A Systematic Analysis of Human Transmembrane E3 RING Proteins

Robert Christopher Jenn

Thesis submitted in accordance with the requirements of the University of Liverpool for the degree of Doctor in Philosophy

December 2011

A Systematic Analysis of Human Transmembrane E3-RING Proteins

Robert Christopher Jenn

Abstract

The reversible covalent conjugation of the small highly conserved ubiquitin protein modifier to selective substrates plays central roles in countless proteolytic and non-proteolytic cellular functions. Substrate protein ubiquitination is co-ordinated by the sequential activity of three distinct classes of proteins: (i) E1-activating enzymes, (ii) E2-conjugating enzymes, and (iii) E3-protein ligases. **R**eally **I**nteresting **N**ew **G**ene (RING) proteins represent the largest family of E3-proteins comprising over half of predicted human E3-ligases. As such, E3-RING proteins play pivotal roles in controlling both specificity and functionality within the ubiquitin system. E3-RING proteins function as catalytically inactive molecular scaffolds that position Ub~E2 and substrate proteins in close proximity for ubiquitination to occur. Within the active ligase complex, E3-RING proteins and E2 conjugating enzymes are believed to select protein substrate(s) and the form of conjugated ubiquitin upon them, respectively. Whilst E3-RING/E2 partners have been investigated in recent HTP screen approaches, a key area of data paucity exists for integral membrane E3-RING (TM-E3-RING) proteins.

As such, high throughput yeast-two-hybrid assays were performed for the entire complement of TM-E3-RING proteins and E2-conjugating enzymes. A broad subset of TM-E3-RING/E2 positive and negative Y2H interactions was

re-tested in secondary luciferase protein complementation assays (PCAs), which increased confidence in Y2H-derived interactions and extended network coverage. Data from these studies was collated with previously published binary TM-E3-RING/E2 interaction data to provide a high-confidence TM-E3-RING/E2 network consisting of 312 unique binary interactions. *In vitro* auto-ubiquitination assays were employed to assign functional activity to TM-E3-RING/E2 protein pairs, revealing high verification rates for both positive and negative Y2H or PCA binary interaction data. Furthermore, novel trends in the generation of different forms of ubiquitin modifications were identified between selective TM-E3-RING/E2 pairs.

Finally, Y2H screens were also performed to identify TM-E3-RING dimerization events, which represent an emerging theme in ubiquitin system regulation. In total 71 TM-E3-RING/TM-E3-RING interactions were reported demonstrating high incidence of these binding events. Novel data was combined with known interactions to generate a TM-E3-RING network containing >500 binary interactions, encompassing both components of the core ubiquitin cascade and non-ubiquitome proteins. This TM-E3-RING-centric network provides a valuable tool for the investigation of specificity and regulation of TM-E3-RING proteins and specific ubiquitin cascades.

Appendices

List of Supplementary files provided on CD:

Supplementary excel files:

E3RING annotation

E3RING dendrogram

TMRING Cloning Summary

Full-length_CRD GAL4Y2H comparison'

E3RING/E2 CRD-Y2H

LexA_CRD comparison

PsortII NLS prediction

Total interaction datasets

Luciferase PCA analysis

TMRING dimerization

TMRING_E2 expression

Abbreviations

3AT	3-amino-1,2,4-triazole
AD	GAL4 activating domain
AMP	Adenosine monophosphate
ATP	Adenosine triphosphate
APS	Ammonium persulphate
BC-PCR	Bacterial colony-PCR
BD	GAL4 DNA binding domain
BP	Base pair
C-terminus	Carboxy-terminus
cDNA	Complementary DNA
CDS	mRNA coding sequence
Co-IP	Co-expression and immuno-precipitation
CRD	Cytoplasmic RING Domain
CRL	Cullin-RING-ligase
Da	Dalton
DMEM	Dulbecco's modified eagle's medium
DNA	Deoxyribonucleic acid
DUB	Deubiquitinating enzyme
E1	E1-activating enzyme
E2	E2-conjugating enzyme
ER	Endoplasmic reticulum
ERAD	ER associated degradation
FL	Full-length
GFP	Green fluorescent protein
GW	Gateway
HECT	Homologous to E6-AP carboxy terminus
HEK	Human embryonic kidney
HPRD	Human Protein Reference Database
HMW	High Molecular Weight
ID	Identifiers
IPTG	Isopropyl-ß-D-thio-galactopyranoside
ISG15	Interferon stimulated gene 15

LMW	Low Molecular Weight
MARCH	Membrane Associated RING Containing Homologues
MINT	Molecular Interactions Database
MYTH	Membrane Yeast Two-Hybrid
N-terminus	Amino-terminus
NCBI	National Centre for Biotechnological information
NEDD8	Neuronal precursor cell-expressed developmentally downregulated protein 8
NLS	Nuclear Localisation Signal
ORF	Open reading frame
PA-TM-RING	Protease associated transmembrane E3 RING protein
PAGE	Polyacrylamide gel electrophoresis
PBS	Phosphate buffered solution
PCA	Protein complementation assay
PCR	Polymerase chain reaction
PDB	Protein data bank
PEG	Polyethylene glycol
PFA	Para-formaldehyde
RefSeq	Reference Sequence
RING	Really interesting new gene
RNA	Ribonucleic acid
SD	Synthetic dropout
SDS	Sodium Dodecyl Sulfate
SUMO	Small ubiquitin-like modifier
TEMED	N,N,N',N'-Tetramethylethylenediamine
TM	Transmembrane
TM-E3-RING	Transmembrane domain containing E3 RING protein
UBAN	Ubiquitin binding in ABIN and NEMO motif
UBC	Ubiquitin conjugating domain
UBD	Ubiquitin binding domain
UBL	Ubiquitin-like
UEV	Ubiquitin E2 variant
UFM1	Ubiquitin-fold modifier 1
UIM	Ubiquitin interacting motif

URM1	Ubiquitin-related modifier 1
UV	Ultra violet
Y2H	Yeast two-hybrid
YC-PCR	Yeast colony-PCR
X-Gal	5-bromo-4-chloro-3indoyl-β-D-galactosidase

Acknowledgements

First and foremost I would like to thank Professor Chris Sanderson for all of his guidance, support and excellent supervision throughout the entirety of this PhD project. Together with members of the lab, both past and present, you have provided an excellent environment to enjoy the highs and persevere through the lows of post-graduate science. To my lab-mates - Jon, Helen, Kelly, Nurulisa, Emily and Amy – you have played no small part in maintaining my sanity and have made the lab a truly enjoyable place to work. I am truly indebted to you all. Special thanks go to Jon for showing me the ropes and always lending a hand whenever I asked and even when I didn't. To the students who have been under my supervision - Fliss, Craig, and Amy – I am grateful to each of you for your dedication and for all the hours you put into the lab. Additional thanks go to the rest of the Physiology Department for providing a friendly place from the outset and to the Wellcome Trust for funding this research.

To all the friends I met along the way and the people who helped me through, I extend my sincere thanks. To Dan Booth, Jon Woodsmith and Hannah McCue thank you for being there. To old and new friends thank you for always being inquisitive and supportive. To Amy, I express my profound appreciation for your encouragement, patience and belief in me. Finally, there is no way that this PhD Thesis could have been completed without the ongoing love and support given to me by my family so to my Mum, Dad, and brothers Phil and Ian (Yan) the final but thoroughly heartfelt thank you is for you.

Table of Contents

Chapter 1: Introduction

1.1. The human ubiquitin system

1.1.1. Intracellular proteolysis and the history of ubiquitin

Intracellular proteins exist in a dynamic state of synthesis and degradation. Prior to the discovery of intracellular protein degradation in mammalian cells, the accepted paradigm was that structural proteins were both stable and static whilst dietary proteins served predominantly as energy providing fuel (Ciechanover 2005). This prevailing notion was challenged by the demonstration that following administration of ^{15}N-labelled tyrosine to rats, only ~ 50% was recovered within urine with the remainder accumulating in tissue proteins (Schoenheimer, Ratner et al. 1939). Subsequent extensive research in the field of protein turnover has elevated intracellular proteolysis from a vague concept to a spatially and temporally controlled process, which is essential for the correct functioning of all eukaryotic cells (Ciechanover 2005).

The discovery of the lysosome provided the first mechanistic description of how proteins could be degraded in a selective manner within the cell ((De Duve, Gianetto et al. 1953) and reviewed in (Luzio, Pryor et al. 2007)). The acidified, hydrolase-rich environment of the membrane-enclosed lysosomal compartment provides an intracellular location where endocytosed and proteins from the late secretory pathways are degraded whilst protecting other cellular contents from non-specific actions of lysosomal hydrolases (Luzio, Pryor et al. 2007). However, subsequent experimental evidence indicated that lysosomal activity could not be entirely responsible for the degradation of all intracellular proteins. Firstly, inhibition of lysosomal proteases by lysosomotropic agents selectively inhibited degradation of

endocytosed proteins while soluble cytoplasmic proteins remained vulnerable to degradation (Poole, Ohkuma et al. 1977). In addition, rabbit reticulocytes, which lack lysosomes, were found to be capable of degrading abnormal haemoglobin proteins in an ATP-dependent manner (Etlinger and Goldberg 1977).

The characterisation of a cell-free proteolytic preparation derived from rabbit reticulocytes identified a heat-stable low molecular weight protein, termed ubiquitin, which could be covalently conjugated to target substrates in a reversible manner upon reconstitution of the entire cell-free proteolytic preparation (Ciechanover, Elias et al. 1980; Wilkinson, Urban et al. 1980). The addition of four or more ubiquitin moieties to substrate proteins was shown to serve as a signal for degradation via the high molecular weight 26S proteasome complex (Ciechanover, Elias et al. 1980; Hough and Rechsteiner 1986; Hough, Pratt et al. 1987; Arrigo, Tanaka et al. 1988). The 26S proteasome is a chambered protease complex comprising a central 20S proteolytic core and two 19S regulatory complexes, which are responsible for the binding of ubiquitinated substrates, the cleavage of ubiquitin, and the unfolding and translocation of substrates into the proteolytic core (Pickart and Cohen 2004).

Following the discovery of ubiquitin as a key regulator of intracellular protein degradation, the importance of the ubiquitin system in countless non-proteolytic processes has been defined. Indeed, much of the recent focus in ubiquitin-related research has focussed on the non-degradative roles of ubiquitin (Welchman, Gordon et al. 2005). As such, the covalent conjugation of ubiquitin to substrate proteins is now recognised as a key regulator of a vast array of cellular functions including protein turnover, DNA repair, cell cycle control, intracellular signalling,

endocytosis and other membrane trafficking events (Welchman, Gordon et al. 2005).

1.1.2. Introduction to the human ubiquitination enzymatic cascade

The canonical mechanism of protein ubiquitination is co-ordinated by the sequential activity of three distinct classes of proteins: (i) E1-activating enzymes, (ii) E2-conjugating enzymes, and (iii) E3-ligases. In addition, ~ 80 deubiquitinating enzymes (DUBs) have been identified, which remove ubiquitin moieties from modified substrates and disassemble ubiquitin chains (Sowa, Bennett et al. 2009). As such, protein ubiquitination should be regarded as a highly dynamic process, which controls the function and stability of a vast array of different cellular components (Figure 1.1).

This chapter provides an overview of the current understanding of the ubiquitin conjugation machinery and how these cascade components operate in a co-ordinated manner to control modification of specific substrates. Finally, a range of protein-protein interaction methods will be reviewed and their potential utility for investigating human ubiquitination networks introduced.

1.2. Ubiquitin and ubiquitin-like molecules

Ubiquitin is a small highly conserved, 76 residue (8.5kDa), protein which undergoes reversible covalent conjugation to target proteins, predominantly via isopeptide bond formation between the C-terminal glycine of ubiquitin and either the ε-amino group of a lysine residue or the N-terminus of substrate proteins (Weissman 2001; Dye and Schulman 2007). Atypical conjugation of ubiquitin to target proteins can also occur by formation of thioester linkages between ubiquitin's C-terminal glycine and target protein cysteine, threonine or serine residues in the presence of

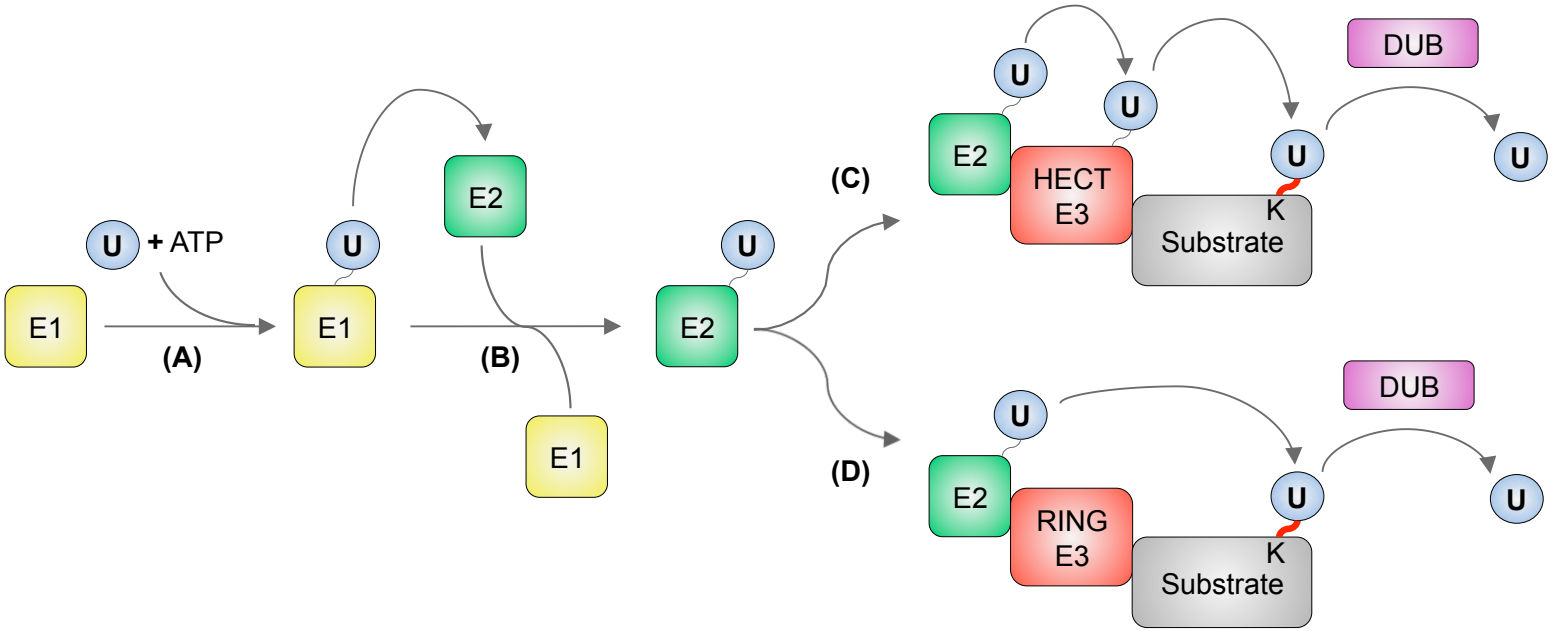

Figure 1.1. The ubiquitination cascade. The conjugation of ubiquitin requires the sequential action of three classes of enzymes: E1 activating enzymes, E2 conjugating enzymes, and E3 ligases. The active site cysteine of the E1-activating enzyme forms a thioester bond with the C-terminal glycine carboxyl group of ubiquitin in an ATP-dependent manner **(A)**. The activated ubiquitin moiety is subsequently transferred to the active site cysteine of an E2-conjugating enzyme via a transthiolation reaction **(B)**. Ubiquitin is attached to substrate lysine residues by an isopeptide bond in a reaction facilitated by E3 ligase proteins. E3 ligases can function either as catalytic intermediates, which bind ubiquitin via a thioester bond (HECT domain containing E3 ligases) **(C)** or act as molecular scaffolds to juxtapose E2 and substrate proteins in close proximity to facilitate direct transfer of ubiquitin from E2 to substrate **(D)**.

viral (Cadwell and Coscoy 2005) and human E3 ligase proteins (Shimizu, Okuda-Shimizu et al. 2010).

Ubiquitin is encoded by 4 genes within the human genome (UBB, UBC, UBA52, RPS27A) that encode either multiple concatenated ubiquitin moieties (UBB & UBC), or ubiquitin-fusion proteins, in which single ubiquitin moieties are fused to the N-terminus of L40 (UBA52) or S27a (RPS27A) proteins (Wiborg, Pedersen et al. 1985; Baker and Board 1991). In each case, post-translational processing of gene products results in the generation of an intracellular pool of unconjugated ubiquitin terminating in a di-glycine motif that is required for 'activation' by specific E1 enzymes for entry into the ubiquitination cascade.

Since the discovery of ubiquitin, 17 other human ubiquitin-like (Ubl) proteins have been identified (Schulman and Harper 2009), which exhibit remarkable structural similarity to ubiquitin despite often exhibiting low sequence similarity (E.g. Figure 1.2B); NEDD8 shows the closest homology to ubiquitin sharing 58% homology (Schulman and Harper 2009). Ubl proteins belong to 9 subfamilies: Neuronal precursor cell-expressed developmentally down-regulated protein 8 (NEDD8, (Kumar, Yoshida et al. 1993; Shen, Pardington-Purtymun et al. 1996)), small ubiquitin-like modifier (SUMO, (Loeb and Haas 1992; Shen, Pardington-Purtymun et al. 1996)), interferon stimulated gene 15 (ISG15, (Loeb and Haas 1992)), gamma-aminobutyric acid receptor-associated protein (GABARAP, (Tanida et al., 2002)), microtubule-associated protein 1 light chain 3 (MAP1LC3, (He, Dang et al. 2003)), ubiquitin-fold modifier 1 (UFM1, (Komatsu, Chiba et al. 2004)), ubiquitin-related modifier 1 (URM1, (Furukawa, Mizushima et al. 2000)), autophagy 12 (ATG12, (Mizushima, Sugita et al. 1998)), and FAT10 (Bates, Ravel et al. 1997).

All Ub/Ubl proteins adopt a similar tertiary structure consisting of a highly compact and tightly hydrogen-bonded tertiary domain, comprising a four-stranded mixed β-sheet, an α-helix, and a flexible C-terminal tail region terminating in a diglycine motif (Welchman, Gordon et al. 2005) (Figure 1.2B). In analogy to ubiquitin, members of the Ubl-subfamilies undergo covalent modification to target proteins (Schulman and Harper 2009).

Ubiquitin, SUMO, and ISG15 moieties are conjugated to a diverse range of intracellular substrates whilst other Ubl proteins often exhibit more restricted substrate profiles, potentially reflecting more specific or restricted cellular functions (Kerscher, Felberbaum et al. 2006). For example, ATG12 has two reported substrates (ATG3 and ATG5) (Mizushima, Sugita et al. 1998; Radoshevich, Murrow et al. 2010), and ATG8 is attached to a specific phospholipid (phosphatidylethanolamine) (Ohsumi 2001) to regulate multiple steps in the process of autophagy. In agreement with potentially more restricted roles of many Ubls, the conjugation machinery for each of these modifiers comprises a limited number of enzymes in comparison to the expansive ubiquitin conjugation system (Kerscher, Felberbaum et al. 2006). The specialised roles of many Ubls may also be inferred by the finding that the expression and/or activation of many Ubl modifiers is controlled by specific cellular events. For example, ISG15 expression is induced by stimulation with type I interferons (IFN) (Loeb and Haas, 1992); ATG12 is activated during autophagy (Mizushima et al., 1998); and FAT10 expression is cell cycle regulated (Lim et al., 2006).

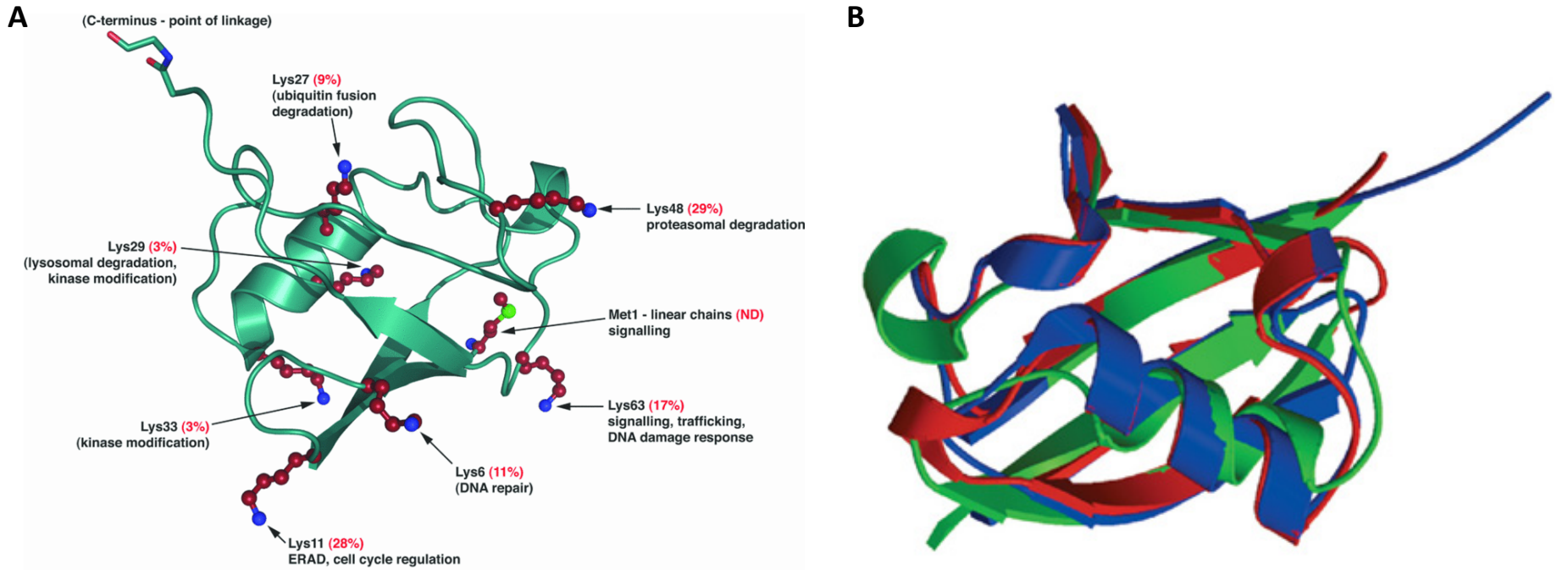

Figure 1.2. The ubiquitin superfold. (A) Ribbon diagram representing the tertiary structure of ubiquitin and the functional implications of specific linkages (Komander 2009). **(B)** Structural similarities of Ub and Ubl moieties through overlay of ribbon diagrams: ubiquitin (blue; PDB code P62988), SUMO-1 (green; PDB code P63165) and NEDD8 (red; PDB code Q15843) (Welchman, Gordon et al. 2005).

1.2.1. Differential architecture of Ub/Ubl modification

Ubiquitin can be conjugated to other ubiquitin molecules through any of the six lysine residues in its primary sequence (K11, K27, K29, K33, K48, K63) or to the free amino group of its N-terminal methionine residue (Figure 1.2A). This allows for the assembly of a diverse range of ubiquitin architectures upon target proteins from conjugation of single ubiquitin moieties to one (mono-ubiquitination) or multiple substrate lysine residues (multi-ubiquitination) to the formation of ubiquitin chains linked through specific lysine residues (poly-ubiquitination). Additionally, linear poly-ubiquitin chains have also been reported by formation of isopeptide bond linkages between the C-terminal glycine and N-terminal methionine residue of ubiquitin molecules both *in vitro* (Kirisako, Kamei et al. 2006) and *in vivo* (Niu, Shi et al. 2011). Mass spectrometric analysis of ubiquitin chain linkage abundance within yeast (Xu, Duong et al. 2009) and humans (Ziv, Matiuhin et al. 2011) revealed that poly-ubiquitin chains of all lysine linkage specificity were detected, in the order of abundance: K48 (29%), K11 (28%), K63 (17%), K6 (11%), K27 (9%), K29 (3%), and K33 (3%) (Xu, Duong et al. 2009). Further complexity is added to the ubiquitin signal by the formation of complex, mixed linkage chain topologies that include branched chains (Komander 2009). The Ubl proteins belonging to the SUMO family (SUMO-1, SUMO-2, SUMO-3) have been also reported to poly-SUMOylate substrate proteins to mediate differential effects compared to mono-SUMOylation (Ulrich, Vogel et al. 2005; Denuc and Marfany 2010).

The elucidation of crystal structures for K11-, K6-, K63-, and linear di-ubiquitin structures and K48-tetra-ubiquitin chains has revealed the adoption of unique conformations dependent upon linkage type (Eddins, Varadan et al. 2007;

Komander, Reyes-Turcu et al. 2009; Bremm, Freund et al. 2010; Matsumoto, Wickliffe et al. 2010; Virdee, Ye et al. 2010) (Figure 1.3). Differences in topology are most evident when comparing K48-linked with K63- or linear-ubiquitin chains. K48-linked tetra-ubiquitin chains predominantly adopt compact folds with intermolecular interactions between hydrophobic patches centred on the Ile44 residue of ubiquitin (Figure 1.3A). In contrast, K63-linked and linear ubiquitin chains exhibit more extended and open conformations with minimal contact between ubiquitin moieties (Figure 1.3D&E). The distinct conformations of ubiquitin modifications on target proteins allows for the selective recognition of ubiquitinated proteins by a multitude of downstream effector proteins via non-covalent interactions with specific Ubiquitin Binding Domains (UBD) to mediate wide-ranging physiological outcomes.

1.3. Ubiquitin binding (UBD) domains

1.3.1. Diversity of ubiquitin binding domains and Ub linkage specificity

The discovery of the first ubiquitin binding domain (UBD) in the yeast S5a subunit of the 26S proteasome provided the first description of how the 26S proteasome was capable of selecting poly-ubiquitinated substrates for degradation (Young, Deveraux et al. 1998). Since this time, ~ 20 different families of UBDs have been described, which show considerable structural diversity and mechanisms of ubiquitin recognition (reviewed in (Dikic, Wakatsuki et al. 2009)). Most ubiquitin binding motifs interact with the hydrophobic patch of ubiquitin centred on the Ile44 residue located within ubiquitin's β-sheet surface (Hicke, Schubert et al. 2005). Whilst these interactions are predominantly mediated by α-helical structures, β-sheets are also employed for ubiquitin binding, for example by E2-conjugating enzymes belonging to UBE2D and UBE2G2 families ((Brzovic, Lissounov et al. 2006; Choi, Jeon et al. 2009) and reviewed in (van Wijk and Timmers 2010)).

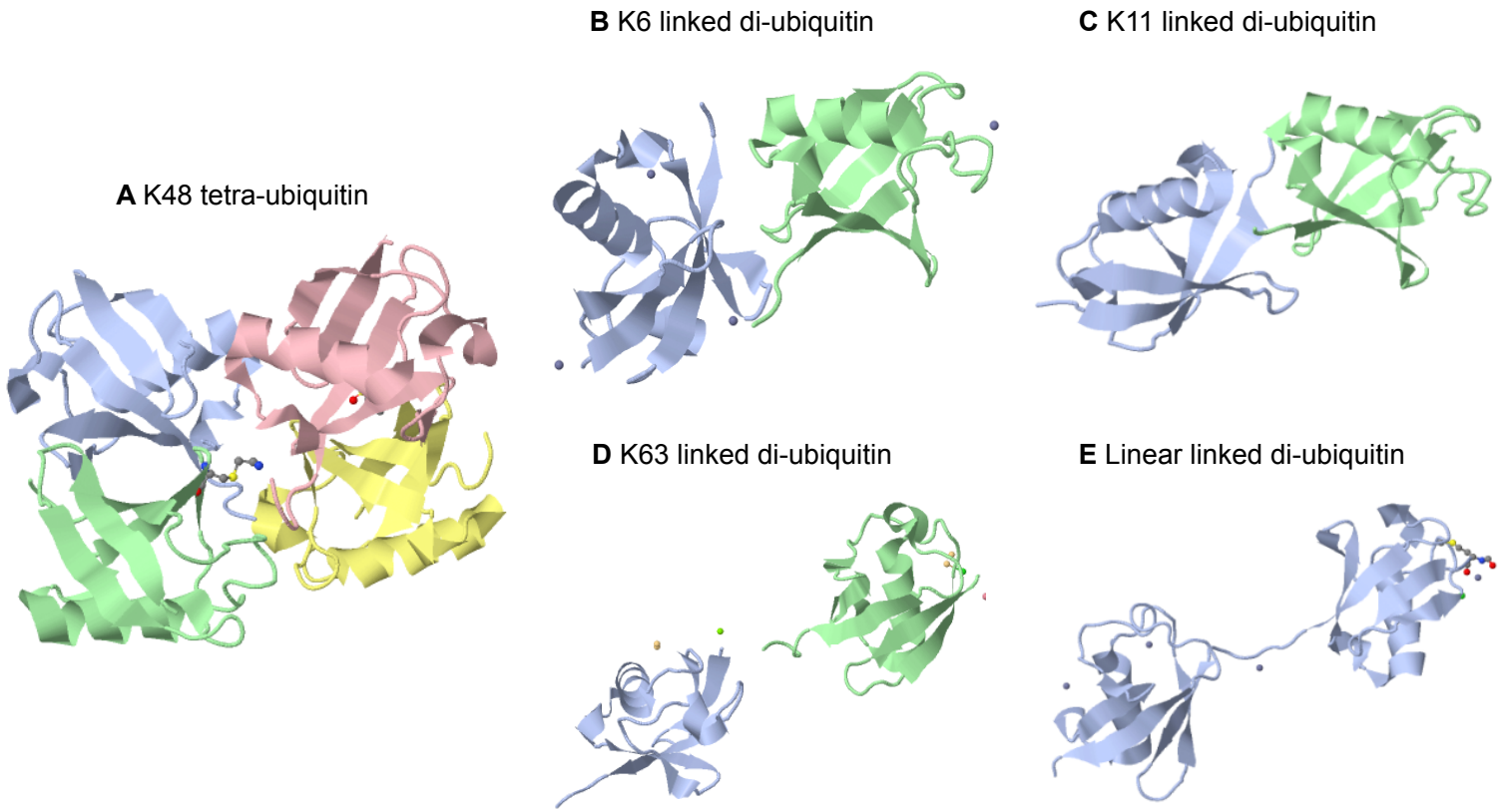

Figure 1.3. Poly-ubiquitin chains adopt different topologies based upon ubiquitin linkage specificity. (A) Ribbon diagram showing structural diagrams of K48 linked tetra-ubiquitin (PDB code 2O6V, (Eddins, Varadan et al. 2007)), **(B)** K6 linked di-ubiqiutin (PDB code 2XK5 (Virdee, Ye et al. 2010)), **(C)** K11 linked di-ubiquitin (PDB codes 3NOB (Matsumoto, Wickliffe et al. 2010)), **(D)** K63 linked di-ubiquitin (PDB code 2JF5 (Komander, Reyes-Turcu et al. 2009)) and **(E)** linear di-ubiquitin (PDB code 2W9N, (Komander, Reyes-Turcu et al. 2009)). Ribbon diagrams were generated using Jmol by Jonathan Woodsmith (Jmol: an open-source Java viewer for chemical structures in 3D. http://www.jmol.org/). Lys48 and Met1 residues in the distal ubiquitin moieties are highlighted in **A** and **E**, respectively.

Pioneering work in the field of linkage-specific UBD recognition revealed distinct preferences for specific poly-ubiquitin chain topologies when investigating 30 different UBDs (Raasi, Varadan et al. 2005). Structural studies have provided mechanistic insights into how UBDs exhibit specificity for ubiquitin chain linkages. For example, the UBA domain of hHR23A utilises the proximity of hydrophobic isoleucine patches in the closed structure of K48-linked ubiquitin to interact with two ubiquitin moieties (Figure 1.3A) (Varadan, Assfalg et al. 2005). In contrast, the extended conformations of the RAP80 UIM and the NEMO UBAN domain exhibit interaction preference for the extended conformations of the K63 and linear linked chains, respectively (Figure 1.3D&E) (Rahighi, Ikeda et al. 2009; Sato, Yoshikawa et al. 2009). DUB family members also exhibit remarkable specificity for poly-ubiquitin linkages, underlying their restricted activity profiles for poly-ubiquitin chains of specific topologies *in vitro* ((Komander, Reyes-Turcu et al. 2009) and reviewed in (Komander 2010)).

1.4. The human ubiquitin conjugational machinery

1.4.1. Introduction

The sequential actions of Ub-activating (E1), Ub-conjugating (E2), and Ub-ligating (E3) enzymes mediate the covalent conjugation of ubiquitin to target proteins. Discrete E1-E2-E3 combinations have been reported for specific attachment of Ub/Ubl moieties to cellular substrates and will be discussed in greater detail below.

1.4.2. Human E1-activating enzymes

Early studies utilising a mouse cancer cell line that exhibited a temperature-sensitive decrease in ubiquitin conjugation led to the isolation of a temperature-sensitive mutant protein required for ubiquitination, termed the E1 ubiquitin-activating enzyme (Finley, Ciechanover et al. 1984). The E1 enzyme functions to activate the C-

terminal glycine residue of Ub moieties in an ATP and Mg^{2+}-dependent adenylation reaction, to form a high-energy acyl-phosphate linkage between ubiquitin and AMP. The E1 catalytic cysteine residue subsequently attacks the Ub-AMP, releasing AMP and forming a thioester linkage with the C-terminal ubiquitin glycine residue (Lee and Schindelin 2008). A second adenylation reaction results in the asymmetric loading of an individual E1 molecule with two molecules of activated Ub (Dye and Schulman 2007), prior to the transfer of the thiol-linked Ub moiety to the catalytic cysteine residue of the next enzyme in the ubiquitination cascade, the E2 conjugating enzyme. Sequence homology between E1 proteins dedicated to Ub and specific Ubl families (Table 1.1) have implicated similar mechanisms of activation for a number of Ubl molecules and has been experimentally confirmed in a limited number of cases (Dye and Schulman 2007).

Ub/Ubl	**E1 Gene Symbol (EntrezID)**
Ubiquitin	UBA1 (7317) & UBA6 (55235)
ISG15	UBA7 (7318)
FAT10	UBA6 (55235)
SUMO	SAE1/2* (10054/10055)
NEDD8	NAE1/UBA3* (8883/9039)
URM1	MOCS3 (27304)
GABARAP family	ATG7 (10533)
UFM1	UBA5 (79876)

Table 1.1. Known E1-Ub and E1-Ubl pairs. Gene symbols and corresponding Entrez gene IDs for known E1-ubiquitin or E1-Ubl pairs. *Two E1s are hetero-dimeric enzymes and therefore have two associated independent genes. Ubiquitin has two annotated E1-activating enzymes.

1.4.3. Human E2-conjugating enzymes

Following activation of Ub, the thiol-linked Ub is transferred from E1 to the active site cysteine of an E2-conjugating enzyme via a transthiolation reaction. E2 proteins are characterised by the presence of an ~ 150 residue ubiquitin conjugating domain (UBC), which provides an interaction platform for E1, E3, and activated Ub proteins. UBC domains are comprised of a core four-stranded antiparallel β-sheet flanked by (i) a C-terminal extension containing a β-hairpin and one or two helices and (ii) an N-terminal extension containing an α-helix (Figure 1.4A). The active-site cysteine residue and other highly conserved residues are located within the C-terminal β-hairpin structure. Upon Ub binding to the catalytic Cys, the C-terminal β-hairpin region undergoes a conformational shift to position the Ub tail for attachment to target lysine residues within protein substrates (Reverter and Lima 2006; Yunus and Lima 2006; Burroughs, Jaffee et al. 2008). Amino acid residues flanking the β-hairpin structure are proposed to provide specificity of E1 binding and to prevent mis-charging of a given E2 with a non-cognate Ub (Pickart 2001).

1.4.3.1. Family Diversity and Ub/Ubl Selection

The human genome encodes 37 E2-conjugating enzymes and 5 ubiquitin E2 variant proteins (UEV; AKTIP, TSG101, UEVLD, UBE2V1, UBE2V2), which adopt the UBC structural fold yet lack a catalytic cysteine residue required for Ub/Ubl conjugation (Figure 1.4 B). The majority of E2 enzymes are composed solely of a UBC domain with variable N- and/or C-terminal extensions (Figure 1.4B), which can provide specificity for particular E3 ligases, enable membrane anchoring, permit E3-ligase independent ubiquitination, or dictate the topology of poly-ubiquitin signals (see Figure 1.4B) (Dye and Schulman 2007). A limited number of E2s contain additional protein domains located within the N- and/or C- terminal tails suggesting functions

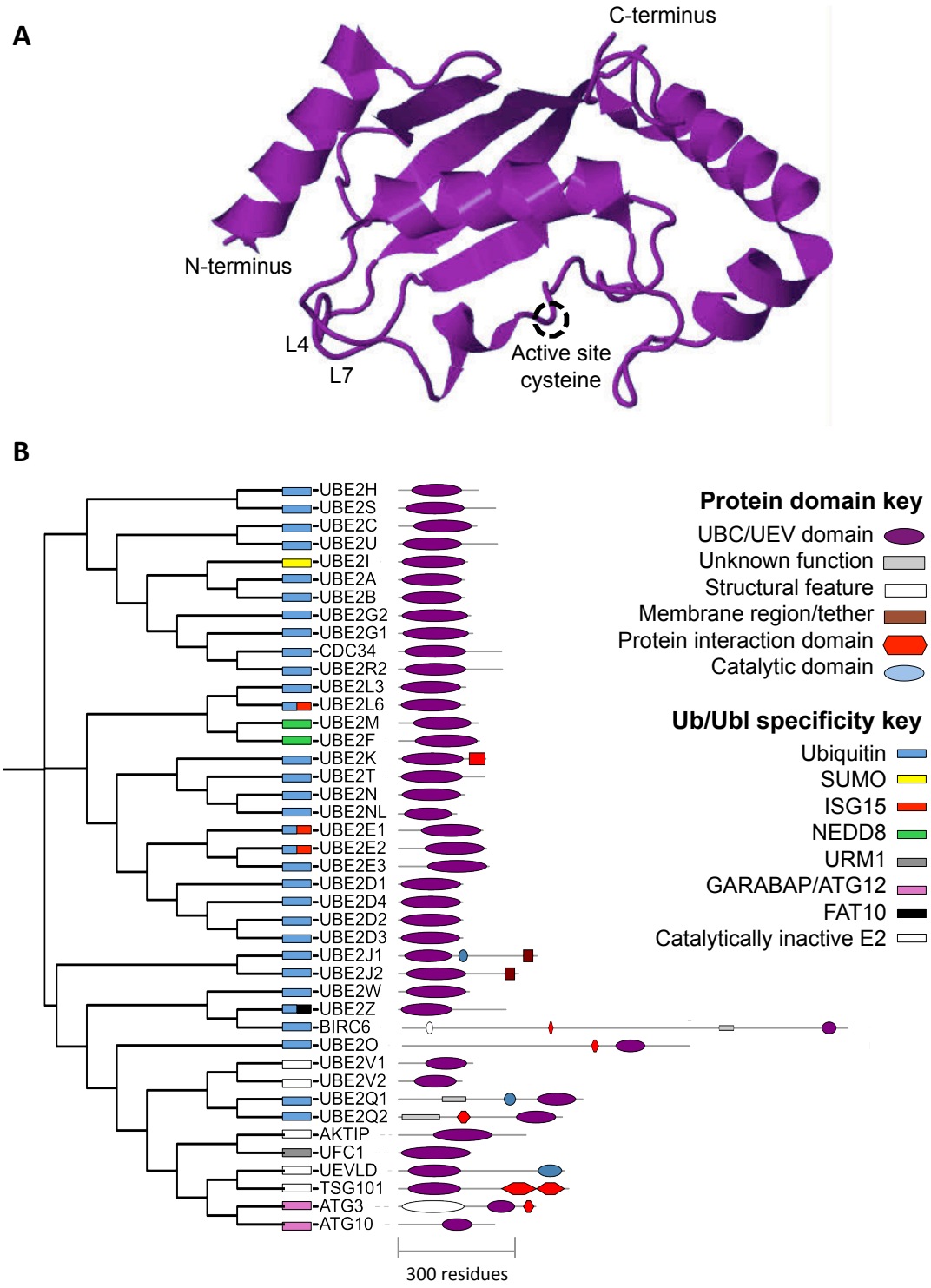

Figure 1.4. The UBC fold and E2-conjugating enzyme family. (A) Ribbon diagram representation of the E2-conjugating enzyme UBE2N, which consists of solely a UBC domain and lacking N- or C-terminal extensions (PDB Code 2GMI (Eddins, Carlile et al. 2006). **(B)** Dendrogram of the human E2-conjugating enzyme family with schematic representations of annotated protein domains. E2 proteins represented by official gene symbols are ordered according to protein sequence alignment in CLUSTALW. BIRC6 and UBE2O are too large to fit to scale on the diagram and are proportional representations of their annotated gene size. Figure generated using ITOL.

within and outside of ubiquitination events. UBE2K contains a C-terminal UBA domain, which contributes to its specificity for generation of K48 poly-ubiquitin chain linkages (Wilson, Edmondson et al. 2011). The BIR domain located within the ~ 5000 residue BIRC6 E2 conjugating enzyme promotes ubiquitination and degradation of both SMAC and caspase-9 proteins to function in the negative regulation of apoptosis (Bartke, Pohl et al. 2004; Zhao, Beaudenon et al. 2004). The Vps23_core domain of the TSG101 UEV protein mediates stable binding of TSG101 to other components of the ESCRT-1 machinery to mediate endosomal sorting (Teo, Gill et al. 2006). Whilst the vast majority of E2 proteins are soluble, UBE2J1 and UBE2J2 proteins contain a single transmembrane region, anchoring both proteins to the ER membrane (Tiwari and Weissman 2001).

The selective recruitment of Ubl~E1 by E2 proteins allows each Ub/Ubl moiety to be equipped with cognate E2-conjugating enzyme(s), responsible for transfer through their specific conjugational cascade (Figure 1.4B, coloured boxes). Indeed the majority of Ubl proteins have a sole and often dedicated E2-protein for their conjugation. Of the well-studied Ubl modifiers, the SUMO family is established to function with a sole dedicated E2, UBE2I, to regulate SUMOylation of a large number of target proteins (Gareau and Lima 2010). The non-redundant and essential role of UBE2I in SUMOylation is illustrated by the embryonic lethality associated with gene knockout in mammals (Nacerddine, Lehembre et al. 2005). Of the lesser characterised Ubl proteins, UFC1 serves as the cognate E2 for Ufm1 (Tatsumi, Sou et al. 2010; Lemaire, Moura et al. 2011), whilst UBE2Z which can mediate ubiquitin transfer, has recently been shown to facilitate FAT10 conjugation to targets (Aichem, Pelzer et al. 2010). Additionally, ATG12 and GABARAP (ATG8) conjugation to substrates is mediated by the autophagy specific E2 proteins, ATG3

and ATG10 (Geng and Klionsky 2008). Ubiquitin, NEDD8, and ISG15 modifiers have each been reported to utilise more than one E2 protein for conjugation. NEDD8 utilises two closely related E2 enzymes (UBE2M and UBE2F) for its selective conjugation to cullin substrates (Huang, Ayrault et al. 2009). Similarly, UBE2L6 is dedicated to ISG15-conjugation whilst UBE2E1 and UBE2E2 can also receive activated ISG15 and are shared between ISG15 and ubiquitin conjugational machineries (Zhao, Beaudenon et al. 2004; Takeuchi, Iwahara et al. 2005). Interestingly, ISG15 exhibits distinct specificity for utilisation of the UBE2L6 but not the closely related E2 protein, UBE2L3 (Durfee, Kelley et al. 2008).

Whilst UEV proteins are not capable of directly conjugating ubiquitin, both UBE2V1 and UBE2V2 act in conjunction with the active E2 conjugating enzyme, UBE2N, to determine the topology of ubiquitin chain linkages (Andersen, Zhou et al. 2005; Eddins, Carlile et al. 2006) and will be discussed in further detail later. Equivalent roles of other UEV proteins (UEVLD, AKTIP, TSG101) in ubiquitination events have not yet been reported.

1.4.3.2. Roles in regulating the architecture of ubiquitin modification on substrate protein

As discussed in section 1.2.1, ubiquitin can be conjugated to target proteins either as single moieties (mono- and multi-ubiquitin) or as poly-ubiquitin chains via any of the six lysine residues within ubiquitin's primary sequence or to the free amino group of its N-terminal methionine residue (Komander 2009; Ye and Rape 2009). Whilst E3 proteins represent the crucial regulators of substrate selection, an increasing body of experimental evidence has highlighted the key role of E2s, alone or in combination with UEV proteins, in dictating the architecture of conjugated ubiquitin on target proteins.

The addition of single ubiquitin moieties to target proteins serves as a distinct cellular signal ranging from receptor trafficking events to epigenetic control and DNA repair (Komander 2009). UBE2A, in complex with different E3-RING proteins, mono-ubiquitinates target proteins to regulate gene expression and participate in the DNA damage response; UBE2A/RNF20-mediated mono-ubiquitination of histone H2B acts to regulate histone H3 methylation levels and gene expression (Kim, Guermah et al. 2009) whilst UBE2A/RAD18-mediated mono-ubiquitination of PCNA functions in the DNA damage and repair response (Hoege, Pfander et al. 2002). Additionally, UBE2T has been reported to mono-ubiquitinate another component of the DNA damage response, FANCD2 (Machida, Machida et al. 2006), suggesting a key role of mono-ubiquitination in nuclear/DNA functions. Members of the UBE2D family have also been implicated in the mono-ubiquitination of substrates *in vivo*. UBE2D3/CBL-mediated mono-ubiquitination has been reported to induce internalisation of RTKs (Mosesson, Shtiegman et al. 2003), whilst UBE2D2 and UBE2D3 mediated mono-ubiquitination is necessary for efficient internalisation of cell surface immunoreceptors (Dodd, Allen et al. 2004). Despite this, members of the UBE2D family predominantly generate ubiquitin chains with broad linkage specificity *in vitro* (Christensen, Brzovic et al. 2007; Kim, Kim et al. 2007). It is plausible that E2 proteins may have context dependent roles in both mono- and poly-ubiquitination and as such further study is necessary to determine the specific activities and functions of individual E2 proteins *in vivo*.

The formation of poly-ubiquitin chains on substrate proteins provides additional and distinct signals for various downstream effectors. A small subset of E3 proteins, termed HECT-E3s, serve as catalytic intermediates to bind and transfer ubiquitin

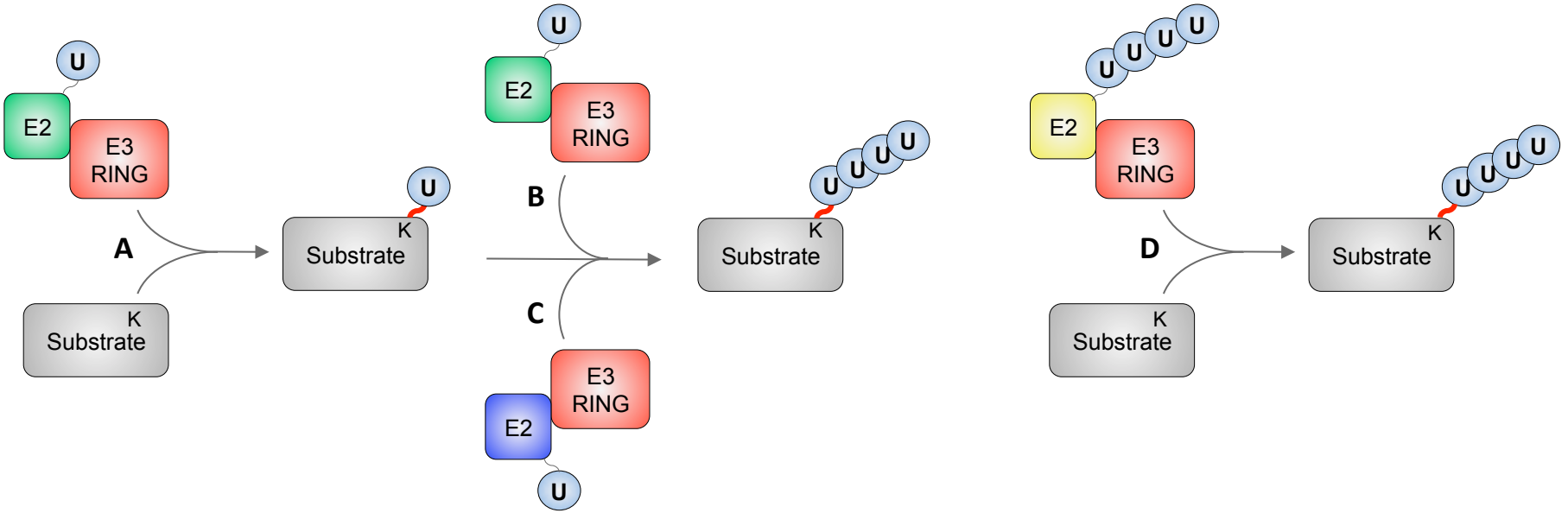

Figure 1.5. Schematic representations of differential architecture of target ubiquitination. (A) Mono- or multi-ubiquitination; ubiquitin is conjugated to target substrates as individual moieties by a single E2-E3 pair. Chains can be formed on target substrates through either the sequential addition of single moieties by a single E2-E3 pair **(A+B)**, through the combinatorial action of different E2 enzymes **(A+C)**, or en bloc transfer of a preformed chain from the E2 enzyme (**D**).

from E2 to substrate, and play key roles in determining poly-ubiquitin chain linkage specificity. For example both the E6AP and KIAA10 HECT E3 proteins catalyse the formation of K48-specific Ub chains either upon their active cysteine residue or as 'free' chains, respectively (Scheffner and Whitaker 2003; Wang, Cheng et al. 2006). However, for the largest number of E3 proteins, the E3-RING family, experimental evidence highlights the central role of E2 proteins in catalysing ubiquitin transfer and dictation of chain topology. Mechanistically, polyubiquitination of substrate proteins can take two main forms: (1) addition of a single Ub moiety, 'initiation', and subsequent 'elongation' of poly-ubiquitin chains on substrates via sequential recruitment of the same or different E2 enzymes (Figure 1.5 A-C) or (2) the transfer of preassembled poly-ubiquitin chains from a single E2 to a substrate (Figure 1.5 D).

During initiation, there can be many sequence or structural variations surrounding target lysine residues. In contrast, elongation of ubiquitin chains is subject to specific sequence determinants surrounding the ubiquitin target lysine. As such, whilst the sequential recruitment of a single E2 can be responsible for both initiation and elongation steps (for example UBE2C generates short K11-linked ubiquitin chains on the APC (Garnett, Mansfeld et al. 2009)) (Figure 1.5 A&B), specialised E2s responsible for initiation and elongation of polyubiquitination chains would represent a more efficient mechanism of chain formation (Ye and Rape 2009) (Figure 1.5 A&C). This mechanism was first reported for the hetero-dimeric E3-RING ligase BRCA1/BARD1 complex which can utilise the UBE2D, UBE2E, UBE2W E2s to nucleate substrate proteins with a single ubiquitin moiety for subsequent K63 and K48 poly-ubiquitin chain elongation by the hetero-dimeric UBE2N/UBE2V1 and UBE2K E2s (Christensen, Brzovic et al. 2007). A similar division of labour is observed for the APC/C E3-RING ligase, which recruits UBE2C to prime APC/C

substrates for subsequent K11-chain elongation by UBE2S during cell cycle regulation (Garnett, Mansfeld et al. 2009; Wu, Merbl et al. 2010). Finally, UBE2D family members can serve as initiation E2s for UBE2N- (Dodd, Allen et al. 2004) and CDC34- (Wu, Kovacev et al. 2010) chain elongation to control K63-mediated internalisation of cell surface receptors and K48-mediated degradation- of the SCF substrate IκB, respectively. In contrast to the mechanism of poly-ubiquitin chain synthesis by initiation and elongation processes, preassembled poly-ubiquitin transfer from E2 to substrate protein is characterised for the UBE2G2 E2 enzyme (Figure 1.5 D). UBE2G2 assembles K48-linked poly-ubiquitin chains at its catalytic cysteine prior to transfer of the preformed chain to a substrate lysine residue facilitated by the E3-RING protein, AMFR (Li, Tu et al. 2007).

1.4.3.3. Control of Chain specificity

The majority of E2 proteins are capable of building ubiquitin chains of specific topology at their catalytic cysteine or on generic substrates *in vitro* (David, Ziv et al.). Whilst the *in vivo* relevance of many of these events remain to be addressed, the finding that E2 proteins exhibit distinct preferences for poly-ubiquitin chain linkages highlights the ability of E2 proteins to control specificity of chain linkages. In agreement with mass spectrometric analyses of poly-ubiquitin chain linkage abundance in yeast (Xu, Duong et al. 2009) and human (Ziv, Matiuhin et al. 2011) cells, these findings demonstrated that E2 proteins exhibit clear preferences for generation of K11, K48 and K63 linkage types.

The prevailing model of linkage specificity is such that elongating E2 proteins, charged with a donor ubiquitin moiety, non-covalently bind a substrate-bound acceptor ubiquitin and optimally positions the acceptor and/or donor ubiquitin

molecules for isopeptide bond formation between a specific lysine residue of the acceptor and the C-terminal glycine of the donor ubiquitin (Wickliffe, Lorenz et al. 2011). In addition, two UEV proteins have been shown to act in conjunction with active E2 conjugating enzymes to determine the topology of poly-ubiquitin chains; both UBE2V1 and UBE2V2 form hetero-dimer complexes with the active UBE2N to catalyse formation of K63-linked poly-ubiquitin chains. Structural studies of the Ub~UBE2N/UBE2V2 complex has revealed that UBE2V2 binds and orients an acceptor ubiquitin to optimally facilitate Lys63 conjugation with the Ub~UBE2N moiety (Eddins, Carlile et al. 2006).

Interestingly, many single-subunit E2 proteins that are capable of elongating poly-ubiquitin chains are capable of non-covalently interacting with ubiquitin. UBE2D proteins utilise a β-sheet surface opposing the active site cysteine to non-covalently interact with Ub moieties and is required for the formation of poly-ubiquitin chains of broad linkage specificity (Brzovic, Lissounov et al. 2006). The UBA domain located within C-terminal tail of UBE2K (Figure 1.4 B) contributes to its selectivity by positioning acceptor Ub moieties in an optimal orientation for K48-linkage formation (Wilson, Edmondson et al. 2011). Finally, the Ub~UBE2S active site transiently recognises acceptor ubiquitin moieties via electrostatic interactions around the acceptor K11 residue. In this complex a single residue (Glu34) in the donor ubiquitin moiety is predicted to suppress the pK_a of the acceptor Lys11 residue to promote linkage-specific ubiquitin chain formation via substrate-assisted catalysis (Wickliffe, Lorenz et al. 2011). Consistent with the non-covalent interaction between E2 proteins and ubiquitin serving a key role in poly-ubiquitin chain formation, a number of E2 proteins that primarily mediate mono-ubiquitination of targets appear incapable in NMR experiments of non-covalently binding ubiquitin moieties

(Christensen, Brzovic et al. 2007). However, whilst UBE2E and UBE2W are capable of assembling poly-ubiquitin chains when expressed in fusion with a generic substrate (David, Ziv et al. 2010), they do not appear capable of non-covalently binding ubiquitin (Christensen, Brzovic et al. 2007). As such, it should be assumed that there must exist diverse mechanisms of poly-ubiquitin chain formation for these E2 proteins. In accordance with the central role of E2 proteins in determining the architecture of conjugating ubiquitin, individual E3 ligases induce the assembly of variable poly-ubiquitin chain architectures depending upon E2 usage (Christensen, Brzovic et al. 2007).

1.4.4. Human E3 'ligases'

1.4.4.1. Role(s) in the ubiquitination cascade

During the final stages of ubiquitination, charged Ub~E2 proteins interact with an E3-ligase to facilitate the formation of an isopeptide bond linkage between ubiquitin's C-terminal glycine residue and the ε-amino group of substrate lysine residues. The human ubiquitin system is hierarchical with few E1-activating enzymes, tens of E2 conjugating enzymes, and hundreds of E3 ligases encoded within the human genome, consistent with a role of E3 proteins in imparting substrate selectivity. Previous bioinformatic analysis has identified > 600 human proteins encoding motifs associated with E3 proteins, which can be divided into 3 broad subfamilies based upon their E2-binding domains: (1) Homologous to E6-AP Carboxy Terminus (HECT), (2) Really Interesting New Gene (RING) and RING-like (including, PIAS, plant homeodomain (PHD), U-box, F-box, and Cullin-RING proteins), and (3) those resembling neither HECT nor RING classes (ZnF A20, para-caspase) (Li, Bengtson et al. 2008). The E3-mediated transfer of ubiquitin to substrate proteins occurs by one of two mechanisms, dependent upon the type of

E3 ligase involved. HECT domain-containing E3 proteins accept ubiquitin from E2 conjugating enzymes by formation of direct thioester linkages with ubiquitin at a catalytic cysteine residue prior to ubiquitin transfer to substrates (Huibregtse, Scheffner et al. 1995; Kee and Huibregtse 2007) (Figure 1.1 C). In contrast, RING-domain containing E3 proteins function as catalytically inactive molecular scaffolds that juxtapose Ub~E2 and substrate proteins to facilitate direct transfer of Ub from E2 to substrate (reviewed in (Deshaies and Joazeiro 2009)) (Figure 1.1 D). RING-domain containing proteins are the principle focus of this thesis and as such this class of E3-ligase is described in greater detail below.

1.4.4.2. RING-type E3 proteins

1.4.4.2.1. RING domain structure

The RING domain was originally identified by Freemont and colleagues and characterised by the presence of a distinct arrangement of conserved cysteine and histidine residues (Freemont, Hanson et al. 1991). The canonical amino acid sequence of the C_3HC_4 RING domain is Cys-X_2-Cys-$X_{(9-39)}$-Cys-$X_{(1-3)}$-His-$X_{(2-3)}$-Cys-X_2-Cys-$X_{(4-48)}$-Cys-X_2-Cys, where X represents any amino acid (Figure 1.6).

Subsequent three-dimensional structural studies of individual RING domains have revealed that the conserved histidine and cysteine residues are buried within the core of the RING domain, where they co-ordinate two Zinc cations (Zn^{2+}) in an interleaved, or cross-brace, arrangement (Figure 1.6 A) (Borden, Boddy et al. 1995). The conserved histidine and cysteine residues play a key role in maintaining structural integrity, enabling the RING domain to adopt a rigid, globular platform for protein-protein interaction. Since the initial characterisation of the canonical RING domain, numerous variations of the RING sequence have been described, typically

involving the interchange of the conserved cysteine and histidine residues (Figure 1.6 B). For example, an atypical RING variant, characterised by the sequence C_4HC_3, is present in the Membrane-Associated RING-CH (MARCH) family of transmembrane domain-containing E3-RING proteins (Bartee, Mansouri et al. 2004). Additionally, exchange of cysteine and histidine residues for other residues capable of chelating Zn^{2+} ions has also been reported; the Rbx1/Roc1 RING domain substitutes an aspartate residue in place of a cysteine at the eighth Zn^{2+} co-ordination site (Zheng, Schulman et al. 2002). An additional variation on this theme is observed for the U-Box domain-containing class of E3 proteins, wherein conserved Zn^{2+}-chelating residues are replaced by charged and polar residues which engage in hydrogen bonding networks to maintain a structure with considerable homology to the RING domain (Vander Kooi, Ohi et al. 2006). Whether the sequence variations observed between RING and RING-like domains have functional significance largely remains unclear. Whilst PHD and LIM domains exhibit a high degree of sequence homology to the RING domain, they have been reported to fold differently and not adopt the interleaved structure characterised by RING domains and have not yet been implicated in the process of ubiquitination (Deshaies and Joazeiro 2009).

In addition to the highly conserved Zn^{2+}-chelating residues, a number of semi-conserved residues exist within RING domain sequences, which are implicated in contributing to the core structure of the RING domain or the recruitment of interacting protein partners, such as E2-conjugating enzymes (Deshaies and Joazeiro 2009).

A

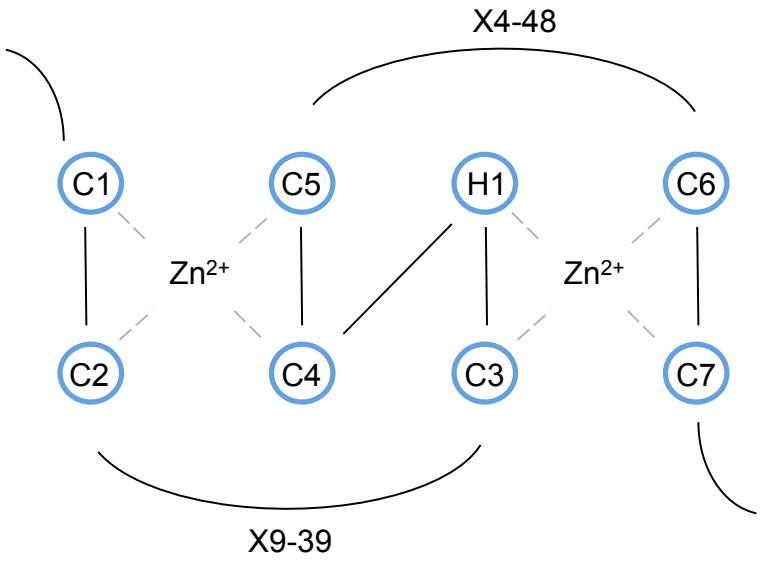

B

RING-HC (C4HC4)	Cys-X-Cys-$X_{(9-39)}$-Cys-$X_{(1-3)}$-His-$X_{(2-3)}$-Cys-X_2-Cys-$X_{(4-48)}$-Cys-X_2-Cys
RING-H2 (C3H2C3)	Cys-X-Cys-$X_{(9-39)}$-Cys-$X_{(1-3)}$-His-$X_{(2-3)}$-His-X_2-Cys-$X_{(4-48)}$-Cys-X_2-Cys
RING-CH (C4HC3)	Cys-X-Cys-$X_{(9-39)}$-Cys-$X_{(1-3)}$-Cys-$X_{(2-3)}$-His-X_2-Cys-$X_{(4-48)}$-Cys-X_2-Cys
C2H2C4	Cys-X-Cys-$X_{(9-39)}$-His-$X_{(1-3)}$-His-$X_{(2-3)}$-Cys-X_2-Cys-$X_{(4-48)}$-Cys-X_2-Cys
C4H4 (Cnot4)	Cys-X_2-Cys-$X_{(9-39)}$-Cys-$X_{(1-3)}$-Cys-$X_{(2-3)}$-Cys-X_2-Cys-$X_{(4-48)}$-Cys-X_2-Cys
RBX1	Cys-X_2-Cys-$X_{(9-39)}$-Cys-$X_{(1-3)}$-His-$X_{(2-3)}$-Cys-X_2-Cys-$X_{(4-48)}$-Cys-X_2-Asp

Figure 1.6. The RING zinc finger fold. **(A)** Schematic representation of the canonical cross-brace RING finger domain and **(B)** variations on the canonical RING finger sequence. C and H are the single letter codes for cysteine and histidine respectively. Less conserved primary protein sequence is represented by a solid black line whilst co-ordinating bonds between amino acid side chains and the chelated Zn^{2+} ion are shown as dashed lines in **(A)**. Variations from canonical Cys and His residues are highlighted by red font in **(B)**.

1.4.4.2.2. The RING domain and ubiquitination

The first evidence of a RING domain-containing protein participating in the process of ubiquitination was reported for Rad18, which promoted ubiquitination of histone H2B in yeast (Bailly, Lauder et al. 1997). Subsequent studies categorically demonstrated that the RING domain binds to E2-conjugating enzymes to promote the direct transfer of Ub-moieties from E2 to substrate (Zheng, Wang et al. 2000; Brzovic, Keeffe et al. 2003). Functional activity for a large proportion of RING-domain containing proteins has been reported indicating that most E3-RING proteins possess ubiquitination activity (Deshaies and Joazeiro 2009). However, there is increasing evidence that some E3-RING proteins may not possess such intrinsic ubiquitin ligase activity. The BARD1, BMI1, and MDMX E3-RING proteins do not exhibit ubiquitin ligase activity in complex with E2 enzymes, but function to stimulate or enhance the ubiquitination activity of their hetero-dimeric E3-RING partners BRCA1, RING1B, and MDM2, respectively (Hashizume, Fukuda et al. 2001; Linares, Hengstermann et al. 2003; Wang, Wang et al. 2004).

1.4.4.2.3. Family Diversity

In total 318 RING domains are currently annotated in the human genome, arising from a total of 308 individual genes ((Rheinbach 2005; Li, Bengtson et al. 2008; Markson, Kiel et al. 2009) and personal communication Jonathan Woodsmith). Previous bioinformatic analyses show that the majority of E3-RING proteins (> 75%) are annotated for at least one of > 65 different domain types outside of their RING domain (Li, Bengtson et al. 2008). The diversity of domain architecture is similarly reflected by use of the Pfam domain batch analysis tool (Finn, Mistry et al. 2009), Human Protein Reference Database (HPRD; (Prasad, Kandasamy et al. 2009)), and transmembrane domain prediction server (TMHMM; (Krogh, Larsson et al. 2001)).

In total, over 1000 individual domains were identified, belonging to 275 distinct Pfam families for the complement of E3-RING proteins. These domains are implicated in diverse processes including membrane anchoring, catalytic and kinase functions, and DNA and protein binding (For a full list of domains see Supplementary File E3RING annotation). The variety of domains observed for the E3-RING proteins is consistent with the proposed pleiotropic role of ubiquitin/Ubl conjugation in cellular physiology and reflects the variety of substrates and mechanisms involved for substrate recognition and for roles outside of ubiquitination.

Sequence homology and domain architecture has been used to define subfamilies of E3-RING proteins. The largest E3-RING subfamily is the tripartite motif (TRIM) subfamily which contain ~ 1/4 of the predicted 308 family members and are characterized by the presence of a RING, B-box and coiled coil domain. The 14 members of the RING-between-RING (RBR) make up the second largest subfamily and exhibit two RING domains separated by an in-between RING (IBR) structural domain. Strikingly, the largest number of a single annotated domain within the E3-RING family is the transmembrane region with 144 domains annotated between 53 E3-RING proteins.

1.4.5. Transmembrane E3-RING proteins

1.4.5.1. Family diversity

Domain architecture varies dramatically amongst TM-E3-RING family members, which contain between 1 and 14 transmembrane domains located either N- or C-terminal to the RING domain (Figure 1.7A). Pfam analysis identified 31 TM-E3-RING proteins that are annotated as possessing only RING and TM domains with a further 22 TM-E3-RING s having one or more additional domains (Figure 1.7A&B).

A

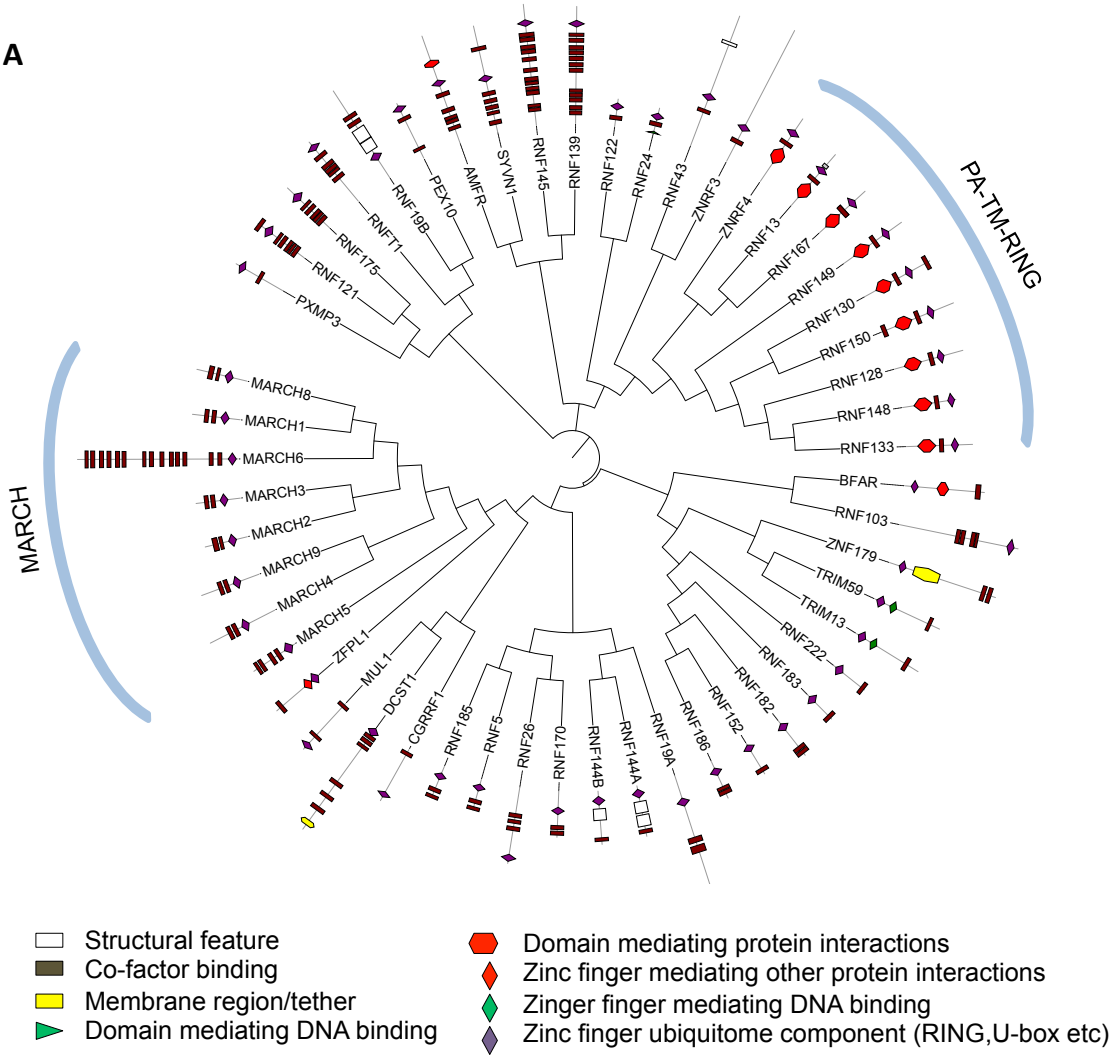

B

Domain	Description	TM E3 RINGs
RING	Protein-protein interaction	All (53)
TM	Membrane anchoring	All (53)
PA	Protein-protein interaction	PA-TM-RING family (9)
IBR	Structural feature	RNF19B, RNF144A, RNF144B, RNF217 (4)
zf-B_box	Unknown	TRIM13, TRIM59 (2)

Figure 1.7. The TM-E3-RING protein family and domain architecture. (A) Dendrogram and schematic representations of TM-E3-RING domain architecture**.** Each TM-E3-RING is represented by official gene symbol and ordered based on a basic primary sequence alignment in CLUSTALW. Figure generated using ITOL (Letunic and Bork 2007). **(B)** Protein domains which are present in ≥ 2 TM-E3-RING proteins.

Outside of the RING and TM region the most commonly occurring domains are PA (nine), IBR (four), and zf-B_box (two) domains (Figure 1.7B).

TM-E3-RING proteins are distributed throughout the phylogeny of E3-RING sub-families suggesting a potential broad range of functions in ubiquitination events (Figure 1.8). Despite the diverse distribution, several TM-E3-RING proteins do cluster into distinct sub-families, which are characterised by the presence of distinct domains or features. For example, each of the eleven MARCH E3-ligase family contain an N-terminal variant RING (vRING; C3HC4) domain and most commonly 2 C-terminal TM regions, yet four (MARCH5), thirteen (MARCH6), and zero (MARCH7 and MARCH10) TM regions are also predicted (Figure 1.7 & 1.8).

A second TM-E3-RING family consists of nine members which share an N-terminal protease associated (PA) domain, TM region, and C-terminal RING-H2 (C2H2C3) domain, with the exception of RNF130, which contains an additional C-terminal TM region (Figure 1.7 & 1.8). The PA domain is proposed to function as a protein–protein interaction domain (Mahon and Bateman 2000). In addition to these families, there are a number of other closely related TM-E3-RING proteins belonging to the TRIM (TRIM13 and TRIM59) and RBR (RNF144A, RNF144B, RNF19A, RNF19B) E3-RING subfamilies.

1.4.5.2. Known roles of TM-E3-RING proteins

The emergence of a large cohort of human TM-E3-RING proteins may underlie a requirement of a range of selective ubiquitination events at cellular membranes. Consistent with this proposal, TM-E3-RING proteins have been shown to mediate a range of cellular functions such as membrane transport, receptor internalisation and

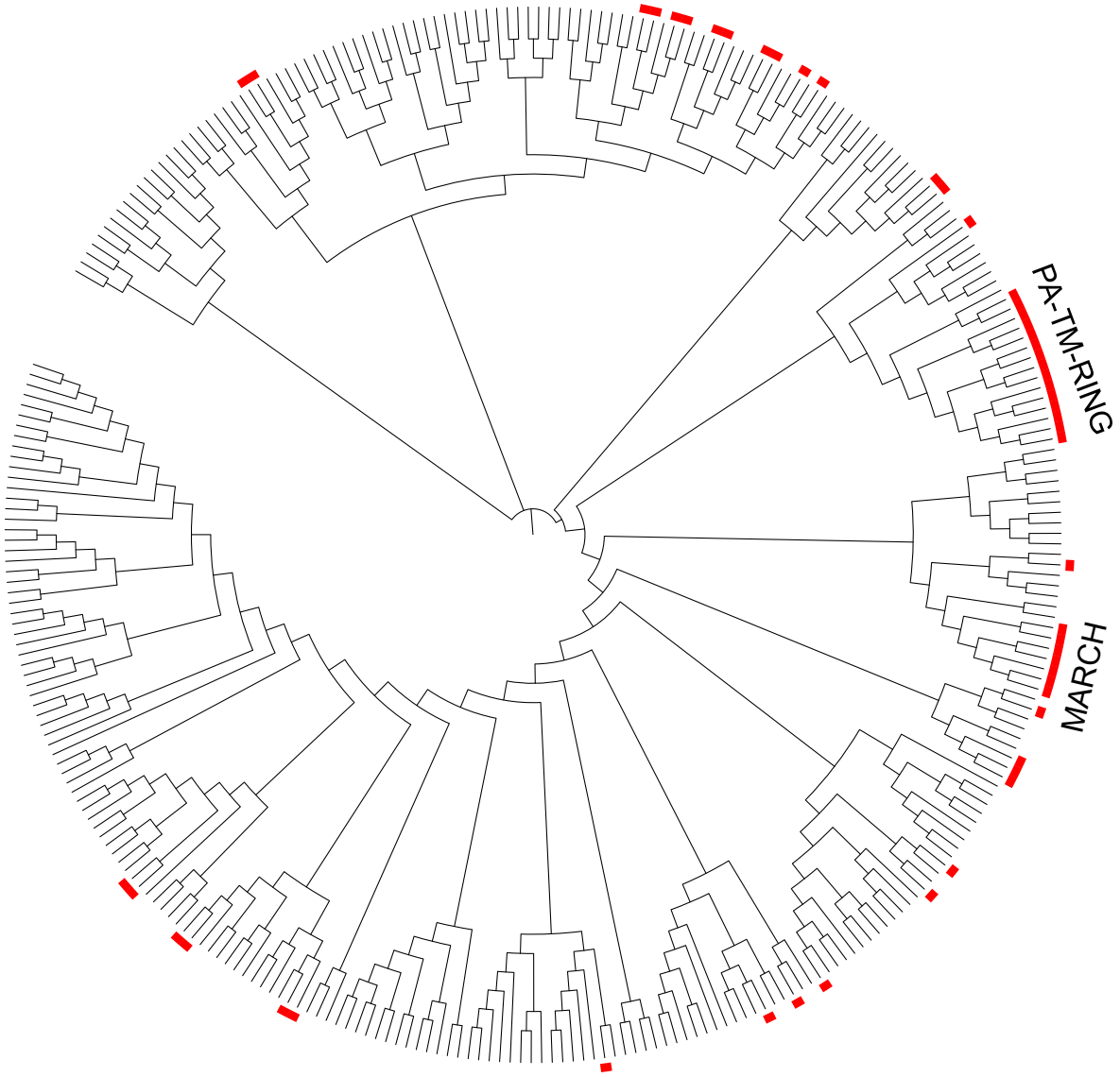

Figure 1.8 Dendrogram of the human E3-RING ligase family showing the diverse distribution of TM-E3-RING proteins within the protein family. Proteins are ordered by primary protein sequence alignment in CLUSTALW. TM-E3-RING are indicated by red bars. The PA-TM-RING and MARCH families of TM-E3-RING proteins are annotated. Figure generated using ITOL (Letunic and Bork 2007). A high-resolution image with gene symbols annotated can be found in Supplementary File E3RING_dendrogram.

other organelle-specific processes including ER-associated degradation (ERAD) and mitochondrial fission/fusion.

Overexpression of several MARCH proteins down-regulates cell surface immunoreceptors such as MHC Class I (Bartee, Mansouri et al. 2004), MHC Class II (Ohmura-Hoshino, Matsuki et al. 2006), CD86 and ICAM1 proteins (Hoer, Smith et al. 2007). In particular, MARCH1 and MARCH8 promote ubiquitination of cell surface MHC II receptors, initiating their internalisation and endolysosomal degradation (Ohmura-Hoshino, Matsuki et al. 2006; Matsuki, Ohmura-Hoshino et al. 2007). Recently these proteins have been shown to target other proteins which are internalized by clathrin-independent endocytosis (CIE) (Eyster, Cole et al. 2011). Alternative roles in intracellular trafficking have been reported for MARCH2 and MARCH3 with overexpression resulting in redistribution of TGN46, a trans-Golgi Network (TGN) marker, presumably through the recognition and ubiquitination of syntaxin 6, which is important for recycling of endosomes to the TGN (Fukuda, Nakamura et al. 2006). Finally, the mitochondrial MARCH5 protein plays a key role in mitochondria organelle dynamics through recognition of proteins involved in mitochondrial fusion (MFN2) and division (Dpn1) (Nakamura, Kimura et al. 2006).

PA-TM-RING family members also have diverse roles in cellular events. RNF128 (gene related to anergy in lymphocytes/GRAIL) represents one of the most extensively studied human PA-TM-RINGs and has reported roles in mediating T-cell anergy, a state of unresponsiveness following antigen challenge (reviewed in (Whiting, Su et al. 2011)). RNF128 utilises the extracellular PA domain to capture CD80 and CD40L integral membrane proteins for RING-mediated ubiquitination within the cytosol (Lineberry, Su et al. 2008). RNF13 has been implicated in cellular

proliferation events with overexpression suppressing cell proliferation in response to extracellular ligands (Zhang, Wang et al. 2010). RNF13 has been proposed to have a key role in nuclear signaling; activation of PKC signaling by Phorbol myristate acetate (PMA) leads to a redistribution of RNF13 from endosomes to the inner nuclear membrane, positioning the RING domain in the nucleoplasm (Bocock, Carmicle et al. 2010).

A well-characterized role of several TM-E3-RING proteins is the degradation of misfolded proteins within the ER in a process termed Endoplasmic Reticulum Associated Degradation (ERAD). In a typical cell one third of all synthesised proteins are predicted to enter the secretory pathway (Nyfeler, Michnick et al. 2005). The ER represents the major entry point for secretory pathway proteins, which are imported into the ER in an unfolded state through the Sec61αβγ protein translocation complex (reviewed in (Mehnert, Sommer et al. 2010)). Following import, nascent polypeptides are folded and post-translationally modified by attachment of sugar moieties and/or formation of disulphide bond linkages to aid folding. ER quality control (ERQC) machinery supports protein biogenesis by retaining misfolded polypeptides to allow further folding (Mehnert, Sommer et al. 2010). Polypeptides that remain in an inappropriate conformation are ubiquitinated, which acts as a signal to undergo retrograde transport into the cytoplasm for proteolysis (Mehnert, Sommer et al. 2010). The TM-E3-RING proteins AMFR (Chen, Mariano et al. 2006) and SYVN1 (Burr, Cano et al. 2011) have been extensively studied in this process leading to the identification of numerous substrates. In addition, a growing number of TM-E3-RING proteins (RNF5, MARCH6 (TEB4), TRIM13 (RFP2), RNF103 (Kf-1), RNF139 (TRC8), and ZNRF4) have also been implicated in ERAD events, although more limited numbers of substrates have been

identified for these TM-RING proteins. Furthermore, recent subcellular analysis revealed 24 of the 53 TM-E3-RING proteins co-localised with the ER resident proteins calnexin or calretinin (Neutzner, Neutzner et al. 2011), suggestive of potential roles of even more TM-E3-RING proteins in ERAD processes.

Finally, TM-E3-RING proteins also participate in a number of specific cellular processes such as the negative regulation of apoptosis (BFAR; (Roth, Kermer et al. 2003)) and control of mitochondrial protein synthesis through recognition of stop codons and peptide release mechanisms in yeast (ZNF179; (Kutner, Towpik et al. 2008))

1.4.6. Deubiquitinating (DUB) enzymes

In analogy to other post-translational modifications such as phosphorylation, ubiquitination is a dynamic and reversible process. In humans, the de-conjugation machinery is composed of 79 active deubiquitinating (DUB) enzymes, which can be divided into five families: ubiquitin C-terminal hydrolases (UCHs), ubiquitin-specific proteases (USPs), ovarian tumour proteases (OTUs), Josephins or Machado-Joseph Disease (MJDs), and Jab1/MPN/MOV34 metalloenzymes (MPNs, also known as JAMMs) (Komander, Clague et al. 2009). DUB enzymes function to: (i) cleave expressed Ub-fusions to generate the ‘free’ ubiquitin pool for conjugation; (ii) remove mono- or poly-ubiquitin from post-translationally modified substrates; (iii) edit the form of ubiquitin modification by trimming of ubiquitin chains (Komander, Clague et al. 2009).

1.5. Protein interactions within the ubiquitin system

The interactions that occur between the constituents of the ubiquitin conjugational machinery confer a high level of complexity and specificity to ubiquitin and Ubl

systems. As such, defining these interactions and the molecular mechanisms underlying them has been intensively studied and has provided insight into the specificity of ubiquitin and Ubl conjugational events.

1.5.1. Ub/Ubl and E2 protein selection by E1-activating enzymes

In addition to their fundamental roles in the initiation of conjugational cascades, E1 activating enzymes establish specificity of Ub/Ubl cascades by selectively binding and matching individual Ub/Ubl moieties with E2 proteins (Table 1.1). The molecular determinants underlying the specificity of E1 enzymes for certain Ub/Ubl moieties are best described for the ubiquitin (UBA1) and NEDD8 (UBA3) E1-activating enzymes. Both E1 enzymes establish selective positive interactions with a single C-terminal tail residue in their cognate Ub/Ubl protein; UBA1 contacts Arg72 of ubiquitin and UBA3 contacts Ala72 of NEDD8. Additionally a unique arginine residue in UBA3 repels ubiquitin moieties to prevent mis-loading (Walden, Podgorski et al. 2003; Lee and Schindelin 2008; Souphron, Waddell et al. 2008).

The interactions that occur between E1 and E2 proteins in each of the Ub, NEDD8, SUMO, and ISG15 cascades are predominantly mediated via hydrophobic interaction surfaces. A Ubiquitin Fold Domain (UFD) within the E1 contacts N-terminal sequences within the E2-UBC domain. The substitution of the UFD domain of UBA6 with UBA1, or the N-terminal UBC-domain sequences of UBE2L3 with that of UBE2L6 alters E1/E2 binding preferences, highlighting the importance of these regions for binding and selectivity (Huang, Walden et al. 2004; Durfee, Kelley et al. 2008). Pathway-specific E1/E2 interactions also exist; N-terminal extensions of the UBE2M and UBE2F proteins form positive interactions with a groove exclusive to UBA3 conferring specificity for NEDD8 conjugation and preventing mischarging with

the non-cognate Ub protein (Huang, Ayrault et al. 2009). Similarly, unique residues in UBA1 (Ub-E1) and UBA2 (SUMO-E1) near their catalytic cysteine residues have also been implicated in their selective binding to cognate E2 proteins and also selects against mischarging with an inappropriate Ub/Ubl protein (Schulman and Harper 2009).

The binding of multiple E2s to any given E1 is a requisite given the increase in their numbers (37 catalytically active E2) compared to E1s. The structural characterisation of UBE2M and UBE2F usage by the sole NEDD8 hetero-dimeric E1 enzyme, NAE1-UBA3, has demonstrated how pliability in the hydrophobic E2 interaction surface allows for recruitment of multiple E2 proteins by a single E1 (Huang, Ayrault et al. 2009).

1.5.2. E2-conjugating enzyme/E3-RING protein interactions

1.5.2.1. Canonical E2/E3-RING binding

To form active ubiquitin ligase complexes E3-RING proteins must selectively interact with E2-conjugating enzymes. E3-RING/E2 interactions reported to date are predominantly weak and transient in nature, typically in the low micromolar range (E.g. UBE2N/TRAF6 K_D=1.2μM (Yin, Lin et al. 2009); UBE2D3/BMI1-RING1B, $K_D \approx 7$ μM (Bentley, Corn et al. 2011)). Structural studies of E1/E2 and E2/E3 complexes have revealed that E1 and E3 binding sites on E2 conjugating enzymes partially overlap, and that these binding events are mutually exclusive (Eletr, Huang et al. 2005). The necessity of E2 discharge from E3-RING proteins to allow recharging with a Ub/Ubl moiety may underlie the low affinity of binding reported for E2/E3 protein pairs.

Despite the weak affinity of E2/E3-RING interactions a limited number of crystal structures have been obtained for this class of interaction, which have revealed key binding determinants in both E3-RING and E2 proteins. From the E2 perspective, the crystal structure determination of UBE2L3 (also called UBCH7) in complex with c-CBL or E6AP identified the Ubiquitin Conjugating domain (UBC) as the major interaction surface for both RING and HECT-type E3 ligases, respectively (Huang, Kinnucan et al. 1999; Zheng, Wang et al. 2000). Subsequent structural and NMR studies of several E3-RING/E2 complexes (E.g. UBE2D1/BRCA1 (Brzovic, Keeffe et al. 2003), UBE2D1/CNOT4 (Dominguez, Bonvin et al. 2004), UBE2N/TRAF6 (Yin, Lin et al. 2009), UBE2D3/BIRC3 (Mace, Linke et al. 2008)) have identified residues in Helix 1 (H1) and Loops 1 and 2 (L1 & L2; also referred to as L4 & L7 in literature) of the UBC domain as providing major contact points for E3-RING partners (Figure 1.9A&B).

From the E3 perspective, the crystal structures of the UBE2L3/c-CBL and subsequent E2/E3-RING complexes identified a shallow groove between the E3-RING's two Zn^{2+}-chelating loop regions and the helix connecting the first and second Zn^{2+} co-ordination site as forming critical contacts for E2 interaction (Figure 1.9 A&B). This surface predominantly consists of a hydrophobic core surrounded by an acidic region. E2 L1 and L2 loops protrude into the shallow groove within the E3-RING and form hydrophobic contacts, which dominate the E2/E3-RING interaction (Zheng, Wang et al. 2000). Mutagenesis of equivalent residues in a number of E3-RING proteins for those important for c-Cbl binding to UBE2L3 (Ile383 and Trp408; Figure 1.9B) ablated almost all interactions detectable via Y2H, highlighting the importance of single residues in contributing to E3-RING/E2 binding (Markson, Kiel et al. 2009). Finally, variable regions immediately N-terminal of the RING domain

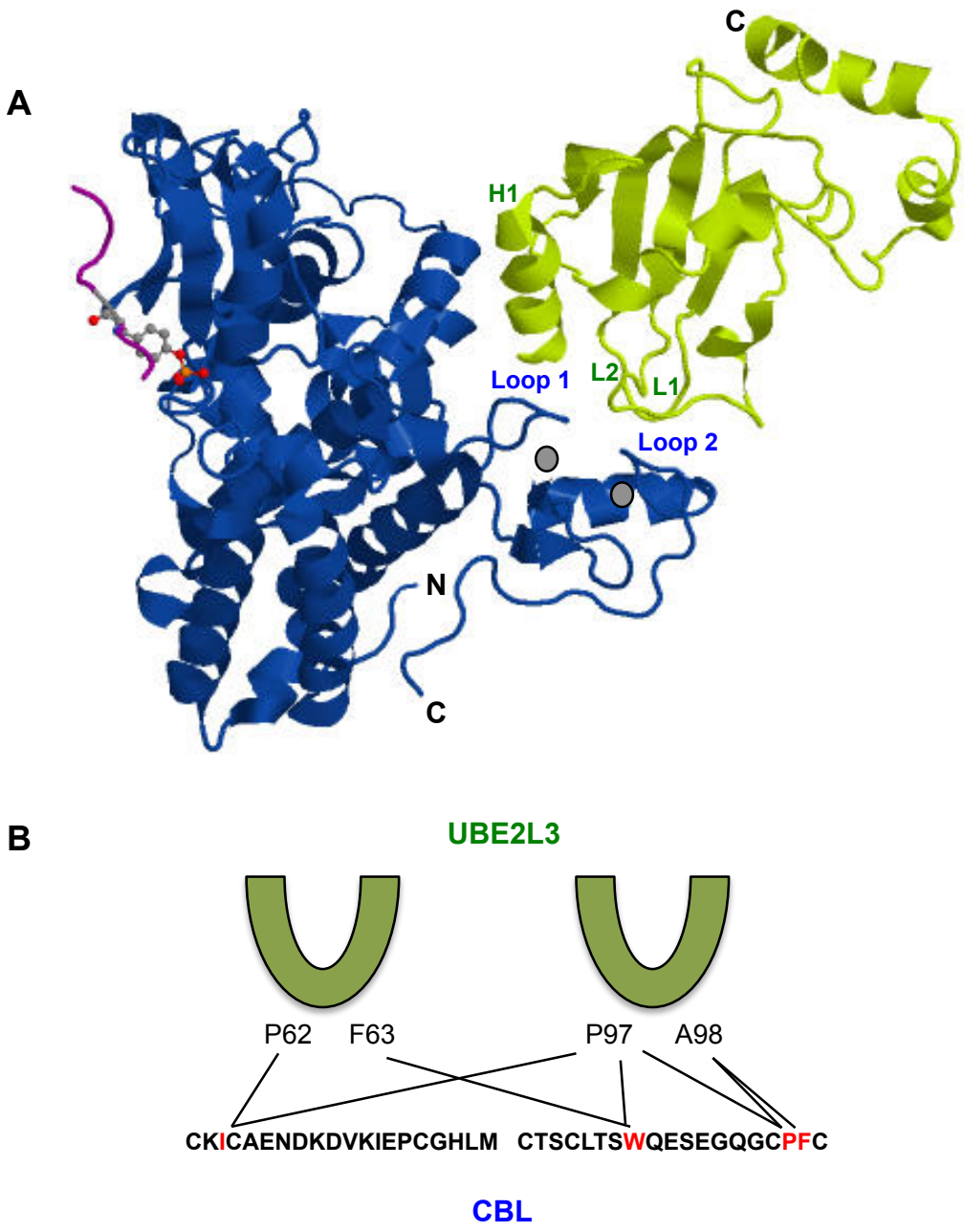

Figure 1.9 E3-RING/E2 interaction surface and contact points. Crystal structure of the E2-conjugating enzyme UBE2L3 (green) bound to the E3-RING ligase CBL (blue) highlighted the key interaction surfaces (PDB Code 1FBV (Zheng et al., 2000)) **(A)** and residues **(B)** involved in E3-RING/E2 binding. Co-ordinated Zn^{2+} ions by the Cbl E3-RING are represented by grey circles in **(A)**.

have also been demonstrated to interact with E2 proteins often via salt bridges with the E2 H1 helix .

Taken together, these findings implicate not only the RING and UBC domains of E3-RING and E2 proteins, but also proximal flanking regions as forming the main interaction surfaces for this class of interaction. Analysis of the growing number of E3-RING/E2 complexes has demonstrated a plasticity of the E2-E3/RING interface, with specific residues within these regions important for formation of different E3-RING/E2 complexes (Wenzel, Stoll et al. 2010).

1.5.2.2. Non-canonical E3-RING/E2 binding

In addition to the canonical E3-RING/E2 interaction surfaces between RING and UBC domains, emerging evidence point towards surfaces outside of these domains as contributing to the formation or stability of E3-RING/E2 complexes. A β-sheet surface opposing the UBC catalytic site and previously reported to form non-covalent interactions with ubiquitin molecules for UBE2D members is important in E3-RING binding to UBE2G2. In this case, the AMFR E3-RING protein utilises a distinct structural UBE2G2-Binding-RING (G2BR) domain ~200 residues from the RING domain, to interact with UBE2G2's β-sheet surface via hydrophobic interactions (Das, Mariano et al. 2009) to increase the affinity of the AMFR/UBE2G2 interaction 50 fold, in comparison to the isolated RING domain (Chen, Mariano et al. 2006). It is plausible that the β-sheet surface of other E2 and UEV proteins could provide an analogous binding site for other E3-RING proteins away from the shared E1/E3 binding site.

Additionally, non-UBC extensions of certain E2 proteins provide interaction binding surfaces for both E3-ligase proteins and substrates. The 37-residue C-terminal extension of CDC34 contains a high density of acidic residues, which reinforces the interaction with the SCF E3-RING complex by forming positive interactions with a basic surface of the CUL1 subunit (Kleiger, Saha et al. 2009). Similarly, the N-terminal extensions of the UBE2E family may form novel interactions with some Cullin-RING-ligases (CRLs) as mutations in canonical E3 and E2 binding sites do not ablate the observed interactions (Plafker, Singer et al. 2009). As such, regions outside the RING and UBC domains of E3-RING and E2 proteins may reflect relevant sites for E3-RING/E2 interactions. In agreement with these findings, comparison of two recent directed Y2H studies revealed a higher rate of E3-RING/E2 interaction detection using full-length E2 clones as opposed to isolated UBC domains with fewer E2 proteins annotated one or more E3-RING interaction partners using UBC domains alone (Markson, Kiel et al. 2009; van Wijk, de Vries et al. 2009).

1.5.3. E3-RING/E3-RING ligase interactions

A limited number of E3-RING proteins have been reported to form dimers to mediate a variety of functions (de Bie and Ciechanover 2011), including recruitment of differential E2 proteins to substrates, auto-ubiquitination of active E3-RING complexes and enhancement of ubiquitination activity of an E3-ligase. Recruitment of differential E2 proteins by hetero-dimeric partners has been demonstrated in yeast whereby the Rad5 E3-RING protein recruits the E2 Rad6 to mono-ubiquitinate its substrate, PCNA. Rad5's hetero-dimeric partner, Rad18, subsequently recruits the Mms2/Uev3 E2 complex to facilitate elongation of K63-linked poly-ubiquitin chains on mono-ubiquitinated PCNA substrates (Parker and Ulrich 2009).

Enhancement of E3-RING ubiquitin ligase activity has been observed for a number of hetero-dimeric complexes including RING1-BMI1 and BRCA1-BARD1 (Buchwald, Stoop et al. 2006; Christensen, Brzovic et al. 2007; de Bie and Ciechanover 2011). In both of these cases one E3-RING recruits E2 enzyme(s) while the second facilitates the efficient ubiquitination of selective substrates (Buchwald, van der Stoop et al. 2006; Bentley, Corn et al. 2011). In addition, both RNF4 and BIRC2 require homo-dimerisation in order to function in ubiquitination events (Mace, Linke et al. 2008; Plechanovova, Jaffray et al. 2011). Recent determination of E3-RING dimerization events by preliminary HTP-Y2H screens within the Sanderson laboratory revealed a high degree of E3-RING dimerization events across the phylogeny of E3-RING proteins with >220 reported interactions (unpublished data; personal communication Jonathan Woodsmith).

Structural studies of several E3-RING homo- and hetero-dimeric partners have highlighted common interaction surfaces responsible for complex formation. For the heterodimer MDM2/MDMX and homodimers, BIRC3 and RNF4, these interaction surfaces predominantly comprise residues in β-strand structures located within and immediately flanking the core RING domain (Linke, Mace et al. 2008; Mace, Linke et al. 2008; Liew, Sun et al. 2010). E3-RING domains therefore perform dual roles in binding both E2 and E3 proteins. For those E3-RING dimers for which both the E2 and E3 binding interfaces have been determined by crystallographic, mutagenesis, or modelling approaches, E2 and E3 interfaces have been shown to reside on distinct surfaces of the three-dimensional RING complex thus allowing both binding events to occur simultaneously.

In addition to these shared binding surfaces, the RNF2/BMI1 and BRCA1/BARD1 hetero-dimers contain additional interaction domains located in larger helical structures outside of the RING domain (Buchwald, Stoop et al. 2006; Christensen, Brzovic et al. 2007). In addition to homo- and hetero-dimerisation, a subset of E3-RING proteins have been reported to form higher order multimeric complexes, which exhibit increased catalytic activity compared to their monomeric subunits (Reymond, Meroni et al. 2001; Kentsis, Gordon et al. 2002; Poyurovsky, Priest et al. 2007). Members of the TRAF E3-RING subfamily have been characterised in the formation of higher order structures using coiled-coil regions to trimerise and RING-domains to dimerise. The TRIM subfamily of E3-RING proteins also utilise coiled-coil regions to homo- and hetero-dimerise, suggesting that this mechanism of regulation is not restricted to TRAF proteins.

Two recent studies have highlighted the importance of E3-RING dimerization for the mechanism and specificity of ubiquitination events (Bentley, Corn et al. 2011; Plechanovova, Jaffray et al. 2011). Computational docking and mutagenesis analysis of the RNF4 homo-dimer in complex with loaded UBE2D1~ubiquitin revealed that upon canonical binding of UBE2D1~ubiquitin to one monomer of RNF4, the thioester-linked ubiquitin extends across the dimer and engages the second RNF4 monomer through ubiquitin's hydrophobic Ile44 patch and a conserved tyrosine residue at the dimer interface. The RNF4 homo-dimer therefore facilitates ubiquitin transfer to substrates by positioning the E2~ubiquitin thioester across the RNF4 dimer and activating the thioester bond for catalysis (Plechanovova, Jaffray et al. 2011). Secondly, the crystal structure determination of a BMI1/RING1B/UBE2D3 complex has demonstrated that whilst E2 recruitment is mediated solely by the RING1B monomer, a basic surface patch unique to the

BMI1/RING1B dimer and provided by both RING domains binds directly to short duplex DNA sequences, with mutation of residues at this surface ablating the selective ubiquitination of H2A. Hetero-dimerization of E3-RING domains can therefore contribute to selection of specific substrates and assist in directing E2s to preferred substrate lysines (Bentley, Corn et al. 2011). Taken together, these findings have challenged the prevailing model of E3-RING proteins as merely 'bridging' proteins by juxtaposing E2 and substrates for ubiquitin transfer.

1.6. Protein interaction networks (PINs)

Physiological processes are regulated by a complex network of interactions occurring between cellular constituents including proteins, metabolites, lipids, and nucleic acids (Barabasi and Oltvai 2004). As such, most proteins do not function in isolation but as components of one or more protein complexes, which in turn regulate selective cellular pathways (Morell, Ventura et al. 2009). Comprehensive knowledge of the protein-protein interactions occurring within a given system is therefore of paramount importance to understanding physiological and pathophysiological processes. The identification of protein-interacting partners for a protein of interest can provide a tool in prediction of protein function according to the 'guilt-by-association' principle whereby the function of an uncharacterised protein can be inferred by the functions of its interaction partners (Oliver 2000), with the caveat that individual proteins may have discrete functions in multiple complexes. Furthermore, protein-protein interactions connect protein complexes involved in disparate cellular processes. The identification of proteins that connect multiple modules or complexes by network analysis approaches can provide an elevated understanding of communication between different biological processes (Cusick, Klitgord et al. 2005). Finally, analysis of biological protein-protein interaction

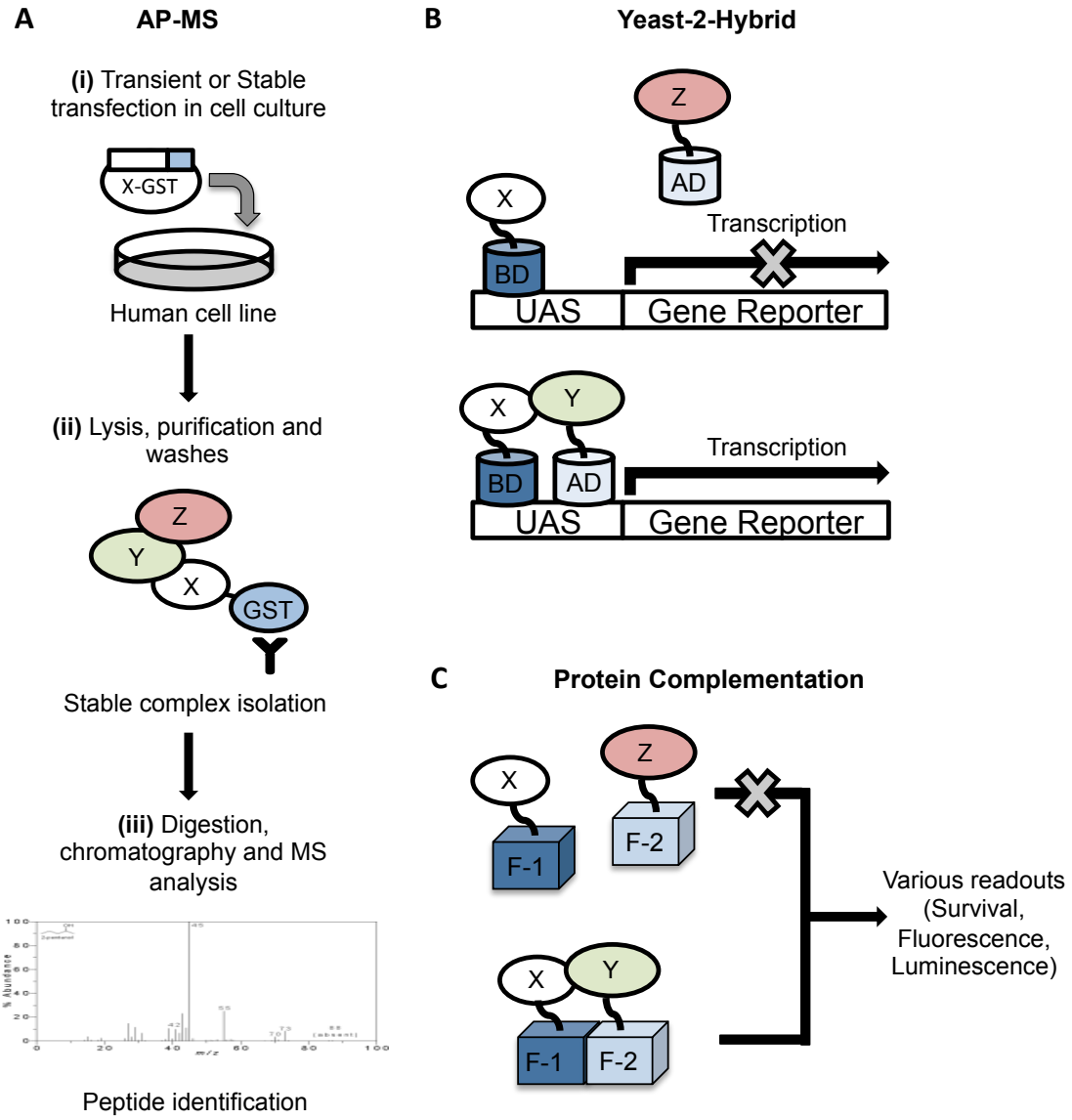

Figure 1.10. Schematic representations of key HTP protein interaction detection techniques. In each case proteins Y and Z represent direct and indirect (co-complex) interaction partners for protein X, respectively. **(A**) **AP/MS**. Transient or stable expression of tagged bait proteins (GST-tagged X) followed by purification and identification of both binary and indirect interacting partners of protein X by MS. (**B) Y2H**. Detection of binary interactions between proteins X and Y through reconstitution of reporter activity. Interaction of fusion proteins reconstitutes transcription factor activity by bringing both binding (BD) and activating (AD) domains to the promoter of reporter genes. **(C) PCA**. Reconstitution of reporter protein (e.g. DHFR, EGFP, Firefly luciferase) upon binary protein-protein interaction allows read-out in various formats depending upon PCA system (Sanderson 2009). F-1 and F-2 represent two fragments of a complete dissected reporter protein.

networks can reveal emergent properties of a given network or the interactome as a whole (Rual, Venkatesan et al. 2005); global analyses of interaction networks have revealed a trend for biological networks to obey a power-law distribution whereby the majority of proteins have few interaction partners with few highly connected proteins, termed hubs. Whilst the biological significance of power law distributions of protein-protein interaction networks have been challenged (Khanin and Wit 2006; Lima-Mendez and van Helden 2009), the removal of hub proteins and 'module-connecting' proteins have however been shown to be more likely to cause the greatest network disruption and be essential gene products in yeast (Jeong, Mason et al. 2001; Yu, Kim et al. 2007).

On a physiological level, protein-protein interactions occur in a spatiotemporal manner within the functional context of the cell. Furthermore, many proteins are predicted to have multiple spliced isoforms, which may have altered protein interaction partners and exert synergestic or even antagonistic functions (Tsai, Ma et al. 2009). Whilst the generation of interaction maps at subcellular and isoform levels will become a necessity to reveal the full complexity of the interactome, it is initially necessary to define interaction partners for the multitude of proteins that still have poorly defined functions. As such, large-scale PPI networks provide new insight into the function of uncharacterised genes and the organisation and interplay between different physiological processes. The integration of secondary datasets such as expression and localization data with binary interaction networks can deliver increased confidence in interaction networks and to define distinct subgroups such as those limited to a given cell type.

1.6.1. Interaction detection methodologies for medium/high throughput screening

At present two main complementary branches of protein interaction analysis have been extensively performed on a HTP or proteome-wide scale. Dissection of protein complexes by affinity purification and mass spectrometry (AP/MS) identifies both directly and indirectly associated proteins (Figure 1.10A). In contrast yeast two-hybrid (Y2H) methods identify only binary, or direct, protein-protein interactions (Figure 1.10B). Split protein complementation assays (PCA) have also recently been utilized in large-scale HTP format to investigate binary protein-protein interactions in eukaryotic systems (Figure 1.10C). In addition, a number of other protein-protein interaction techniques have been employed in increasingly HTP formats, including LUMIER, mammalian protein-protein interaction trap (MAPPIT), membrane yeast-two-hybrid (MYTH) and nucleic acid programmable protein array (NAPPA). In analogy to Y2H, both MAPPIT and MYTH rely on transcription factor activation following protein-protein interaction whilst LUMIER and NAPPA utilise affinity purification of tagged bait proteins and enzymatic activity measurements to deliver readouts of protein-protein interactions.

1.6.1.1. Yeast-two hybrid (Y2H) matrix matings and library screens

The Y2H system was first described by Fields and Song in 1989 as a genetic method to study protein-protein interactions using the model organism *Saccharomyces cerevisiae* (Fields and Song 1989). Transcription factors are modular proteins containing two functionally required domains, which mediate transcription factor binding to DNA promoter regions (BD) and activation of transcription (AD). The separation of BD and AD domains and fusion to the interaction partners SNF1 and SNF4 reconstituted transcription factor activity and reporter gene activation, which could not be observed when isolated BD and AD

domains were co-expressed (Fields and Song 1989) (Figure 1.10B). Since its inception, the Y2H system has been utilised for the identification of interaction partners between predicted or unknown protein pairs. Numerous Y2H systems have been developed to improve both sensitivity and accuracy, including truncation of promoters to reduce protein expression levels and employing more than one reporter gene to reduce the incidence of non-specific activation being reported as true-positive interaction (James, Halladay et al. 1996). Interestingly, it is now clear that Y2H systems which utilise different vectors and yeast strains generate distinct but overlapping protein interaction profiles (Chen, Rajagopala et al. 2010). The use of different Y2H systems can therefore increase the coverage of a given interaction space and enables detection of a broader spectrum of interactions.

There have now been several proteome-wide HTP-Y2H studies and the potential application of Y2H screens for human proteome-wide interactome mapping has been demonstrated by two major studies. Initially, the matrix testing of ~7200 human full-length ORFs identified 2754 positive protein interactions (Rual, Venkatesan et al. 2005). Secondly, Y2H arrays generated from a human foetal brain cDNA library and a collection of full-length ORFs identified 3156 positive protein interactions (Stelzl, Worm et al. 2005). Combined, these two datasets identified over 5900 protein interactions, a large proportion of which were novel (Rual, Venkatesan et al. 2005; Stelzl, Worm et al. 2005).

Recently, two focused medium-scale Y2H studies systematically assessed the interactions that occur within the human ubiquitin system, between E2 conjugating enzymes and E3-RING proteins (Markson, Kiel et al. 2009; van Wijk, de Vries et al. 2009). Together, these studies have contributed to a higher-density E3-RING/E2

interaction map, delivering new insights into the combinatorial nature of the human ubiquitin system.

Advantages of Y2H systems:

1) Using *S.cerevisiae* as a model organism allows for very large numbers of protein coding sequences to be assayed quickly in a cost-effective and relatively simple manner.
2) The *in vivo* nature of the Y2H assay provides advantages over *in vitro* assays. A recent comparative analysis revealed five of eight phosphorylation-dependent interactions were detectable within Y2H screens suggesting that some post-translational modification dependent interactions can be detected (Chen, Rajagopala et al. 2010).
3) A broad range of interaction affinities can be detected. Interactions with a dissociation constant (Kd) > 70μM can be detected (Yang, Wu et al. 1995). This is not true for many other binary interaction assays, which fail to detect many weak or transient interactions.

Disadvantages of Y2H systems:

1) Interactions involving full-length proteins which contain transmembrane regions are found comparatively less often than by other methods (Rual, Venkatesan et al. 2005).
2) Human proteins are not in their native cellular environment and binding occurs within the yeast nucleus, which may not be the site of endogenous interactions.
3) Cooperative binding cannot be assessed in traditional Y2H systems as only two proteins are tested at any one time.

1.6.1.2. Affinity purification and mass spectrometry

Co-affinity purification and mass spectrometry (MS) represents the prevailing strategy for detection of stable protein complexes, which can be purified from cells (Poetz, Hoeppe et al. 2009). Typically, affinity tags are fused to a protein of interest (bait) enabling affinity-purification with an epitope-specific antibody or column. Protein complexes are separated by column or polyacrylamide gel electrophoresis methods prior to trypsin digestion. Peptide samples are subsequently ionized by laser pulses and the mass-to-charge ratio (m/z) of each composite peptide fragment measured by mass spectrometry. The m/z ratio values provide a 'peptide-mass fingerprint' that can be correlated with reference peptide MS sequences in online databases. This technique has been used in human cells utilizing tagged baits within transient expression systems on a HTP scale with 338 disease-associated bait proteins yielding ~6500 interactions between >2000 distinct proteins (Ewing, Chu et al. 2007). Additionally, this technique has been performed using stable cell lines in more directed studies for example to define the interaction landscape for the family of DUB enzymes, identifying ~770 candidate interaction partners for 75 DUBs (Sowa, Bennett et al. 2009).

Recently, mass spectrometry technologies targeting the ubiquitin system have focussed upon analysing the ubiquitinated proteome in both yeast (Peng, Schwartz et al. 2003) and human cells under basal conditions and following induction of **E**pidermal **G**rowth **F**actor (EGF) signalling (Argenzio, Bange et al. 2011).

Advantages of AP/MS systems:

1) Enables the unbiased study of a vast array of proteins simultaneously *in vivo*.
2) Identifies functional protein complexes that may be dependent on multiple

protein components.

3) Proteins can be expressed in the context of their normal cellular environment and correct localisation and in some cases at endogenous expression levels.
4) Proteins are subject to their appropriate post-translation modifications such as phosphorylation and ubiquitination (reviewed in (Choudhary and Mann 2010)).
5) Tandem MS/MS enables the assessment of post-translational modifications of peptide sequences, and identification of ubiquitin chain linkages upon modified substrates (reviewed in (Kirkpatrick, Denison et al. 2005)).

Disadvantages of AP/MS systems:

1) Proteins that exhibit weak binding affinities are likely to avoid detection due to dissociation during washing steps.
2) Discrimination between direct and indirect protein-protein interaction partners is not possible.
3) Reduced ability to detect membrane proteins due to solubility/extraction problems and reduced ionization of resulting peptides (Eichacker, Granvogl et al. 2004).
4) Detects a snapshot of potential interactions in a given cellular context and will therefore likely have a degree of false negative interactions.
5) AP/MS systems are more technically demanding and incur higher costs compared to the relatively simple and cheap Y2H interaction assay.

1.6.1.3. Protein complementation assays (PCA)

Protein complementation assays (PCA) operate on the principle that two separated fragments of a reporter protein will spontaneously refold into their native

conformation when brought into close proximity by the binary interaction of fused interacting protein pairs (Morell, Ventura et al. 2009) (Figure 1.10C). This reconstitution strategy has been successfully employed in the reassembly of several reporter genes including dihydrofolate reductase (DHFR), Firefly/Renilla luciferase, and fluorescent proteins (EGFP and its spectral variants) (Morell, Ventura et al. 2009). As such, the experimental read-out varies depending upon the PCA system used, but these include: fluorescence (E.g. EGFP); luminescence, (E.g. Firefly luciferase), survival (E.g. DHFR) or colorimetric (E.g. Beta-Lactamase, DHFR), assays.

A recent proteome-wide protein-interaction study covering 93% of all *S.cerevisiae* ORFs utilised DHFR as a survival readout to identify ~ 2770 interactions amongst > 1100 proteins. The DHFR screen demonstrated high correlation (16-41%) with previous interactions from large-scale Y2H and AP/MS screens and identified a large number of novel protein pairings, thus highlighting the complementary nature of data from different interaction technologies (Tarassov, Messier et al. 2008). The survival readouts of the DHFR PCA system offer many of the same advantages and disadvantages as described for the Y2H assay, whilst also allowing for interactions of soluble and integral membrane proteins in yeast at appropriate subcellular localisations.

Advances in technologies such as retroviral vectors to efficiently activate and tag host genes within cDNA libraries have recently enabled the characterisation of protein interaction partners on a large-scale in mammalian cells. For example, a YFP-based fluorescent complementation assay was recently employed to systematically test 6 telomere-associated proteins for interaction partners against

12212 prey proteins, identifying ~300 interaction partners providing a high-resolution map of the telomere interactome (Lee, Kim et al. 2011).

Luciferases form a family of proteins that emit light following oxidation of bioluminescent substrates. The *Photinus pyralis* (Firefly) luciferase enzyme was the first to be adapted for protein complementation assays, with reconstitution of enzymatic activity upon the interaction of fusion proteins MyoD and Id proteins (Paulmurugan, Umezawa et al. 2002). Since the initial description of a Firefly luciferase PCA system, a number of luciferases have been similarly adapted for PCA-based interaction detection including *Renilla reniformis* (Paulmurugan and Gambhir 2003), and *Guassia princeps* (Remy and Michnick 2006). Split-luciferase based systems exhibit very low background luminescence and higher sensitivity compared to other split fluorophore-based PCA techniques, which require exogenous illumination, which can 'bleach' signal and contribute to higher background signals (Massoud and Gambhir 2003). Additionally, the faster folding of split luciferase fragments and the reversible nature of luciferase reconstitution have culminated in the use of this system in the evaluation of protein-protein interactions in both living cells and whole organisms (Hida, Awais et al. 2009).

Advantages of mammalian PCA systems:

1) Proteins are expressed in the context of their normal cellular environment enabling correct localisation and appropriate post-translational modifications.
2) Transmembrane-domain containing proteins can be localised to their appropriate subcellular compartment.
3) Protein pairs that exhibit a broad range of interaction affinities can be detected within PCA methodologies. Interactions can be detected for

interactions with dissociation constants in the micromolar range and above (Magliery, Wilson et al. 2005; Morell, Espargaro et al. 2007)

4) Fluorophore-based, and to a limited extent split-luciferase-based, PCA systems can now provide spatial and temporal annotation to protein-protein interactions (Ding, Liang et al. 2006; Stefan, Aquin et al. 2007).
5) Reversible nature of split-luciferase reconstitution allows for investigation of the dynamics of protein-protein interactions and conditional or signal dependent interactions in mammalian cells (Hida, Awais et al. 2009).

Disadvantages of mammalian PCA systems:

1) Cooperative binding cannot be assessed in traditional PCA systems as only two proteins are tested at any one time.
2) PCA-based systems are more technically demanding and incur higher costs compared to the relatively simple and low-cost Y2H interaction assay.

1.6.1.4. Comparative analysis between interaction detection techniques

Each protein-protein interaction methodology will have inherent limitations that dictate the potential interaction space covered by individual methods. Each protein-protein interaction system utilises different protein tags in distinct *in vivo* or *in vitro* environments and variable interaction read-outs and stringencies. As such, it is perhaps unsurprising that early comparisons of AP/MS, Y2H, and literature curated protein-protein interactions screens exhibited only modest overlap in reported interactions (Yu, Braun et al. 2008). Comparative analyses of data obtained from independent orthogonal assays have highlighted the utility of using data from multiple experimental methodologies to obtain higher coverage of interaction

partners across common clone sets (Braun, Tasan et al. 2009; Rajagopala, Hughes et al. 2009; Chen, Rajagopala et al. 2010).

A recent comparative analysis of a gold-standard interaction dataset using five distinct techniques (Y2H, LUMIER, MAPPIT, MYTH, and NAPPA) verified ~60% of the total positive reference dataset yet each of five distinct techniques reconfirmed only 21-36% of known binary protein pairs (Braun, Tasan et al. 2009). When tested against a random reference clone set to assess potential false positive discovery rates, each assay reported a < 5% false discovery rate. Significantly, investigation of the same positive and negative reference datasets in five independent Y2H systems revealed differential Y2H approaches to have overlapping but distinct interaction coverage providing an equivalent level of specificity and accuracy to that observed using distinctly orthogonal interaction detection systems (Chen, Rajagopala et al. 2010).

These analyses highlight the benefits of utilising multiple protein-protein interaction methodologies to enable maximal coverage of a given interaction space (Braun, Tasan et al.). Furthermore, while the use of orthogonal interaction screens is valuable for assessing systematic bias in any individual assay system, the degree of complementarity between data from different assays stipulates that 'verification' between different assay systems should not be considered absolute and should be based upon a process of increasing confidence through benchmarking.

1.7. Aims of this study

In this chapter the human Ub/Ubl conjugational machinery has been introduced. Furthermore, the combinatorial interactions that occur between constituents of this

conjugational machinery and how such interactions underlie selectivity of ubiquitination events have been discussed. To ascertain the existing coverage of ubiquitin system interactions E3-RING/E2 interactions were extracted from publically available databases and recent HTP-Y2H TM-E3-RING data published by our laboratory to generate a high density network of ~ 700 binary full length E3-RING/E2 protein interactions (Markson, Kiel et al. 2009). As can be seen from Figure 1.11 there exists a key area of data paucity for E3-RING proteins, which contain transmembrane domains (TM-E3-RING protein) with approximately half of all TM-E3-RINGs annotated having no cognate E2 partners. This highlights the necessity for directed interaction studies to address areas of low network density, which remain following proteome-wide studies.

A major drawback of conventional Y2H approaches is that interactions involving full-length proteins that contain transmembrane regions are found comparatively less often than by other methods (Rual, Venkatesan et al. 2005). Y2H systems are based upon the principle that protein interaction mediated reconstitution of an active transcription factor within the nucleus enables the expression of reporter genes (Fields and Song 1989). Furthermore, transmembrane domain containing proteins have a tendency to become insoluble or form aggregates when expressed outside of cellular membranes. Therefore, ORFs encoding full-length transmembrane proteins are poor candidates for interaction detection in these systems. To address the poor coverage of TM-E3-RING/E2 interactions it was proposed that a directed Y2H approach using TM-E3-RING ORF clones encoding the entire cytoplasmic RING-domain (CRD) containing region for each human TM-E3-RING protein would maintain an optimal E2 binding surface whilst overcoming the associated issues of using transmembrane domains in Y2H analyses.

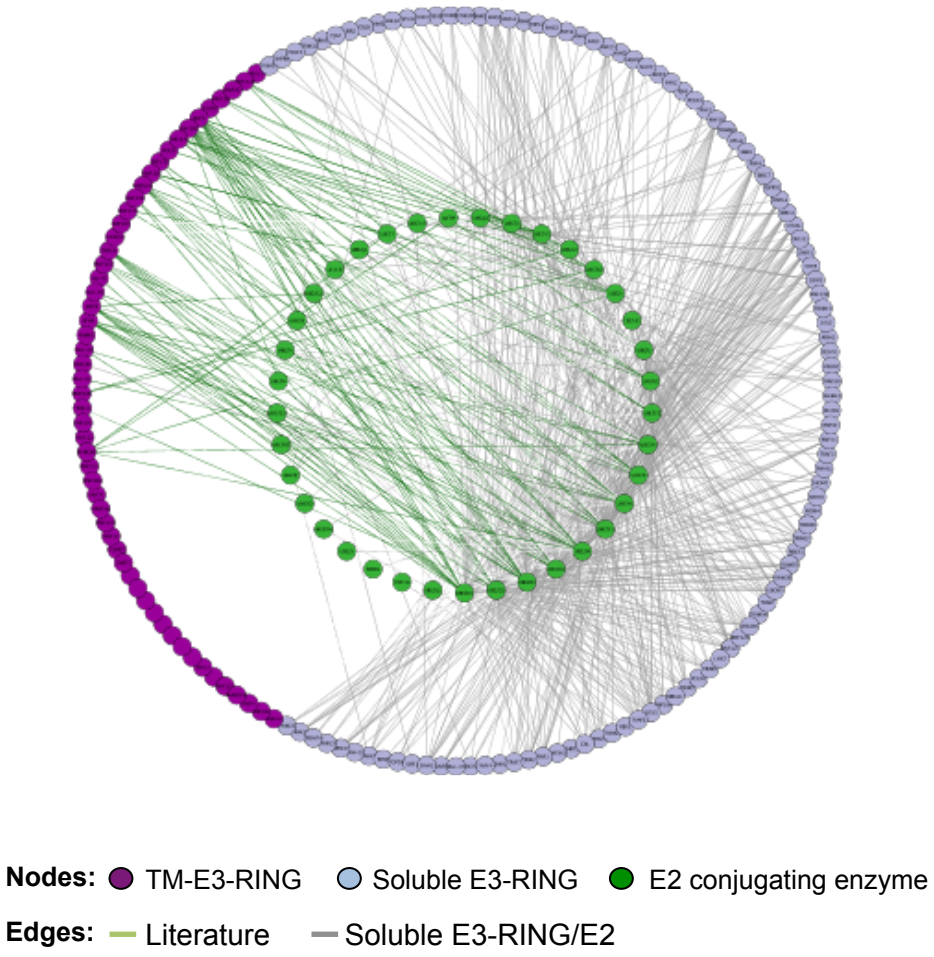

Figure 1.11 Binary TM-E3-RING/E2 interaction network. (A) E3-RING/E2 interaction coverage at the time of initiating the current study with data collated from full-length GAL4 screens (Markson, Kiel et al. 2009) and other literature-derived interaction data. Nodes (circles) represent proteins and edges (lines) represent binary interactions between proteins.

The aims of this study were:

1. To systematically generate comprehensive binary protein-protein interactions maps of human TM-E3-RING/E2 using Y2H as a primary interaction detection method.
2. To validate and extend interaction coverage in secondary protein-protein interaction detection systems.
3. To integrate datasets with publically and commercially available datasets to generate higher coverage TM-E3-RING interaction maps.
4. To investigate the potential functional significances of TM-E3-RING/E2 pairings using *in vitro* ubiquitination assays.

2. Chapter 2: Materials and methods

2.1. Molecular biology

2.1.1. Reagents

Human Brain and Testes Marathon-Ready cDNA libraries were obtained from Clontech (Mountain View, Ca, USA). One Shot ccdB Survival 2 T1R Competent Cells, Gateway® BP and LR reaction kits, the RfB-Gateway® cassette, SybrSafe DNA gel stain and primers were purchased from Invitrogen (Paisley, UK). Human KOD HotStart DNA Polymerase was obtained from Merck Chemicals Ltd (Nottingham, UK). BIOTaq DNA polymerase, α-select chemically competent silver efficiency cells, DNA HyperLadder and Agarose were from BioLine (London, UK). $_{d}$NTPs (100 mM solutions) were from GE Healthcare (Buckinghamshire, UK). Tris/Borate/EDTA buffer (TBE; 10X) was obtained from VWR International Ltd (Lutterworth, UK). Restriction endonucleases, antarctic phosphatase and T4 DNA ligase were obtained from New England Biolabs (Hertfordshire, UK). Wizard® Plus SV Miniprep kits were obtained from Promega (Southampton, UK). QIAfilter^{TM} Midiprep kits and QIAQuick^{TM} DNA purification kits were from Qiagen (Crawley, UK). Tryptone was from Fisher (Loughborough, UK). Yeast extract and BioAgar were from BioGene (Cambridge, UK) and glucose from Formedium (Norfolk, UK). All other chemicals were obtained from Sigma-Aldrich (Poole, UK).

2.1.2. Agarose gel electrophoresis

Agarose gels (0.8% to 1%) were prepared by the addition of electrophoresis grade agarose to 0.5X TBE buffer and heating in a microwave for ~ 2 min or until agarose had dissolved completely. Sybr Safe DNA gel stain was added to cooled agarose/TBE solution at a 1:20,000 dilution to allow visualisation of DNA bands. 1% Orange G buffer (5% w/v sucrose, 0.05% Orange G) was added to PCR products

prior to sample loading and resolving in 0.5X TBE buffer using a horizontal mini-electrophoresis tank (BioLine, UK). DNA HyperLadder (5 µl/well) was loaded alongside DNA samples to facilitate estimation of PCR product base pair size and DNA concentration. DNA bands were visualised using an ultraviolet (U.V.) light source.

2.1.3. Sequencing

Sequencing of DNA constructs was performed by automated fluorescent DNA sequencing at GATC BioTech (London, UK). PCR products amplified from transformed yeast colonies were PCR purified and 5' end sequenced-tagged by automated fluorescent DNA sequencing at GATC BioTech (London, UK) to ensure correct ORF insertion into Y2H vectors.

2.1.4. Bacterial glycerol stocks

Glycerol stocks of transformed bacterial cells were generated from 9 ml 2xTY overnight cultures (plus appropriate antibiotic) inoculated with an individual bacterial colony and incubated for 16 h at 200 rpm, 30 °C. 200 µl samples of individual bacterial cultures were combined with 80 µl 80% autoclaved glycerol in 1.5 ml microfuge tubes and stored at -80 °C.

2.1.5. TM-E3-RING Gene Identifier (ID) acquisition

Initial identification of human E3-RING proteins was performed by interrogation of InterPro (http://www.ebi.ac.uk/interpro) and Human Protein Reference Database (http://www.hprd.org) databases for any human proteins predicted to contain RING-finger domains. Each E3-RING protein was allocated an Entrez Gene ID – uniquely assigned to individual genes by the National Centre for Biotechnology Information (NCBI) – and duplicates removed to generate a non-redundant list of human E3-RING proteins. To identify putative TM-E3-RING proteins, Reference cDNA

Sequences (RefSeq) for isoform 1 of each E3-RING protein were extracted from GenBank and used as query for transmembrane domain prediction using the batch search function of the transmembrane domain prediction server TMHMM (http://www.cbs.dtu.dk/services/TMHMM-2.0/).

Gateway™-compatible nucleotide primer sequences were manually designed using cDNA RefSeq to facilitate PCR amplification of full-length and cytoplasmic RING domain (CRD) TM-RING-E3 ORF clones. Full-length primers were designed from the 5' region ATG start to the penultimate 3' codon to remove STOP codons. CRD-E3 primers were designed to amplify solely the cytosolic RING domain region according to RING and TM domain architecture predicted using the Pfam domain batch analysis tool (Finn, Mistry et al. 2009). Gateway®-compatible 5' and 3' primers typically contained 18-25 gene specific base pairs (bp) and included attB flanking regions to enable Gateway® transfer of PCR-amplified products into the pDONR223 'Entry' vector by a BP reaction. TM-E3-RING ORFs were amplified by high-fidelity HotStart KOD DNA polymerase from either (i) Brain or Testes derived Marathon-ready cDNA libraries, (ii) available yeast constructs within our laboratory or (iii) Mammalian Gene Collection (MGC) I.M.A.G.E. clones.

All PCR reactions were performed using either the MJ Research PTC-200 or PTC-225 Peltier Thermal Cycler (supplied by GRI Ltd, Essex, UK). Size verification and estimation of DNA was performed by analysis of PCR products by agarose gel electrophoresis prior to utilisation in BP recombination reactions.

A

Reagent	µl / reaction	[Conc]
Forward Primer (10µM)	0.5	0.2µM
Reverse Primer (10µM)	0.5	0.2µM
$_{d}$NTPs (2mM)	2.5	0.2mM
KOD Buffer (10x)	2.5	1x
$MgSO_4$ (25mM)	1.5	1.5mM
HotStart KOD	0.5	0.5 U
$_{d}H_2O$	17 – x	-
*Brain/Testis cDNA library	x (0.5-1)	-
**Yeast lysis sol.	x (2)	-
***cDNA clone	x (0.5)	-
Total	25	-

B

Step	Cycles	Temp (°C)	Duration
1	1	95.0	2 min
2	29-39*	95.0	30 secs
		60.0	60 secs
		70.0	30 secs /kb
3	1	4.0	For ever

Table 2.1. KOD HotStart PCR amplification. (A) Reagents and typical concentrations for high-fidelity HotStart KOD PCR reactions. All components were added to a thin walled PCR tube on ice. * denotes cDNA-library PCR, ** denotes YC-PCR, *** denotes MGC cDNA clone PCR. **(B)** Typical PCR thermocycling conditions; annealing temperature (step 2; row 2) varied according to predicted primer Tm to facilitate primer-DNA annealing; extension temperature (step 2; row 3) varied according to template DNA source (YC-PCR was performed for 39 cycles).

2.1.6. TM-RING-E3 ORF amplification from cDNA libraries

The majority (40/53) of TM-E3-RING ORFs obtained during the course of this study were amplified from Brain or Testes Marathon-ready cDNA libraries. PCR reagents and typical concentrations for cDNA library PCR experiments are outlined in Table 2.1 A and typical thermo-cycling conditions are outlined in Table 2.1 B.

2.1.7. TM-RING-E3 ORF amplification from Y2H expression constructs

Seven TM-E3-RING ORF clones were amplified from yeast pACTBE-B clones, previously generated by *in vivo* gap-repair cloning techniques (Semple, Prime et al. 2005; Markson, Kiel et al. 2009). TM-E3-RING ORFs were amplified directly from specific yeast colonies by KOD HotStart DNA polymerase Yeast Colony PCR (YC-PCR) using the Gateway® compatible vector specific primers, A1F and A2R (Supplementary file TMRING Cloning Summary). Initially, yeast colonies were lysed in 10 µl 20 mM NaOH for 20 min and cell debris pelleted by centrifugation at 10,000 rpm for 10 s. 2 µl of supernatant was combined with all other components of YC-PCR mix (Table 2.1A) prior to thermo-cycling (Table 2.1B).

2.1.8. TM-E3-RING ORF amplification from cDNA I.M.A.G.E. clones

Finally, four TM-E3-RING ORFs were amplified from MGC cDNA clones obtained from the Integrated Molecular Analysis Of Genomes And Their Expression Consortium (IMAGE; http://image.hudsonalpha.org). PCR reagents and typical concentrations for PCR experiments using I.M.A.G.E. clones are described in Table 2.1A and typical thermo-cycling conditions are outlined in Table 2.1B.

2.1.9. Gateway® BP reaction to generate Gateway ENTR™ vector

PCR products were combined with the Gateway® vector pDONR223 by BP recombination reactions to generate an ENTR™ vector to enable future shuttling of TM-E3-RING ORFs into Gateway®-compatible expression vectors. BP reaction

components were combined on ice as described in Table 2.2. BP Clonase® enzyme mix was combined immediately prior to incubation of reaction mixtures at 25°C for 16 h. BP recombination reactions were terminated by addition of 0.5 µl Proteinase K enzyme and incubation at 37°C for 10 min.

2.1.10. Gateway® LR reaction to generate Gateway™ expression vector

To rapidly transfer TM-E3-RING ORFs into expression vectors for further study LR reactions were undertaken. LR recombination reaction components were combined on ice as described in Table 2.2. LR Clonase® enzyme mix was added immediately before incubation of reaction mixtures at 25 °C for 16 h. LR reactions were terminated by addition of 0.5 µl Proteinase K enzyme and incubation of samples at 37 °C for 10 min. Gateway® destination vectors utilised within this study are described in the text where appropriate. A schematic representation of the Gateway recombination cloning methodology is shown in Figure 2.1.

BP Reaction	**LR Reaction**	**µl / reaction**
BP Clonase® Enzyme Mix	LR Clonase® Enzyme Mix	2
BP Reaction Buffer	LR Reaction Buffer	2
AttB flanked PCR Product	pDONR223 AttL Entry Construct	x (200ng of PCR product)
AttP pDONR223 Vector	AttR Expression vector	y (200ng of vector DNA stock)
dH_2O	dH_2O	6 -x-y
Total	Total	10

Table 2.2 BP and LR reaction components. All components were added to a thin walled 1.5 ml microfuge tube on ice prior to incubation in a heat block at 25 °C for 16 h.

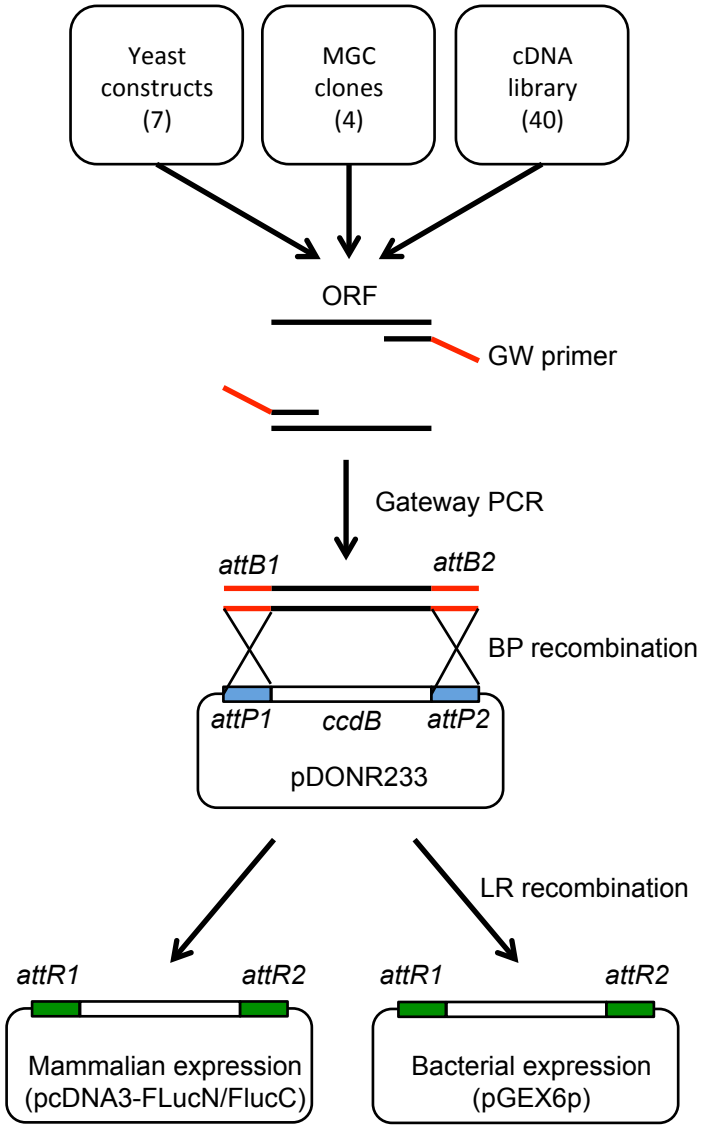

Figure 2.1 The Gateway system. Full-length and CRD TM-E3-RING ORFs were amplified with Gateway primers with 5' (forward) or 3' (reverse) overhangs. Amplified TM-E3-RING ORFs are flanked by the *attB1* and *attB2* sites (in red). This PCR product can be recombined with the *attP1* and *attP2* sites (in blue) on an entry vector (pDONR223) to produce an entry construct flanked by *attL1* and *attL2* sites (not shown) in what is called a BP reaction. This entry construct can be subjected to further recombination with destination vectors (for bacterial or mammalian expression) containing the *attR1* and *attR2* sites (in green) in a Gateway® LR reaction.

2.1.11. Transformation of competent bacterial cells, DNA amplification and purification

BP and LR reaction products were transformed into α-select silver efficiency competent bacterial cells to propagate individual clones and allow generation of DNA stock solutions. Typically, 6 µl BP or LR reaction product was combined with 30 µl α-select cells, which were thawed on ice immediately prior to use. Transformation mixtures were incubated on ice for 30 min prior to heat shock treatment at 42°C for 45 s and incubation on ice for a further 2 min before addition of 200 µl room temperature Super Optimal broth with Catabolite repression media (SOC; tryptone, 2% (w/v); yeast extract, 0.5% (w/v); glucose, 0.4% (w/v); NaCl, 10mM; KCl, 2.5mM; $MgCl_2$, 10mM; $MgSO_4$, 10mM) and incubation for 1 h at 37°C, 220 rpm. 150 µl reaction product was evenly distributed onto 2xTY solid medium (yeast extract, 1% (w/v); BioAgar, 2% (w/v); tryptone, 1.6% (w/v); NaCl, 85mM; plus appropriate antibiotic), using a sterile glass spreader and incubated for 16 h at 37 °C.

Size-verification of ORF inserts was performed by diagnostic Bacterial Colony diagnostic PCR (BCPCR) and agarose gel electrophoresis using BIOTaq™ DNA polymerase and vector specific primers flanking the Gateway®-recombination sites (For a list of Gateway™-compatible primers see supplementary file TMRING Cloning Summary). Reaction components were combined on ice and an individual bacterial colony transferred from 2xTY solid medium to PCR reaction mixture followed by 2xTY liquid media using a sterile toothpick (yeast extract, 1% (w/v), tryptone, 1.6% (w/v), NaCl, 85 mM; plus appropriate antibiotic). For size-verified BC-PCR bacterial colonies, the corresponding 2xTY liquid media was incubated overnight at 37°C, 220 rpm in 9 ml or 25 ml 2xTY liquid media (plus appropriate

A

Reagent	µl / reaction	[Conc]
Forward Primer (10µM)	0.7	0.7µM
Reverse Primer (10µM)	0.7	0.7 µM
$_{d}$NTPs (25mM)	0.25	0.625mM
NH_4 Buffer (10x)	1.0	1x
$MgCl_2$ (50mM)	0.45	2.25mM
$_{d}H_2O$	6.9 - x	-
BIOTaq	0.05	-
DNA	Individual bacterial colony	-
TOTAL	10	-

B

Step	Cycles	Temp (°C)	Duration
1	1	95.0	5 min
2	35	95.0	1 min
		55.0 - 68.0	1 min
		72.0	1 min/kb
3	1	72.0	5 min
4	1	4.0	Forever

Table 2.3. Concentration and reaction conditions for bacterial colony (BC-PCR). A All components were added to a thin walled PCR tube on ice. **B** Typical thermocycling conditions for BC-PCR. The annealing temperature (second segment of step 2) is dependent on the primer pair used, according to primer Tm. The extension step of the polymerase (third segment of step 2) is dependent on the polymerase used and the length of the insert in the vector.

A

$$RfB\ cassette\ DNA\ (ng) = \frac{Vector\ DNA\ (ng)\ x\ RfB\ cassette\ size\ (kb)}{Vector\ size\ (kb)}$$

B

	1:1	**1:3**	**Insert alone**	**Vector alone**
Vector	x µl	x µl	-	x µl
Insert	y µl	3y µl	y µl	-
10x T4 Ligase buffer	1µl	1µl	1µl	1µl
T4 Ligase	1µl	1µl	1µl	1µl
dH_2O	10µl – x – y	10µl – x – y	10µl – x – y	10µl – x – y
Total	10µl	10µl	10µl	10µl

Table 2.4 Ligation reaction using T4 DNA ligase. (A) Formula to calculate appropriate ratios for blunt end ligation. **(B)** Ligation mixtures were set up on ice as indicated. Volumes of vector (y) and insert (x) DNA solutions used varied depending on concentration.

antibiotic) for miniprep or midiprep DNA stock preparation, respectively. Mini- and midi-preps were performed according to manufacturer's instructions. Concentrations of DNA stocks were

estimated by measuring optical density at 260nm wavelength (OD_{260}).

2.1.12. Gateway® destination vectors

Gateway® destination vectors used in this study contain either an N- or C-terminal tag. pEGFP-N2 GW, pcDNA3-myc GW, pGEX6P1 GW were previously available as Gateway®-converted vectors within the laboratory. pcDNA3-FLucC and pcDNA3-FLucN vectors were converted into Gateway®-compatible vectors in house. Briefly, pcDNA3-FLucC and pcDNA3-FLucN split luciferase vectors were digested with

BamHI and XhoI prior to removal of 3' overhangs by T4 DNA polymerase. The 5' ends of blunt end digested vectors were dephosphorylated by incubation with Antarctic Phosphatase according to manufacturer's instructions to prevent re-ligation. Linear pcDNA3-FLucC and pcDNA3-FLucN vectors were blunt-end ligated with the Reading frame B (RfB) Gateway® conversion cassette using T4 DNA ligase at 1:1 and 3:1 RfB Cassette:Vector molar ratios (Table 2.4). Reaction mixtures were incubated for 16 h at 4 °C. For transformation, 2 µl of ligation reaction was used to transform 50 µl OneShot ccdB 2T1 Survival cells. Transformation reactions were evenly spread onto 2xTY solid medium containing Ampicillin (100 µg/ml) and Chloramphenicol (27 µg/ml), conferred by the pcDNA3 vector and RfB Gateway cassette, respectively. OneShot ccdB 2T1 Survival cells are permissive to growth of constructs expressing the ccdB gene product encoded within the Gateway® Reading frame cassette, which is otherwise lethal to bacteria. Diagnostic BC-PCR, mini-prep DNA purification, vector sequencing, and glycerol stocks were undertaken as described previously. Once the correct ligated product was obtained and sequenced, midipreps were performed from individual bacterial colonies streaked onto selective 2xTY agar containing Ampicillin (100 µg/ml) and Chloramphenicol (27 µg/ml) from the corresponding sequenced glycerol stock. To distinguish between vectors, the Gateway®-converted pcDNA3-FLucC and pcDNA3-FLucN were renamed pcDNA3-FLucC GW and pcDNA3-FLucN GW.

2.2. Yeast clone generation

2.2.1. Reagents

Salmon testis DNA and primers were from Invitrogen (Paisley, UK). Polyethylene glycol (PEG), amino acid powders, and chemicals were obtained from Sigma Aldrich (Poole, UK). Peptone, yeast nitrogen base lacking amino acids, yeast extract and

glucose were purchased from Formedium (Norfolk, UK). The yeast two-hybrid host bait and prey strains utilised within this study were PJ69-4A (MatA trp1-901 leu2-3, 112 ura3-52, his3-200 gal4Δ gal80Δ LYS2::GAL1-HIS3 GAL2-ADE2 met2::GAL7-lacZ), and its switch mating type PJ69-4α, respectively (provided by Phil James; University of Wisconsin, USA). Yeast strains carried three independent GAL4-responsive reporter genes (GAL1-*HIS3*, GAL2-*ADE2* and GAL7-*lacZ*).

2.2.2. Media constituents

Media for yeast experiments were prepared according to Table 2.5. YPAD media provides strong growth conditions for yeast growth. Synthetic defined (SD-X) media allows for selection of yeast transformed with a given expression vector and determination of binary protein-protein interactions (Table 2.5D).

2.2.3. Yeast Glycerol Stocks

Successfully transformed MatA and Matα yeast colonies were grown for 3-4 days on synthetic deficient solid medium lacking appropriate selective nutrients (SD-X); growth selection markers conferred by all yeast vectors used within this study are outlined in Table 2.5D and Figure 2.2. Glycerol stocks were generated from 200 µl SD-X liquid media inoculated with an individual yeast colony in 1.5 ml microfuge tubes and incubated for 24 h at 200 rpm, 30°C. 80 µl of 80% autoclaved glycerol was added to yeast cultures prior to storage in at -80°C.

2.2.4. Yeast two hybrid vectors

All bait and prey Y2H expression vectors used in Y2H screens encoded the GAL4 DNA-binding domain (BD) or Activation Domain (AD), respectively. TM-E3-RING ORFs were inserted into prey and bait vectors for the generation of N- and C-terminal fusion proteins (Figures 2.2). E2-conjugating enzymes were previously generated within the laboratory within the pGBAE-B vector and were used for all

A Basic yeast media constituents

YPAD (500 ml)	
D-glucose	10 g
BioAgar (solid media)	10 g
Yeast Extract	5 g
Peptone	10 g
Adenine	0.1 g

SD-X (500 ml)	
D-glucose	10 g
BioAgar (solid media)	10 g
Yeast Nitrogen Base	3.35 g
Amino acid mix	0.1 g

B SD-X amino acid supplements for yeast gap repair and transformation.

A/H/L/W/U DO	
Amino acid	**Grams / 100L**
Arginine	2
Isoleucine	3
Lysine	3
Methionine	2
Phenylalanine	5
Threonine	20
Tyrosine	3
Valine	15
Total (g/L)	**0.53**

SD-X mix (for 10 L)		
Amino acid	**Grams / 100L**	
	L*	W*
Adenine	0.6	0.6
Leucine	-	1.0
Histidine	0.2	0.2
Uracil	0.2	0.2
A/H/L/W/U DO	5.3	5.3
Total g / L	**0.63**	**0.73**

C SD-X amino acid supplement mixes for autoactivation and interaction studies

	SD-X mix (for 10 L)							
	LA*	**LH*/****	**WA**	**WH****	**WL**	**WLA**	**WLH****	**WLU**
Adenine	0.6	0.6	-	0.6	0.6	-	0.6	0.6
Leucine	-	-	1.0	1.0	-	-	-	-
Histidine	0.2	-	0.2	-	0.2	0.2	-	0.2
Uracil	0.2	0.2	0.2	0.2	0.2	0.2	0.2	-
A/H/L/W/U	5.3	5.3	5.3	5.3	5.3	5.3	5.3	5.3
Total g / L	**0.63**	**0.61**	**0.67**	**0.71**	**0.63**	**0.57**	**0.61**	**0.61**

D

Name	Deficiency	Selection
YPAD	None (Nutrient rich)	None (Strong growth of yeast)
-W	Tryptophan	Bait yeast (pGBAE-B/pBGBD)
-L	Leucine	Prey yeast (pACTBE-B/pBACT2)
-WA	Tryptophan and Adenine	Autoactivation of bait constructs
-WH(AT)	Tryptophan and Histidine	
-LA	Leucine and Adenine	Autoactivation of prey constructs
-LH(AT)	Leucine and Histidine	
-WL	Tryptophan and Leucine	Diploid yeast
-WLA	Tryptophan, Leucine, and Adenine	Protein-Protein Interactions
-WLH(AT)	Tryptophan, Leucine, and Histidine	

Table 2.5 Yeast media. (A) Basic yeast media constituents for YPAD and synthetic defined (SD-X) media. **(B)** SD-X amino acid supplements for yeast gap repair and transformation. **(C)** SD-X amino acid supplements for auto-activation and interaction studies. Amino acid supplement mixes for autoactivation and interaction studies. *Filter-sterile Tryptophan was added to SD-X media post-autoclaving to a final concentration of 20 mg/L. **Histidine dropout media was supplemented with a competitive analogue of histidine, 3-amino-1,2,4-triazole (3AT) to a final concentration of 2.5 mM, to increase the stringency of the reporter. **(D)** Selection/use of different yeast growth medias. YPAD provides strong conditions for yeast growth. Synthetic defined (SD-X) media allows for selection of yeast transformed with a given expression vector, auto-activation, and determination of binary protein-protein interactions, as indicated.

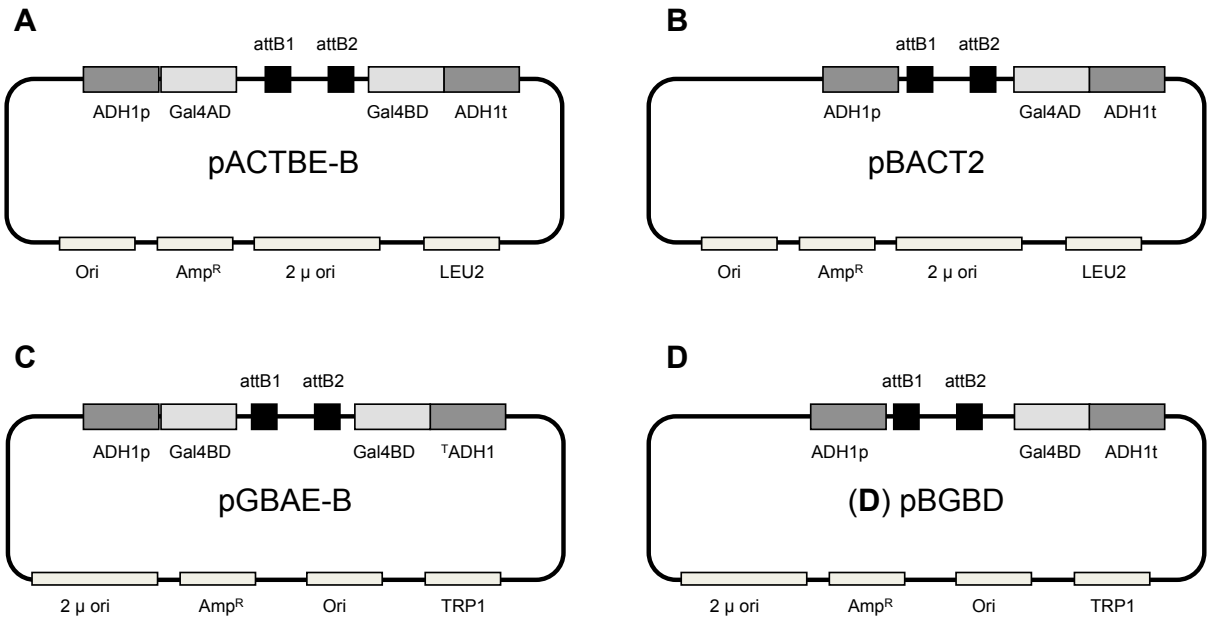

E

Vector	GAL4 Domain	GAL4 position	Yeast	Amino acid synthesis gene
pACTBE-B	AD	N-terminal	PJ69-4α (prey)	LEU2
pBACT-2	AD	C-terminal	PJ69-4α (prey)	LEU2
pGBAE-B	BD	N-terminal	PJ69-4A (bait)	TRP1
pBGBD	BD	C-terminal	PJ69-4A (bait)	TRP1

Figure 2.2 Y2H vectors used in this study. (A & B) pACTBE-B and pBACT2 prey vectors based on pACT2 and **(C&D)** pGBAE-B and pBGBD bait vectors based on pGBD-C1. pACTBE-B and pGBAE-B have a one base-pair insertion at the recombination site separated by the attB flanking regions to allow frame-shift and stop codon insertion following homologous recombination. **(E)** Y2H vector growth selection markers and GAL4 domain conjugation.

interaction assays. The selection of TM-E3-RING ORFs for either N- or C-terminal fusion protein generation is described in Chapter 3 and shown in Figure 2.3. To accommodate ORFs lacking stop codons, the N-terminal vectors pACTBE-B (prey) and pGBAE-B (bait) were designed to insert a stop codon 3' of the recombination site upon ORF insertion.

2.2.5. Yeast clone generation

To enable the *in vivo* homologous recombination of CRD TM-E3-RING ORFs with the desired Y2H-expression vectors (Figure 2.2), generic primers (pDONR223 gap repair F and pDONR223 gap repair R) were utilised to amplify ORFs from pDONR223 ENTR™ constructs by proof-reading KOD HotStart PCR, as described in section 2.1.3.

pACTBE-B, pBACT2, pGBAE-B, and pBGBD vectors were linearised by restriction enzyme digestion with BamHI and diluted to a working concentration of 20 ng/μl in dH_2O. Linearised DNA vector and PCR-amplified insert were recombined in MatA and Matα yeast strains by lithium acetate transformation (Ito, Fukuda et al. 1983). All yeast incubations described below were performed at 30 °C in an orbital shaking incubator at 220 rpm. Briefly, 2 ml YPAD liquid media was inoculated with a single colony of MatA or Matα yeast and incubated for 16 h. Following this period, an additional 8 ml YPAD liquid media was added and cultures incubated for a further 5 h. Yeast were harvested by centrifugation at 2300 rpm for 5 min and resuspended in 5 ml 100 mM Lithium acetate. For 10 yeast transformations, 1.5 ml of yeast suspension was transferred to a microfuge tube and cells harvested by centrifugation at 2300 rpm for 5 min, the supernatant discarded, and the pellet resuspended in transformation mixture described in Table 2.6.

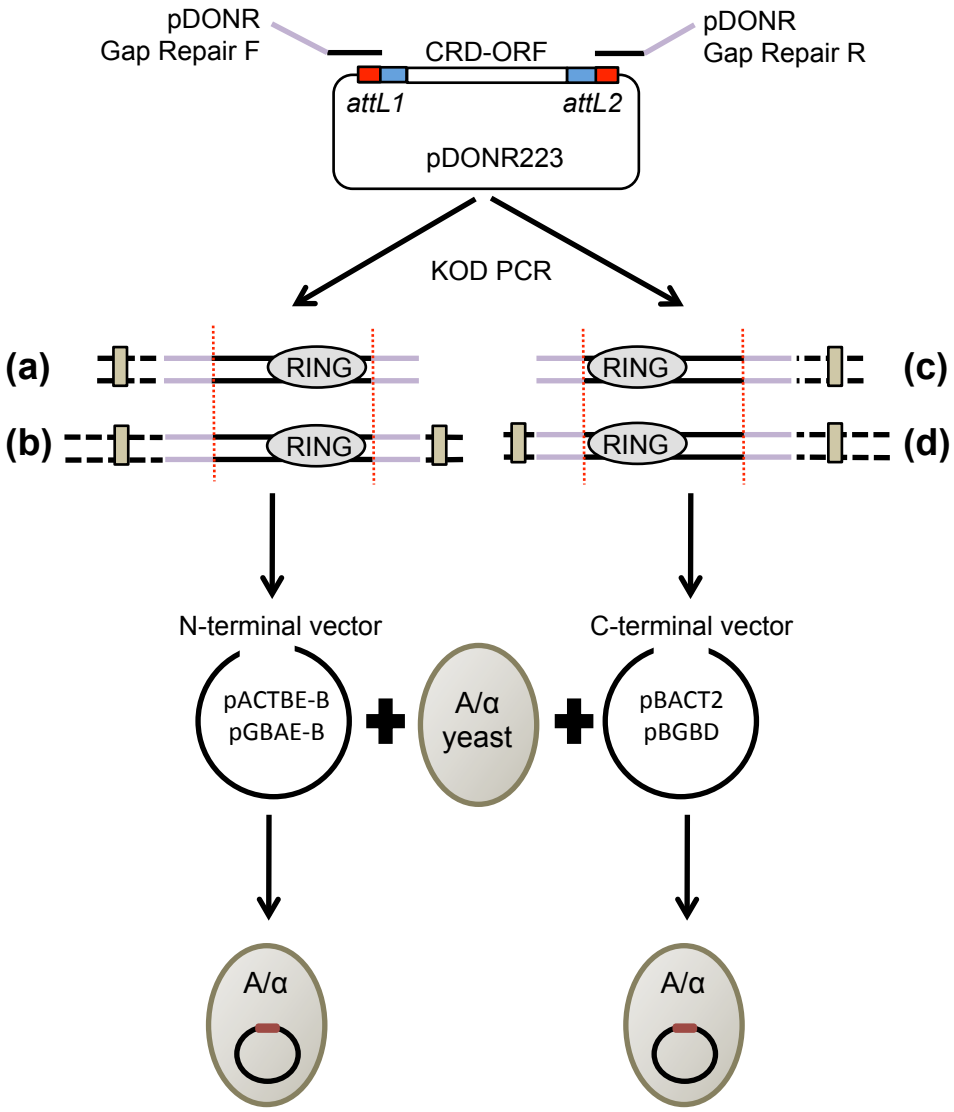

Figure 2.3 Selection and generation of N- and C-terminal GAL4 fusion proteins by *in vivo* gap repair cloning. CRD TM-E3-RING ORFs (black solid bars within red dotted lines) are amplified from pDONR223 with vector specific primers with 5' (forward) or 3' (reverse) overhangs for *in vivo* homologous recombination with Y2H expression vectors in yeast following lithium acetate transformation. Purple represents flanking region. Brown rectangles in **(a-d)** represent transmembrane domains and are therefore located outside of the CRD region. For those TM-E3-RING proteins, which contain TM-domains solely N- or C-terminal **(a&c)** to the RING domain, prey vectors were chosen such that the GAL4 domain substituted the cleaved TM-domain region at that terminus. However, for TM-E3-RING proteins that contain both N- and C-terminal TM-domains **(b&d)**, the GAL4 domain was positioned at the terminus of the CRD domain most distally located to the RING domain, to reduce the potential of steric hindrance of the GAL4 domain.

Reaction Component	Volume (μl)
50% (w/v) PEG 3350	230
1M Lithium acetate	35
Denatured salmon testes DNA (10 mg/ml)	9
20 ng/μl BamHI linearised DNA	1
Distilled H_2O	45

Table 2.6. Typical reaction mixture for transformation of yeast with linearised DNA vector and PCR product. Sufficient for 10 transformation reactions. Transformations were performed at room temperature.

32 μl of yeast transformation mixture was combined with 4 μl of PCR reaction for *in vivo* gap repair recombination reactions, or 4 μl dH_2O for determination of undigested vector contamination. Samples were incubated in a thermal cycler as follows:

i. 30°C for 30 min
ii. 42°C for 25 min
iii. 30°C for 1 min

The resulting reaction mixture was spread onto appropriate SD-X media as described in Table 2.5D and incubated for 3-4 days at 30 °C prior to diagnostic yeast colony PCR and auto-activation tests.

2.2.6. Diagnostic yeast colony PCR (YCPCR) and auto-activation

Colonies were tested for transformation and homologous recombination of linear DNA vector and PCR products by diagnostic yeast colony PCR (YCPCR) and agarose gel electrophoresis using BIOTaq™ DNA polymerase and vector specific primers flanking the homologous recombination sites (Supplementary file TMRING Cloning Summary). Reaction components were combined on ice and an individual yeast colony transferred using a sterile toothpick from SD-X media to 5 μl 0.02 M

NaOH followed by 10 µl SD-W or SD-L media, as appropriate. Yeast / NaOH solutions were incubated for ~ 15 min at room temperature prior to centrifugation at 10,000 rpm for 10 s. 12 µl of YCPCR mix (Table 2.7A) was combined with 3 µl yeast / NaOH solution and incubated in a thermal cycler as described in Table 2.7B. 5 µl of the resulting PCR product was size-verified by agarose gel electrophoresis. Colonies exhibiting a DNA band of the correct estimated size following diagnostic YCPCR were spotted (3 µl) onto selective SD-X media for determination of auto-activation.

2.2.7. Auto-activation screening

Auto-activation tests were performed to identify haploid yeast clones capable of constitutively activating reporter genes within the PJ69-4A/α strain in the absence of the reciprocal GAL4 domain fusion protein. Of the three GAL4-responsive reporter genes present in PJ69-4A/α (GAL1-HIS3, GAL2-ADE2 and GAL7-lacZ), both the HIS3 and ADE2 reporters were assayed for auto-activation; colonies were incubated at 30°C for 10 days on selective SD-X media described in Table 2.5D. Yeast colonies that did not display auto-activation growth phenotypes upon –His or –Ade reporters were selected for generation of glycerol stocks. Prior to Y2H screening, ≥ 3 individual glycerol stocks of each TM-E3-RING clone were pooled, and 4 µl spotted onto SD-L or SD-W agar for further experimentation. Each pooled yeast colony was sequence-tagged to confirm the presence of the desired insert.

2.2.8. Yeast construct clone set coverage and storage

Gap repair cloning resulted in the generation of bait (pGBAE-B/pBGBD; MatA) and prey (pACTBE-B/pBACT2; Matα) constructs representing 51 and 50 unique TM-E3-RING genes, respectively. Bait and prey yeast constructs were stored in two separate 96 well plate arrays.

A

Reagent	µl / reaction	[Conc]
Forward Primer (10µM)	0.75	0.5 µM
Reverse Primer (10µM)	0.75	0.5 µM
$_{d}$NTPs (25mM)	0.25	0.42 mM
NH Buffer (10x)	1.5	1 x
$MgCl_2$ (50mM)	0.45	1.5 mM
BIOTaq (5 U / µl)	0.15	0.75 U
DMSO	0.3	-
$_{d}H_2O$	7.35	-
NaOH yeast suspension	3.0	-
TOTAL	15	-

B

Step	Cycles	Temp (°C)	Duration
1	1	95.0	5 min
2	39	95.0	1 min
		55.0 - 68.0	1 min
		72.0	1 min/kb
3	1	72.0	5 min
4	1	4.0	For ever

Table 2.7. YCPCR. (A) Reaction mix for a yeast colony PCR. DMSO was added to increase the efficiency of primer annealing to the template DNA. The PCR mix was combined on ice prior to addition to thin walled PCR tubes. **(B)** Typical thermo-cycling conditions for YCPCR reactions.

2.3. Yeast two hybrid matrix matings

2.3.1. Reagents

5-bromo-4-chloro-3indoyl-β-D-galactosidase (X-Gal) reagent was purchased from Melford Laboratories (Ipswich, UK). Whatman filter paper (3mm) was purchased from Fisher Scientific (Loughborough, UK). All plasticware was from VWR (Lutterworth, UK). All other chemicals were purchased from Sigma Aldrich, unless otherwise stated.

2.3.2. Y2H matrix mating screen protocol

Yeast glycerol stocks were spotted onto the appropriate selective SD-X media and incubated at 30 °C for 3-5 days for yeast colony growth. Bait and prey yeast constructs were re-suspended to a similar opacity (assessed by eye) in 3 μl SD-X liquid media per yeast colony to be tested against. Initially, 2 μl prey yeast suspension was spotted onto YPAD agar in an 8 x 12 format and allowed to dry at room temperature. 2 μl of each of the bait yeast suspensions was subsequently spotted on top of the dried prey yeast constructs and dried at room temperature. YPAD agar plates were incubated at 30 °C for 24 h to encourage MatA and Matα yeast mating. Yeast spots were replica-transferred onto SD-WL media using a sterilised velvet cloth and incubated for 48 h at 30 °C for diploid yeast selection prior to replica-transfer onto SD-WL, SD–WLA and SD-WLH(AT) selection media. SD-WL media plates were incubated for 5 days at 30 °C and processed for determination of β-Galactosidase activity (described in Section 2.3.3). SD-WLA and SD-WLH(AT) media plates were incubated at 30 °C for 10 days with selective yeast growth scored and recorded following 3 days and subsequently every 2-3 days; scoring was based upon number of colonies per pairwise interaction tested: 0-5 colonies, background growth (0), 5-20 colonies, weak growth (1), 20-200 colonies, medium growth (2), full

plaque, strong growth (3). An overview of the Y2H matrix mating protocol is shown as a schematic in Figure 2.4.

2.3.3. LacZ enzymatic assay

In addition to the biosynthetic reporter assays described above, the lacZ assay was utilised as an alternative for identification of interacting partners. For transfer of diploid yeast growth from SD-WL media, a dry 15 x 20 cm 3mm Whatman filter paper was placed on the yeast growth and an even downward pressure applied to transfer an equal amount of yeast from each plaque to the filter paper. The filter paper was submerged in liquid nitrogen for 20 s and allowed to thaw, and the process repeated to maximise lysis of yeast. Following thawing, the filter paper was positioned yeast-side-up onto two sheets of Whatman filter paper saturated with β-gal reagent (6 ml Z-buffer (60 mM Na_2HPO_4, 40 mM $Na_2H_2PO_4$, 10 mM KCl, 1 mM $MgSO_4$, pH 7.0), 1.6 mg/ml X-Gal reagent (100 mg/ml in N,N-dimethylformamide), 11 µl β-mercaptoethanol), in a 150 mm petri-dish. β-gal plates were incubated at 37 °C for up to 12 h to allow the progressive development of a white to blue colour change, diagnostic of β-Galatisidase production within yeast and as such a positive binary interaction. β-gal plates were scored every hour for 6 h and at 12 h to optimise positive results observed over background. Each biosynthetic/enzymatic assay was undertaken twice and the results from each recorded.

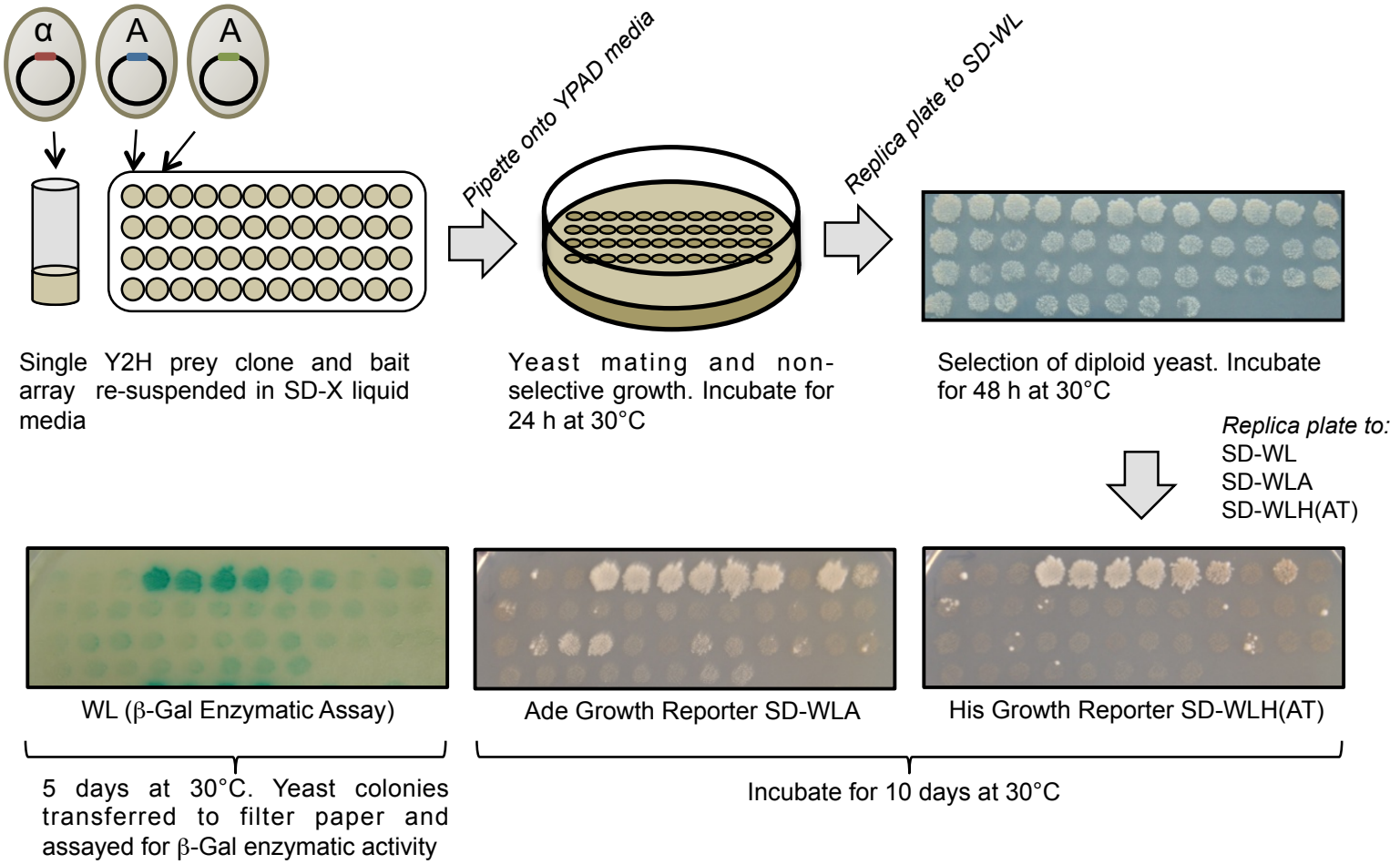

Figure 2.4. A flow diagram representation of the experimental procedure undertaken for Y2H determination of protein interactions. Construct generation was undertaken prior to insertion of the ORF of interest into MatA or Matα yeast. Yeast constructs were verified by PCR band size and assayed for activation of the growth reporter genes in the absence of a binding partner. Non-autoactivating clones were then moved forward in to yeast two hybrid matrix matings.

2.3.4. Y2H scoring and data storage

To allow integration and comparison of interaction data with that previously obtained a scoring methodology was adopted from that utilised in a recently published E3-RING/E2 Y2H screen within our laboratory (Markson, Kiel et al. 2009). Each tested protein pair was assigned an interaction score of 0-7 dependent upon both the number and combination of reporter genes activated as described in Table 2.8. Scores above zero required reproducible reporter activation in two independent matrix-mating screens with growth of ≥ 5 yeast colonies per interaction in both screens. The lowest positive interaction score, 1, was awarded to activation of the enzymatic LacZ reporter alone due to the predominantly subjective nature of this experimental readout. The ADE reporter is reported to be inherently more stringent than the HIS reporter (James, Halladay et al. 1996) and therefore activation of the ADE reporter alone represented an unexpected growth phenotype and assigned a lower confidence score than the HIS reporter alone. Interaction scores increase incrementally according to the above criteria and number of reporters activated.

Reporter activated	Number reporters activated	Interaction Score
None	0	0
$LacZ^+$	1	1
Ade^+	1	2
His^+	1	3
$Ade^+ LacZ^+$	2	4
$His^+ LacZ^+$	2	5
$His^+ Ade^+$	2	6
$His^+ Ade^+ LacZ^+$	3	7

Table 2.8 Y2H Stringency Criteria and Interaction Score. A Table to show each possible positive interaction phenotype and the corresponding interaction score.

2.4. Cell biology

2.4.1. Reagents

All cell culture reagents were obtained from Invitrogen unless otherwise stated. All plasticware, including 96 well opaque luminometry plates (white) were obtained from Corning Inc. (NY, USA). GeneJuice was obtained from Merck Biosciences (Nottingham, UK). Dual-luciferase® reporter assay system was purchased from Promega (Southampton, UK); reagents were prepared according to manufacturer's instructions.

2.4.2. Mammalian cell culture

HEK 293T cells were cultured in a humidified 5% CO_2 atmosphere at 37 °C in Dulbecco's Modified Eagle's Medium (DMEM) supplemented with 10% foetal bovine serum (FBS), 1% non-essential amino acids (NEAA), and 1% penicillin/streptomycin sulphate. Cells were maintained by growing to ~ 80% confluency in 75 cm^2 flasks prior to trypsin treatment and transfer to fresh 75 cm^2 flasks at 1:5 or 1:10 dilutions every 2-4 days as appropriate.

2.4.3. Mammalian cell transfection

HEK 293T cells were typically seeded at such a density such that they would reach ~ 50% confluency at the time of transfection and cells lysed 24 h post-transfection. Cells were routinely transfected with GeneJuice in 1 ml DMEM media lacking additional supplements at a ratio of 3 µl transfection reagent to 1 µg total DNA. Medium was changed to complete DMEM including supplements 4 h post-transfection. MG132, proteosomal inhibitor, was added to a final concentration of 100 nM where indicated.

2.4.4. Split Luciferase Protein Complementation Assay (PCA)

HEK 293T cells were seeded in 12-well cell culture plates at a density of 1.5 x 10^5 cells per well. Split Firefly luciferase (pcDNA3-FLucC GW and pcDNA3-FLucN GW) and Renilla luciferase (pRL-SV40) constructs were transfected at 0.5 ng / well and 0.1 ng / well, respectively, 24 h post-transfection. For sequential measurement of Firefly and Renilla luciferase activities the Dual-luciferase® reporter assay system was utilised, according to manufacturer's instructions (Promega Ltd), and photon emission recorded using a VICTOR Light luminometer (Perkin Elmer, Cambridge, UK).

Briefly, cells were washed twice with room temperature PBS and lysed by addition of 200 μl 1X Passive Lysis Buffer (PLB) with gentle rocking at room temperature for 5 min. Lysates were collected in pre-cooled sterile 1.5 ml microfuge tubes and placed on ice. 20 μl sample was added to individual wells of a pre-cooled 96-well opaque (white) luminometry plate. For measurement of Firefly luciferase activity, 100 μl Luciferase Assay Reagent II (LARII; containing Firefly luciferase substrate, luciferin) was combined to each well and photon emission (Relative Light Units (RLUs)) recorded for a period of 4 s. Subsequently, Firefly luciferase activity was quenched and Renilla luciferase activity measured by addition of 100 μl Stop & Glo® Buffer plus Stop & Glo® Reagent (contains Renilla luciferase substrate, coelenterazine) and RLUs recorded over a period of 0.2 s. To prevent depreciation of RLU signals, LARII and Stop & Glo® reagents were combined with only batches of 6 samples at a time for recording of RLU measurements.

To minimise experimental variation caused by differences in cell viability, transfection and cell lysis efficiency, Firefly luciferase values were normalised to the internal Renilla luciferase control (Firefly RLU / Renilla RLU) and a normalised average RLU obtained from two separate transfections calculated. To reduce false positive interaction detection, for each TM-E3-RING/E2 pair, TM-E3-RING-FLucC and E2-FLucN constructs were co-transfected with the predicted non-interaction partners FKBP-pcDNA3-FLucN and FRB-pcDNA3-FLucC, to provide appropriate negative normalisation controls for each tested protein pair.

2.5. Protein biochemistry

2.5.1. Reagents

Agar, peptone, tryptone and yeast extract were from Formedium. Sodium chloride, zinc chloride, 2-mercaptoethanol, ammonium persulphate (APS), N,N,N',N'-Tetramethylethylenediamine (TEMED) and mammalian protease inhibitor cocktail were from Sigma. Amersham Hybond™ ECL™ nitrocellulose membrane was from GE Healthcare. BenchMark Prestained Protein Ladder was from Invitrogen. Protogel electrophoresis buffers (ProtoGel® 30% Acrylamide/Bisacrylamide solution (37.5:1 w/v ratio), ProtoGel resolving buffer, ProtoGel stacking buffer) were from GeneFlow. Glycine and Tris-Base were from Fisher. Isopropyl-ß-D-thio-galactopyranoside (IPTG) was from Melford Laboratories Ltd. Rosetta™ 2(DE3) Singles™ Competent Cells were from Merck. Glutathoine Sepharose was from Bioline.

2.5.2. SDS polyacrylamide gel electrophoresis (SDS-PAGE)

Gels were assembled in a Mini-Protean® electrophoresis system, according to manufacturer's instructions (Bio-Rad). Samples were suspended in 5X Laemmli Sample buffer (Tris-HCl pH 6.8, 60 mM; SDS, 2% v/v; glycerol, 10% v/v; β-

mercaptoethanol, 5% v/v; bromophenol blue, 0.01% v/v) and protein content denatured by boiling at 98 °C for 5 min. Polyacrylamide gel recipes for the stacking and resolving of protein samples are given in Table 2.9. 4% acrylamide stacking gels were used in all SDS-PAGE experiments whilst the percentage of acrylamide for resolving gels varied depending upon the expected size of proteins being analysed. Samples were run in 1X electrophoresis running buffer (Tris-HCl, 50 mM; SDS, 0.1%; glycine, 380 mM), typically for 15 min at 125 V for protein stacking, followed by 40 to 60 min at 175 V to achieve optimal separation of protein bands. Polyacrylamide gels were removed from the electrophoresis system for processing. For assessing total protein content, gels were incubated for 1 h at room temperature in Coomassie-Blue stain (methanol, 50% (v/v); acetic acid, 7% (v/v); Coomasie Blue R250, 0.1% (w/v)) and excess dye was removed with de-stain solvent (methanol, 5% (v/v); $_dH_2O$, 85% (v/v); acetic acid, 10% (v/v)) prior to scanning polyacrylamide gels using the 700 nm wavelength channel of a Licor Odyssey infrared imaging system.

Reagent	Stacking Gel	Resolving Gel		
	4%	8%	10%	12%
Protogel Acrylamide Solution (ml)	1.3	2.67	3.33	4.0
Resolving Buffer (ml)	-	2.6	2.6	2.6
Stacking Buffer (ml)	2.5	-	-	-
$_dH_2O$ (ml)	6.1	4.62	3.96	3.29
TEMED (ml)	0.01	0.01	0.01	0.01
10% APS (ml)	0.05	0.05	0.05	0.05
Total Volume (ml)	9.95	9.95	9.95	9.95

Table 2.9. Recipes for SDS-PAGE gels. Resolving gels of differing acrylamide percentage were utilised dependant on size of expected protein molecular weight.

2.5.3. Western blotting

Following SDS-PAGE, resolved proteins were transferred to nitrocellulose membranes using a Mini-Trans Blot Cell system (BioMol, Exeter, UK) at a constant current of 300 mA for 90 min in Transfer Buffer (Tris, 25 mM; glycine, 192 mM; methanol, 20%). Nitrocellulose membranes were stained with Ponceau S to ensure efficient protein transfer followed by incubation at room temperature for 1 h in TBS Blocking Buffer (Tris-HCl, 50 mM; NaCl pH 7.6, 150 mM; Tween 20, 0.1% (w/v); Marvel, 5% (w/v)). Membranes were incubated overnight at 4°C on a rocker in TBS Blocking Buffer supplemented with specific primary antibody. Unbound antibodies were removed by 3 X 5 min washes in TBS-Tween prior to incubation for 1 h in blocking buffer containing IRDye-linked secondary antibodies. Unbound secondary antibody was removed by 3 X 5 min washes in TBS-Tween followed by an additional 5 min wash in TBS to remove detergent. Immunoreactive bands were detected using a LI-COR Odyssey infrared imaging system. A complete list of primary and secondary antibodies and the dilutions used within this study are listed in Table 2.10.

Antibody Antigen	Source	Company	Dilution in Blocking Buffer
Anti-GST (AB92)	Mouse	Abcam	1 : 1000
Anti Ubiquitin (07-375)	Rabbit	Millipore	1 : 2000
Anti-mouse IRDye 800CW	Donkey	Licor BioSystems	1 : 15000
Anti-rabbit IRDye 680CW	Donkey	Licor BioSystems	1 : 15000

Table 2.10. A list of primary and secondary antibodies utilised in western blotting analysis.

2.6. In vitro ubiquitination assay

2.6.1. Reagents

His-tagged E1 activating enzyme was purchased from Boston BioChem (MA, USA). Bovine ubiquitin and adenosine tri-phosphate (ATP) were from Sigma-Aldrich (Poole, UK).

2.6.2. GST-tagged construct generation

TM-E3-RING and E2 ORFs were transferred into the Gateway®-converted bacterial expression GST-tag vector, pGEX6p-GW, by LR recombination reactions. Typically, 7 μl of LR reaction product was directly transformed into 35μl Rosetta™ 2(DE3) Singles™ Competent Cells prior to overnight incubation at 37 °C on 2xTY solid media plus antibiotic. Rosetta™ 2(DE3) Competent Cells have been optimised to enhance the expression of eukaryotic proteins by supplying tRNAs for 7 rare human codons (AGA, AGG, AUA, CUA, GGA, CCC, and CGG). Diagnostic BCPCR was performed and glycerol stocks generated from size-verified bacterial colonies, which were subsequently streaked using a sterile wire loop onto 2xTY solid media supplemented with Ampicillin (100 μg/ml) and Chloramphenicol (27 μg/ml), conferred by the pGEX6p vector and a plasmid encoded by Rosetta™ 2(DE3) Singles™ Competent Cells, respectively.

2.6.3. GST-tagged TM-E3-RING protein production

A single transformed Rosetta bacterial colony was picked into 5 ml of 2xTY plus appropriate antibiotics and incubated overnight at 37°C, 220 rpm. This culture was combined with 45 ml 2xTY liquid media plus antibiotics and supplemented with 100 μM $ZnCl_2$, to facilitate the correct folding of the zinc-chelating RING domain. Cultures were incubated to an OD_{600} of 0.8-1.0 and protein expression induced by addition of 100 μM isopropyl β-D-1-thiogalactopyranoside (IPTG) followed by

incubation for 16-18 h at 18 °C, 220 rpm. Bacterial cells were harvested by centrifugation at 4300 rpm for 20 min at 4°C, the supernatant discarded and the pellet re-suspended in 1 ml filter sterilised, ice-cold PBS. Protease inhibitors were added (PMSF, 1 mM; leupeptin hemisulphate, 1 μM; pepstatin, 1 μM) and samples were snap-frozen by immersion in liquid nitrogen for 1 min prior to storage at -80 °C. Samples were thawed in ice-cold water prior to the addition of 1 mg/ml lysozyme and incubation on ice for 30 min. Bacterial cell lysis was performed by sonication of samples for 3 x 10 s (1 s pulse, 1 s rest). To reduce viscosity of sonicated samples 1 μl DNAse1 was added and samples passed through a hypodermic needle (25 gauge) three times. Samples were centrifuged at 33 000 rpm for 1 h at 4 °C and the supernatant carefully transferred to a 2 ml microfuge tube and incubated with 50 μl glutathione cellulose beads for 2 h at 4 °C with rotation at 50 rpm to bind GST-conjugated TM-E3-RING protein. Beads were washed three times in 1 ml High Salt Buffer (NaCl, 500 mM; Tris, 25 mM pH 8.5) followed by three washes in 1 ml Low Salt Buffer (NaCl, 150-200 mM; Tris, 25 mM, pH 8.5). GST-conjugated TM-E3-RING proteins were eluted in 1 ml Elution Buffer (Tris, 50 mM; NaF, 50 mM; sucrose, 270 mM; glycerol 2-phosphate disodium salt hydrate, 10 mM; reduced glutathione, 20 mM pH 8.0) by incubation for 20 min at room temperature with rotation at 50 rpm. Beads were pelleted by centrifugation at 3000 rpm for 5 min, and the supernatant carefully removed and snap-frozen by immersion in liquid nitrogen prior to storage at -80 °C. The procedure outlined above was repeated twice to obtain a second and third eluate for an individual sample.

2.6.4. E2-conjugating enzyme production

To produce unconjugated E2 proteins for *in vitro* ubiquitination assays volumes of 2xTY culture (lacking $ZnCl_2$), inhibitors, and glutathione cellulose beads were

ratiometrically scaled from those described in section 2.6.3 to generate a 500 ml culture. Cells were harvested and re-suspended in 10 ml PBS for snap-freezing. A more vigorous sonication procedure was employed with pulses for 3 X 20 s (1 s pulse, 1 s rest). Incubation and wash steps were undertaken using an Econo-Column (Bio-Rad) to accomodate the increased volumes of lysate, wash, and elution solutions. Lysates were incubated with 500 µl glutathione cellulose beads for 2 h at 4 °C to bind GST-conjugated E2 proteins. Beads were sequentially washed with 500 ml High Salt Buffer and 500 ml Low Salt Buffer prior to incubation with 5 ml Low Salt buffer supplemented with 50 µl PreScission™ Protease (2 U / µl) overnight at 4°C. Cleaved protein was eluted from the column in 10 ml Elution Buffer lacking reduced glutathione. Samples were concentrated to ~ 5 µg/µl (assessed by OD_{280}) using a Vivaspin 6 3kDa MWCO column (GE Healthcare) by centrifugation at 4300 rpm, 4 °C. Concentrated samples were snap-frozen and stored at -80 °C until use.

All eluates of GST-tagged TM-E3-RING and unconjugated E2 protein were analysed by SDS-PAGE to size-verify protein products.

2.6.5. *In vitro* ubiquitination assay

All *in vitro* ubiquitination assay reagents were thawed on ice and combined in pre-cooled thin-walled PCR tubes. *In vitro* ubiquitination reaction components were combined to make mastermixes for each TM-E3-RING or E2 protein tested, dependent upon experiment. A typical ubiquitination reaction mastermix for a TM-E3-RING tested against a panel of E2 conjugating proteins is described in Table 2.11. In this scenario, E2 conjugating enzymes were added individually to specific tubes. Typically, reaction mixtures were incubated at 37 °C for 90 min, unless stated otherwise. Following incubation, 3.75 µl 5 X Laemmli sample buffer

was added and proteins denatured at 95 °C for 5 min. Samples were subjected to analysis by SDS-PAGE and western blotting using rabbit anti-ubiquitin antibody or anti-GST antibody as described in Section 2.5.3.

Reagent	Stock Conc	[Conc]	*Vol Required (µl)
E1 Activating Enzyme	5 µM	250 nM	9.0
E3/RING Protein	~1 µg/µl	2 µg	2.0
L-Buffer	20 X	1 X	9.0
ATP	0.1 M	10 mM	18.0
Ubiquitin	20 mg/ml	5 µg	1.5
Total (dH_2O)	-	15 µl	180

Table 2.11 Mastermix for a TM-E3-RING assayed within *in vitro* ubiquitination assays against a panel of E2 proteins. *Volume required represents the volume of mastermix required for 12 individual reactions. E2 conjugating enzymes were added individually to each reaction to a final amount of 1 µg. 20X L-Buffer contained 800 mM Tris-HCl pH 7.5, 200 mM $MgCl_2$ and 12 mM DTT.

2.7. Construction and analysis of binary protein-protein interaction networks

2.7.1. Data storage

When dealing with high-throughput data it is crucial to minimise error by ensuring accurate data storage. Additionally, accurate storage and curation of high-throughput data is of paramount importance in the performance of computational analyses, to provide meaningful insights from protein interaction networks.

For interaction data, ORFs were assigned an entrez gene ID as a unique identifier to allow removal of duplicates. All tested interactions were recorded to reduce user input error when scoring interactions and also allow tested but negative results to be reported. Standard methods of storing data were established to facilitate

comparative and integrative analysis of obtained data with literature datasets. All tested interactions from Y2H, protein complementation, and *in vitro* ubiquitination assays were stored as tab delimited flat files containing all associated interactions.

2.7.2. Database curation

Four public databases and one commercial database (MetaCore™) were mined by Russell Hyde and Jonathan Woodsmith to provide overlapping yet complementary datasets to detail as many literature-reported interactions as possible. The four public databases were Human Protein Reference Database (HPRD) (Keshava Prasad, Goel et al. 2009), Molecular Interactions database (MINT) (Ceol, Chatr Aryamontri et al. 2010), IntAct (Aranda, Achuthan et al. 2010) and BioGrid (Breitkreutz, Stark et al. 2008). As a result of this data integration approach the final combined human 'interactome' network contains both binary protein-protein interactions observed and more ambiguous protein interactions derived from co-complex detection techniques. All unique identifiers were converted to entrez gene IDs to standardise interaction reporting. In order to ensure the highest possible coverage of the TM-E3-RING interaction networks, three of the public databases (HPRD, Biogrid, and IntAct) were again mined for TM-E3-RING interactions in June 2011 prior to performance of computational analyses.

2.7.3. Data integration, analysis and visualisation

To integrate interaction data obtained within the present study with other available datasets and to analyse the interaction data obtained on a systematic level computational filters written by Jonathan Woodsmith using the PERL computational language were utilised. For visualisation of some protein-protein interaction networks, such as heatmap representations, R statistical programming environment was implemented. PERL and R tools are more flexible in their implementation than

standard software such as Microsoft Excel allowing visualisation of data from a wide variety of experimental input.

Visualisation of integrated protein-protein interaction data in the form of node and edge graphs were generated using the open source bioinformatics software platform Cytoscape. All cytoscape Figures were generated using Cytoscape version 2.8.1.

3. Chapter 3: TM-E3-RING/E2 Conjugating Enzyme Interaction Mapping

3.1. Introduction

The selection and differential modification of cellular substrates by the ubiquitin system is to a large extent regulated by the E3-RING and E2 protein components of the ubiquitin machinery. The combinatorial interactions that occur between E3-RING and E2 proteins therefore represent a key regulatory step within the ubiquitin cascade, orchestrating the differential architecture of ubiquitin modifications to determine the fate or function of specific substrate proteins. To develop a deeper understanding of how E3-RING and E2 proteins cooperate to coordinate substrate selection and specific ubiquitination events, the determination of E3-RING/E2 protein partner preferences would provide an invaluable resource for interrogation and provide a framework for future hypothesis-driven research. During the early stages of this project, a high-throughput Y2H study directed at E3-RING/E2 protein interactions was published by our laboratory which was integrated with literature-derived information to generate a high density network consisting of ~ 700 binary E3-RING/E2 protein interactions (Markson, Kiel et al. 2009).

Despite the increased coverage of human E3-RING/E2 pairs, analysis of the integrated E3-RING/E2 network revealed a key area of data paucity for those E3-RING proteins predicted to contain transmembrane regions with ~ 1/2 of all TM-E3-RING proteins having no known E2 partners (Figure 3.8A&D). The poor representation of TM-E3-RING/E2 protein partners may result from the lack of amenability of proteins containing transmembrane regions to Y2H analysis due to a tendency to become insoluble, or form aggregates when expressed outside of lipid membranes. Additionally, as protein-protein interaction mediated reconstitution of an

active transcription factor must occur within the nucleus, proteins that contain transmembrane regions are poor candidates for determination of interaction partners by Y2H analysis. Indeed, a number of genome-wide Y2H screens have highlighted the poor coverage of protein interaction partners for integral membrane proteins in yeast (Uetz, Giot et al. 2000; Ito, Chiba et al. 2001) and human (Rual, Venkatesan et al. 2005) protein interaction networks.

This study sought to address the poor coverage of TM-E3-RING/E2 interactions by employing a directed Y2H approach using TM-E3-RING ORF clones encoding the entire cytoplasmic RING-domain (CRD) specific region for each human TM-E3-RING protein (see methods Figure 2.3). To this end, both CRD- and full-length TM-E3-RING ORF libraries were constructed for use in directed CRD GAL4-based Y2H matrix interaction studies and complementary secondary assays.

During the course of this project a second HTP Y2H screen directed at binary E3-RING/E2 interactions was published (van Wijk, de Vries et al. 2009). In comparison with our study, the interaction network compiled by van Wijk and colleagues utilised truncated E3-RING ORF clones. However, this study differed from the CRD-GAL4 Y2H screen in three key respects: (i) a LexA rather than GAL4-based Y2H system was used, (ii) UBC-domain specific E2 clones rather than full-length E2 clones were used, and (iii) RING-domain specific E3 clones rather than the entire cytoplasmic RING domain were used. A recent comparative study of different Y2H vector systems has highlighted the value of utilising different Y2H systems to increase coverage of interaction datasets (Chen, Rajagopala et al. 2010). Therefore, comparison of interactions observed in the CRD-GAL4 Y2H screen with the LexA screen and all other publically available TM-E3-RING/E2 interaction data was

performed (Markson, Kiel et al. 2009; van Wijk, de Vries et al. 2009), prior to collation into the most comprehensive TM-E3-RING/E2 interaction network available.

3.2. pBACT2 vector validation

Interactions between E3-RING and E2 proteins have been reported to be both weak and transient (Deshaies and Joazeiro 2009). As such, directed Y2H studies performed within our laboratory have utilised Y2H expression vectors containing an ADH1 promoter that drives moderate, rather than low, expression of N-terminal GAL4-fusion proteins (pACTBE-B/pACTBD-B E3-RING, Matα, Prey; pGBAE-B/pGAD-B, E2, MatA, Bait) (Markson, Kiel et al. 2009). Previous work within the Sanderson laboratory has demonstrated that the rational use of C-terminal GAL4 fusion constructs, which leave N-terminal regions more accessible for binding can reveal interactions that are not detected by conventional N-terminal Gal4 domain fusions (Tsang, Connell et al. 2006). In this study Y2H prey vectors were selected to generate N-terminal (pACTBE-B) or C-terminal (pBACT2) fusion-proteins to reflect the *in vivo* topology of each TM-E3-RING protein. For those TM-E3-RING proteins that contain TM-domains solely N- or C-terminal to the RING domain, Y2H vectors were chosen such that the GAL4AD domain substituted the cleaved TM-domain region at that terminus. However, for TM-E3-RING proteins that contain both N- and C-terminal TM-domains, the GAL4AD domain was positioned at the terminus of the CRD domain most distally located to the RING domain, to reduce the potential of steric hindrance of the GAL4 domain (see methods Figure 2.3).

As the previous directed E3-RING/E2 Y2H studies performed within our laboratory utilised only N-terminal fusions (Markson, Kiel et al. 2009), it was necessary to

validate the use of C-terminal pBACT2 vector constructs for GAL4-Y2H based determination of binary interactions between TM-E3-RING and E2 proteins. Therefore, 12 TM-E3-RINGs with domain architecture that fulfilled the criteria for testing as C-terminal GAL4AD fusions were generated as both pACTBE-B (N-terminal) and pBACT2 (C-terminal) GAL4AD prey constructs within Matα yeast. Each clone was then mated against the available array of 44 bait E2 conjugating enzyme pGBAD-B/pGBAE-B GAL4BD clones (representing 39 unique E2 genes) (Figure 3.1A). In this study all interaction data is related to Entrez Gene ID numbers, with interactions for different isoforms of a given gene product being collapsed onto a single node. As such, positive and negative interactions refer to binary interactions between the 53 TM-E3-RING proteins and the 39 unique E2 conjugating enzyme ORFs.

TM-E3-RING proteins demonstrated selective interactions on both biosynthetic reporters across many of the E2 enzymes in both pACTBE-B (N-terminal) and pBACT2 (C-terminal) prey vectors (Figure 3.1). For example, RNF185 exhibited an extensive E2 partner profile over a range of E2 families including the UBE2D1-4, UBE2E1-3, UBE2W, and UBE2K whilst RNF144A displayed a more restricted E2 interaction profile, interacting with UBE2L3 and UBE2L6 in both pACTBE-B and pBACT2 vectors (Figure 3.1B&C; blue boxes). Extended E2 interaction profiles were reported for a number of TM-E3-RING proteins when tested in the pBACT2 vector compared with pACTBE-B as exemplified by RNF152 (Figure 3.1D; blue and red boxes).

Analysis of total interactions revealed > 55% (35/63) of interactions were observed in both pBACT2 and pACTBE-B screens. Significantly, > 80% (35/43) of pACTBE-B

A

UBE2 A	UBE2 B	UBE2 C	UBE2 D1	UBE2 D2	UBE2 D3	UBE2 D4	UBE2 E1	UBE2 E3	UBE2 G1	UBE2 G2	UBE2 H
UBE2 I	UBE2 L3	UBE2 L3	UBE2 L6	UBE2 M	UBE2 N	UBE2 V1	UBE2 V2	UBE2 S	CDC 34	UBE2 K	UBE2 R2
UBE2 J1	UBE2 J2	UBE2 W	UBE2 E2	UEV LD	UEV LD	UBE2 W	UBE2 Z	AKT IP	UBE2 O	UBE2 Q1	UBE2 T
UBE2 I	UBE2 F	BIRC 6	UBE2 U	UBE2 DNL	UBE2 Q2	UBE2 Z	TSG 101	-	-	-	-

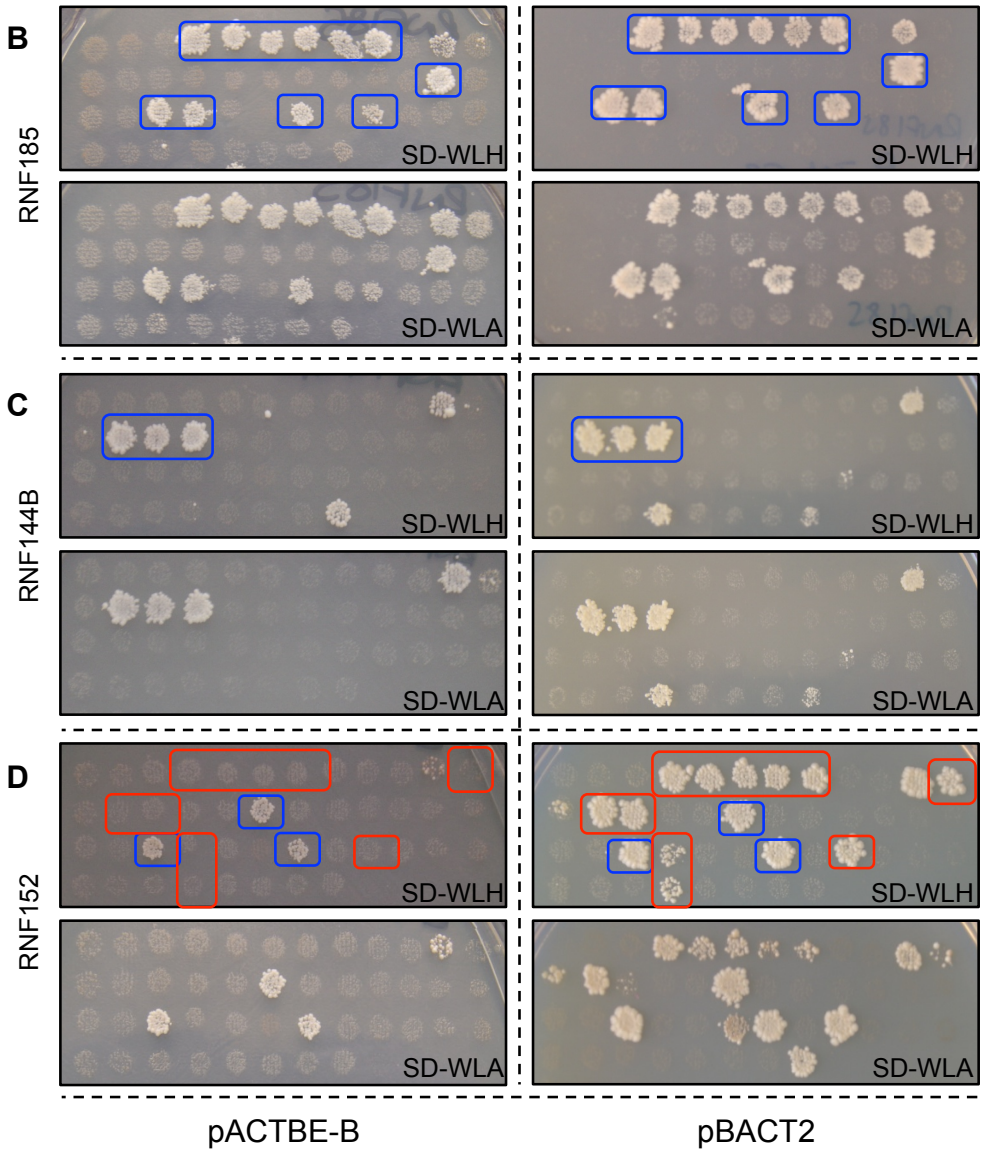

Figure 3.1. CRD-GAL4 Y2H matrix matings (A) E2 bait array layout. Each clone is represented by its official gene symbol. **(B-D)** Representative images of TM-E3-RING/E2 binding profiles observed on SD-X media selective for histidine (SD-WLH) or adenine (SD-WLA) reporter activity for CRD E3-RING clones expressed in either pACTBE-B (left) or pBACT2 (right) prey Y2H vectors. **(B)** RNF185, **(C)** RNF144B, and **(D)** RNF152. Images were recorded 9 d after replication onto triple selection SD-X plates. Blue and red boxes on WLH arrays represent shared and differential interaction profiles, respectively.

derived TM-E3-RING/E2 interactions were reconfirmed in pBACT2 screens (Figure 3.2A; black and grey segments). Furthermore, pBACT2 screens identified 20 novel TM-E3-RING/E2 interactions, which were not reported in pACTBE-B screens. Importantly, 32/33 higher stringency pACTBE-B interactions observed on –HIS and –ADE biosynthetic reporter arrays were reconfirmed in pBACT2 screens, on both biosynthetic reporters (Figure 3.2B). Therefore 7/8 unconfirmed pACTBE-B interactions were observed in -HIS reporter array alone (Figure 3.2B). To establish the main differences between datasets the degree contribution of pBACT2 and pACTBE-B screens for each TM-E3-RING was calculated (Figure 3.2C); 6/8 pACTBE-B interactions that were unconfirmed in pBACT2 screens were restricted to a single TM-E3-RING ORF construct (**bif**unctional **a**poptosis **r**egulator (BFAR)) (Figure 3.2C). This analysis also highlights that novel interactions observed in the pBACT2 screen result from both extension of pACTBE-B derived interaction profiles, exemplified by RNF152 and RNF144A, and detection of E2 interaction partners for TM-E3-RING clones which have no interaction partners in the pACTBE-B screen (MARCH8, MARCH1, MARCH6) (Figure 3.2 C).

The high reproducibility of pACTBE-B interactions and extension of E2 partners for a number of TM-E3-RING proteins in pBACT2 compared to pACTBE-B supported the rational use of the pBACT2 C-terminal GAL4AD-tag for appropriate TM-E3-RING proteins during Y2H assays.

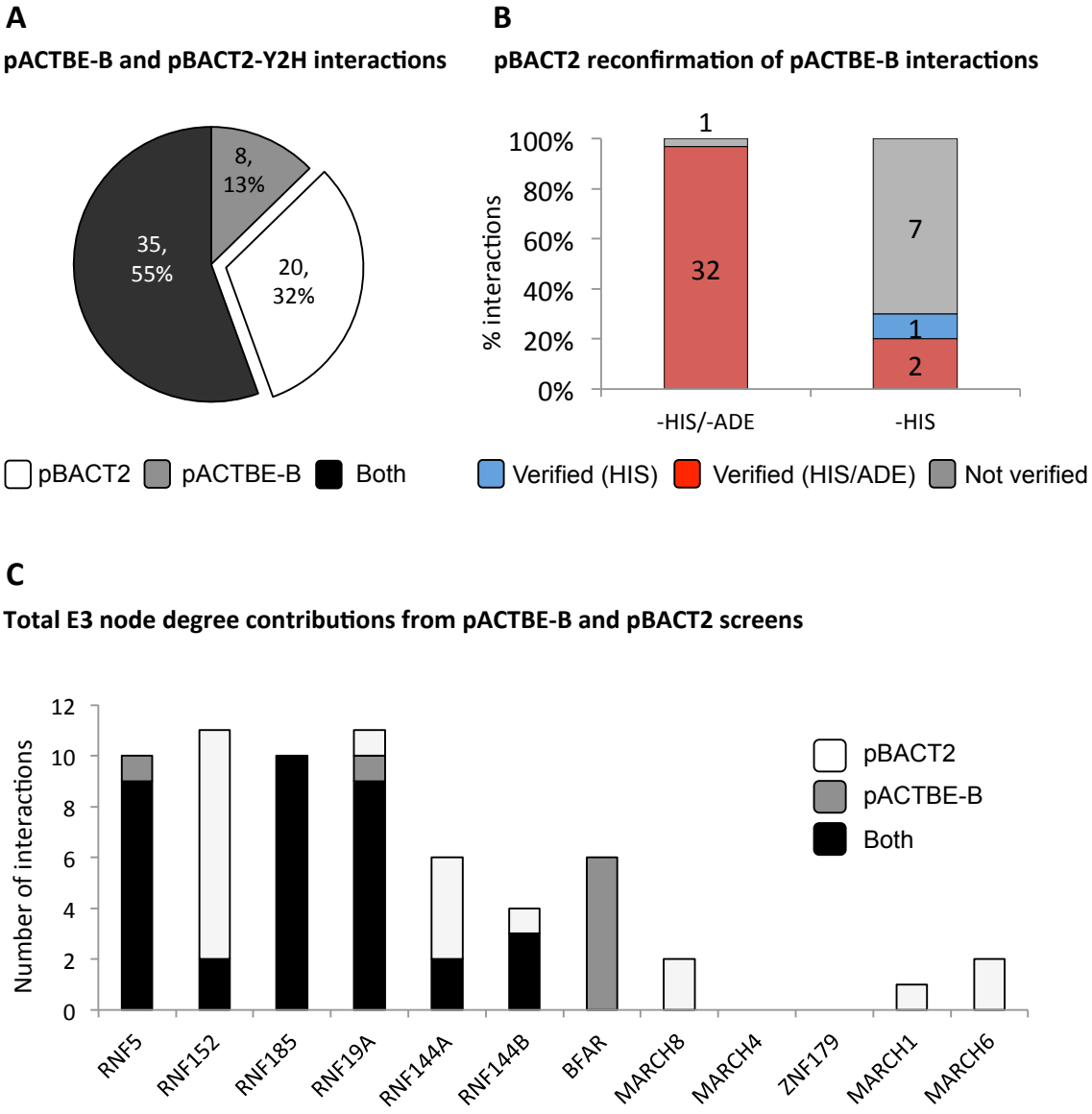

Figure 3.2. pACTBE-B and pBACT2 Y2H vector comparison. (A) Breakdown of co-tested CRD-Y2H interactions observed in pACTBE-B and pBACT2 screens. **(B)** Verification of pACTBE-B derived interactions by pBACT2 screening according to activation of different biosynthetic reporters. **(C)** Relative degree contributions of pACTBE-B and pBACT2 CRD E3-RING vector constructs to total number of E2 interaction partners for co-tested CRD TM-E3-RING ORFs.

3.3. CRD TM-E3-RING ORF strategy validation

The proposed utilisation of truncated TM-E3-RING ORFs encoding the entire cytoplasmic RING domain-containing (CRD) region was based on two principles. Firstly, previous structural and binding studies demonstrated that E3-RING residues responsible for interaction with E2 conjugating enzymes reside within or immediately flanking the RING domain ((Zheng, Wang et al. 2000) and discussed in section 1.5.2.1). Secondly, use of transmembrane domain containing proteins in Y2H analyses often lead to high false negative and/or false positive rates. Therefore, CRD TM-E3-RING ORFs would maintain an optimal E2 interaction surface whilst circumventing the inherent problems associated with using integral membrane proteins in Y2H screens. Finally, inclusion of the entire cytoplasmic RING domain may reduce the incidence of steric hindrance that may occur using RING-domain specific clones in Y2H fusions. Data from the published TM-E3-RING/E2 GAL4-Y2H network, which employed a number of full-length TM-E3-RING clones (Markson, Kiel et al. 2009), provided an opportunity to assess the applicability of CRD TM-E3-RING ORFs for the determination of E2 protein interaction partners using the identical Y2H technology, E2 conjugating enzyme ORFs, and comparable Y2H expression vector backgrounds.

Studies performed using full-length E3-RING clones identified 74 interactions between 27 TM-E3-RING and 21 E2 proteins (Markson, Kiel et al. 2009) and supplementary file ‘full-length_CRD GAL4Y2H comparison’). To test whether the CRD TM-E3-RING screening strategy facilitated detection of previously observed interactions and also increased interaction profiles, 7 highly connected TM-E3-RING proteins that accounted for 54/74 interactions full-length interactions, and 3 TM-E3-RING proteins that exhibited zero full-length interactions were tested as CRD clones

against the 44 E2 ORFs (39 unique genes). As incomplete β-gal reporter data was available for full-length interactions, comparisons between studies were based on the activation of two biosynthetic reporters, -HIS and -ADE. In total, 390 binary TM-E3-RING/E2 interactions were tested in both screens. A strong positive correlation was observed between screens with 53% of total interactions detected in both datasets (Figure 3.3A). Importantly, a high reconfirmation rate (39/54; 72%) of full-length screen interactions were observed using equivalent CRD clones, with an additional 20 interactions observed solely in the CRD screen (Figure 3.3A). Significantly, 25/28 high confidence (-HIS/-ADE positive) full-length screen interactions were reconfirmed within the CRD-Y2H screen with 20/25 reconfirmed on both biosynthetic reporter arrays. As such, 12/15 unconfirmed full-length interactions were only observed in –HIS reporter full-length arrays (Figure 3.3B).

To investigate differences in interaction profiles between CRD and full-length datasets, degree contributions of TM-E3-RING proteins from each screen were calculated (Figure 3.3C). Differential interaction partners were observed 7/10 TM-E3-RING proteins between screens whilst 2 TM-E3-RING proteins (MARCH8 and RNF13) were found to interact with E2 proteins in CRD- but not full-length screens (Figure 3.3C). The data was further interrogated to identify E2 proteins responsible for the differential profiles between TM-E3-RING clones that showed interaction partners in both screens (Figure 3.3D). A number of E2 proteins displayed remarkable correlation of TM-E3-RING interaction profiles between full-length and CRD-Y2H screens; the UBE2D, UBE2E, UBE2L, and UBE2W families display 100% overlap between functional TM-E3-RING clones in both full-length and CRD screens. However, a number of E2 proteins exhibit unique interactions in either the

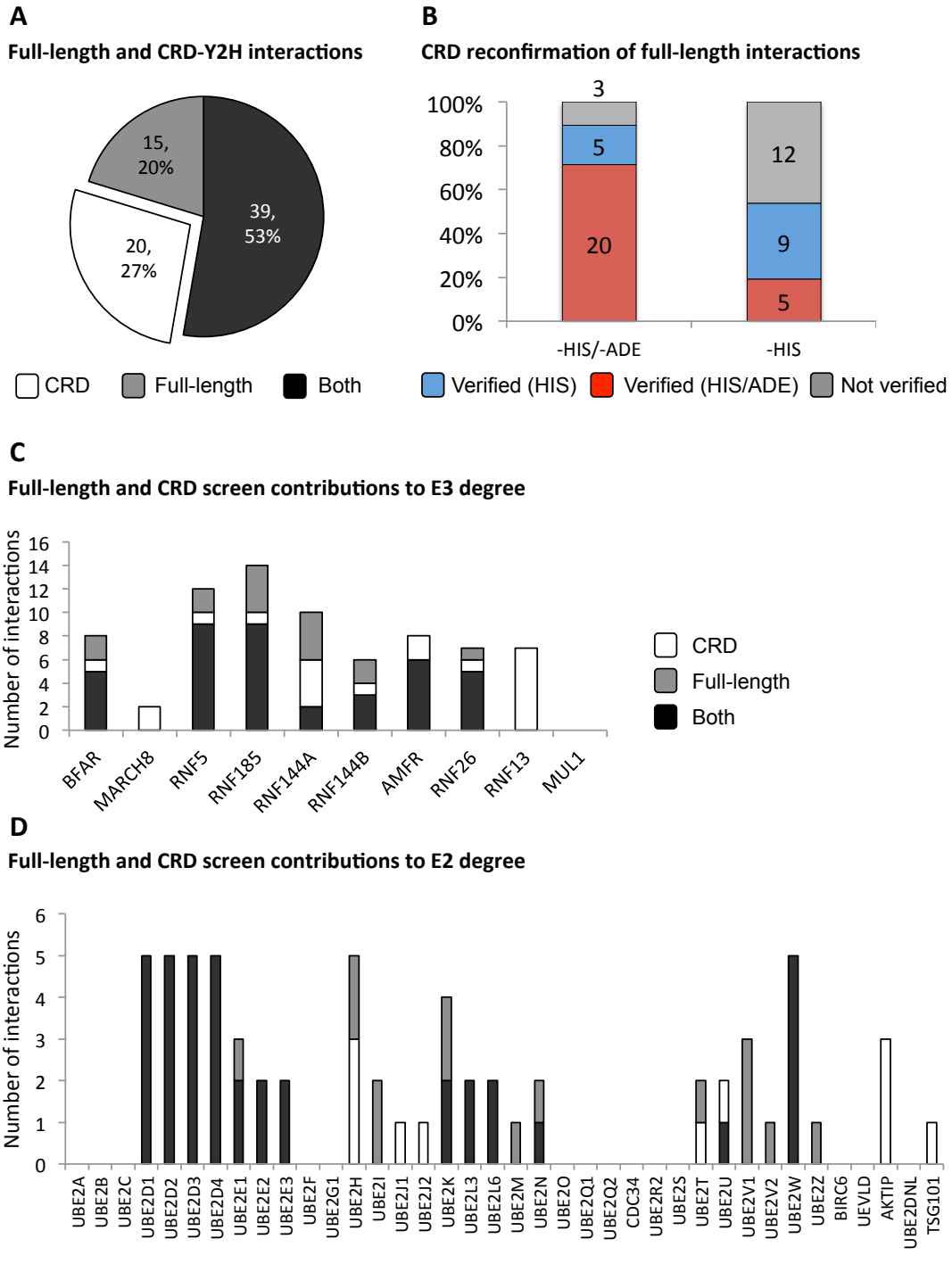

Figure 3.3. Comparison of data from full-length and CRD TM-E3-RING/E2 Y2H screens. (A) Percentage of total co-tested Y2H interactions observed in full-length and CRD Y2H screens. **(B)** Verification of full-length Y2H interactions in CRD screens, according to activation of different biosynthetic reporters. **(C)** Relative contribution of full-length and CRD screens to total number of E2 interaction partners for co-tested TM-E3-RING proteins. **(D)** Relative contribution of full-length and CRD screens to E2 degree for TM-E3-RINGs that were functional in both screens (≥ 1 E2 interaction partner in each screen).

full-length or CRD-Y2H screen; UBE2J1/2 and the UEV proteins, AKTIP and TSG101 exhibit interactions with CRD E3 clones whilst UBE2I, UBE2M, UBE2Z, and the UEV proteins UBE2V1/V2 exhibit interactions with full-length E3 clones (Figure 3.3D). The high rate of correlation between full-length and CRD screens supports the use of CRD TM-E3-RING ORFs for large scale screening of TM-E3-RING/E2 partner profiles.

3.4. High-throughput yeast 2-hybrid screen results

In total 51 sequence-verified TM-E3-RING CRD ORFs were successfully amplified from cDNA libraries, cDNA I.M.A.G.E. clones, or previous yeast constructs and cloned into Y2H prey vectors (pACTBE-B or pBACT2) by *in vivo* gap repair cloning. Of these haploid TM-E3-RING yeast constructs, only RNF103 displayed any auto-activation phenotype, which activated both –ADE and -HIS biosynthetic growth reporters and was therefore not used in directed Y2H matrix screens. As such, a total of 50 TM-E3-RING proteins were used in directed Y2H matrix matings against the panel of 44 available E2 conjugating enzyme bait constructs (representing 39 unique E2 genes). This strategy enabled the systematic investigation of 1950 potential binary TM E3-RING/E2 protein interactions. Following repeated matrix matings, 196 reproducible Y2H positive interactions involving 33 TM-E3-RING and 22 E2-proteins were detected. Of these, 49% were detected on at least two reporters with a further 51% being reproducibly detected on the -HIS reporter alone (Figure 3.4A). Importantly, a high rate of reproducibility of positive interactions was reported between repeats of the CRD-Y2H screen; > 92% of interactions observed on –HIS or multiple reporter arrays were reported in both screens (supplementary file E3RING/E2 CRD-Y2H).

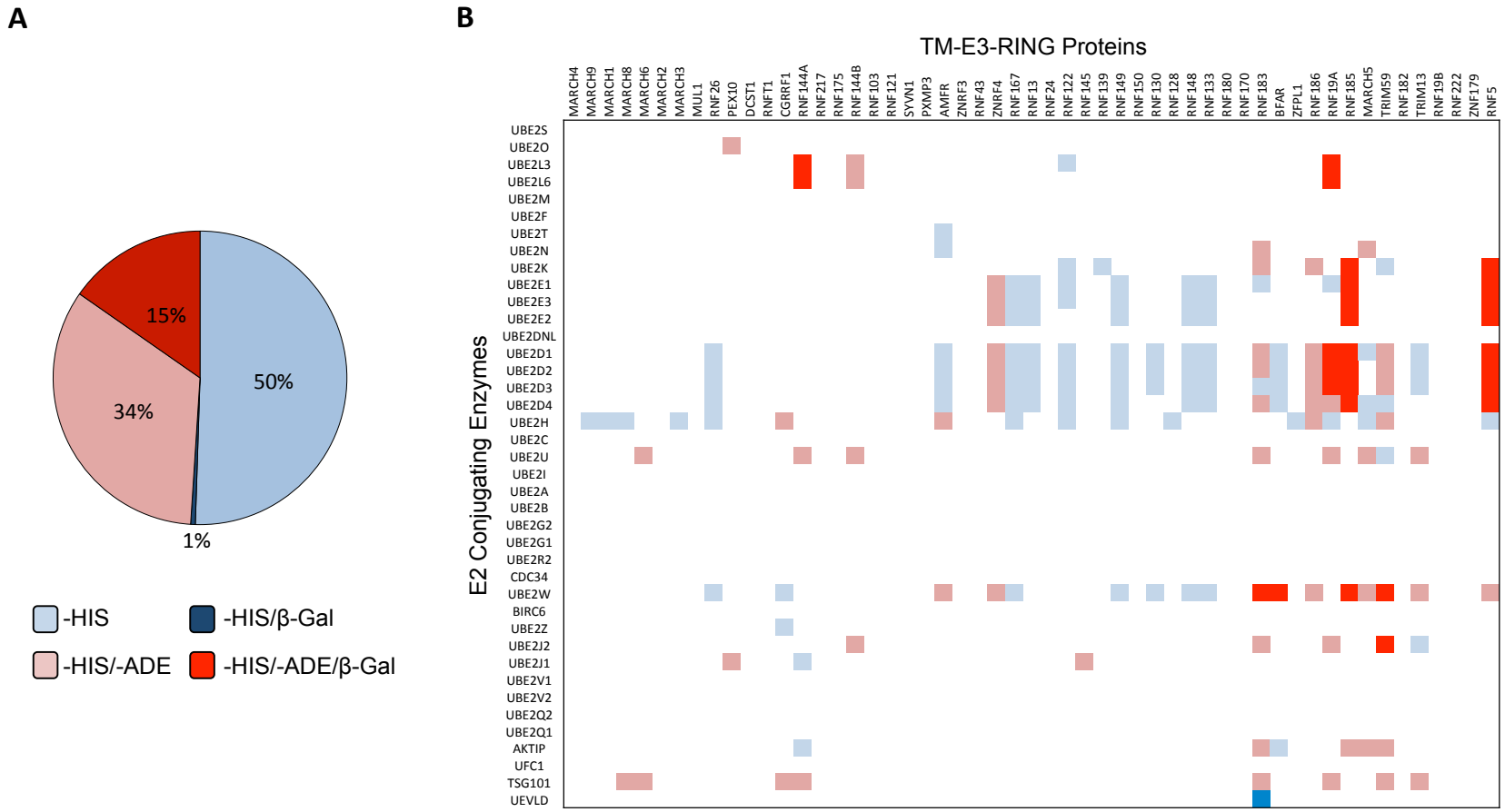

Figure 3.4 CRD GAL4 Y2H interactions. (A) Breakdown of positive CRD-Y2H interactions according to differential Y2H reporter activation. **(B)** Heatmap representation of TM-E3-RING/E2 interactions obtained in CRD-Y2H screens. TM-E3-RING (horizontal) and E2-conjugating enzyme (vertical) entrez gene symbols are ordered based on primary protein primary sequence alignment in ClustalW. Differential reporter gene activation is indicated by colour code.

The heatmap representation of TM-E3-RING/E2 interactions shown in Figure 3.4B highlights a large proportion of TM-E3-RING proteins to have selective E2 interaction partners, with individual TM-E3-RING proteins binding multiple E2 proteins. In agreement with E3-RING/E2 profiles reported in recently published TM-E3-RING/E2 datasets (Markson, Kiel et al. 2009; van Wijk, de Vries et al. 2009), a small subset of E2 proteins, notably UBE2D, UBE2E and UBE2W E2 family members, appear responsible for a high proportion of total TM-E3-RING/E2 interaction partners (Figure 3.4B).

3.4.1. Full-length TM-E3-RING GAL4 system comparison

In total, 27 full-length TM-E3-RING proteins had been previously tested against the identical panel of 44 E2 clones used in this study. The total number of E2 interactions observed for the complement of co-tested TM-E3-RING proteins was considerably higher using CRD (102 interactions) compared to full-length E3 clones (73 interactions) (Figure 3.5A). Of the 73 interactions observed within the full-length screen, 42 (> 58%) were reconfirmed within the truncated study (Figure 3.5A; black and grey segments). Importantly, 25/28 high stringency (-HIS/-ADE positive) interactions observed within the full-length screen were reconfirmed using truncated TM-E3-RING clones (Figure 3.5B). As such, 28 of the 31 unconfirmed full-length interactions were reported solely on -HIS biosynthetic reporter arrays (Figure 3.5A&B). Finally, a total of 60 and 31 interactions were uniquely detected using CRD or full-length clones, respectively (Figure 3.5A). To determine the main differences between Y2H screen datasets, the degree contribution for each TM-E3-RING and E2 protein from full-length and CRD Y2H datasets was calculated (Figure 3.5C&D). Notably, 5 TM-E3-RING proteins that exhibited a degree of zero in full-length screens interacted with 23 E2 partners in CRD screens (Figure 3.5C)

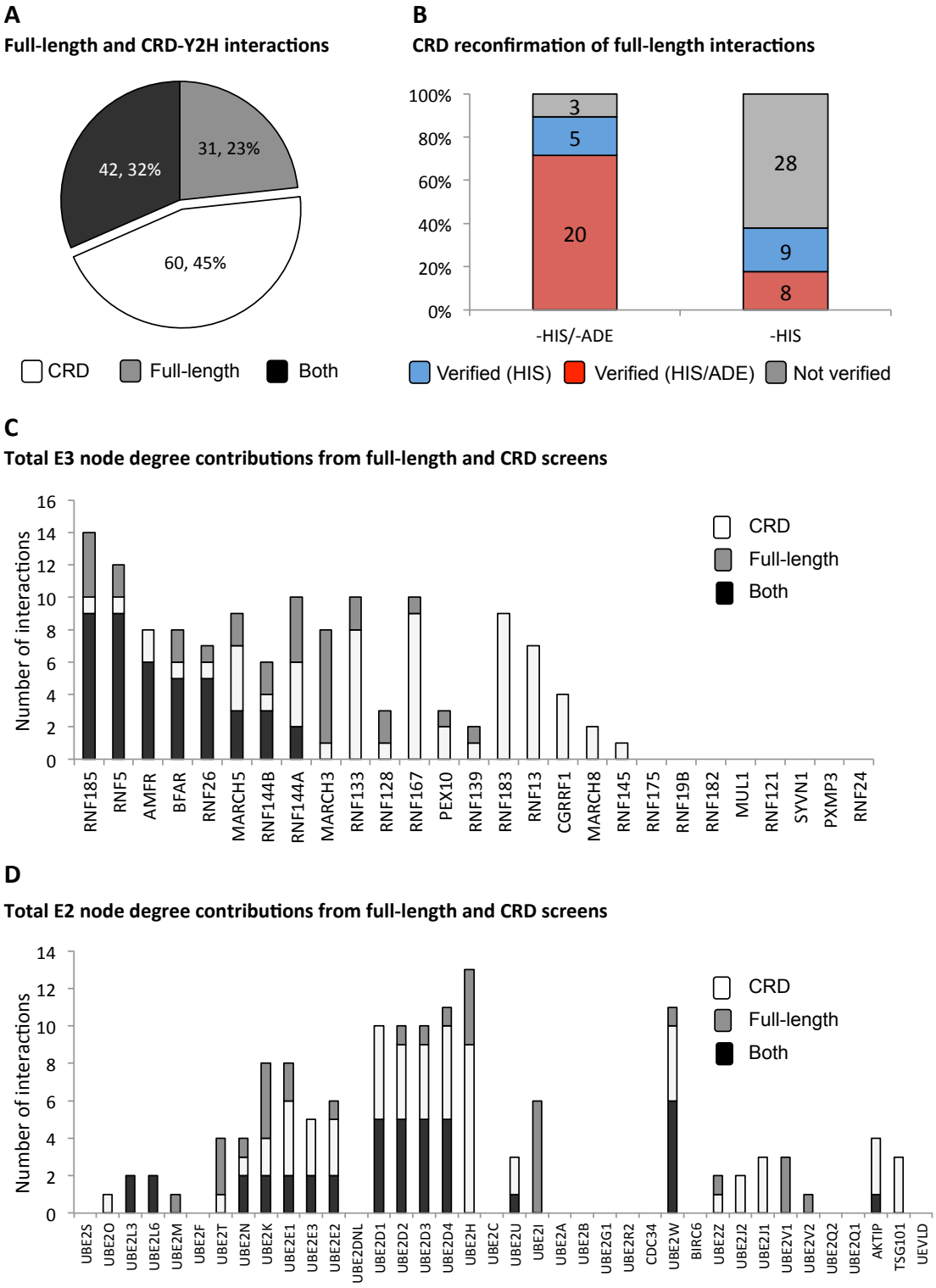

Figure 3.5. Total full-length and CRD TM-E3-RING Y2H comparison. **(A)** Breakdown of total co-tested Y2H interactions observed in full-length and CRD screens. **(B)** Verification of full-length Y2H interactions by CRD screens according to activation of different biosynthetic reporters. **(C)** Degree contribution of full-length and CRD TM-E3-RING clones for each co-tested TM-E3-RING protein. **(D)** Degree contribution of full-length and CRD Y2H screens for each co-tested E2 protein.

demonstrating the value of CRD TM-E3-RING ORF clones in the Y2H determination of TM-E3-RING/E2 protein interaction profiles.

TM-E3-RING clones that were functional in both screens revealed 68 interactions that reflected different binding profiles between CRD and full-length TM-E3-RING clones; 31 and 37 interactions were unique to full-length or CRD screens, respectively (Table 3.1). A small subset of TM-E3-RING and E2 clones within the full-length screen were responsible for a large proportion of the differential interactions that were not seen when respective CRD clones were analysed. For example, MARCH3 exhibited 7 interactions in the full-length screen, however only one was identified using the CRD clone (Figure 3.5C). Also higher numbers of TM-E3-RING interactions were observed for the UBE2T (3), UBE2K (4), UBE2V1/V2 (4) and UBE2I (6) E2s in full-length compared to CRD screens (Figure 3.5D).

	Full-length	**CRD**	**Union**	**Intersection**
Co-tested TM-E3-RING clones	27			
TM-E3-RING/E2 Interactions	73	102	133	42
Interacting TM-E3-RING clones	14	19	19	14
Interacting TM-E3-RING clones in one screen	0	5	5	-
Interactions from TM-E3-RING ORFs with degree 0 in alternative screen	0	23	23	-
Differential interactions if degree ≥ 1 in both screens	31	37	68	-

Table 3.1. Tabular breakdown of total interactions observed in full-length and CRD GAL4-Y2H screens. ‘Union’ refers to interactions or clones in either dataset. ‘Intersection’ refers to common interactions or clones in both screens.

3.4.2. Comparison with LexA Y2H-derived interaction data

During the course of this study, an E3-RING/E2 interaction network was published using an orthogonal LexA-based Y2H system with RING and UBC domain specific clones to identify selective binding partners (van Wijk, de Vries et al. 2009). Data from the LexA-based Y2H study provided an opportunity to compare protein-protein interaction data between two non-identical but orthogonal Y2H systems involving 32 common TM-E3-RING and 34 common E2 ORFs (1088 co-tested protein-protein interactions) (supplementary file LexA_CRD comparison). The union of co-tested TM-E3-RING/E2 pairs revealed a total of 170 interactions of which 25% (42) were detected in both studies, 25% (42) were only observed in the LexA screen and 50% (86) were uniquely observed in our GAL4-based screen (Figure 3.6A). The 25% overlap between HTP Y2H interactions observed in this analysis is comparable to correlation rates previously reported between orthogonal Y2H systems for an identical 'gold-standard' positive protein interaction reference dataset (Chen, Rajagopala et al. 2010). Similarly, a considerably higher correlation between screens was observed compared to that described for the LexA versus total E3-RING/E2 study (8% overlap; personal communication Jonathan Woodsmith). This highlights the value of using differing Y2H systems for interaction detection, as ORFs may not function in any given screen for numerous reasons including steric hindrance, mis-folding, or poor expression.

The percentage of interactions observed for each E2 conjugating enzyme was analysed to investigate similarities in TM-E3-RING binding profiles between studies (Figure 3.6B&C). Highly similar trends in E2 binding pattern were observed between LexA and CRD-GAL4 Y2H screens with UBE2D, UBE2E, and UBE2W families exhibiting broad TM-E3-RING partner preference in both screens; the UBE2D and

UBE2E E2 families account for approximately half of all interactions within GAL4 (49%) and LexA (54%) systems (Figure 3.6B). Highly comparable patterns of E2 degree contributions for TM-E3-RING proteins were also observed in full-length GAL4 Y2H screens and were also observed in the extended E3-RING/E2 networks, encompassing all E3-RING proteins tested in LexA and full-length GAL4 screens (Figure 3.6C). UBE2D, UBE2E, UBE2W proteins display similar interaction coverage for TM-E3-RING proteins between CRD-GAL4, full-length-GAL4 and LexA Y2H screens with the exception of UBE2E2, which reported a sole soluble E3-RING interaction partner in the entire LexA interaction screen (Figure 3.6C). Considering the high sequence similarity between members of the UBE2D and UBE2E families and the highly connected nature of this protein in GAL4 screens it is plausible that the UBE2E2 clone had limited functionality in the LexA screen. Despite considerable similarities in TM-E3-RING/E2 binding profiles between studies, a number of functional E2s (UBE2H, UBE2N, UBE2Z and the highly promiscuous UBE2U clone) show considerable differences in the proportion of (TM-)E3-RING binding partners derived from LexA and GAL4 screens (Figure 3.6B&C). Additionally, UBE2K appears non-functional in the LexA screen yet reported 7 interactions in the CRD-GAL4 screen whilst UBE2G2 displayed a strong autoactivation phenotype in GAL4-based Y2H screens but had 3 specific TM-E3-RING interaction partners in the LexA-based study. As such, whilst highly comparable interaction profiles were observed between screens the collation of datasets provides a higher density network of TM-E3-RING/E2 interactions (Figure 3.6B&C).

Taking into consideration the highly similar trends in E2 degree between screens the modest overlap in total interactions between studies (~ 25% intersection) was surprising. Therefore, a comparative analysis of TM-E3-RING clone binding profiles

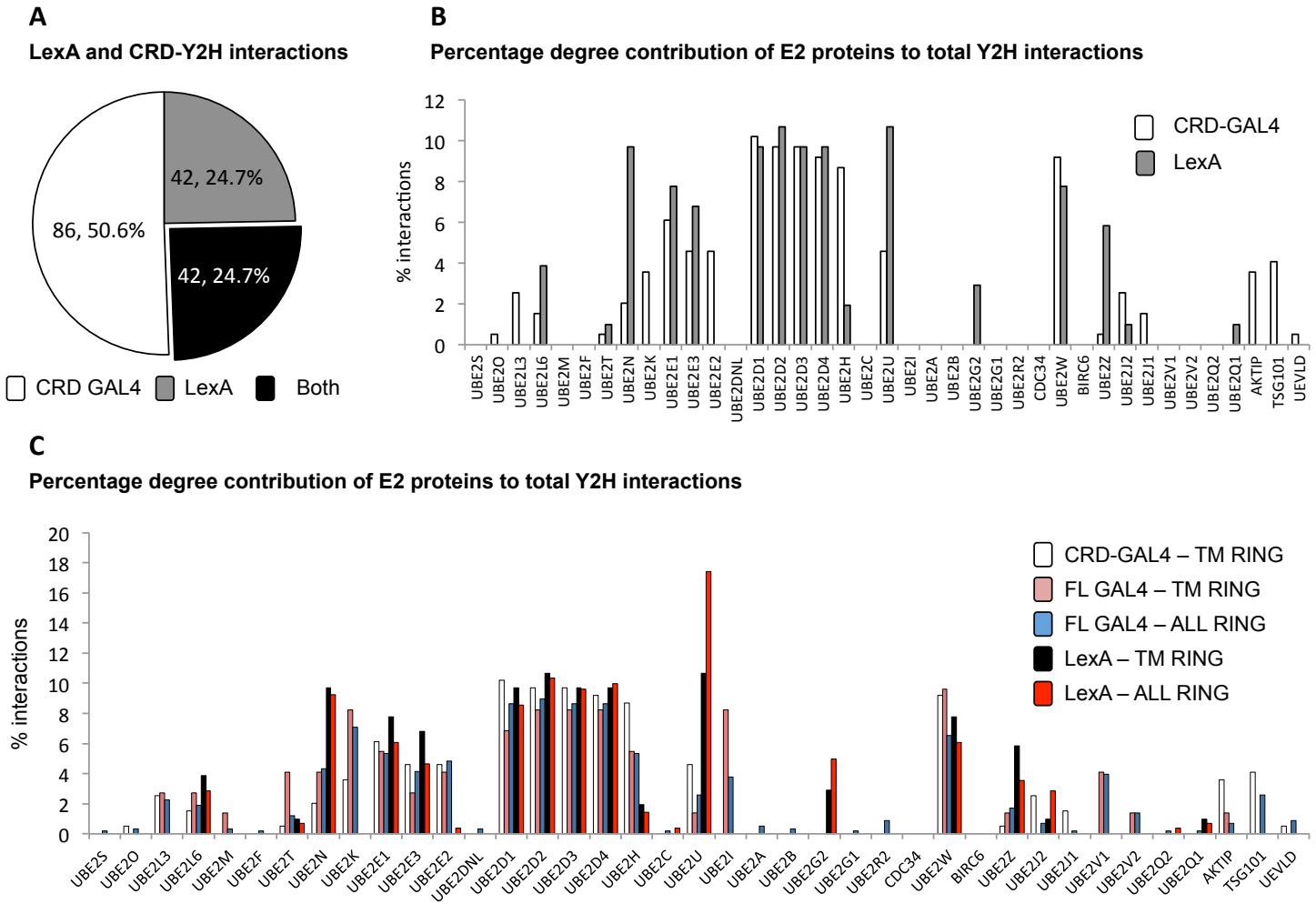

Figure 3.6. Comparison of data from LexA and CRD-GAL4 Y2H studies. (A) Breakdown of co-tested TM-E3-RING/E2 Y2H interactions observed in LexA and CRD-GAL4 Y2H screens. **(B)** Percentage degree contribution of each E2 protein to total TM-E3-RING interactions in the LexA and CRD-GAL4 based Y2H screens **(C)** Percentage degree contribution of each E2 protein to total (TM-)E3-RING interactions in the LexA, CRD-GAL4, and full-length GAL4 Y2H systems.

was undertaken to investigate whether the modest overlap between screens was due to individual TM-E3-RING clones that were functional in one or the other screen, or the result of differential E2 binding patterns of individual TM-E3-RING clones between screens. In total, 62 interactions were uniquely observed in a given system for TM-E3-RING proteins, which displayed a degree of zero in the alternate screen (Figure 3.7A&C). Taking into consideration only those TM-E3-RING proteins that were functional in both screens (i.e. degree ≥ 1 in both screens) the total number of total interactions that could be reported in both screens was 108, of which 39% (42/108) were common to both studies. Therefore, 66 interactions unique to one or the other screen belonged to TM-E3-RING proteins that were functional in both studies yet exhibited differential E2 binding partners; CRD-GAL4 screens generated more extended profiles than the LexA screen with 49 unique interactions compared to 17 within the LexA screen (Figure 3.7C). A large proportion of TM-E3-RING/E2 interactions unique to the LexA screen belong to a small number of E2 clones (UBE2N, UBE2U, and UBE2Z) (Figure 3.7B), which account for 12/17 interactions.

Comparison of data obtained in CRD-GAL4 and isolated RING-domain LexA clones with that derived from comparable full-length E3-RING screens reveals 4 E2 enzymes (UBE2M, UBE2I, UBE2V1 and UBE2V2) that interact with full-length but not truncated E3-RING clones (Figure 3.6C). These findings may indicate that regions outside of the cytoplasmic RING domain may contribute to E2 protein binding. Conversely, the hydrophobic or charged regions of full-length TM-E3-RING clones may lead inappropriate interaction profiles with this sub-set of E2 proteins in our Y2H system.

A

Total E3 node degree contributions from LexA and CRD screens

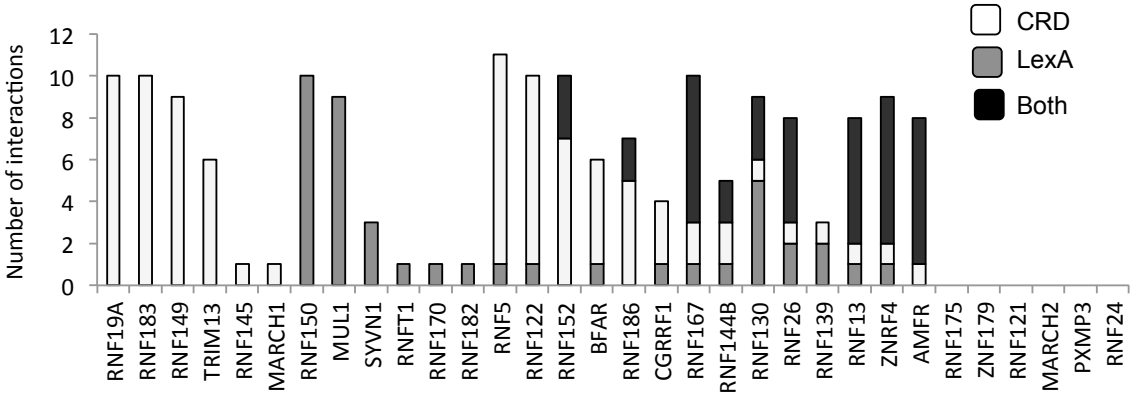

B

Total E2 node degree contributions from LexA and CRD screens

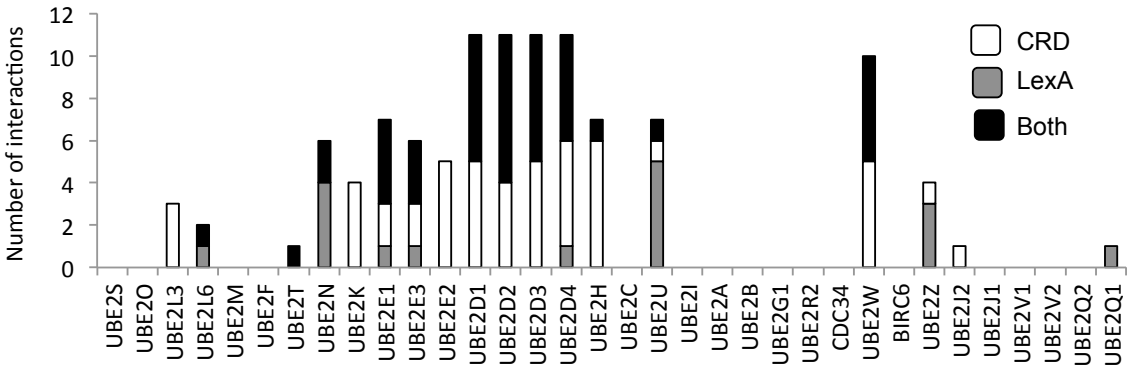

C

Co-tested TM-E3-RING/E2 interactions collapsed onto single Entrez Gene ID				
	LexA	**CRD-Y2H**	**Union**	**Intersection**
Co-tested RING ORFs	32			
Total Interactions	84	128	170	42
Interacting RING clones	20	20	26	14
Interactions from clones with degree 0 in alternative vector systems	25	37	62	-
Novel interactions from clones with degree > 0 in both vector systems	17	49	66	-

Figure 3.7 Comparison of LexA and CRD-Y2H contributions to total TM-E3-RING and E2 degree. (A) Degree contribution of LexA and CRD-GAL4 Y2H screens to total interactions for TM-E3-RING proteins tested in both screens. **(B)** Contribution of LexA and CRD-GAL4 screens to E2 degree for TM-E3-RING proteins that are functional in both screens. **(C)** Tabular format showing interactions observed in LexA and CRD-GAL4 based Y2H studies.

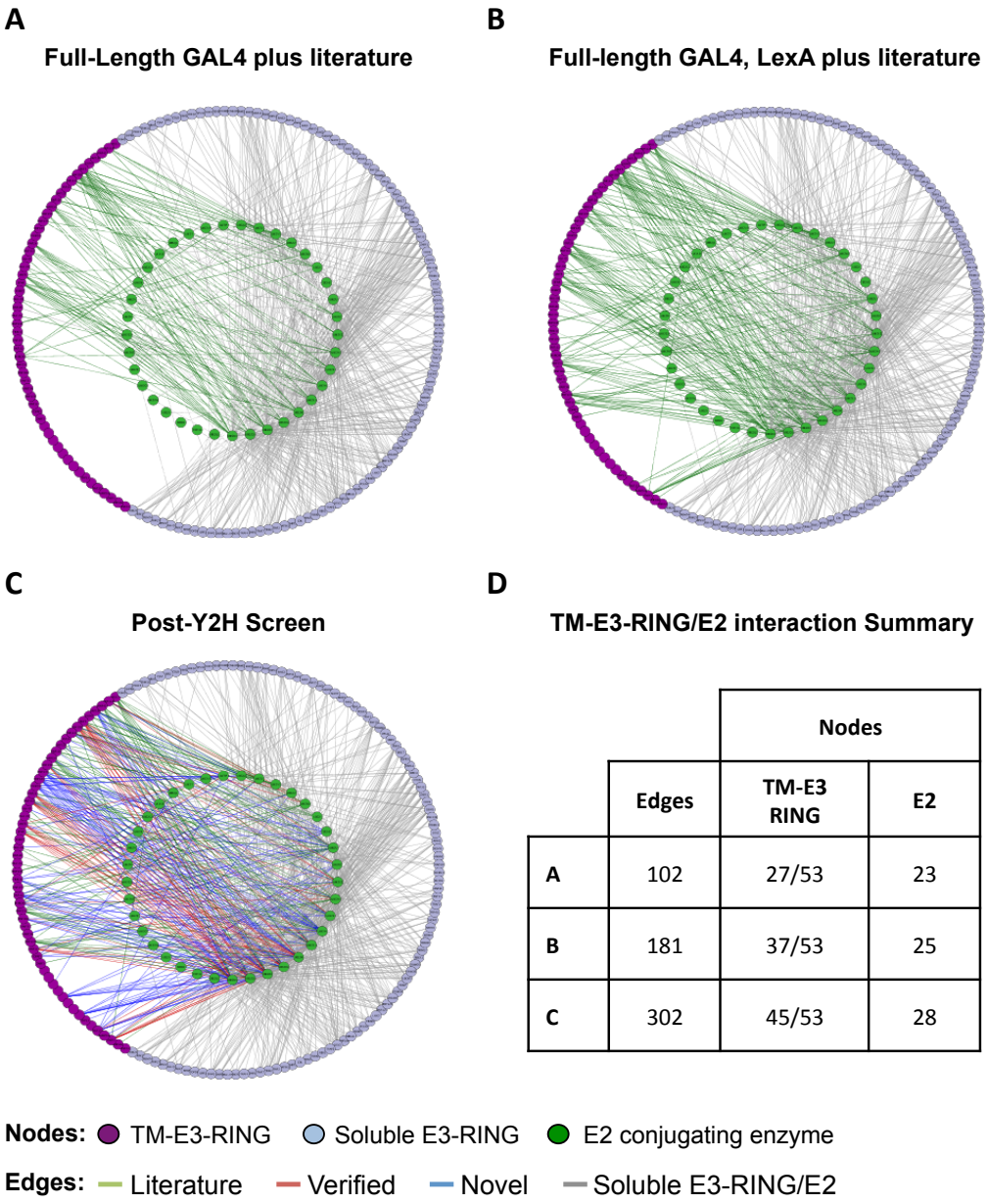

Figure 3.8 Binary TM-E3-RING/E2 interaction networks. Comparative coverage of the human TM-E3-RING/E2 interaction network before **(A & B)** and after **(C)** the CRD-GAL4 screen. **(A)** TM-E3-RING/E2 interaction coverage at the time of initiating the current study with data collated from full-length GAL4 screens (Markson, Kiel et al. 2009) and other literature-derived interaction data. **(B)** Integration of full-length GAL4 plus literature data with LexA-based Y2H data (van Wijk, de Vries et al. 2009) and **(C)** integration with CRD-GAL4 screen data. Nodes (circles) represent proteins and edges (lines) represent binary interactions between proteins. **(D)** Tabular display of TM-E3-RING/E2 network coverage showing interactions and number of TM-E3-RINGs and E2s represented in each network (panels A, B & C).

Comparative analysis of interaction data from CRD-GAL4 screens with full-length GAL4 and LexA based Y2H screens emphasise the value of utilising CRD TM-E3-RING clones in directed Y2H assays. Despite the high number of novel interactions identified in our CRD-GAL4 screen, the orthogonal LexA and full-length GAL4 Y2H screens provide additional coverage of TM-E3-RING/E2 interactions and therefore represent highly complementary datasets.

3.5. Generating a high-density TM-E3-RING/E2 interaction network

In order to develop a high-density TM-E3-RING/E2 interaction network, data from CRD GAL4, full-length GAL4, and LexA Y2H screens was collated with other literature-derived interactions. In terms of network coverage, ~ 80% of TM-E3-RINGs were tested in at least two screens with only 11/53 TM-E3-RING proteins being tested in only one Y2H screen. Similarly 38/39 E2 proteins were tested in more than one study, with UBE2G2 being the exception, as this clone displays an autoactivation phenotype in both GAL4 based Y2H screens.

Literature-derived interactions were obtained from the two directed TM-E3-RING/E2 Y2H studies (Markson, Kiel et al. 2009; van Wijk, de Vries et al. 2009), manual curation and data derived from three independent databases (HPRD, BioGrid, IntACT). All data was combined to form a non-redundant binary network of all known human E3-RING/E2 protein interactions (Figure 3.8B). Upon collation with CRD-Y2H data obtained within this study, the unified TM-E3-RING/E2 network incorporated 28 E2 proteins and 45 TM-E3-RING proteins (Figure 3.8C), with the number of known TM-E3-RING/E2 interactions increasing from 181 to 302. This represents a 67% increase in network density with 121 previously unreported

interactions detected in CRD-GAL4 screens highlighting the novelty of data obtained in this study (Figure 3.8B-D).

Analysis of E2 degree profiles before and after inclusion of CRD-Y2H data reveals 20 E2 proteins to have novel TM-E3-RING interaction partners as a result of the CRD-Y2H screen (Figure 3.9A). Furthermore, UBE2O and the UEV proteins TSG101 and UEVLD are annotated specific TM-E3-RING partners in CRD-Y2H screens, which were previously not linked into the TM-E3-RING/E2 network. Striking differences in connectivity of E2 proteins is observed in the collated network, ranging from highly restricted to broad-specificity interaction profiles (Figure 3.9A). Members of the UBE2D, UBE2E, UBE2U, UBE2W, UBE2N, and UBE2K families all exhibit high TM-E3-RING degree with ≥ 10 TM-E3-RING interaction partners. The UBE2D family accounts for approximately one third of all TM-E3-RING interactions in the combined TM-E3-RING/E2 network with 101 interactions observed between the four family members. Members of the closely related UBE2E family account for a further 42 interactions between the 3 family members (Figure 3.9A). In contrast a number of E2 proteins such as UBE2O, UBE2M and UBE2Q1, represent highly specific E2s with ≤ 2 selective TM-E3-RING protein partners. Finally, a number of E2 proteins (UBE2S, UBE2F, UBE2C, UBE2A, UBE2B, UBE2G1, UBE2R2, CDC34, BIRC6, UBE2Q2) still lack any known TM-E3-RING interaction partners (Figure 3.9A) despite several of these proteins were found to interact with soluble E3-RING proteins (supplementary file ‘full-length_CRD GAL4Y2H comparison’).

From the TM-E3-RING perspective, the integration of all available interaction data resulted in ~ 85% (45/53) of TM-E3-RING proteins being assigned selective E2 interaction partners (Figure 3.9B). CRD-Y2H screens identified novel E2 interaction

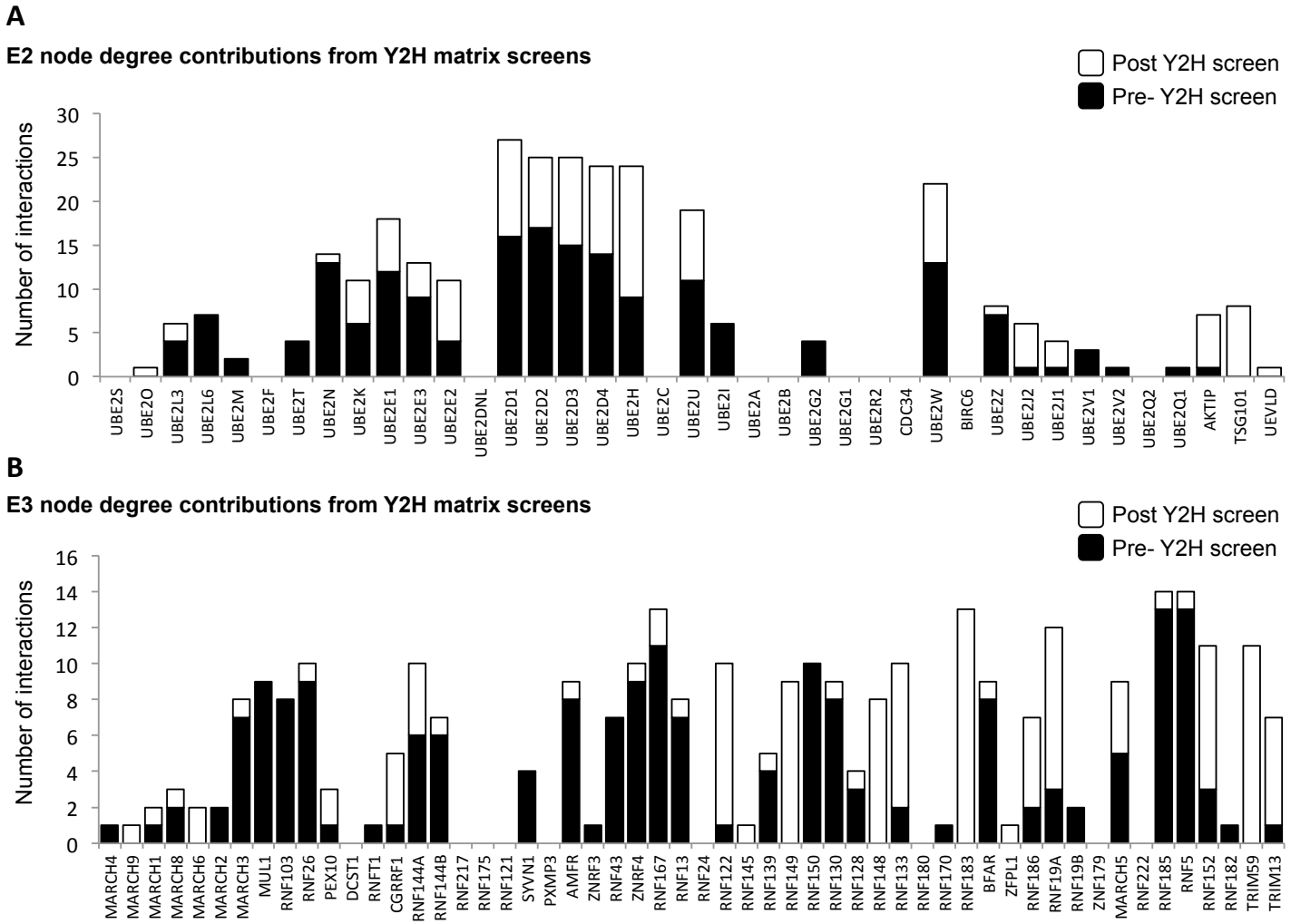

Figure 3.9 CRD-Y2H and literature contributions to TM-E3-RING and E2 degree. **(A)** E2 degree and **(B)** TM-E3-RING degree pre- (black bars) and post- (white bars) CRD-GAL4 Y2H screens. Pre-screen data (black bars) incorporates both previous directed HTP-Y2H screens (Markson, Kiel et al. 2009; van Wijk, de Vries et al. 2009) and all literature curated information.

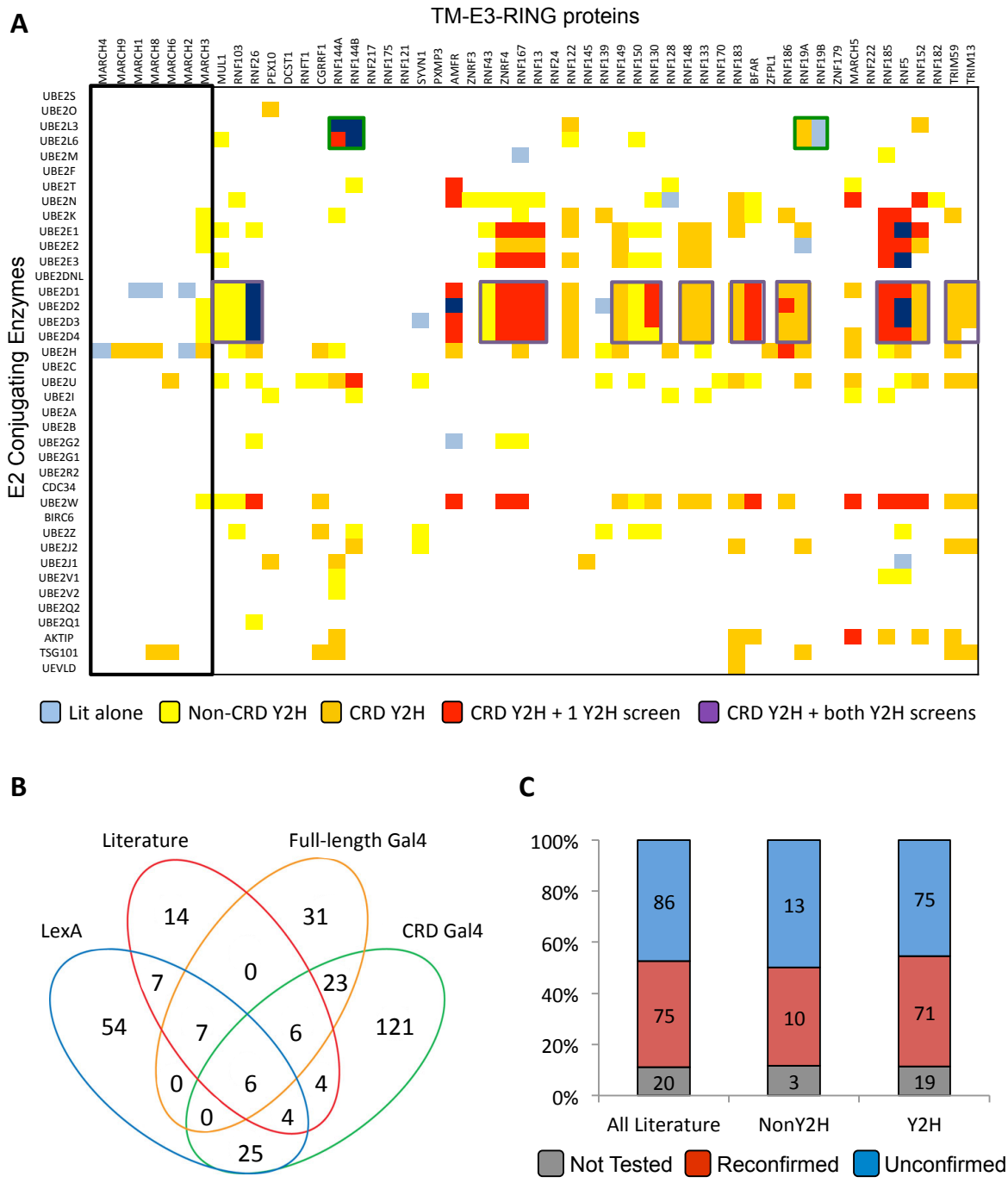

Figure 3.10 Total binary TM-E3-RING/E2 interactions provided by all available datasets. (A) Heatmap representation of binary TM-E3-RING/E2 interactions according to the number of data sources in which a given interaction has been observed. E2 and TM-E3-RING proteins are ordered based on primary sequence similarity in ClustalW. **(B)** Breakdown of total TM-E3-RING/E2 binary interactions according to interaction data source. (**C)** Reconfirmation rates of total, non-Y2H, and Y2H literature derived interactions in CRD-Y2H screens.

partners for 33/53 TM-E3-RING proteins whilst E2 partners were identified for 8 TM-E3-RING proteins, which previously had none (Figure 3.9B).

To assess the contribution of the CRD-GAL4 Y2H screen to overall network density the verification rate of reported interactions and novelty of CRD-GAL4 Y2H data was calculated. Importantly, 65% (196/302) of total TM-E3-RING/E2 interactions were observed in the CRD-GAL4 screen, of which 121/302 (> 40%) represent novel interactions, demonstrating a significant contribution to overall network density (Figure 3.10B). Of the literature interactions retested in our study 47% (75/161) were reconfirmed (Figure 3.10C), reflecting a high rate of verification compared to that expected between orthogonal Y2H assay systems (Braun, Tasan et al. 2009; Chen, Rajagopala et al. 2010). Retested interactions derived from literature databases were also analysed to establish verification rates of data derived from different interaction methodologies revealing comparable reconfirmation rates for Y2H (71/146; 49%) and non-Y2H (10/23; 43%) interaction sources (Figure 3.10 C).

TM-E3-RING/E2 interactions observed in the total network are dispersed throughout the phylogeny of TM-E3-RING proteins with few areas of data paucity (Figure 3.10A & 3.11). However, a number of TM-E3-RING proteins, including several members of the MARCH sub-family (black box in Figure 3.10A) and TM-E3-RINGs closely related to the peroxisomal PXMP3 and PEX10 proteins exhibit few or zero E2 interaction partners. To observe phylogenetic trends in TM-E3-RING/E2 interaction patterns combined interaction data was plotted in phylogenetic order in heatmap format (Figure 3.10A). Despite the observation of clusters of TM-E3-RING/E2 interactions, there are few distinct patterns based on E2 or TM-E3-RING primary sequence similarity. For example, whilst clusters of phylogenetically

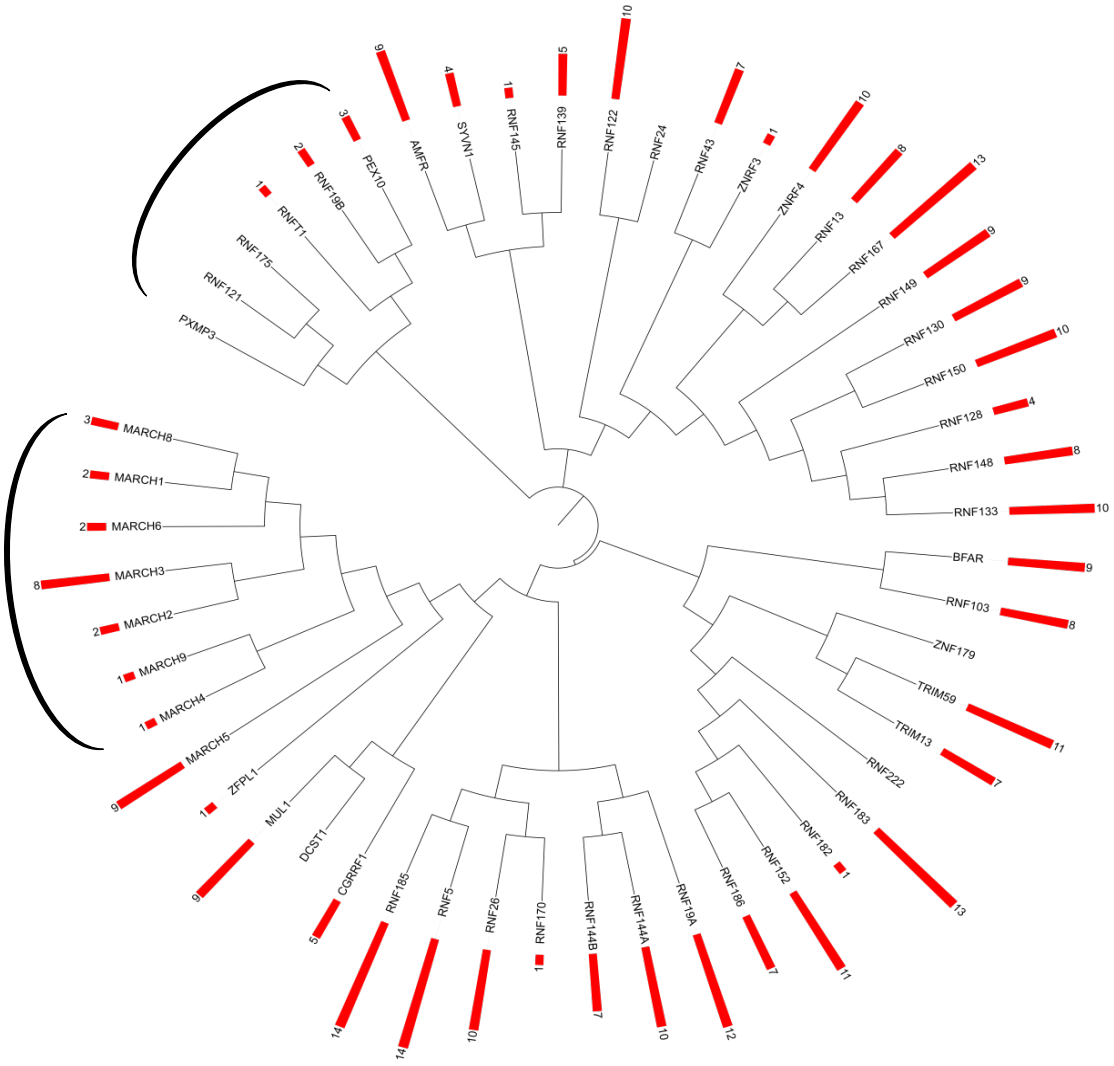

Figure 3.11 Dendrogram showing E2 binding degree across the TM-E3-RING family. TM-E3-RING entrez gene symbols are ordered within the dendrogram according to primary protein sequence similarity in ClustalW. Red bars and associated numbers for each TM-E3-RING protein represent E2 degree. Clusters of related TM-E3-RING proteins with limited/no E2 interaction partners are highlighted by black bars. Figure generated using ITOL (Letunic and Bork 2007).

similar TM-E3-RING proteins interact with members of the UBE2D family of E2 proteins, this can be observed across the entire family of TM-E3-RING proteins (Figure 3.10A; purple boxes). This is also apparent for other highly connected, or promiscuous, E2 proteins (E.g. UBE2E, UBE2W, UBE2U) as well as those that exhibit more restricted TM-E3-RING interaction profiles. For example RNF144A and RNF144B interact with the closely related UBE2L3 and UBE2L6 TM-E3-RINGs as well as the phylogenetically distinct RNF19A and RNF19B proteins (Figure 3.10 A; green boxes).

To further investigate phylogenetic trends, TM-E3-RING/E2 interaction data was mapped onto the total combined E3-RING/E2 interaction network (Figure 3.12). In similarity to the TM-E3-RING/E2 heatmap, clusters of E2 interactions are observed between phylogenetically similar E3-RING proteins yet this can be observed across the entire family of E3-RING proteins. For example, whilst clusters of soluble and transmembrane TM-E3-RING proteins interact with the UBE2L3 and UBE2L6 proteins, they are dispersed across the entire phylogeny of E3-RING proteins (Figure 3.12; green boxes). In addition, numerous clusters of related E3-RING proteins interact with UBE2D family members (Figure 3.12; purple box). As such, prediction of interaction partners based on sequence similarity remains a difficult challenge. It is however interesting to note that soluble E3-RING proteins closely related to the MARCH family of E3-RING proteins largely also appear to lack interactions with UBE2D, UBE2E and other highly promiscuous E2 proteins with a more limited selection of E2-binding partners.

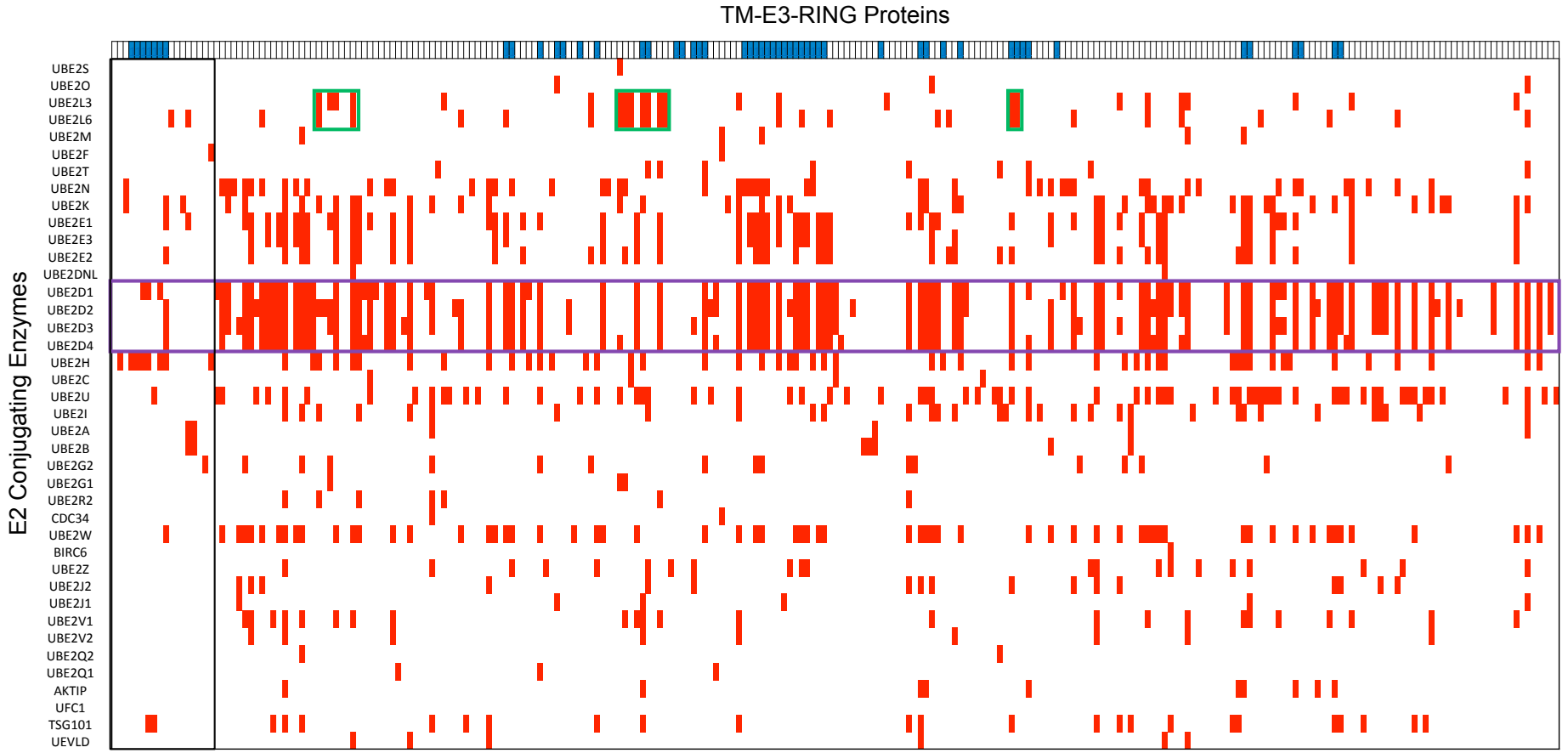

Figure 3.12 Total E3-RING/E2 interactions (A) Heat-map showing all known E3-RING/E2 interactions. E2 and TM-E3-RING proteins are ordered based on primary sequence similarity. TM-E3-RING proteins are indicated by blue bars above heatmap. UBE2D interaction promiscuity with E3-RINGs is highlighted by purple bar. A cluster of E3-RING proteins, which includes MARCH TM-E3-RINGs and a number of soluble RINGs, that exhibit restricted E2 interaction profiles are highlighted by black bar.

3.5.1. Co-occurrence of E2 partners for a given TM-E3-RING

Whilst E3 proteins are largely considered to regulate substrate selection, E2 proteins have been shown to play a central role in dictating the architecture of poly-ubiquitin chain formation on modified substrates (David, Ziv et al. 2010). Mechanistically, the poly-ubiquitination of substrate proteins can be controlled by designated 'initation' and 'elongation' E2 proteins, which can be recruited by the same E3-RING protein ((Christensen, Brzovic et al. 2007) and see section 1.4.3.2). To identify potential functionally linked E2 proteins, co-occurrence analyses were performed to determine the frequency with which any two E2 proteins appear together in the binding profiles of TM-E3-RING or soluble E3-RING proteins. The frequency that pairs of E2s exhibit common TM-E3-RING protein partners was calculated and expressed in heatmap format as a ratio of the total number of interactions detected for each E2 protein. To limit potential biases as a result of low coverage and to allow meaningful insights to be drawn, only those E2 proteins that exhibited $\geq$ 4 TM-E3-RING interactions (with the exception of UBE2V1 and UBE2V2) were investigated. This analysis could address a number of questions, including; 'if a given E2 (X) is present in a subset of E3-RING binding profiles, what proportion of these E3-RINGs also bind to a second common E2 protein (Y)?' As such, it was also possible to determine if a pair of E2 proteins always co-occur in the interaction profiles of E3-RING proteins, or whether the interaction profile of one E2 is the subset of a second.

Naturally, a single E2 enzyme will always occur in 100% of its own E3 interaction profiles and is represented in Figure 3.13A&B by the dark blue diagonal line. Given their primary sequence similarity, E2s within the same subfamily may be expected

to exhibit highly similar binding profiles (Figure 3.13C). This trend is observed for both the expansive UBE2D and UBE2E families, whereby individual family members largely co-occur in the binding profiles of TM-E3-RING proteins. This analysis reveals several emergent properties of E3-RING/E2 interaction networks, which may be important in guiding future investigations into the molecular basis of E3-RING/E2 specificity. Notably, the UBE2E and UBE2W families are largely restricted to a subset of TM-E3-RING partners that interact with the UBE2D subfamily. However, UBE2D does not always co-occur with UBE2E or UBE2W (Figure 3.13A; red and yellow boxes). Highly similar patterns of co-occurrence were also observed for these E2 proteins when investigating the more expansive soluble E3-RING/E2 network implying a general trend within the ubiquitome network (Figure 3.13B). The high rate of co-occurrence between UBE2D, UBE2E and UBE2W proteins may suggest functional linkages between these proteins and members of the UBE2D family, whilst UBE2D proteins may have a range of different functions independent of UBE2E and UBE2W proteins.

Members of the UBE2D family have been shown to prime substrates with a single ubiquitin moiety prior to UBE2N (Dodd, Allen et al. 2004) and CDC34 (Wu, Kovacev et al. 2010) mediated K63 and K48 poly-ubiquitin chain elongation, respectively. Additionally, independent studies revealed that a single E3-ligase complex (BRCA1/BARD1) can utilise the UBE2D, UBE2E, UBE2W E2s to nucleate substrate proteins with a single ubiquitin moiety, which acts as an initiation signal for subsequent K63 and K48 chain elongation by the hetero-dimeric UBE2N/UBE2V1 and UBE2K E2s (Christensen, Brzovic et al. 2007). In agreement with these reports, the present analysis reveals a high degree of co-occurrence between the elongation E2s UBE2N and UBE2K with members of the UBE2D and UBE2W families (and to

a lesser extent UBE2E) (Figure 3.13A&B; black boxes). Additional functional linkages may be inferred for several other E2 proteins, including UBE2G2, UBE2Z, and UBE2J2, that exhibit a similar rate of co-occurrence with the UBE2D/UBE2W/UBE2E families.

Interrogation of the soluble and transmembrane E3-RING/E2 network reveals additional trends. Interestingly, the four catalytically inactive UEV proteins with ≥ 4 E3-RING partners in these datasets exhibit differential patterns of E2 co-occurrence. Three of the UEV proteins (UBE2V1, UBE2V2 and AKTIP) bind almost exclusively to a small subset of E3-RING proteins that bind to the UBE2D family of E2 proteins (Figure 3.13A&B; central turquoise box), whilst TSG101 co-occurs less frequently with UBE2D family members (Figure 3.13A; central turquoise box). Despite their high sequence similarity, UBE2V1 and UBE2V2 appear to have different co-occurrence patterns. UBE2V2 is present almost exclusively in a subset of UBE2V1 E3-RING binding profiles yet co-occurs with UBE2N to a much higher degree than UBE2V1 (left turquoise box) which in contrast exhibits an increased frequency of co-occurrence with UBE2W (right turquoise box). AKTIP exhibits a highly similar profile to UBE2V1 whilst TSG101 appears to have a diverse co-occurrence binding profile to other UEV proteins.

Whilst UEV proteins are not capable of directly conjugating ubiquitin, UBE2V1 and UBE2V2 act in conjunction with UBE2N to specify formation of K63-linked poly-ubiquitin chains in NF-kB signalling (Andersen, Zhou et al. 2005) and DNA repair (Windheim, Peggie et al. 2008), respectively. This is achieved by UBE2V1 or UBE2V2-mediated orientation of a donor ubiquitin moiety for optimal formation of K63 chains by the active E2, UBE2N (Eddins, Carlile et al. 2006). Equivalent roles

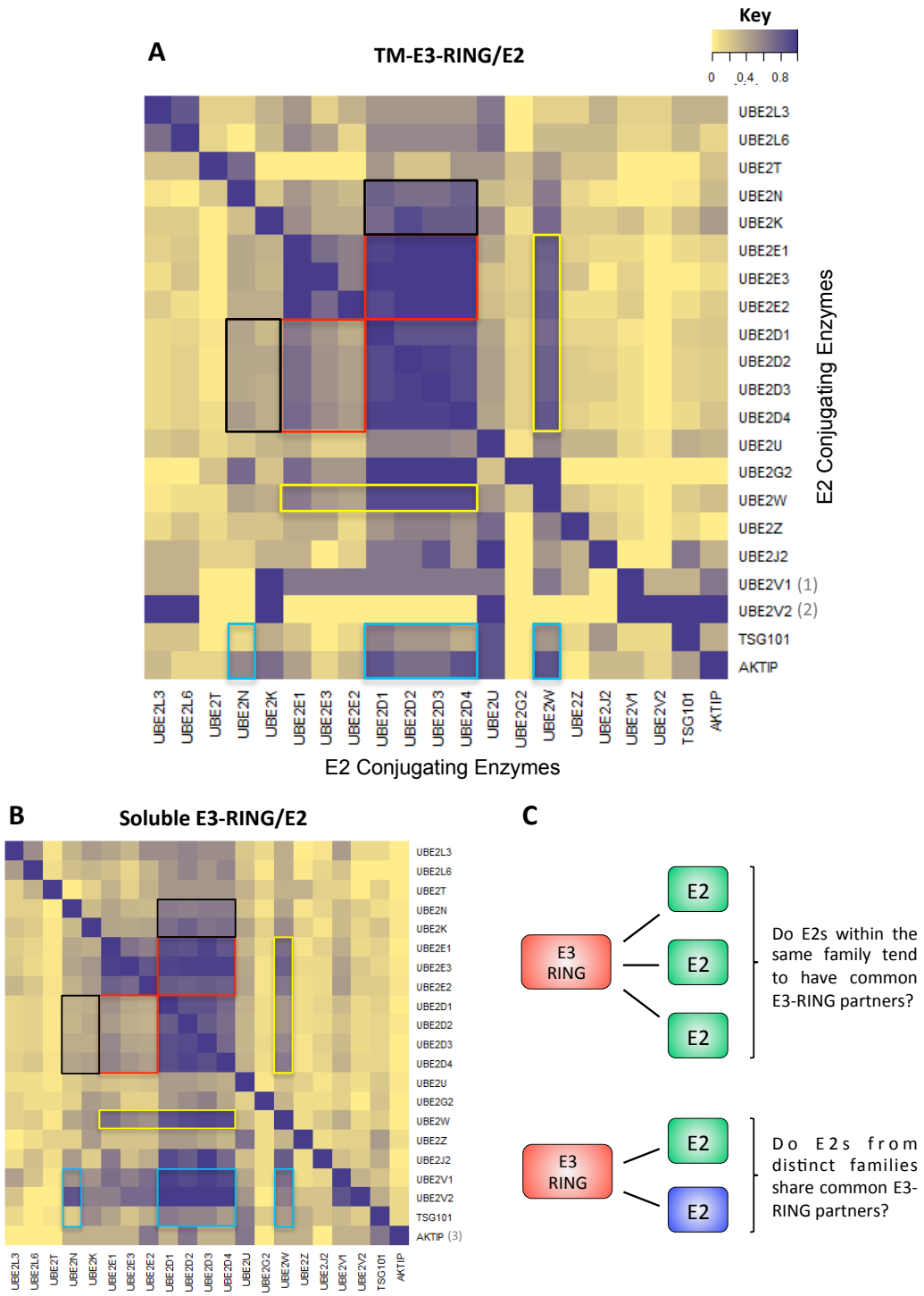

Figure 3.13 Co-occurrence of E2 proteins in (TM-)E3-RING binding profiles. Heatmap representation of E2 co-occurrence within TM-E3-RING **(A)** and soluble-E3-RING **(B)** interaction profiles. Colour scheme represents the proportion of E3-RING interactions mediated by E2s on the vertical axis that are also mediated by E2s on the horizontal axis. Dark blue tends towards 100% of TM-E3-RING interactions by E2s on the vertical axis shared by E2s on the horizontal axis. Pale yellow represents low-scale values. Schematic representation of E2s within **(A)** the same or **(B)** different families co-occurring in E3-RING binding profiles.

of other UEV proteins have not currently been reported. However, the highly similar co-occurrence profiles of UBE2V1 and AKTIP may implicate a similar role and mechanism of action of AKTIP in ubiquitination events. Similarly, TSG101 may also fulfil a similar role but aid polyubiquitination with other active E2 enzymes.

3.6. Discussion

To develop a comprehensive understanding of how specificity and functionality is controlled within the human ubiquitin system it is essential that we first define the interactions that occur between its composite parts. The combinatorial nature of TM-E3-RING/E2 interactions was initially proposed by small-scale studies (Brzovic and Klevit 2006; Christensen, Brzovic et al. 2007) with subsequent HTP Y2H analysis revealing the true complexity of the E3-RING/E2 network (Markson, Kiel et al. 2009; van Wijk, de Vries et al. 2009). Despite the resulting increase in coverage of E3-RING/E2 interactions, a considerable area of data paucity remained for the subset of E3-RING proteins predicted to contain transmembrane regions. The work described in this chapter provides the first comprehensive and high-density binary interaction map of the human TM-E3-RING/E2 protein network through the adoption of a Y2H approach using the cytosolic RING domain (CRD) containing fragments of individual TM-E3-RING proteins, preserving the E2-binding RING domain region whilst removing problematic hydrophobic transmembrane domains. This data dramatically increased network density, and revealed new trends in TM-E3-RING/E2 partner preferences.

3.6.1. Orthogonal Y2H-systems generate different interaction profiles

Recent analyses of data derived from independent orthogonal assays highlights the value of using different interaction assays to increase coverage across common clone sets (Braun, Tasan et al. 2009; Rajagopala, Hughes et al. 2009; Chen,

Rajagopala et al. 2010). Interestingly, different Y2H approaches have been shown to enhance detection of novel protein-protein interactions as using a combination of more diverse orthogonal interaction assays (Chen, Rajagopala et al. 2010).

Comparative analysis of data from CRD-Y2H or full-length Y2H screens demonstrated the utility of CRD-clones for identifying novel E2 interaction partners, exhibiting considerably elevated numbers of total interactions for co-tested TM-E3-RING/E2 protein pairs coupled with a high rate of reconfirmation of full-length interactions (58%). An additional 60 novel interactions were observed for 5 TM-E3-RING clones which were only functional in CRD-Y2H screens. As such, CRD fragment clones represent a valuable tool in determination of this class of protein-protein interaction. Despite these findings, 30 interactions were only observed in full-length TM-E3-RING screens. These interactions were subsequently shown to be attributed to E2s that exhibit higher numbers of interaction partners then observed with full-length compared to CRD TM-E3-RING clones (UBE2K, UBE2I, UBE2M, UBEV1, UBE2V2). It remains to be seen whether these findings implicate regions outside of the cytosolic RING domain in the formation of positive interactions with these E2 proteins, or whether hydrophobic or charged regions of transmembrane domains result in interaction detection with this cohort of E2 proteins within the Y2H system.

During the course of this study, a second directed E3-RING/E2 interaction network was published using a LexA-based Y2H system and UBC or E3-RING domain-specific clones (van Wijk, de Vries et al. 2009). Comparison of data for TM-E3-RING/E2 pairs tested in both studies revealed a 25% overlap between screens, which is comparable to the degree of similarity expected between other orthogonal

Y2H studies (Chen, Rajagopala et al. 2010). As different Y2H vectors, yeast strains, and domain regions were used in the two studies it is difficult to ascribe differences in interaction profiles to any one factor. Comparative analysis of data from the CRD-GAL4 Y2H study with analogous data from both the LexA-based and full-length GAL4 Y2H screens revealed similar emergent properties of the TM-E3-RING/E2 interaction network, which are discussed below. Furthermore, these analyses revealed how different Y2H approaches can provide highly complementary data. As such, the utilisation of multiple Y2H and other interaction approaches is necessary to enable maximal coverage of binary protein-protein interaction networks to be achieved

3.6.2. Emergent trends in TM-E3-RING/E2 interaction partners

3.6.2.1. Highly connected E2 enzymes and TM-E3-RING protein pairs

Interrogation of TM-E3-RING/E2 interaction profiles reveals several emergent properties of the network. Notably, the UBE2D and UBE2E families of E2 proteins were responsible for almost half of the total TM-E3-RING/E2 interactions. Additionally, a single UBE2W clone displayed similar interaction coverage in comparison to UBE2D or UBE2E members. The ‘promiscuous’ nature and diffuse localisation (cytosolic and nuclear) of UBE2D family members (Plafker, Plafker et al. 2004) may reflect a broad role of this E2 family in cellular ubiquitination events (Markson, Kiel et al. 2009). The UBE2E and UBE2W family display more restricted TM-E3-RING partner profiles to UBE2D and exclusively bind to a subset of TM-E3-RINGs that interact with UBE2D proteins with the sole exception of CGRRF1, which interacts with UBE2W but not UBE2D or UBE2E proteins. Both UBE2E and UBE2W family members exhibit restricted subcellular localisation patterns and are predominantly expressed within the nucleus yet shuttle between this compartment

and the cytosol dependent upon ubiquitin 'loading' of their active site cysteine residue (Plafker and Macara 2000; Yin, Ji et al. 2006). Taken together these findings may implicate more specific roles of the UBE2E and UBE2W family in nuclear ubiquitination events compared to potential 'housekeeping' functions of the UBE2D family, which is in agreement with previous reported functions for UBE2E (Lee, Hong et al. 2008) and UBE2W (Zhang, Zhou et al. 2011) proteins.

A large number of TM-E3-RING proteins that interact with UBE2E (50%; 8/18) or UBE2W (32%; 7/22) belong to a discrete subset of TM-E3-RING proteins, the PA-TM-RING subfamily. In agreement with potential nuclear roles of this subfamily, a member of the PA-TM-RING subfamily (RNF13) has been reported to undergo retrograde transport from endosomes to the inner nuclear membrane (INM) following activation of PKC signalling, positioning the RING domain in the nucleoplasm where it may mediate ubiquitination events (Bocock, Carmicle et al. 2010). Furthermore, Nuclear Localisation Signals (NLS) are predicted for 4 PA-TM-RING proteins between their N-terminal TM-region and C-terminal RING-domain (RNF13, RNF130, RNF150, and RNF167) whilst another PA-TM-RING has a predicted N-terminal NLS (ZNRF4) (supplementary file PsortII NLS prediction). Cytoplasmic tails of proteins released from the membrane by regulated proteolysis frequently undergo NLS-mediated import into the nucleus where they modulate transcription (Wolfe 2009). Regulatory proteases can promote the intramembranous cleavage of RNF13 allowing for dissociation of the C-terminal RING-domain from the membrane to enable ubiquitination events at multiple subcellular locations (Bocock, Carmicle et al. 2009; Bocock, Carmicle et al. 2011). Similarly, *in vitro* translation of a second PA-TM-RING in the presence of microsomal membranes led to the production of two forms of RNF128, with a cleavage of the full-length E3-

RING protein in the ER or cis-Golgi resulting in the generation of a smaller isoform (Guais, Siegrist et al. 2006). As such, intramembrane-cleavage or retrograde transport to the INM may reflect a recurring theme within the PA-TM-RING family, which enables participation in nuclear ubiquitination events. In addition to the PA-TM-RING proteins, a number of other UBE2E and UBE2W interactors are also predicted to either contain NLSs (RNF43, MARCH3, and RNF103) or have been previously localised to the nuclear membrane (RNF19A, RNF43, MUL1, RNF5, and AMFR) (supplementary file PsortII NLS prediction).

3.6.2.2. Highly specific E2 proteins and TM-E3-RING protein pairs

Results from this study also highlight a number of E2 proteins that have highly specific TM-E3-RING interaction partners. For example, UBE2O, UBE2M and UBE2Q1 all have ≤ 2 TM-E3-RING partners, which may reflect highly specialised roles in cellular ubiquitination events. As UBE2M is a NEDD4 specific E2 our data indicates a potentially novel role for RNF167 and RNF185 in NEDDylation events. Both RNF167 and RNF185 also interact with ubiquitin-specific E2 proteins and therefore both may direct ubiquitination and NEDDylation events. The UBE2O and UBE2Q1 E2 enzymes remain relatively uncharacterised in the literature, however identification of selective TM-E3-RING partners may provide new insight into the mode of action of these E2 proteins. A number of E2 proteins (UBE2S, UBE2F, UBE2C, UBE2A, UBE2B, UBE2G1, UBE2R2, CDC34, BIRC6, UBE2Q2) have no known TM-E3-RING interaction partners. These findings are largely mirrored in the total E3-RING/E2 network, with the majority of these E2 proteins exhibiting ≤ 3 E3-RING interaction partners (with the exception of UBE2R2, UBE2A, UBE2B which have 6, 4, and 5 E3-RING partners, respectively; supplementary file ‘total interaction datasets’).

Whilst further investigation is required to determine whether the apparent fidelity of some E2 proteins is a true reflection of highly selective ubiquitination events, annotation of selective TM-E3-RING partners within this study may be used to inform future studies of E2 function. For example, the highly specific interaction observed between UBE2O and the peroxisomal TM-E3-RING ligase, PEX10, may implicate a role for this uncharacterised E2 protein in ubiquitination events at the peroxisomal membrane, potentially relating to PEX10-mediated peroxisomal biogenesis and protein import mechanisms (Cepinska, Veenhuis et al. 2011). As such, the comprehensive TM-E3-RING/E2 protein interaction map has provided a resource to direct future hypothesis-driven research and determine the physiological relevance of individual interactions reported in this study.

3.6.3. Combinatorial complexity of TM-E3-RING/E2 interactions

Analysis of the integrated TM-E3-RING/E2 network clearly demonstrates that the majority of TM-E3-RING proteins have the potential to interact with multiple E2 protein families. Such combinatorial complexity may underlie the ability of individual TM-E3-RING proteins to mediate distinct ubiquitination events within context-dependent complexes for selective ubiquitination of substrates. In addition, such combinatorial complexity may underlie the sequential activity of E2 proteins in the initiation and elongation of different forms of poly-ubiquitin chains (Christensen, Brzovic et al. 2007). The generation of a comprehensive TM-E3-RING/E2 interaction map in the present study has enabled the computational prediction of such potential functional linkages by determination of E2 co-occurrence in TM-E3-RING profiles. In agreement with the role of UBE2D, UBE2W, and UBE2E in priming substrates with a single ubiquitin moiety prior to subsequent elongation by UBE2N or UBE2K proteins (Christensen, Brzovic et al. 2007), a high degree of co-

occurrence was observed between UBE2N and UBE2K with UBE2D and UBE2W family members, and to a lesser extent UBE2E. The similarly high rate of co-occurrence of other E2s (UBE2G2, UBE2Z, UBE2J2) with UBE2D/UBE2W/UBE2E families may be suggestive of analogous functional linkages and may imply a general role of the UBE2D and UBE2W proteins in polyubiquitin chain 'initiation' for a number of other E2 proteins.

3.6.4. Remaining area of data paucity

Nine human TM-E3-RING proteins still have no known E2 interaction partners. Furthermore, certain phylogenetic TM-E3-RING sub-families exhibit lower numbers of E2 interactions including the MARCH family and the peroxisomal (PEX10 and PXMP3) and closely related TM-E3-RING proteins. It remains to be seen whether those TM-E3-RING proteins that have no E2 interaction partners have lost their ability to interact with E2 proteins or reflect false-negative interactions within Y2H studies. One additional possibility may be that some TM-E3-RING proteins may bind indirectly to E2 proteins through a process of heterotypic E3-RING/E3-RING interaction as described for a growing number of soluble E3-RING proteins (Brzovic, Keeffe et al. 2003; Linares, Hengstermann et al. 2003; Buchwald, van der Stoop et al. 2006). As such, it would be of interest to determine whether the restricted or lack of E2 partners for certain TM-E3-RING proteins reflects a true physiological fidelity of these TM-E3-RING/E2 pairings or whether additional co-factors or dimerization events are required in order for E2 binding to occur (Deshaies and Joazeiro 2009). Finally, it remains to be established whether E2 proteins, which exhibit lower numbers of interaction partners using CRD compared to full-length TM-E3-RING clones represent protein interactions which require determinants outside of the cytosolic RING domain in E2 binding.

A key question to be addressed is which of the interactions observed in this study represent physiologically relevant interactions *in vivo*. This is a difficult question to address due to the diverse range of cellular processes that could be regulated by different E2/TM-E3-RING combinations. However, development of interaction assays which can be used in live human cells, such as the firefly luciferase protein complementation (PCA) assay described in the next chapter may begin to deliver insights into the spatial, temporal and conditional nature of putative interaction profiles identified in this study.

4. Chapter 4: Secondary Verification of Y2H-derived TM RING/E3-E2 Network by Protein Complementation in mammalian cells

4.1. Introduction

To assess confidence in binary protein-protein interaction data it is important to re-assess a representative selection of primary interactions in alternative interaction systems or functional screens (Braun, Tasan et al. 2009). Detection of E3-RING/E2 protein interactions has proven to be problematic in most protein interaction systems. Whilst co-immunoprecipitation methods have been utilised to verify a subset of domain specific RING/UBC interactions (van Wijk, de Vries et al. 2009), the transient and weak nature of most E3-RING/E2 interactions has limited the applicability of this approach (Deshaies and Joazeiro 2009). For this reason, *in vitro* ubiquitination assays have been widely used to assess the potential relevance of putative E3-RING/E2 interactions detected in primary Y2H screens (Christensen, Brzovic et al. 2007; Markson, Kiel et al. 2009).

To provide an initial measure of interaction network confidence, TM-E3-RING/E2 interactions reported by CRD-GAL4 Y2H screening was compared in the previous chapter with two high-quality orthogonal Y2H datasets, which share many common tested TM-E3-RING/E2 pairs (Markson, Kiel et al. 2009; van Wijk, de Vries et al. 2009). Whilst favourable correlation was observed between CRD-Y2H and orthogonal Y2H assays was that was comparable to previously reported orthogonal studies assayed using an identical 'gold-standard' positive interaction ORF collection (Chen, Rajagopala et al. 2010), we sought to investigate the utility of a protein complementation assay (PCA) system to examine selective TM-E3-RING/E2 interactions *in vivo*.

4.2. Protein complementation assay (PCA)

Protein complementation assays (PCA) exploit the modular nature of certain reporter proteins in order to identify and quantify protein interactions in prokaryotic or eukaryotic cells (Morell, Ventura et al. 2009). Following the rational dissection of a reporter protein into two non-functional fragments, functional activity can be restored upon proximity induced refolding of reporter fragments. The co-expression of potential interaction partners in fusion with reciprocal reporter fragments therefore allows for binary protein interactions to be investigated, which position the two complementary PCA reporter fragments in close proximity facilitating protein refolding and reconstitution of functional activity (Hu and Kerppola 2003). The PCA reconstitution strategy has been successfully utilised in the investigation of binary protein interactions for several different PCA systems including luminescent (e.g. Firefly and *Renilla* luciferase (Paulmurugan and Gambhir 2003; Hida, Awais et al. 2009)), fluorescent (e.g. GFP and spectral variants (Lee, Kim et al. 2011)) and other enzymatic reporters (e.g. DHFR and Beta-Lactamase (Tarassov, Messier et al. 2008)).

Fluorescence-based PCA systems may represent useful tools for detection of weakly-associating or transient protein interactions in mammalian cells due to the irreversible nature of fluorescent reporter refolding (Nyfeler, Michnick et al. 2005). However, previous studies within the Sanderson laboratory have suggested that split-GFP PCA interaction systems are ineffective in the study of E3-RING/E2 interactions (personal communication, Prof. Christopher Sanderson), which may result from the requirement for de novo formation of the chromophore within the reassembled reporter protein providing a relatively slow response to protein-protein interactions (Reid and Flynn 1997). Furthermore, the lack of enzymatic amplification

and requirement for exogenous illumination may limit the interaction sensitivity of split-fluorophore based systems compared to other PCA-based systems (Massoud and Gambhir 2003; Misawa, Kafi et al. 2010). As such, binary TM-E3-RING/E2 interactions may avoid detection in these assay systems due to their low affinity and transient nature or may require high levels of expression to achieve signals above background cellular fluorescence.

In contrast, the reversible and instantaneous reconstitution of functional activity associated with luciferase fragment complementation, coupled with low background luminescence in mammalian cells, promotes the use of luciferase-based PCA systems for investigation of transient or conditional interactions in human cells (Hida, Awais et al. 2009). The previous exhaustive examination of N- and C-terminal polypeptide fragments of the dissected Firefly luciferase reporter have identified the optimal amino acid fragments for generation of superior signal-to-noise ratio for reporter refolding as: 1-416 (N-terminal fragment; FLucN) and 398-550 (C-terminal fragment; FLucC) (Ozawa, Kaihara et al. 2001; Luker, Smith et al. 2004; Hida, Awais et al. 2009). The previously characterised pcDNA3-FLucN and pcDNA3-FLucC firefly luciferase PCA vectors were selected as a candidate mammalian PCA assay system for investigation of binary TM-E3-RING/E2 interactions and were Gateway^{TM}-converted to exploit the available library of sequence verified TM-E3-RING and E2 proteins. To this end, the RfB Gateway^{TM} cloning cassette was introduced into the pcDNA3-FLucC and pcDNA3-FLucN split firefly luciferase vectors, which were conFigured to generate either N-terminal (FLucN) or C-terminal (FLucC) domain fusions, in accordance with the orientation used in preliminary studies (Luker, Smith et al. 2004). As the available ORF library contained E2 proteins with in-frame stop codons and TM-E3-RING proteins without stop codons,

E2 and TM-E3-RING ORFs were expressed as FLucC and FLucN fusion proteins, respectively.

In addition to Firefly luciferase, a number of additional luciferase enzyme reporters have been identified and utilised in mammalian systems (Remy and Michnick 2006; Stefan, Aquin et al. 2007). In particular, firefly and Renilla luciferases catalyse the oxidation of different substrates with no crossover in activity or bioluminescence emission spectra; D-luciferin, 440-550 nm and coelenterazine, 575-610 nm, respectively (Fan and Wood 2007). As such, an 'unsplit' luciferase can be expressed in tandem with an alternative split luciferase reporter to provide an internal control for transfection efficiency and cell death (Hida, Awais et al. 2009). In the current PCA system, the Renilla luciferase was adopted as the internal control for normalisation of split firefly luciferase activity.

4.3. Validation of Gateway^{TM} converted firefly luciferase PCA vectors

Preliminary studies have highlighted optimization of linker length in luciferase-fusion proteins as an important factor in improving the efficiency of luciferase reporter fragment complementation and generation of optimal luminescence signals upon protein-protein interaction (Remy and Michnick 2001; Misawa, Kafi et al. 2010). To assess the effect of introducing Gateway^{TM} flanking sequences into the linker regions of pcDNA3-FLucC and pcDNA3-FLucN PCA vectors upon the efficiency of protein complementation reactions, firefly luciferase reporter activity was compared for the rapamycin-dependent interaction between FK506-binding protein (FKBP) and FKBP-binding domain of human mTOR (residues 2024-2113; FRB) using conventional and Gateway-converted pcDNA3-FLucC and pcDNA3-FLucN vectors.

In each case, reciprocal luciferase-fusion proteins were co-expressed in human HEK 293T cancer cells, and luciferase activity was measured 24 h post-transfection in the presence or absence of rapamycin (100 nM for 4 h). Reconstituted Firefly luciferase activity was measured following addition of D-luciferin substrate (LARII reagent) by total photon counts over a period of 4 s. Firefly luciferase signals were quenched and Renilla luciferase activity measured by total photon counts over 0.2 s following addition of co-elenterazine substrate (Stop&Glo reagent). Expression of a sole PCA fusion protein (FLucC-FRB or FLucN-FKBP), or co-expression of FKBP-FLucN and FRB-FLucC constructs in the absence of rapamycin, generated low-level luminescence signals in the presence of D-luciferin. The addition of rapamycin resulted in a dramatic increase in firefly luminescence signal for the FRB-FKBP positive interaction pair compared to identically transfected cells that were not subjected to rapamycin treatment for both conventional and Gateway^{TM}-converted luciferase PCA fusion constructs (Figure 4.1A; $p < 0.005$, $n = 5$). Importantly, no statistical difference was observed in reconstituted firefly luminescence signal between conventional and Gateway^{TM}-converted PCA fusion constructs.

To account for differences in firefly luminescence that may result from variations in transfection efficiency or cell death, firefly luciferase PCA signal was normalised to the internal un-split Renilla luciferase signal for each individual sample and expressed as fold change in normalised luciferase activity from HEK 293T cells transfected with the Renilla control alone. This normalised luciferase activity similarly revealed no statistical difference between conventional and Gateway^{TM} fusion constructs (Figure 4.1B). As such, Gateway^{TM}-converted firefly luciferase vectors were used for investigation of all future TM-E3-RING/E2 interactions in PCA screens.

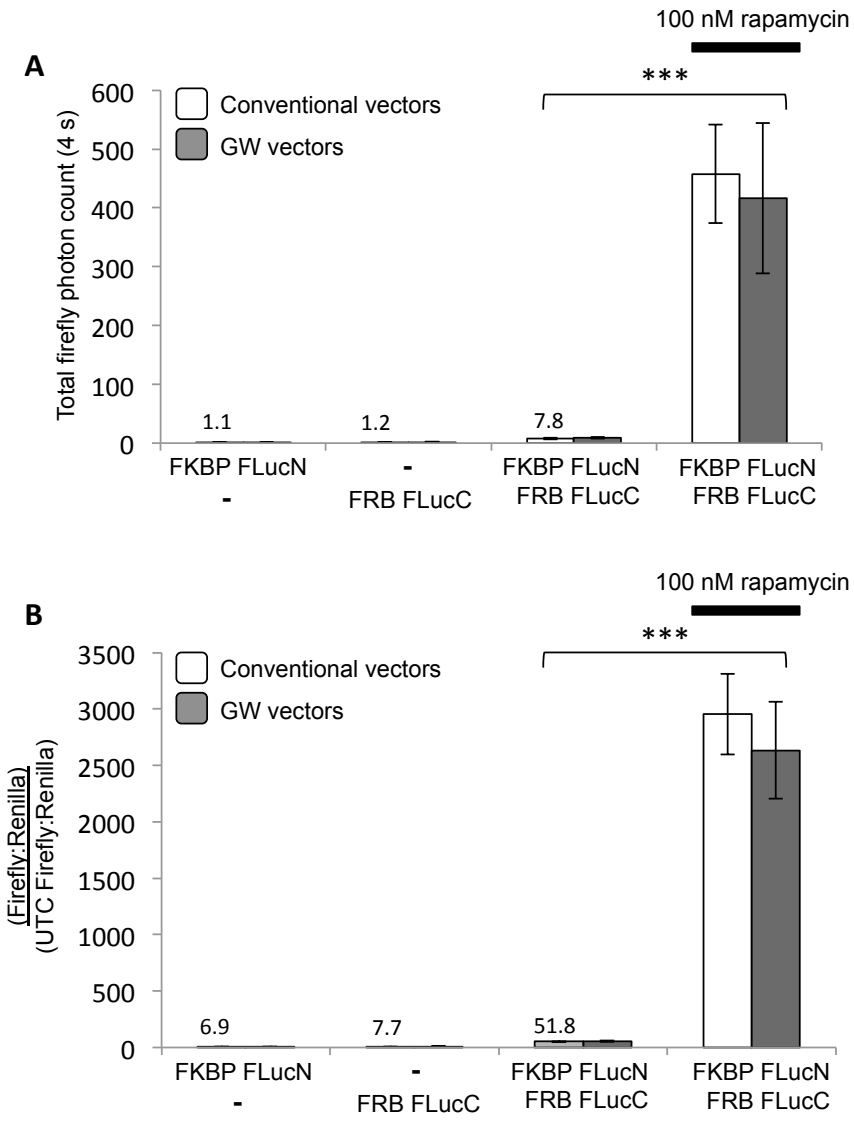

Figure 4.1 Gateway™ conversion of firefly luciferase PCA vectors does not adversely affect interaction-induced reconstitution of luciferase PCA activity. Using the characterised rapamycin-dependent FKBP/FRB interaction, HEK 293T cells were transiently transfected with conventional or GW-converted firefly luciferase vectors (FKBP-FlucN and/or FRB-FLucC; 0.5 ng/well) and pRL-SV40 (Renilla luciferase; 0.1 ng/well). Luciferase activity was measured 24 h post-transfection in the presence or absence of rapamycin (100 nM for 4 h). HEK 293T cells were lysed using PLB and sequential measurements of firefly and Renilla luciferase activity was measured upon addition of appropriate substrate. Total photon counts were recorded for 4 s (Firefly) and 0.2 s (Renilla). **(A)** Total firefly luciferase activity and **(B)** normalised relative light units (RLU) are shown (n = 5). Error bars represent std dev. Student's T-Test was performed for analysis. P-values < 0.005 (***) are indicated.

4.4. Direct orthogonal luciferase PCA assays

To perform a direct comparison with data obtained in primary CRD-Y2H screens, sequence-verified CRD TM-E3-RING and full-length E2 ORFs were transferred by LR recombination reactions into FLucC GW and FLucN GW Firefly luciferase PCA vectors, respectively. This strategy enabled the investigation of potential interactions between distantly related TM-E3-RING proteins across a broad range of E2 conjugating enzyme families (UBE2Ds, UBE2Es, UBE2L, UBE2W, and UBE2N families).

4.4.1. Catalytically-inactive and wild type E2 comparison

The ability of E3-RING proteins to catalyze their own auto-ubiquitination in the presence of E2 enzyme partners is a recurring theme in ubiquitin systems (de Bie and Ciechanover 2011), as exemplified by the MDM2 and CBL ligases (Fang, Jensen et al. 2000; Ryan, Davies et al. 2006). This may represent a potential obstacle for the detection of TM-E3-RING/E2 interactions within mammalian cells, in which turnover of active complexes could limit interaction detection of protein interaction partners.

To address this possibility, putative TM-E3-RING/E2 complexes involving UBE2D2, UBE2E1, and UBE2W proteins were generated and tested in luciferase PCAs as wild-type and catalytically-inactive mutant FLucN fusions. Inactive mutant clones were generated by substitution of the E2 UBC domain catalytic cysteine with an alanine residue to render E2s incapable of becoming charged with ubiquitin moieties.

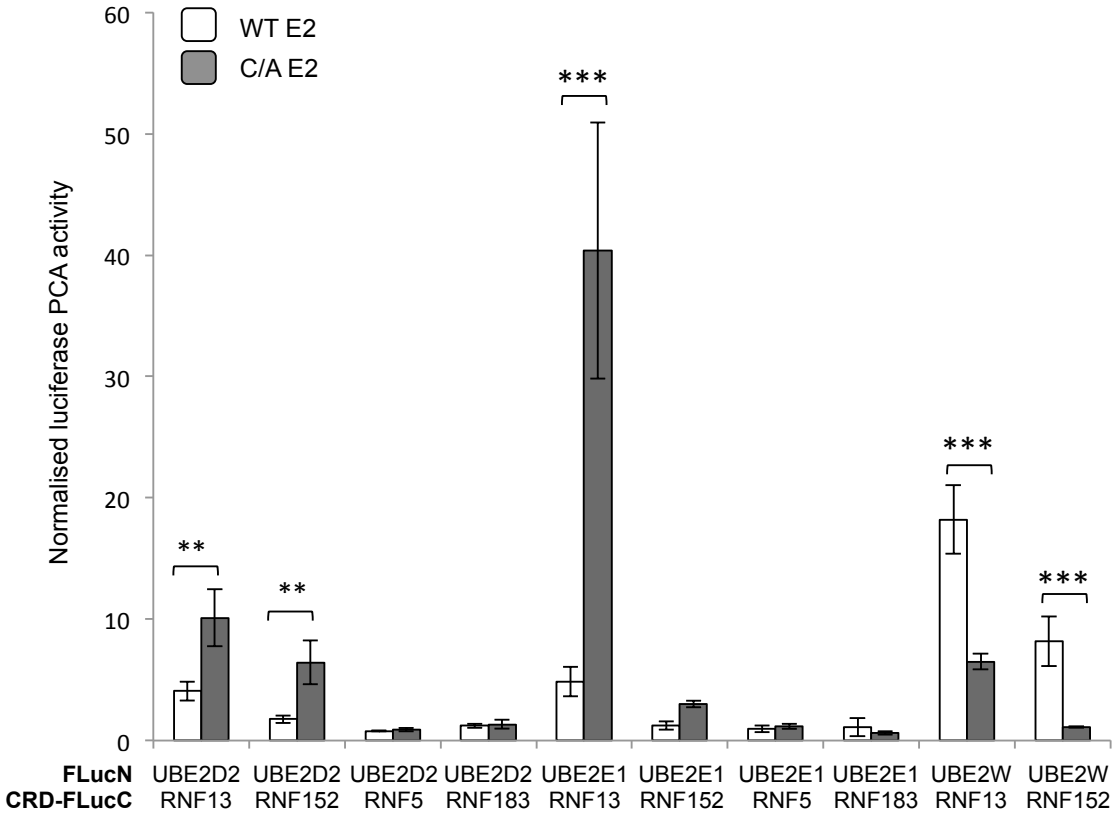

Figure 4.2 E2 protein inactivation confers differential effects upon CRD TM-E3-RING/E2 activity in luciferase PCA assays. HEK 293T cells were transiently transfected with pRL-SV40 (0.1 ng / well), FlucC GW and FlucN GW (0.5 ng / well) fusion constructs. Luciferase activity was measured 24 h post-transfection. Total photon counts were recorded for 4 s (Firefly luciferase) and 0.2 s (Renilla luciferase). Results are a normalised ratio of Firefly:Renilla activity and expressed as fold change from the most stringent negative control for each TM-E3-RING/E2 pair (n = 3). Error bars represent std dev. Student's T-Test was performed to determine statistical differences in luciferase PCA activity for wild type and C>A E2 proteins in combination with each TM-E3-RING protein. P-values < 0.01 (**) and and < 0.005 (***) are indicated.

E2 mutations used in this study were: UBE2D2 (C85A), UBE2E1 (C131A) and UBE2W (C91A). To provide appropriate normalisation controls for each tested TM-E3-RING/E2 pair, CRD-E3-RING FLucC and FLucN E2 constructs were co-transfected with a reciprocal non-interacting firefly luciferase fusion protein (FRB-FLucN or FKBP-FLucC). UBE2D2 C85A-FLucN and UBE2E1 C131A-FLucN fusions exhibited significantly elevated normalised luciferase PCA activity with RNF13-FLucC and RNF152-FLucC compared to the corresponding wild-type E2 fusion protein (p-value < 0.01, $n = 3$) (Figure 4.2). A striking ~ 20 fold increase in normalised luminescence signal was observed for UBE2E1 C131A compared to UBE2E1 WT when co-expressed with RNF13 as firefly luciferase PCA fusions. No significant decrease in luminescence signal was observed for UBE2D2 C85A or UBE2E1 C131A compared to corresponding wild type fusions in combination with any of the 4 TM-E3-RING FLucC fusions. In contrast, UBE2W C91A exhibited significantly reduced normalised luminescence signal compared to UBE2W WT when co-expressed with RNF13 and RNF152 FLucC fusions (p-value < 0.005, $n = 3$).

As a result of these findings, UBE2D2 C85A, UBE2E1 C131A and UBE2W WT E2-FLucN fusion proteins were utilized in subsequent luciferase PCA assays with a selection of TM-E3-RING FLucC fusions. Wild type UBE2E3, UBE2L3, UBE2L6 and UBE2N-FLucN fusions each generated strong luciferase PCA signals in luciferase PCA screens (Figure 4.3B) and therefore catalytic inactive C>A mutants were not generated for use in this system.

4.4.2. Comparison of orthogonal luciferase CRD-PCA and CRD-Y2H assays

In total, 16 CRD TM-E3-RING FLucC constructs were systematically co-expressed with 7 E2 FLucN clones, representing 112 potential binary protein interactions

(Figure 4.3). It is likely that individual CRD E3-RING FLucC and E2-FLucN fusion proteins exhibit different levels of background luciferase activity when co-expressed with fusion proteins encoding reciprocal luciferase fragments. As described in section 1.4.1. CRD-E3-RING FLucC and FLucN E2 constructs were co-transfected with a reciprocal non-interacting luciferase PCA fusion protein (FRB-FLucN and FKBP-FLucC, respectively) to provide two appropriate normalisation controls for each tested TM-E3-RING/E2 pair. Interactions were only considered positive if a reproducible ≥ 1.5 fold increase in firefly:Renilla luciferase activity was observed relative to the most stringent appropriate negative control (i.e. either TM-E3-RING FLucC/FRB FLucN or FKBP FLucC/E2 FLucN). Averages of two independent positive values were recorded and represent 'normalised luciferase PCA activity' (Figure 4.3B).

In total > 20% (45/196) of primary CRD-Y2H interactions were retested in the CRD-luciferase PCA system. CRD-PCA screens revealed 37 binary TM-E3-RING/E2 interactions (Figure 4.3B&C). The union of CRD-Y2H and CRD-PCA data showed 37% of total interactions to be observed in both CRD-Y2H and CRD-PCA screens (Figure 4.4A), representing comparable reconfirmation rates to those previously reported using identical clone sets in orthogonal interaction assay systems (Braun, Tasan et al. 2009). Of the 45 interactions observed in primary CRD-Y2H screens, 22 (~ 50%) were reconfirmed by CRD-PCA screens with an additional 15 interactions observed in CRD-PCA studies that were not reported in the CRD-Y2H dataset (Figure 4.4A). Significantly, ~ 80% (52/64) of negative CRD-Y2H interactions were also found to be negative in CRD-luciferase PCA screens (Figure 4.3C), representing a high degree of interaction specificity between screens. Interestingly,

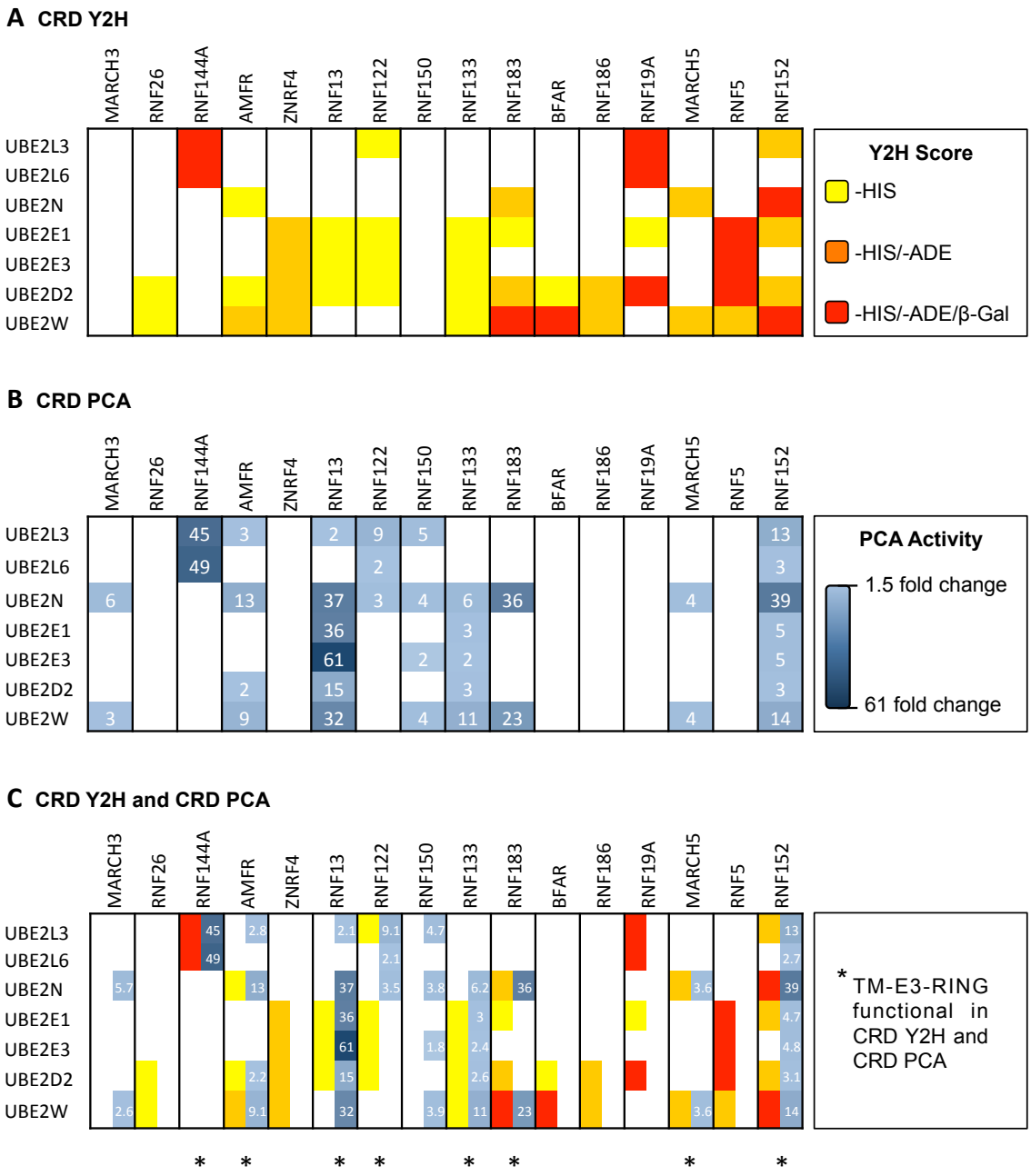

Figure 4.3 Co-tested TM-E3-RING/E2 interactions in CRD-luciferase PCA and CRD-Y2H screens. (A) Results from CRD-Y2H assays showing interaction score. Different colour represent number of Y2H reporters activated for each TM-E3-RING/E2 pair. **(B)** Normalised luciferase PCA activity observed in CRD-luciferase PCA studies. All positive values represent normalised average fold change for protein pairs a reproducible ≥ 1.5 fold increase in normalised Firefly luciferase activity (represented by light to dark blue colour gradient). **(C)** Comparison of data from CRD-Y2H and CRD-luciferase PCA assays. Asterisks represent TM-E3-RING proteins functional in CRD-luciferase PCAs. TM-E3-RINGs are shown on horizontal axis and E2-conjugating enzymes on the vertical axis.

for the subset of TM-E3-RING proteins that displayed ≥ 1 interaction partner in CRD-PCA screens and were therefore demonstrated functional in this system (Figure 4.3; denoted by asterisks), > 80% (22/27) of CRD-Y2H interactions were reconfirmed.

The activation of multiple reporters in Y2H systems has been proposed to represent higher confidence interactions (Serebriiskii and Golemis 2001), with the -ADE reporter inherently more stringent than the -HIS reporter in the GAL4-based Y2H system (James, Halladay et al. 1996). CRD-PCA reconfirmation of CRD-Y2H interactions on different reporter combinations was therefore calculated to investigate correlations between interaction 'strength' between interaction detection systems and to establish reasonable criteria for benchmarking CRD-Y2H positive interactions. CRD-PCA screens reconfirmed equivalent proportions of -HIS (10/18; 56%), -HIS/-ADE (7/15; 47%), and -HIS/-ADE/β-gal (5/12; 42%) CRD-Y2H screen interactions (Figure 4.4B). These findings are in agreement with *in vitro* functional reconfirmation of interactions observed on the -HIS reporter alone in previously published GAL4-Y2H screens from our laboratory (Markson, Kiel et al. 2009) and benchmarks CRD-GAL4 Y2H interactions of this reporter strength as true positives for this particular class of protein interaction in primary screens.

A strength of the firefly luciferase PCA system is its ability to quantify the magnitude as well as dynamics of protein interactions in cell-based assays (Luker, Gupta et al. 2009), whilst additional PCA readouts such as fluorescence generated by fluorophore-based PCAs can correlate with the interaction strength of a given protein pair (Morell, Espargaro et al. 2007). Correlative analysis between CRD-Y2H and CRD-PCA reporter strengths revealed CRD-Y2H interactions observed on all 3

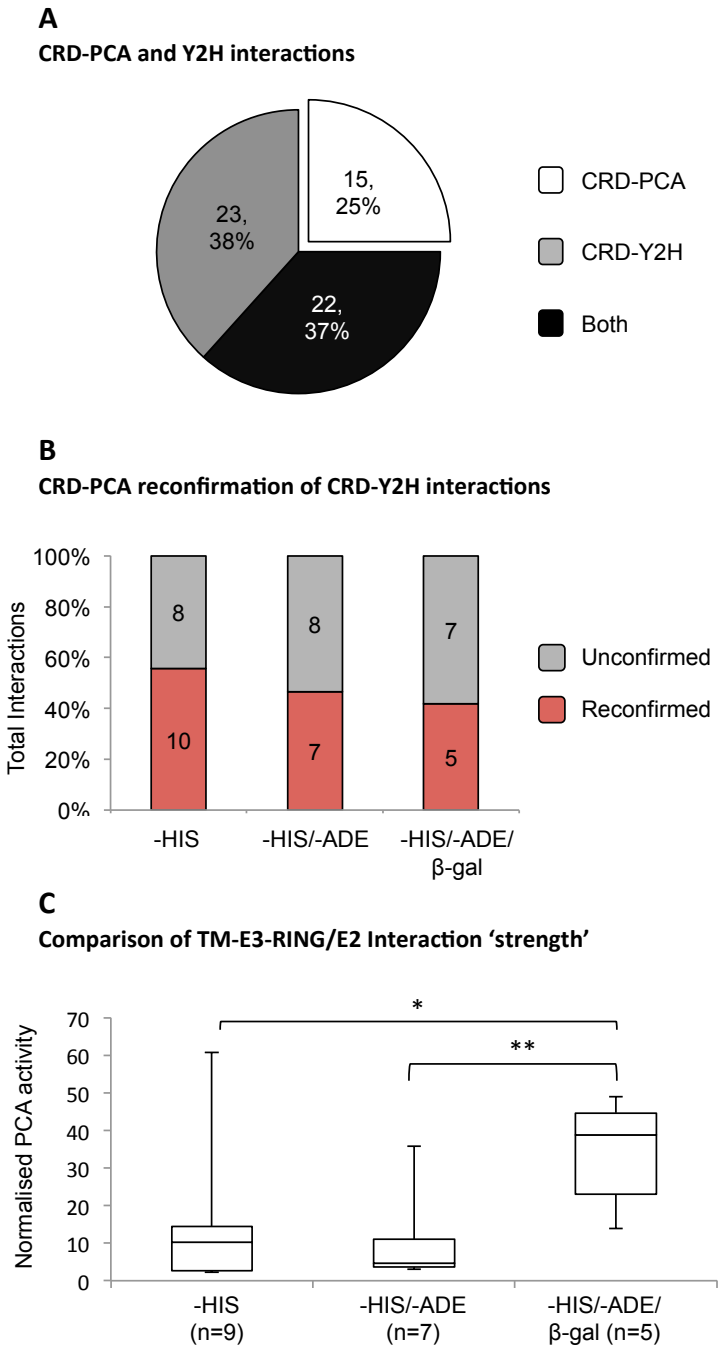

Figure 4.4 Comparison of co-tested TM-E3-RING/E2 interactions from CRD-PCA and primary CRD-Y2H screens. (A) Total overlap between CRD-PCA and CRD-Y2H screens. **(B)** Verified and unverified CRD-Y2H interactions within CRD-PCA assays according to number of Y2H reporters activated. **(C)** Comparison of CRD-Y2H and CRD-PCA interaction 'strength' for TM-E3-RING/E2 interactions observed in both interaction systems. The Student's T-Test was performed to determine statistical differences in normalised luciferase PCA signals for TM-E3-RING/E2 interactions observed by differential reporter activation in CRD-Y2H assays. P-values < 0.05 (*) and < 0.01 (**) are indicated.

reporters exhibited an elevated median luciferase PCA signal compared to interactions observed on –HIS ($p < 0.05$) or -HIS/-ADE selection ($p < 0.01$) (Figure 4.4C). Whilst this trend appears logical, it is important to note that the maximal signal observed in CRD-PCAs was observed for a protein pair observed solely on –HIS selection in primary CRD-Y2H screens, RNF13/UBE2E3 (Figure 4.3C).

4.4.3. Contribution of PCA signal derived from interactions occurring prior to or after cell lysis

As TM-E3-RING FLucC and E2 FlucN fusion proteins are co-expressed in HEK 293T cells, the presumption is that positive luciferase PCA activity results from interaction of fusion proteins and luciferase complementation *in vivo*. However, the lysis of HEK 293T cells prior to addition of the firefly luciferase substrate raised the possibility that the formation of positive binary interactions between fusion proteins may occur post-lysis. To investigate which of these two scenarios is responsible for the observed luciferase activity in our PCA system, a subset of CRD-PCA positive TM-E3-RING FLucC and E2 FLucN interaction partners were (i) co-expressed in HEK 293T cells and (ii) expressed individually in HEK 293T cell cultures and mixed post-lysis to compare luciferase activity for corresponding protein pairs following between experimental protocols (Figure 4.5A). For each tested CRD TM-E3-RING/E2 pair, a statistically significant increase in normalized firefly luciferase activity was observed for co-expressed fusion proteins compared to single expression and lysis mixing (Figure 4.5B). Significantly, RNF26/UBE2W and AMFR/UBE2N each exhibited > 10 fold increase in normalised luciferase PCA activity compared to their most stringent appropriate negative control for co-expression expression experiments yet did not exceed interaction cut-off criteria (≥ 1.5 fold increase) following single transfection and lysate mixing (Figure 4.5B).

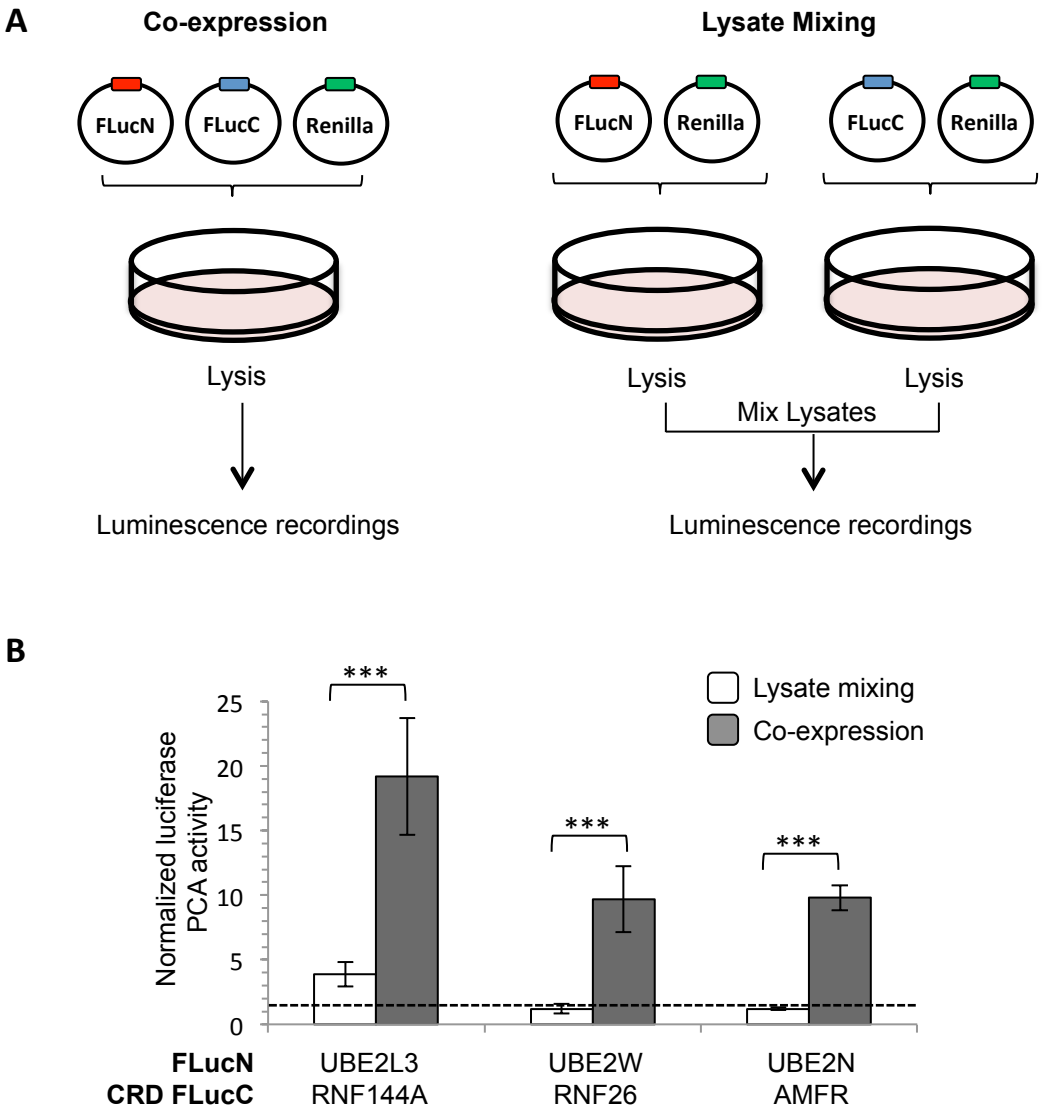

Figure 4.5 Luciferase PCA activities for CRD TM-E3-RING/E2 partners following co-expression and lysate mixing protocols. (A&B) HEK 293T cells were (i) co-transfected with CRD TM-E3-RING-FLucC and E2-FLucN constructs (0.5 ng / well) (grey bars) or (ii) transfected individually (0.5 ng / well) prior to lysate mixing (white bars). All HEK 293T cells were also transfected with the pRL-SV40 un-split Renilla luciferase vector (0.1 ng / well, respectively). Luciferase activity was measured 24 h post-transfection. Total photon counts were recorded for 4 s (Firefly) and 0.2 s (Renilla). Results are represented as fold change in Firefly:Renilla activity ratio compared to the most stringent negative control for each corresponding protein pair and experimental protocol. Error bars represent std dev. Student's T-Test was performed to determine statistical differences in normalised PCA activity between co-expression and lysate mixing protocols for each CRD TM-E3-RING/E2 protein pair. P-values < 0.005 (***) are indicated.

Additionally, whilst the RNF144A FLucC and UBE2L3 FLucN protein pair passed the positive PCA interaction criteria following lysate mixing, significantly higher normalised luciferase PCA activity was observed when the partners were co-expressed (Figure 4.5B). These findings indicate that interactions detected within the luciferase PCA system predominantly result from interactions occurring *in vivo*.

4.4.4. Full-length luciferase PCA screen results

An important advantage of the luciferase PCA system over several interaction techniques is the ability to investigate binary protein interactions in mammalian cells at an appropriate subcellular location. Therefore, unlike primary GAL4 Y2H screens that require soluble fusion protein generation for interaction detection at the yeast nucleus, integral membrane proteins can be investigated in luciferase PCA systems allowing spatial aspects of protein interactions to be considered in human cells (Morell, Ventura et al. 2009). 14 full-length TM-E3-RINGs were generated as FLucC fusion proteins for determination of interaction profiles with all available E2 FLucN fusions. Full-length TM-E3-RING FLucC fusions were selected to allow direct comparison of binary interaction data in CRD-PCA screens. As such, 12/14 tested TM-E3-RING full-length clones were also tested as CRD-fusions with 84/98 tested full-length interactions common to both screens.

Initial inspection of data revealed that full-length TM-E3-RING FLucC fusion proteins yielded fewer E2 interaction partners than their corresponding CRD FLucC fusions with a total of 14 full-length TM-E3-RING/E2 interactions detected (Figure 4.6B). The union of co-tested full-length PCA and CRD PCA protein pairs generated 30 binary TM-E3-RING/E2 interaction partners of which: 9 (30%) were common to both datasets, 18 (60%) were only observed in CRD-PCA screens, and 3 (10%) were

only detected in full-length PCA screens (Figure 4.6A-C and supplementary file luciferase PCA analysis). Significantly, interactions derived from full-length PCA screens predominantly represent a subset (9/12) of CRD-PCA screen interactions. Furthermore, the 3 interactions unique to full-length PCA screens observed for 2 TM-E3-RING clones (RNF26 and ZNRF4) that exhibited zero interaction partners as CRD TM-E3-RING fusions (Figure 4.6C, red boxes). These findings represent high specificity of full-length PCA screen interactions in the reconfirmation of CRD-PCA data. Two TM-E3-RING proteins (RNF185 and RNF148) were tested solely as full-length PCA fusions and extended the PCA TM-E3-RING/E2 network by an additional 2 interactions (Figure 4.6B&C).

As TM-E3-RINGs represent integral membrane proteins they can exhibit either cytosolic/nuclear or extracellular/luminal C-terminal topologies. In contrast, tested E2 conjugating enzymes are soluble proteins and exhibit N- and C-terminal cytosol/ nuclear topologies. Current Gateway^{TM} firefly luciferase PCA vector availability solely allowed the expression of TM-E3-RING proteins in fusion with the C-terminal FLucC domain. This topological constraint may preclude interaction detection between TM-E3-RING and E2 proteins that display alternative C-terminal FLucC and N-terminal FLucN locations as the physical separation of PCA fragments by cellular membranes could prevent complementation of luciferase PCA fragments. TM-E3-RING protein topology prediction demonstrated only 64% correlation in C-terminal location for tested TM-E3-RING proteins using two independent prediction tools (TMHMM and HMMTOP) (supplementary file ‘luciferase PCA analysis’), highlighting the current difficulty in calculating the orientation of integral membrane proteins in cellular membranes by primary protein sequence alone. Based on RING and TM domain architecture, and the assumption that RING domains are oriented to

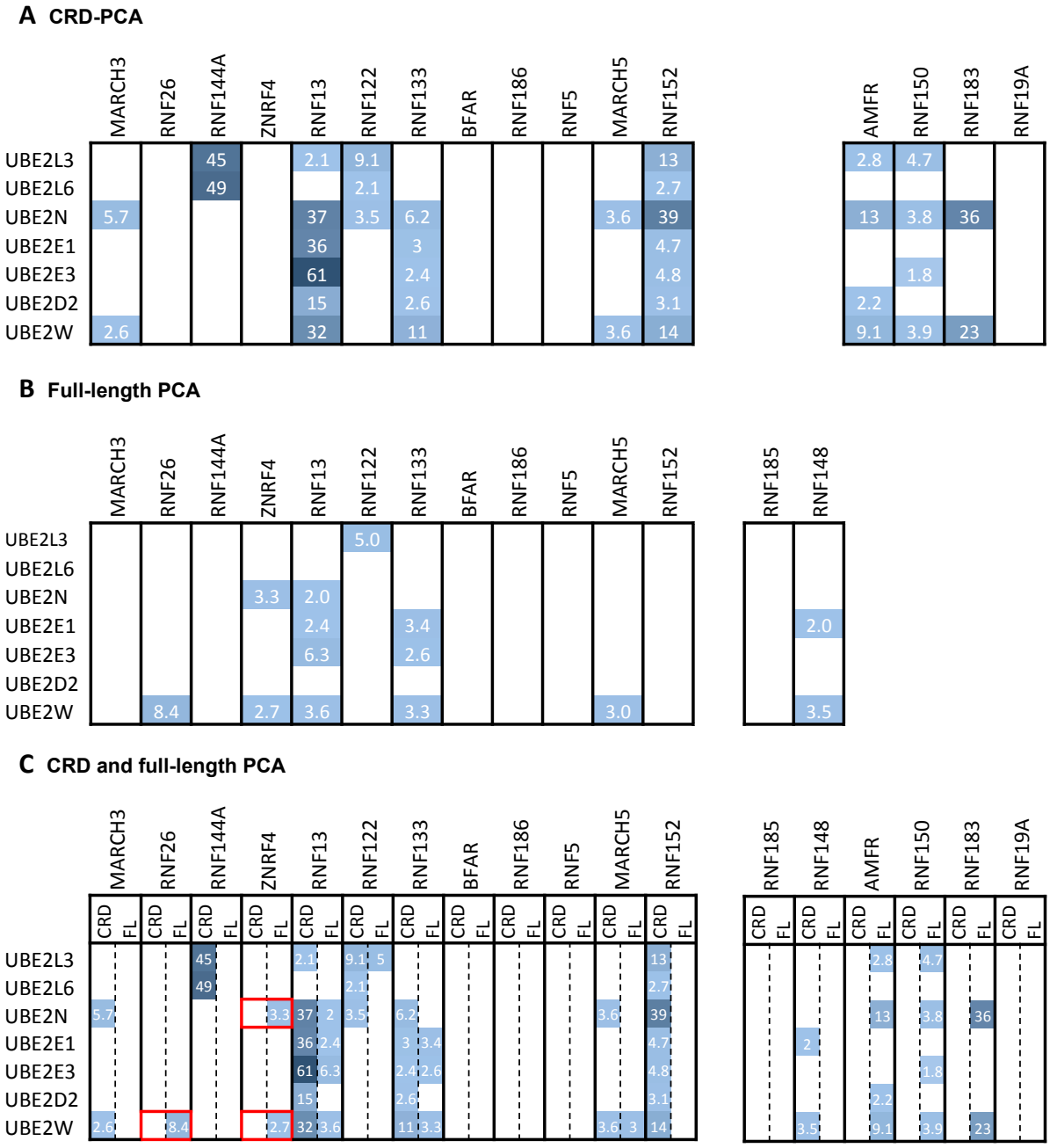

Figure 4.6 CRD and full-length luciferase PCA comparison. Normalised luciferase PCA activity is shown for CRD-luciferase PCA screen **(A)** and full-length luciferase PCA screen **(B)**. Comparison of data from co-tested clones in CRD-luciferase (left column) and full-length luciferase (right column) PCA assays **(C)**. Values ≥ 1.5 represent average normalized fold change relative to most stringent negative control. Light to dark blue colour scale represents lower to higher normalised PCA signal for TM-E3-RING/E2 pairs.

the cytosol/nucleus to enable interaction with E2 proteins, 3/14 tested TM-E3-RING proteins (RNF152, RNF144A, BFAR) full-length and CRD-PCA screens were interpreted to encode extracellular/luminal C-terminal topologies (see supplementary 'luciferase PCA analysis'). Significantly, this subset of TM-E3-RING proteins did not yield any E2 interactions in full-length PCA screens yet E2 partners were reported for both RNF144A and RNF152 when tested as CRD TM-E3-RING clones that lack the topological constraints associated with membrane insertion, (Figure 4.6B&C).

4.4.5. Collation of data from luciferase PCA and CRD-Y2H screens to form a secondary interaction dataset

Upon completion of CRD and full-length luciferase PCA studies, TM-E3-RING/E2 PCA interaction data was collated and compared with available literature data to determine overlap and novelty of reported interactions. In total 126 potential binary interactions were tested in CRD- and/or full-length luciferase PCA assays revealing a total of 42 TM-E3-RING/E2 interaction pairs. 45 of the tested protein pairs were reported positive in the combined previous literature ((Markson, Kiel et al. 2009; van Wijk, de Vries et al. 2009) and others), of which 21/45 (47%) were reconfirmed by luciferase PCA screens (supplementary file supplementary file 'luciferase PCA analysis'). As such, 21 PCA-derived interactions were novel compared to previous literature.

A similar reconfirmation rate of CRD-Y2H data alone (26/53; 49%; Figure 4.7A – red and grey segments) or CRD-Y2H plus total literature data (32/66; 48%; Figure 4.7B – red and grey segments) by luciferase PCA screens was observed. Significantly, 6 PCA-derived TM-E3-RING/E2 interactions that were not observed in CRD-Y2H screens reconfirm previously unverified interactions from other HTP interaction

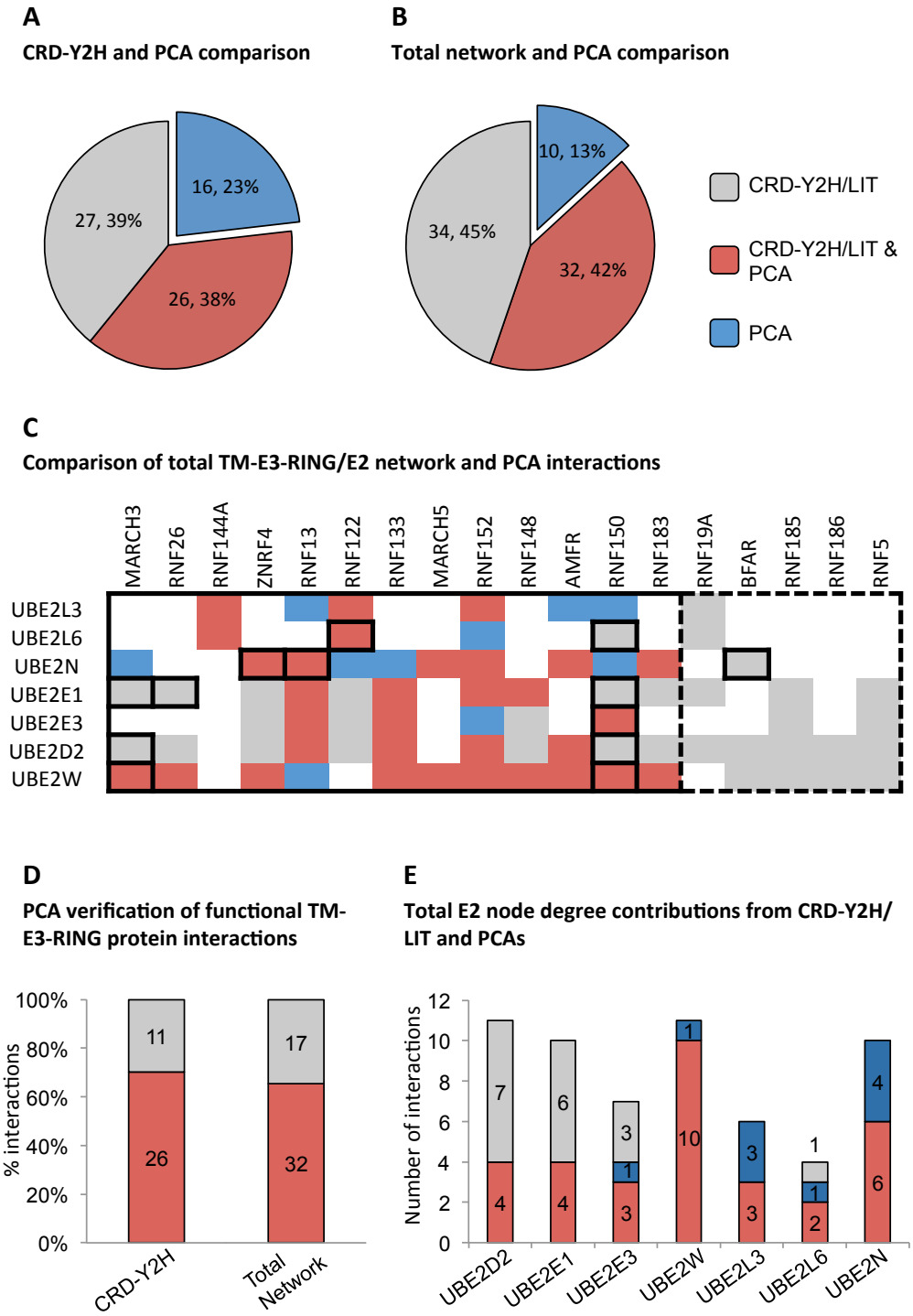

Figure 4.7 CRD-Y2H and total TM-E3-RING/E2 comparison with PCA interaction data. (A) Comparison of PCA positive interactions with CRD-Y2H data and **(B)** CRD-Y2H plus literature data (total network). **(C)** Heat-map representation of PCA and total TM-E3-RING/E2 interactions. TM-E3-RING clones with no interactions in luciferase PCAs are contained in broken black border. Squares with black outlines represent binary interactions reported in literature but not CRD-Y2H screens. **(D)** Verification of CRD-Y2H and total network interactions by functional TM-E3-RING clones in PCA screens. **(E)** Known and PCA interaction contributions to E2 degree for functional TM-E3-RING clones. Functional TM-E3-RING clones have ≥1 interaction in both screens.

studies (Markson, Kiel et al. 2009; van Wijk, de Vries et al. 2009) (Figure 4.7C; red box with black border). The remaining, 10/42 interactions observed in luciferase PCA screens represent novel TM-E3-RING/E2 interactions that have not been reported in primary CRD-Y2H or other studies (Figure 4.7B). A high rate of negative reconfirmation was also reported for luciferase PCA system with 86% of non-interacting TM-E3-RING/E2 pairs in the total interaction network also negative in PCA screens (Figure 4.7C – white boxes; and supplementary file 'luciferase PCA analysis').

Given the relatively strict topological constraints inherent in PCA systems, it is possible that several constructs may not be effective as PCA partners. Discounting TM-E3-RING fusions that exhibit no E2 interactions in PCA screens (Figure 4.7C; broken black border), results in > 65% reconfirmation of CRD-Y2H and CRD-Y2H plus literature datasets (Figure 4.7D). Furthermore, the vast majority of unconfirmed TM-E3-RING/E2 interactions in the total dataset (94; 16/17) were attributed to UBE2D and UBE2E family members, suggesting that these E2 proteins may not function effectively as FLucN fusions in the present PCA system (Figure 4.7E). As such, high rates of reconfirmation of CRD-Y2H and literature-derived interactions were observed for the four remaining E2 proteins (UBE2W, UBE2L3, UBE2L6, and UBE2N).

4.5. Discussion

No single interaction detection system is absolute in its scope and different interaction systems cover distinct interaction spaces (Braun, Tasan et al. 2009; Sanderson 2009). As such, the utilization of multiple interaction assays can increase network coverage and provide increased confidence in interactions detected in a

given interaction system(s). Previous HTP Y2H studies have used different methods to reassess putative E3-RING/E2 interactions including co-immunoprecipitation (Co-IP) assays (van Wijk, de Vries et al. 2009) and *in vitro* interaction partners observed in recent HTP-Y2H screens. Aside from these studies, very few methods have been successfully employed for the detection of a broad range of E2/E3-RING protein interactions and fewer still have attempted to reconfirm interactions between E2 and TM-E3-RING proteins. The instantaneous reconstitution of luciferase activity in PCA systems upon reporter protein refolding coupled with a low background luminescent signal in mammalian cells may enable a luciferase-based PCA system to detect transient interactions of low affinity (Hida, Awais et al. 2009), such as those reported for TM-E3-RING/E2 complexes (Yin, Lin et al. 2009; Bentley, Corn et al. 2011).

4.5.1. Generation and validation of an orthogonal Gateway compatible luciferase PCA system

The work in this chapter has described the Gateway modification and successful application of a firefly luciferase-based PCA system for investigation of CRD and full-length TM-E3-RING/E2 interaction partners within human cells. Importantly, considerable overlap was observed between CRD-Y2H and CRD-luciferase PCA screens (37% total overlap), corresponding well with previous reports of reconfirmation rates between orthogonal interaction assay systems using identical ORF clones (Braun, Tasan et al. 2009). This analysis validated the use of the luciferase PCA assay system for detecting TM-E3-RING/E2 interactions and enabled us to benchmark CRD-Y2H interactions reported on the –HIS biosynthetic reporter alone as high confidence interactions. As such, the generation of the luciferase PCA assay provides an orthogonal system for benchmarking positive Y2H interactions. Furthermore, full-length TM-E3-RING clones generated E2 interaction profiles which represented a subset of CRD-TM-E3-RING/E2 interactions for TM-

E3-RING clones functional in both screens. The union of CRD- and full-length luciferase PCA screens and comparison with the total TM-E3-RING/E2 network revealed strong positive and negative verification rates, representing high accuracy and specificity of detected interactions.

4.5.2. Luciferase PCA system extends TM-E3-RING/E2 interaction coverage

Orthogonal interaction techniques cover different interaction spaces due to limitations of individual techniques and differential assay stringency (Braun, Tasan et al. 2009). As such, alternative binding profiles between orthogonal screens should not automatically be considered false-positive in either system. Therefore, In addition to increasing confidence in primary interaction data, orthogonal assay systems can also serve to extend interaction coverage. The luciferase PCA system undertaken identified 16 interactions that were not observed in CRD-Y2H screens. 6 of these interactions were however present as previously unverified interactions in the combined TM-E3-RING/E2 network with 10 interactions entirely novel to luciferase PCA screening. As such the TM-E3-RING/E2 interaction network is extended to 312 binary protein-protein interactions with novel data provided from CRD-Y2H, literature, and luciferase PCA screens (Figure 4.8), thus highlighting how different experimental approaches contribute to increasing network density.

4.5.3. Luciferase PCA system measures interactions occurring within mammalian cells *in vivo*

Preliminary experiments indicate that interactions detected within the PCA system largely occur *in vivo*. Current vector availability only allowed for the expression of TM-E3-RING FLucC and E2 FLucN proteins as C-terminal and N-terminal fusions, respectively. Given the belief that interactions occur *in vivo* it was argued that TM-E3-RING proteins predicted to have C-terminal luminal/extracellular topologies may avoid E2 interaction detection due to physical separation of firefly luciferase reporter

fragments by cellular membranes. In accordance with this proposal, proteins with predicted luminal/extracellular C-terminal domains did not yield any interactions in full-length luciferase PCA arrays. In addition, breakdown of reconfirmed interactions for individual E2 proteins revealed ~95% (16/17) of total unconfirmed TM-E3-RING interactions were attributed to members of the UBE2D and UBE2E families, suggesting that these proteins may not function effectively as fusions in this PCA system.

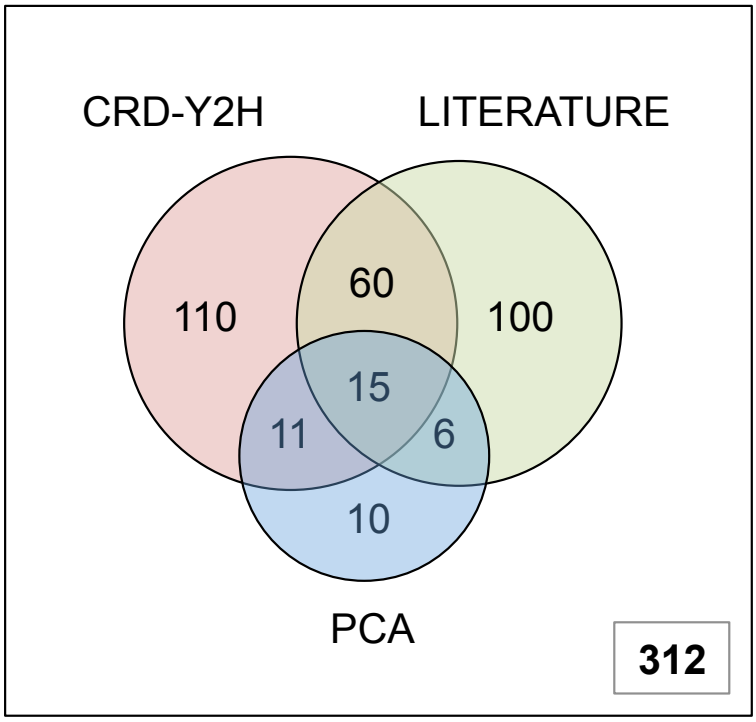

Figure 4.8. Complementary interaction detection systems contribute to higher density binary protein-protein interaction maps. Total interactions reported in CRD-Y2H, Literature and PCA screens and the overlap between datasets are annotated.

4.6. Differential effects of wild-type and mutant E2 proteins

Interestingly, the use of catalytically inactive E2 proteins revealed differential effects during luciferase PCA screens compared with wild type clones; UBE2D2 and UBE2E1 exhibit increased levels of activity as mutant clones whilst UBE2W exhibit decreased activity as mutant clones. Whilst our rationale was such that the catalytically inactive clones may enhance the stability of TM-E3-RING/E2 complexes, there are further possibilities that could underlie the increased luciferase activity observed with mutant clones. Firstly, the nuclear distribution of UBE2E and UBE2W families is dependent upon the 'loading' of their respective active site cysteine residues with ubiquitin (Plafker and Macara 2000; Yin, Ji et al. 2006) and as such these E2s shuttle between nuclear and cytoplasmic compartments dependent upon their ubiquitinated state. Therefore, whilst these E2s have the potential to come into contact with TM-E3-RING proteins in both nuclear and cytosolic compartments, UBE2E1 C131A and UBE2W C91A FLucN fusions may display a more cytoplasmic localisation, which could result in increased interaction with cytosolic TM-E3-RING proteins. E3-RING proteins appear to bind both free and loaded forms of E2 proteins (Deshaies and Joazeiro 2009). However, limited experimental evidence supports the notion that E3-RING/E2 binding is stronger with charged E2~Ub proteins (Siepmann, Bohnsack et al. 2003; Saha and Deshaies 2008). The decrease in luciferase PCA activity for the UBE2W C91A compared to wild type UBE2W FLucN fusion proteins may therefore result from a decreased affinity of UBE2W C91A for its cognate TM-E3-RING proteins. As such, the precise mechanisms underlying the differential activity of catalytic inactive E2 FlucN fusion proteins remain unclear and may differ between different E2 families.

4.6.1. Future Directions

A major strength of the firefly luciferase PCA is the ability to quantify the magnitude as well as dynamics of protein interactions in cell-based assays (Luker, Gupta et al. 2009). This luciferase-based PCA system described in this chapter could therefore be utilized to investigate conditional or signal-dependent TM-E3-RING/E2 interactions (Hida, Awais et al. 2009). As such, the development of this assay may aid future investigation of TM-E3-RING/E2 interactions following the initiation of specific physiological events such as Endoplasmic Reticulum Associated Degradation (ERAD) to identify putative protein partners, which function within a given process.

5. Chapter 5: TM-E3-RING/E2 *in vitro* ligase activity

5.1. Introduction

E3-RING proteins must bind selectively to E2-conjugating enzymes to facilitate the modification of selective substrate proteins. In total 312 unique binary TM-E3-RING/E2 complexes have been identified (Figure 4.8): 181 literature-reported interactions (Markson, Kiel et al. 2009; van Wijk, de Vries et al. 2009) were extended by 131 previously unreported interactions in CRD-Y2H and/or PCA screens. However, few of these potential TM-E3-RING/E2 complexes have been investigated to test their ability to function as active ligase complexes *in vitro*.

A recurring theme in ubiquitin cascades is the ability of E3-RING proteins to drive auto-ubiquitination events in the presence of an appropriate E2 partner (de Bie and Ciechanover 2011), exemplified by the MDM2 and the CBL ligases (Fang, Jensen et al. 2000; Ryan, Davies et al. 2006). Auto-ubiquitination activity has previously been used to assess the functional potential of several putative E3-RING/E2 complexes (Christensen, Brzovic et al. 2007; Markson, Kiel et al. 2009). These studies have shown a strong correlation between primary Y2H data and *in vitro* ubiquitination activity and revealed novel relationships between E3-RING/E2 partner preference and the formation of different forms of ubiquitin modification (Christensen, Brzovic et al. 2007). Given the established utility of this approach similar combinatorial *in vitro* ubiquitination assays were undertaken to investigate a representative selection of putative TM-E3-RING/E2 pairings including interactions observed in: (i) CRD-Y2H screens with different reporter stringencies (ii) complementary PCA screens and (iii) as yet unverified interactions observed in other high throughput Y2H studies.

To perform ***in vitro*** auto-**u**biquitination **a**ssays (IUAs) sequence-verified CRD TM-E3-RING clones were transferred by LR reactions into the pGEX6p GW vector to allow bacterial expression of human TM-E3-RING proteins in fusion with N-terminal GST moieties that would provide additional substrate lysine residues for modification in auto-ubiquitination reactions. A number of E2 proteins expressed in fusion with a red fluorescent protein (RFP) protein tag have been previously shown to become auto-ubiquitinated within IUAs in the absence of cognate E3-RING proteins (David, Ziv et al. 2010). For this reason, expressed E2-GST fusion proteins were cleaved and E2s purified prior to use within *in vitro* auto-ubiquitination assays. Furthermore, E2 proteins were independently assayed in the presence and absence of potential E3-RING partners to define the extent and form of E3-RING dependant modifications.

5.2. *In vitro* auto-ubiquitination assays

Previous studies have typically performed *in vitro* ubiquitination assays at 30°C or 37°C for 1:30 h (Lorick, Jensen et al. 1999; Christensen, Brzovic et al. 2007). To optimise assay conditions the efficiency of auto-ubiquitination was assessed at either 30°C or 37°C for 1:30 h using two TM-E3-RING GST fusion proteins (RNF152 and RNF167) and a panel of E2 conjugating enzymes (Figure 5.1). Auto-ubiquitination activity was assessed qualitatively following Western blot analysis using rabbit polyclonal anti-ubiquitin antibody (1:2000; 07-375; Millipore). Auto-ubiquitination activity of functional TM-E3-RING/E2 complexes was observed as generation of high molecular weight (HMW) ubiquitin bands or smears and was more pronounced following incubation at 37 °C compared to 30 °C (Figure 5.1A&B). As such, subsequent auto-ubiquitination reactions were performed at 37°C for 1:30 h.

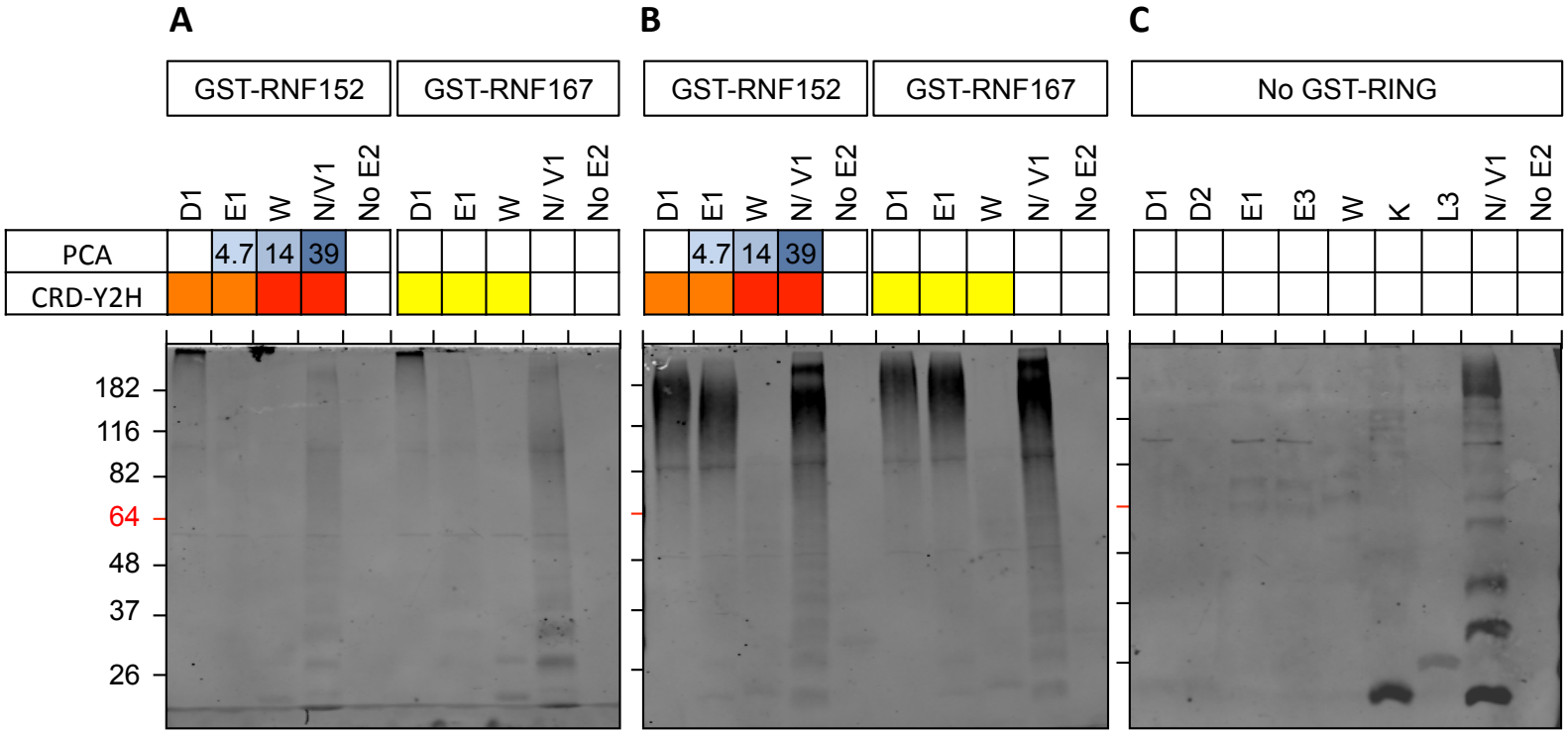

Figure 5.1 Optimization of incubation temperature for *in vitro* ubiquitination assays. E2 conjugating enzymes, CRD TM-E3-RING GST-fusion proteins, and all other assay components were combined on ice. *In vitro* auto-ubiquitination reactions were initiated by addition of MgATP and reactions were incubated at either 30°C **(A)** or 37°C **(B)** for 1:30 h. E2 auto-ubiquitination activity was assessed by incubation of reaction components for 1:30 h at 37°C in the absence of TM-E3-RING fusion proteins **(C)**. Auto-ubiquitination activity was qualitatively assessed by Western blot analysis using rabbit polyclonal anti-ubiquitin antibody (1:2000; 07-375; Millipore) and is signified by HMW ubiquitin bands or smears. CRD-Y2H and PCA scores for binary TM-E3-RING/E2 protein pairs are indicated above each lane.

In the absence of TM-E3-RING GST fusions, the majority of E2 proteins were incapable of generating HMW ubiquitin modifications (Figure 5.1C). As such, the majority of auto-ubiquitination activity was dependent on the formation of active E3-RING/E2 complexes. However, in agreement with previous reports (Markson, Kiel et al. 2009; Wilson, Edmondson et al. 2011) UBE2K and the UBE2N/UBE2V1 hetero-dimer generated HMW ubiquitin modifications in the absence of TM-E3-RING GST fusion partners (Figure 5.1C).

5.2.1. TM-E3-RING/E2 *in vitro* auto-ubiquitination assays

In total, 10 CRD TM-E3-RING GST fusion proteins and 10 E2 conjugating enzymes were successfully expressed and assayed in the *in vitro* auto-ubiquitination assay system, enabling the analysis of functional ligase activity across the phylogeny of TM-E3-RING and E2 proteins (UBE2D1/2, UBE2E1/3, UBE2L3, UBE2W, UBE2N/UBE2V1 and UBE2K). UBE2N and UBE2V1 were tested in combination due to the known co-operative role of this E2/UEV hetero-dimer complex in the formation of poly-ubiquitin chains (Hofmann and Pickart 1999).

Probing IUA reaction products for total ubiquitin revealed HMW ubiquitin smears for 8/10 TM-E3-RING GST fusion proteins in combination with UBE2D and UBE2E protein family members (Figure 5.2 A-J). For this subset of E2 proteins, *in vitro* ubiquitin ligase activity exhibits strong correlation with primary interaction data; 100% of CRD-Y2H positive interactions (25/25) exhibited functional *in vitro* ligase activity. Significantly, two TM-E3-RINGs that did not interact with UBE2D or UBE2E family members in either CRD-Y2H or PCA screens were not functionally active *in vitro* (8/8 negative interactions reconfirmed; Figure 5.2I&J). However, 2 TM-E3-RING fusions that exhibited ubiquitin ligase activity *in vitro* with

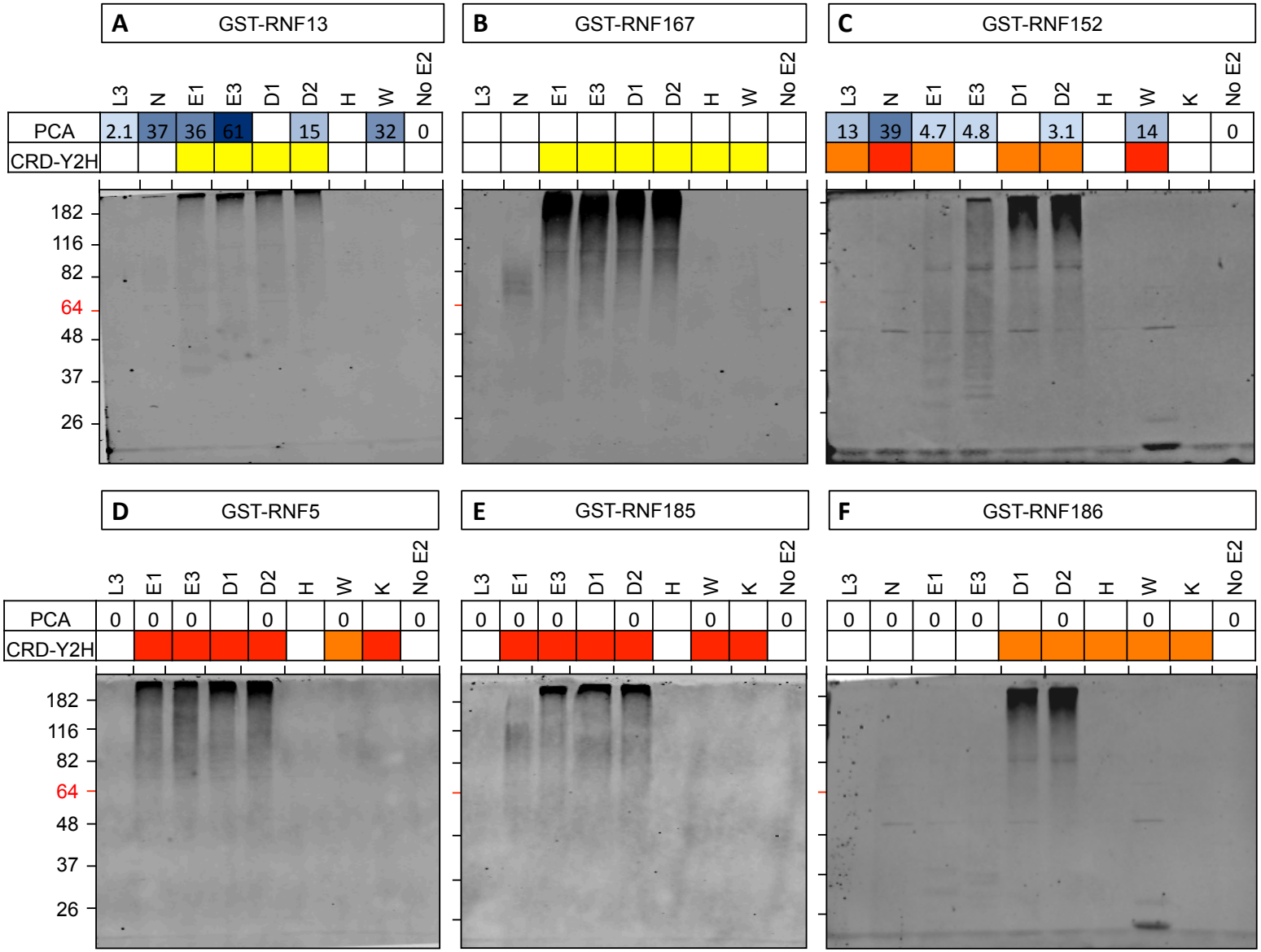
A
GST-RNF13
B
GST-RNF167
C
GST-RNF152
L3
N
E1
E3
D1
D2
H
W
K
No E2
PCA
CRD-Y2H
2.1
37
36
61
15
32
0
13
39
4.7
4.8
3.1
14
182
116
82
64
48
37
26
D
GST-RNF5
E
GST-RNF185
F
GST-RNF186

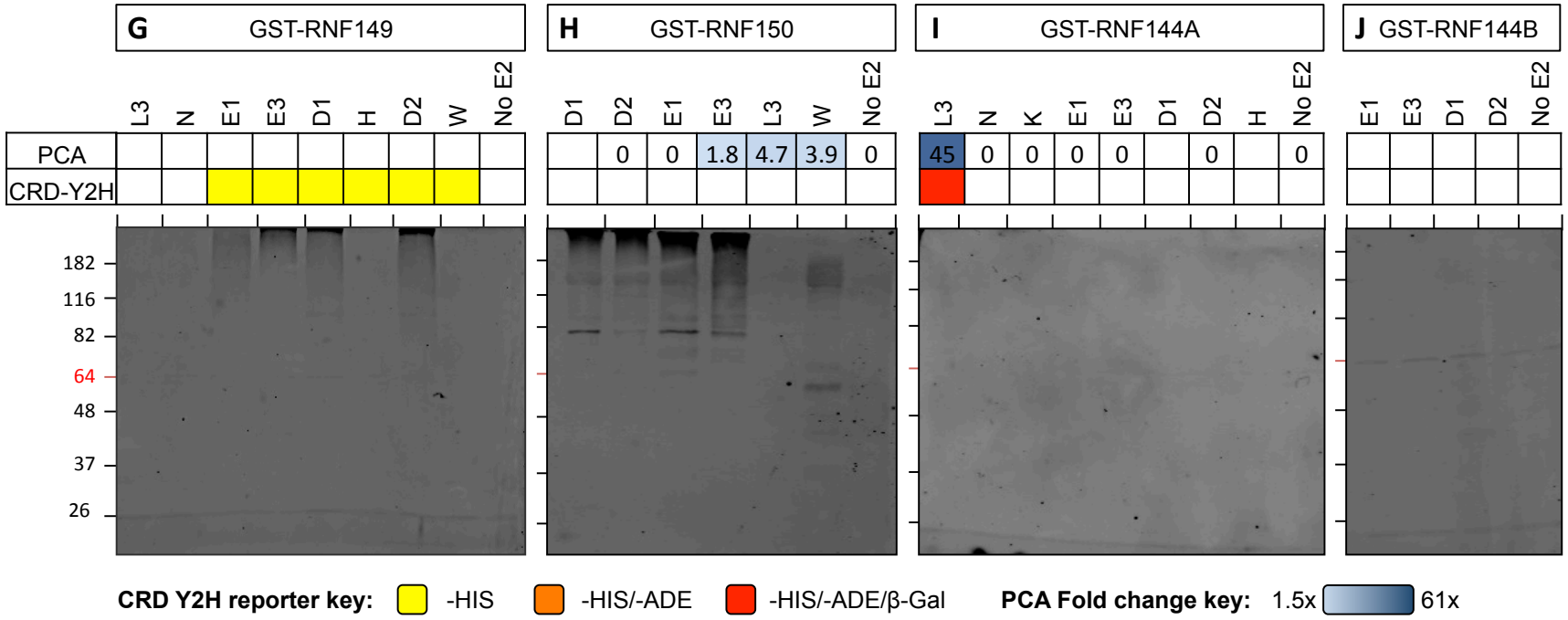

Figure 5.2 *In vitro* ubiquitination assay screen. 10 TM-E3-RING GST fusion proteins were tested for functional auto-ubiquitination activity against a panel of E2 conjugating enzymes. All assay components were combined on ice. *In vitro* auto-ubiquitination reactions were initiated by addition of MgATP and reactions incubated at 37°C for 1:30 h. Auto-ubiquitination activity was qualitatively assessed by Western blot analysis using rabbit polyclonal anti-ubiquitin antibody (1:2000; 07-375; Millipore) and is signified by HMW ubiquitin bands or smears. CRD-Y2H and PCA positive interactions for each TM-E3-RING/E2 pair are indicated according to number of biosynthetic reporters activated and normalized firefly luciferase fold change, respectively. As all TM-E3-RING/E2 pairs were tested in CRD-Y2H but not all in luciferase PCA screens, non-tested pairs in PCA screens are represented by empty box whilst tested but negative interactions are indicated by a 0.

UBE2D/E family members were not reported as binary interaction pairs in CRD-Y2H screens; RNF150 formed active ubiquitin ligase complexes with all tested UBE2D and UBE2E proteins (Figure 5.2H), whilst RNF152 formed a functional pairing with UBE2E3 (Figure 5.2C). Interestingly, 2 of these 5 CRD-Y2H negative pairs were detected as positive binary interactions in PCA screens (RNF152/UBE2E3 and RNF150/UBE2E3), highlighting the utility of using multiple orthogonal assay systems to increase network coverage and further emphasising the value of the developed luciferase PCA system for detection of potential functionally relevant TM-E3-RING/E2 interactions.

Increasing the concentration of E3-RING and/or E2 proteins within *in vitro* auto-ubiquitination assays did not extend activity profiles beyond members of the UBE2D and UBE2E families (personal communication, Jonathan Woodsmith). This suggests that shifting the reaction equilibrium in favour of catalysis by mass action does not affect the activity of these E2 proteins within IUAs. Additionally, modification of reaction conditions to incorporate an ATP-regeneration system (1 mM creatine phosphate and 15 U creatine phosphokinase, as previously reported (Lee, Choi et al. 2001)) similarly did not reveal additional activity profiles for E2s outside of these subfamilies (data not shown).

E3-RING proteins have been reported to yield different forms of ubiquitin modification (from mono- to poly-ubiquitin conjugates) in combination with different E2 partners (Christensen, Brzovic et al. 2007; Garnett, Mansfeld et al. 2009). Therefore, IUA products were probed with monoclonal anti-GST antibody to selectively analyse modifications occurring on TM-E3-RING GST-conjugates in an attempt to allow better detection of lower molecular weight (LMW) ubiquitin

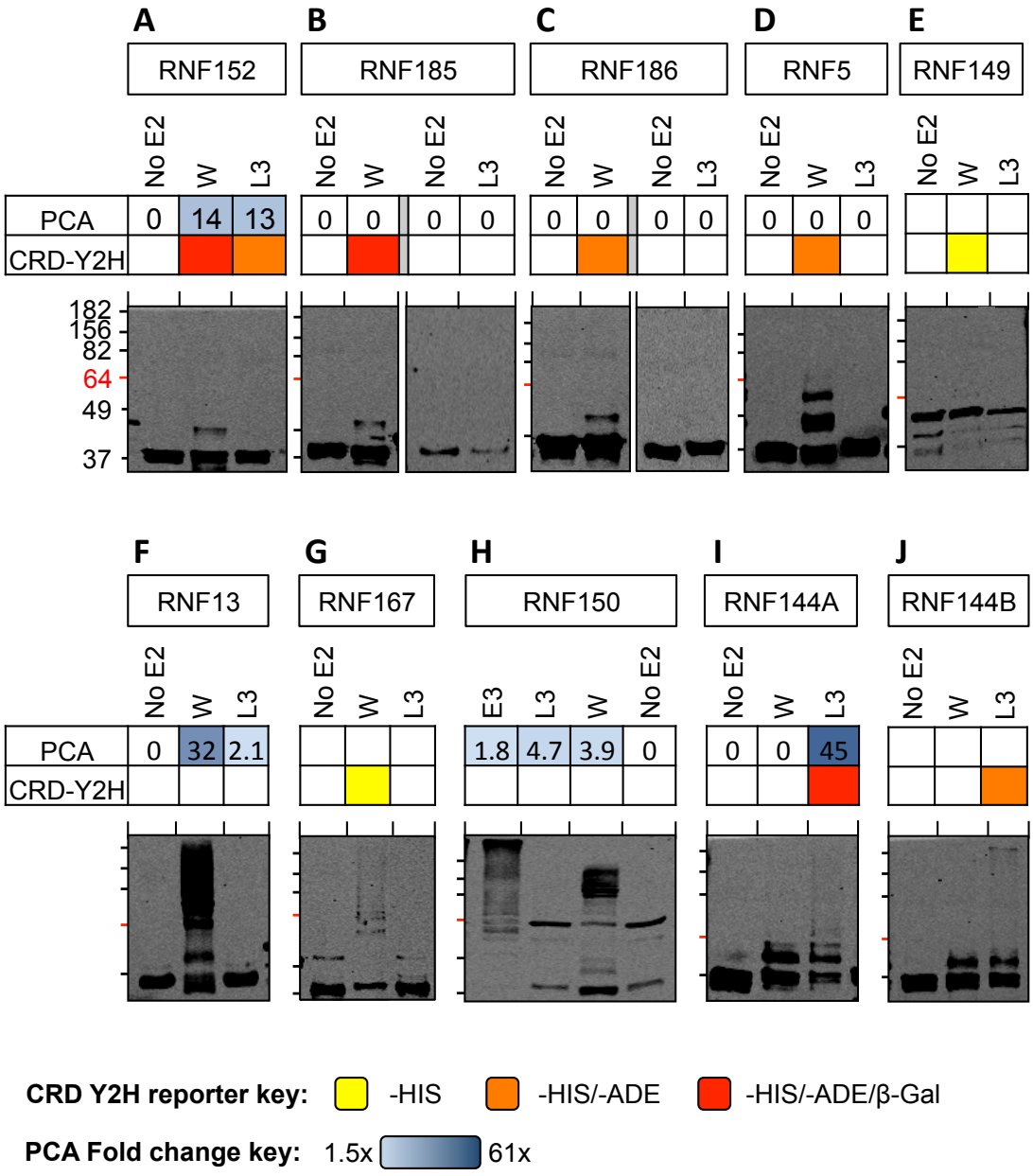

Figure 5.3 Systematic *in vitro* auto-ubiquitination assays involving 10 GST-TM-E3-RING proteins in combination with UBE2W and UBE2L3 E2 conjugating enzymes. Ubiquitin ligase activity was assessed by the formation of HMW or LMW ubiquitin modifications upon TM-E3-RING GST fusions with anti-GST antibody (1:1000; AB92; Abcam) (**A-J**). CRD-Y2H (red) and luciferase PCA (blue) positive interactions are indicated above each lane. Pre-stained protein ladder molecular weight (kDa) are shown in **(A)** and by corresponding dashes in **(B&J)**.

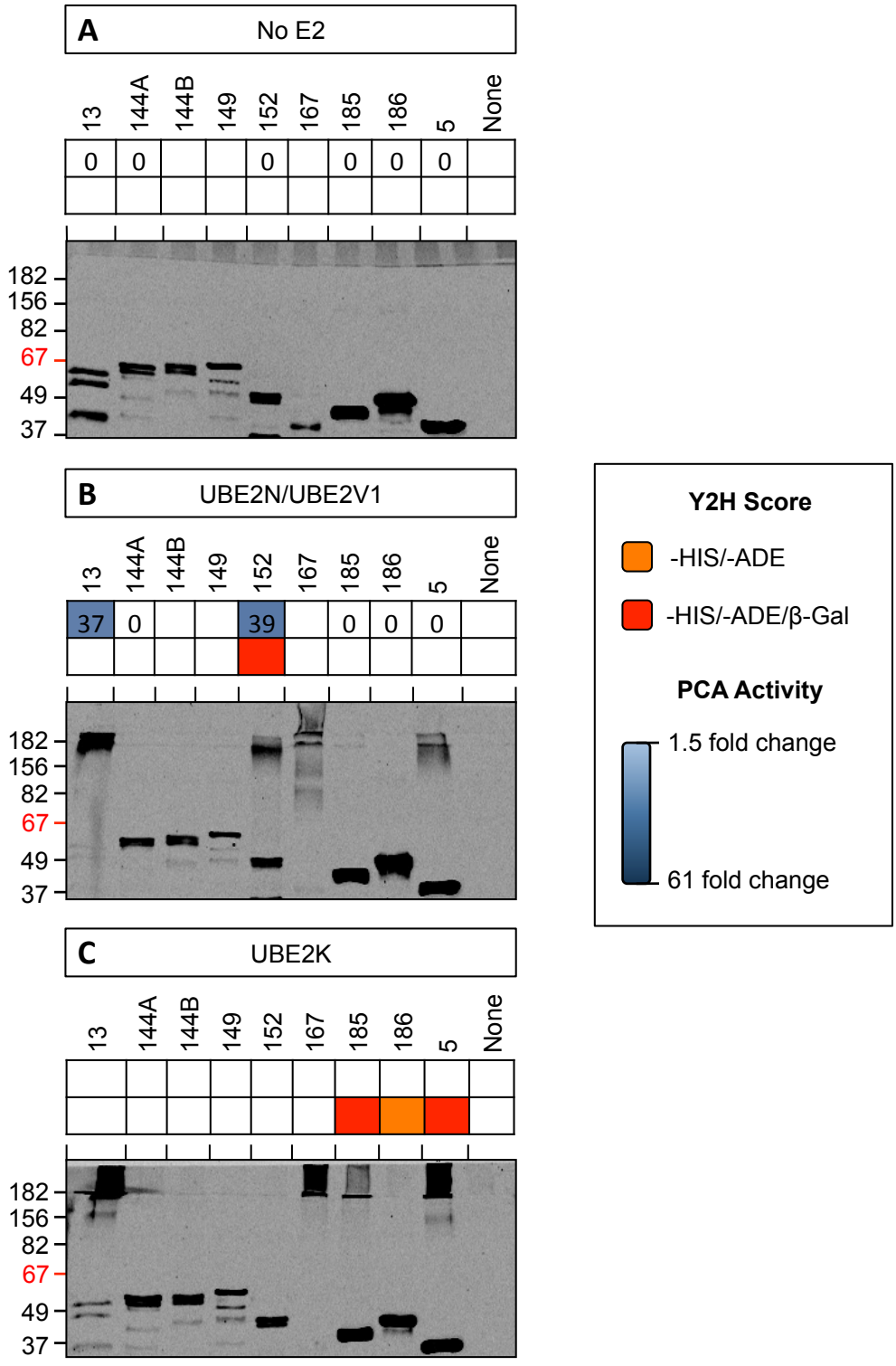

Figure 5.4 Systematic *in vitro* auto-ubiquitination assays involving 10 GST TM –E3-RING proteins in combination with UBE2N/V1 and UBE2K E2 conjugating enzymes. Ubiquitin ligase activity was assessed by the formation of HMW or LMW ubiquitin modifications upon TM-E3-RING GST fusions with anti-GST antibody (1:1000; AB92; Abcam) (**A-C**). CRD-Y2H and PCA positive interactions are indicated above each lane.

modifications. This strategy revealed additional LMW and HMW ubiquitin modifications for selective TM-E3-RING proteins in complex with UBE2W and/or UBE2L3 E2 proteins that were not previously detected by probing for total ubiquitin alone (Figure 5.3A-J). This approach also provided an effective method of distinguishing between auto-ubiquitination of active TM-E3-RING/E2 complexes and E3-independent activity observed for UBE2K and UBE2N/V1 proteins (Figure 5.4C). As a result of this optimized Western blotting procedure, 19 additional active TM-E3-RING/E2 complexes were observed, increasing the total number of active TM-E3-RING/E2 ligase complexes to 49 between 8 E2 proteins and 10 TM-E3-RING specific CRDs.

5.2.2. Comparison of *in vitro* activity with data from Y2H and Luciferase PCA methods

Upon completion of *in vitro* auto-ubiquitination assays, all functional data was compared with CRD-Y2H, PCA and literature curated interaction datasets. Significantly, 89% (40/45) of binary TM-E3-RING/E2 interactions detected in CRD-Y2H and/or PCA screens exhibited ubiquitin ligase activity *in vitro*, with only 5 predicted interaction partners not exhibiting functional activity within IUAs (Figure 5.5A).

A modest reconfirmation (26/35, 74%) of CRD-Y2H and/or PCA negative TM-E3-RING/E2 pairs was observed with 9 TM-E3-RING/E2 pairs exhibiting ubiquitin ligase activity that could not be predicted from CRD-Y2H or PCA interaction data (Figure 5.5A; blue segment). However, 5/9 of these functionally active pairs, belonging to RNF150 and RNF167, reconfirm previously unverified interactions reported in other interaction studies (Figure 5.5C; red square, black outline).

Comparison with all known TM-E3-RING/E2 interactions revealed an overall more favourable negative reconfirmation rate compared to CRD-Y2H and/or PCA data obtained in the course of this study alone (86%; 25/29 predicted negative TM-E3-RING/E2 pairs did not exhibit ligase activity *in vitro*), whilst positive reconfirmation rates remain comparable to CRD-Y2H plus PCA screen data (88%; 45/51 positive interactions reconfirmed). This is reflected across all families of E2 proteins with each showing a high positive correlation with IUA data (Figure 5.5E). As such, *in vitro* activity showed strong correlation with CRD-Y2H, PCA, and literature data datasets (Figure 5.5D). Finally, only 6 active ubiquitin ligase complexes were observed that were reported as negative in the combined TM-E3-RING/E2 network (Figure 5.5B&C).

Remarkable specificity was observed between functional ligase activity and binary protein-protein interaction data. This is exemplified by the specificity of RNF186 for UBE2D but not UBE2E sub-families in both primary interaction screens and functional ubiquitin ligase activity (Figure 5.5C). Additionally, the highly specific binary interaction profiles observed for RNF144A and RNF144B TM-E3-RING proteins (UBE2L3 but not UBE2D or UBE2E) are largely mirrored in their functional activity profiles. For those binary interactions that were not verified by functional IUA activity, three belonged to a single E2 clone, UBE2L3 (Figure 5.5C&E). Specifically, RNF152 did not exhibit *in vitro* activity with UBE2L3 despite binary interactions having been reported in both CRD-Y2H and PCA screens (Figure 5.5C). These findings may suggest an inability of certain physical TM-E3-RING/E2 complexes to function as active ligase complexes.

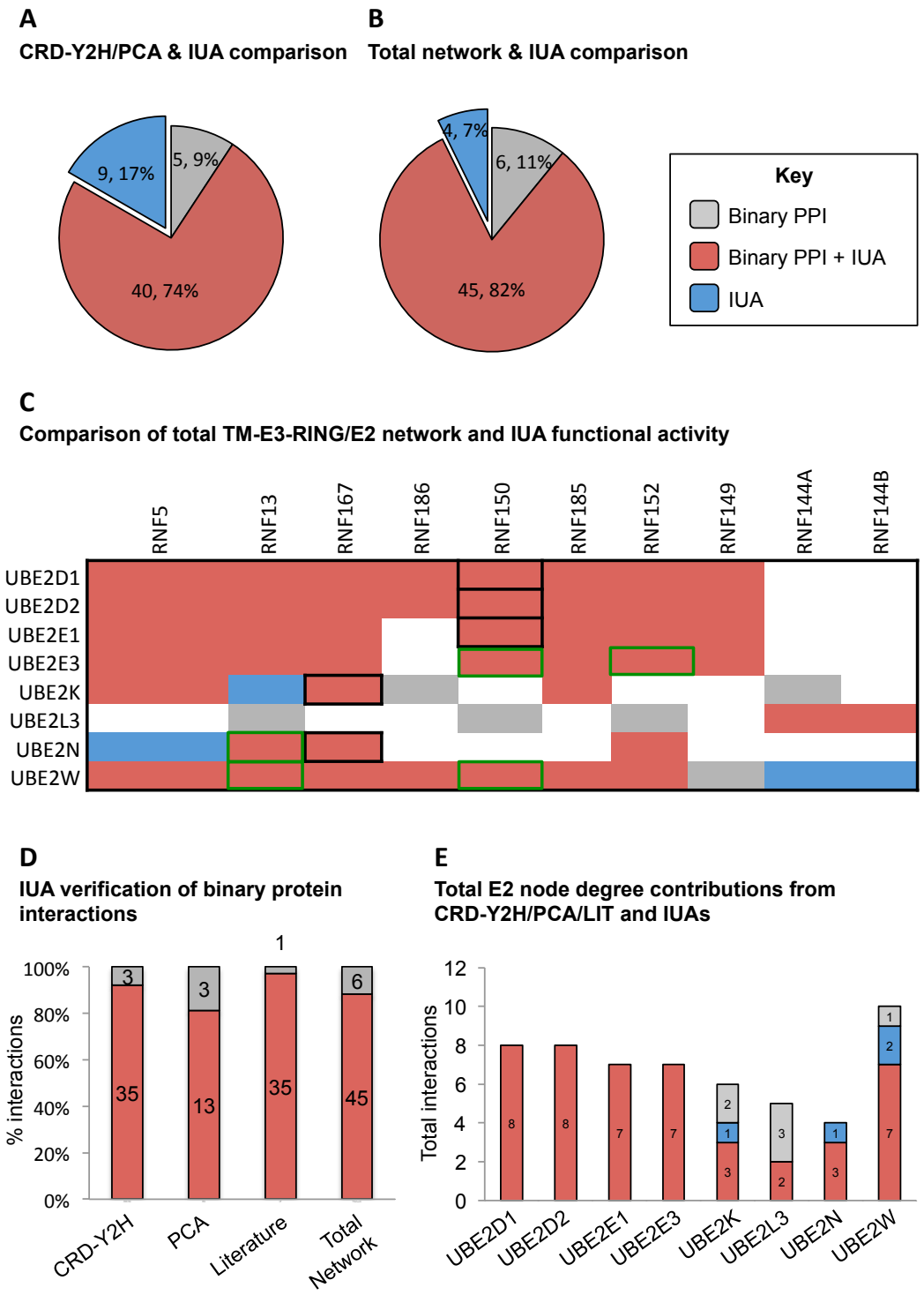

Figure 5.5. Binary protein-protein interaction (PPI) and *in vitro* activity comparison for TM-E3-RING/E2 pairs tested in IUAs. Overlap between IUA activity and binary PPI data obtained from CRD-Y2H and/or PCA screens alone **(A)** or in combination with all literature known TM-E3-RING/E2 pairs **(B)**. **(C)** Heatmap representation of reported TM-E3-RING/E2 interactions and IUA activity. **(D)** *In vitro* functional 'verification' of TM-E3-RING/E2 interactions by interaction source. **(E)** Breakdown of binary PPIs and *in vitro* ubiquitination activity for tested E2 proteins.

The *in vitro* functional testing of a broad range of TM-E3-RING and E2 proteins allowed investigation of positive and negative ubiquitin ligase activity for TM-E3-RING/E2 pairs that were reported at different stringencies of interaction in CRD-Y2H (number of reporters activated) and PCA (luciferase activity fold change) screens. In agreement with the high rate of PCA reconfirmation of CRD-Y2H interactions reported on –HIS arrays in Chapter Four, 13/14 CRD-Y2H interactions of this strength represented functionally active ligase complexes *in vitro* (Figure 5.2 A, B, G and 5.3 E & G). This is highly comparable to the positive correlation rate between in vitro functional activity and CRD-Y2H interactions detected on double (-HIS/-ADE; 8/10) and triple (-HIS/-ADE/β-gal; 14/14) selection. With respect to luciferase PCAs, 13/16 positive interactions exhibited auto-ubiquitination activity *in vitro* (Figures 5.2, 5.3, 5.4 and Figure 5.5D) with 5 PCA positive interactions demonstrated activity *in vitro* that were not reported in CRD-Y2H screens (Figure 5.5C; red box with green outline). Importantly, *in vitro* functional activity was observed for PCA-reported positives across the broad range of signal strengths; for example the RNF150/UBE2W protein pair reported a 1.8 x fold change in normalized luciferase PCA signal and delivered strong *in vitro* ubiquitination activity.

5.2.3. Different TM-E3-RING/E2 ubiquitin ligase complexes induce different ubiquitin modifications *in vitro*

E2 proteins are largely responsible for determining the form of ubiquitin modification conjugated to substrates (Christensen, Brzovic et al. 2007; David, Ziv et al. 2010). As such, it is interesting to note that several TM-E3-RING proteins (RNF5, RNF152, RNF185 and RNF186) induce different patterns of ubiquitin modification in combination with different E2 proteins within *in vitro* auto-ubiquitination reactions (Figures 5.2-5.4 and summarised in Table 5.1). In conjunction with UBE2D, UBE2E, UBE2N/V1, and UBE2K proteins all functional TM-E3-RING partners facilitated the

generation of HMW ubiquitin modifications, consistent with previous reports that each of these E2 proteins dictate formation of poly-ubiquitin chains in the presence of cognate E3-RING partners (Haldeman, Xia et al. 1997; Eddins, Carlile et al. 2006; Kim, Kim et al. 2007). LMW ubiquitin modifications represented the dominant product of active UBE2L3/TM-E3-RING complexes, again in agreement with previous *in vitro* findings (Wenzel, Lissounov et al. 2011).

In contrast to UBE2D, UBE2E, UBE2N/V1, UBE2K, and UBE2L3 E2 conjugating enzymes, UBE2W generated variable patterns of auto-ubiquitination signals within IUAs dependant upon differential TM-E3-RING protein usage (Table 5.1). Specifically, 6/9 functional UBE2W/TM-E3-RING complexes dictated the formation of LMW ubiquitin modifications upon the TM-E3-RING GST fusion whilst HMW auto-ubiquitination signals were observed for UBE2W in conjunction with TM-E3-RING

	UBE2D	**UBE2E**	**UBEW**	**UBE2L3**	**UBEN/V1**	**UBE2K**
Linkage specificity (David, Ziv et al. 2010)	All possible	K11 + K48	Mono + K11	K11	K63	K48
RNF13	+++	+++	+++	-	+++	+++
RNF167	+++	+++	+++	-	+++	+++
RNF152	+++	+++	+	-	+++	-
RNF5	+++	+++	+	-	+++	+++
RNF185	+++	+++	+	-	-	+++
RNF186	+++	-	+	-	-	-
RNF149	+++	+++	-	-	-	-
RNF150	+++	+++	+++	-	-	-
RNF144A	-	-	+	+	-	-
RNF144B	-	-	+	+	-	-

Table 5.1 Tabular display of positive and negative TM-E3-RING/E2 pairs tested in IUAs. Individual TM-E3-RING proteins were tested against each E2 protein within IUAs. Functional activity is shown according to the dominant reaction product formed for each TM-E3-RING/E2 protein pair: no activity (- , white box), LMW modifications (+ , yellow box), HMW modifications (+++ , red box).

proteins (RNF13, RNF167 and RNF150) (Figure 5.6A-C and Table 5.1). As such, different TM-E3-RING/UBE2W combinations have the ability to confer different forms of substrate modification *in vitro*. Interestingly, TM-E3-RING proteins that were shown to function with UBE2W to generate HMW ubiquitin modifications all belong to a discrete subfamily of closely related TM-E3-RING proteins characterised by the presence of an N-terminal protease associated (PA) domain, TM region, and C-terminal RING domain (PA-TM-RING).

The HMW ubiquitin modifications observed for 3 TM-E3-RING/UBE2W complexes could potentially represent poly-ubiquitination or multiple mono-ubiquitination signals. To investigate both possibilities and explore the specific nature of these HMW modifications, a selection of ubiquitin mutant proteins was utilized within *in vitro* auto-ubiquitination reactions with the RNF13/UBE2W TM-E3-RING/E2 pair (Figure 5.6D). Substitution of wild-type ubiquitin in the IUA reaction mixture with a Ub-K0 mutant protein (UM-NOK; BostonBiochem) in which all 7 lysine residues had been mutated to arginine led to a reduction in HMW ubiquitin modifications and concomitant increase of modifications in the LMW range (Figure 5.6D; anti-GST blot). As the K0-ubiquitin mutant prevents lysine-dependent ubiquitin chain elongation, the diverse modification pattern observed compared to wild-type ubiquitin implicates poly-ubiquitin chains as a major reaction product for selective TM-E3-RING/UBE2W complexes. Whilst remaining HMW modifications lack precise description they are consistent with either multiple mono-ubiquitination events or linear poly-ubiquitin chain formation.

To investigate potential linkage specificity of HMW ubiquitin signals, IUAs were performed using ubiquitin mutants encoding a single lysine > arginine mutation.

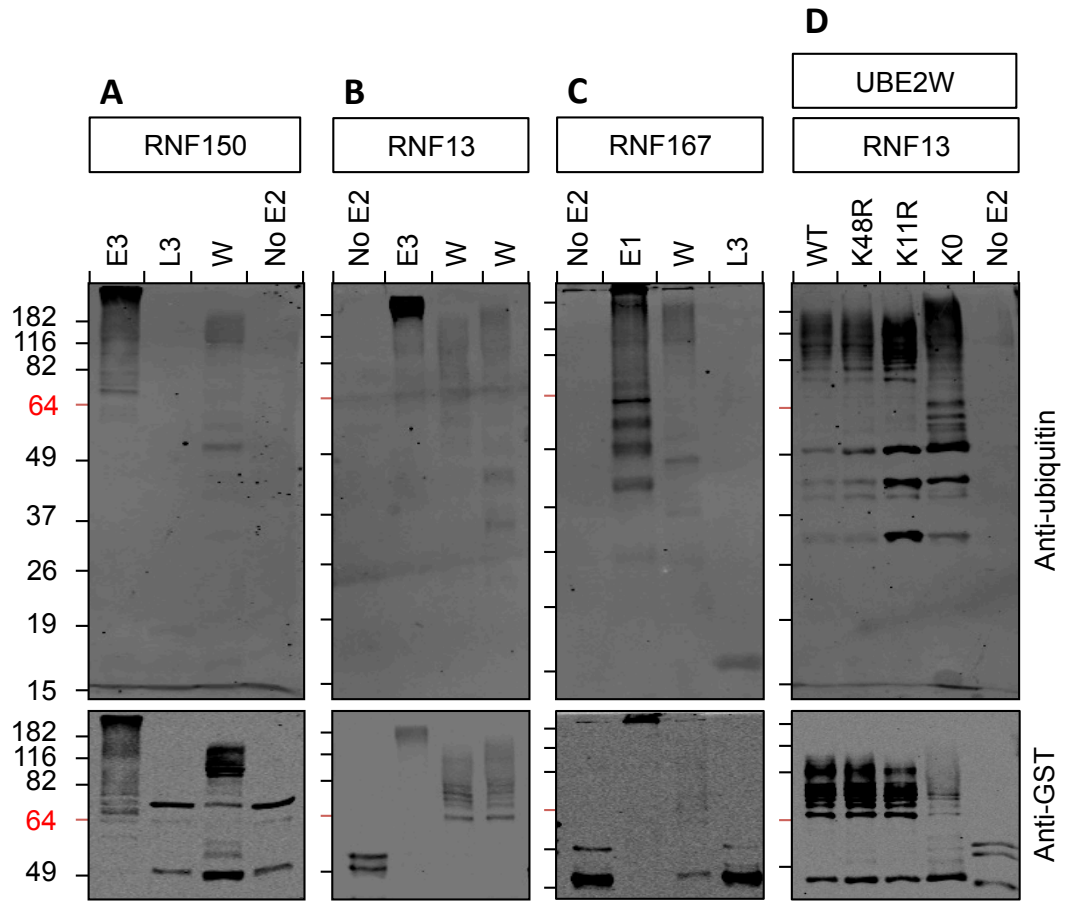

Figure 5.6 PA-TM-RING/UBE2W protein complexes generate HMW ubiquitin modifications a dominant reaction product *in vitro*. (A-D) TM-E3-RINGs, E2s and all other assay components were combined on ice. IUA reactions were initiated by addition of MgATP and reactions incubated at 37°C for 1:30 h. Auto-ubiquitination activity was qualitatively assessed by Western blot analysis using rabbit polyclonal anti-ubiquitin antibody (1:2000; 07-375; Millipore) and anti-GST antibody (1:1000; AB92; Abcam) and is signified by either HMW or LMW signals. **(D)** Wild-type ubiquitin was substituted for specific ubiquitin mutants in reaction buffer as indicated above each lane for investigation of HMW signals (WT, wild-type; K48R and K11R, single lysine to arginine mutants; K0, all lysines to arginine mutant)

Specifically, K11R and K48R ubiquitin mutants were selected as: (i) UBE2W-RFP fusion proteins have been reported capable of selectively synthesising K11-specific ubiquitin chains upon the RFP substrate chains *in vitro* (David, Ziv et al. 2010) and (ii) K48-linked polyubiquitin chains represent the most abundant ubiquitin linkage type in yeast (Xu, Duong et al. 2009) and human cells (Ziv, Matiuhin et al. 2011). However, neither of these single residue ubiquitin mutants exerted any clearly observable effect on the HMW ubiquitin modifications generated by RNF13/UBE2W within the *in vitro* auto-ubiquitination system.

5.3. Discussion

The majority of E3-RING proteins are thought to mediate protein ubiquitination events (Deshaies and Joazeiro 2009). Despite this, there is growing evidence that some E3-RING proteins may not possess intrinsic E3 ubiquitin ligase activity. For example the E3-RING proteins BARD1, BMI1, and MDMX are well characterised to lack intrinsic ligase activity and function to enhance or activate the ubiquitination activity of hetero-dimeric E3-RING partners (BRCA1 (Hashizume, Fukuda et al. 2001), RING1B (Wang, Wang et al. 2004), and MDM2 (Linares, Hengstermann et al. 2003), respectively). The demonstration that all 10 TM-E3-RING proteins tested for *in vitro* ubiquitination activity, which are dispersed throughout the TM-E3-RING family according to primary sequence similarity, form active ligase pairs with selective E2 proteins implies a direct role of the majority of TM-E3-RING proteins in substrate ubiquitination events.

5.4. Several E2-conjugating enzymes appear to dictate the form of ubiquitin modifications *in vitro*

Target ubiquitination can take two general forms in the cell; mono-/multi-ubiquitination whereby single target lysine residue(s) are modified by a single ubiquitin moiety and poly-ubiquitination, which is characterised by the assembly of

ubiquitin chains often via specific iso-peptide linkages (Ye and Rape 2009). The differential architecture of ubiquitin modification determines the function or fate of modified substrate proteins. The *in vitro* ubiquitination assays described in this chapter demonstrate individual TM-E3-RING proteins in combination with different E2 partners to yield different forms of ubiquitin modification. These findings are in agreement with the prevailing perception that whilst TM-E3-RING proteins determine substrate specificity, E2 conjugating enzymes dictate the form of ubiquitin modification upon substrates (David, Ziv et al. 2010).

In conjunction with TM-E3-RING proteins the major *in vitro* reaction product observed for a number of E2 proteins (UBE2D1, UBE2D2, UBE2E1, UBE2E3, UBE2K, UBE2N/V1) in the present study is that of HMW ubiquitin signals. Importantly, these findings support previous findings of E2 specificity including: UBE2D proteins generate poly-ubiquitin chains using all possible isopeptide bond linkages *in vitro* (Kim, Kim et al. 2007); the UBE2N/UBE2V2 hetero-dimer and UBE2K specify poly-ubiquitin chains of Lys63- (Chen and Pickart 1990; Eddins, Carlile et al. 2006) and Lys48- specificity (Haldeman, Xia et al. 1997). The UBE2N/UBE2V2, UBE2K, and UBE2D1 proteins non-covalently bind ubiquitin to facilitate poly-ubiquitin chain formation, with differences in the geometry of ubiquitin binding between E2s suggested to control the different ubiquitin chain linkage specificities (Haldeman, Xia et al. 1997; McKenna, Spyracopoulos et al. 2001; Brzovic, Lissounov et al. 2006). However, UBE2W and UBE2E proteins are reported to be incapable of non-covalently binding ubiquitin moieties. In light of the data presented in this chapter and previous *in vitro* evidence it should therefore be assumed that there must exist a diverse mechanism of poly-ubiquitin chain formation for UBE2E members (Christensen, Brzovic et al. 2007).

5.5. UBE2W generates either HMW or LMW ubiquitin modifications in complexes with different TM-E3-RING proteins

Several examples exist of E2s acting in concert to facilitate the initiation and elongation of ubiquitin chains. In particular, UBE2W has been shown to be an initiation factor for both the K63-specific UBE2N/UBE2V1 hetero-dimer and K48-specific UBE2K in BRCA1/BARD1 mediated ubiquitination, by nucleation of substrates with a single ubiquitin moiety (Christensen, Brzovic et al. 2007). The generation of (multi) mono-ubiquitin conjugates by active TM-E3-RING/UBE2W complexes supports their role in the process of mono-ubiquitination either as a distinct signal or as initiators of poly-ubiquitin chain elongation processes. However, in addition to the (multi) mono-ubiquitination activity observed for TM-E3-RING/UBE2W complexes, a subset of TM-E3-RING proteins promoted the formation of HMW ubiquitin modifications in complex with UBE2W. Therefore, specific E3-RING proteins in combination with UBE2W appear capable of dictating ubiquitin architecture on protein substrates. The use of a lysine-less ubiquitin mutant highlighted poly-ubiquitin chains as major contributors to these signals. K11R and K48R ubiquitin mutants did not significantly alter TM-E3-RING/UBE2W ubiquitination patterns. Whilst this may implicate alternative lysine residues in this poly-ubiquitin chain type, single lysine ubiquitin mutants may result in the utilisation of proximal lysine residues (K6/K11, K27/K29, K29/K33) within *in vitro* ubiquitination reactions (Kim, Kim et al. 2007; Komander 2009).

TM-E3-RING proteins responsible for HMW ubiquitin modifications with UBE2W all belong to a closely related TM-E3-RING subfamily, which are characterised by the presence of an N-terminal protease associated (PA) domain, TM region, and C-terminal RING domain (PA-TM-RING). As such, these findings may suggest a

conserved mechanism of action with UBE2W to generate HMW, to regulate disparate ubiquitination events to mono-ubiquitination signalled dictated by distinct TM-E3-RING/UBE2W pairs. Members of the PA-TM-RING subfamily are expressed at low levels in all mammalian tissues and are conserved between species, although no orthologs appear to exist in yeast; implying metazoan specific functions. The physiological roles of PA-TM-RING proteins in humans are diverse ranging from ERAD (ZNRF4) (Neutzner, Neutzner et al. 2011) to regulation of T-cell anergy and cellular proliferation (RNF128/GRAIL; (Lineberry, Su et al. 2008); RNF13 (Bocock, Carmicle et al. 2011)). Whilst the PA-TM-RINGs have a broad range of cellular functions, the E2 proteins with which they function *in vivo* remains largely unknown. Given the conserved interactions and *in vitro* ubiquitination profiles between PA-TM-RING protein and UBE2W it would be of interest to determine whether any of these cellular functions are controlled by a potentially novel mechanism of poly-ubiquitin chain synthesis *in vivo* implied from IUAs. Finally, the observation that UBE2W can participate in distinct mono- and poly-ubiquitination events with different E2 proteins may underlie the ability of TM-E3-RING/UBE2W complexes to participate in distinct processes by the selective and variable decoration of substrate proteins.

The dominant reaction product for active TM-E3-RING/UBE2L3 complexes is mono-ubiquitination, with evidence of some HMW modifications. UBE2L3 has been shown to exhibit broad specificity for HECT-type E3s (Anan, Nagata et al. 1998) but has frequently been shown to lack ubiquitin ligase activity in combination with E3-RING proteins with which they form specific complexes (Brzovic, Keeffe et al. 2003; Huang, de Jong et al. 2009). Despite these findings, UBE2L3 has been shown to exhibit ligase activity with members of the RING-in-between-RING (RBR; defined by the presence of two RING domains separated by an IBR domain) E3-RING

subfamily, which can function as RING/HECT hybrids by forming thioester-linkages with donor Ub-moieties prior to transfer to substrates (Wenzel, Lissounov et al. 2011). In the current *in vitro* functional assays the RBR proteins (RNF144A and RNF144B) but not the non-RBR proteins (RNF13, RNF150 and RNF152) exhibit ubiquitin ligase activity in conjunction with UBE2L3, despite all being predicted to interact with the E2 from binary interaction screens. These findings highlight that whilst TM-E3-RING/E2 proteins may form interacting complexes, this alone is not always sufficient for transfer of ubiquitin moieties.

6. Chapter 6: TM-E3-RING ubiquitome network generation and analysis

6.1. Introduction

E2 and E3-RING proteins control the architecture of ubiquitin modification and substrate specificity in the E1/E2/E3-RING enzymatic cascade. The generation of a comprehensive TM-E3-RING/E2 network by directed CRD-Y2H and luciferase PCA screens has revealed the combinatorial complexity of interactions between these ubiquitination cascade components. Furthermore, *in vitro* functional investigation has delivered insight into the potential regulation of the type of ubiquitin modification by selective TM-E3-RING/E2 complexes. To develop a deeper understanding of TM-E3-RING function and regulation the identification of additional E3-RING partners would provide a list of potential ubiquitination targets and/or regulators of specific E3-RING/E2 pairs. To this end, we sought to create an extended TM-E3-RING one-step network incorporating additional core cascade components (CCCs) of the ubiquitin system as well as components external to the ubiquitin system.

6.2. TM-E3-RING dimerization

An increasing mass of experimental evidence points towards a central role of E3-RING/E3-RING interactions in the regulation of ubiquitination cascades (de Bie and Ciechanover 2011). Several structurally and/or functionally characterised E3-RING dimer complexes are composed of a non-E2 binding E3-RING protein that provides structural or activating roles to an active E3-RING partner. Several ‘activating’ E3-RING proteins have been identified including BARD1, BMI1, and MDM4 E3-RING proteins, which enhance the ligase activity of the hetero-dimeric partners BRCA1 (Brzovic, Keeffe et al. 2003), RNF2 (Buchwald, van der Stoop et al. 2006), and MDM2 (Linares, Hengstermann et al. 2003) towards cognate substrate(s). Certain ubiquitin cascades require E3-RING dimerization for the facilitation of ubiquitin

transfer from E2 conjugating enzymes to substrates (e.g. RNF4 homo-dimerization (Plechanovova, Jaffray et al. 2011)) whilst E3-RING dimerization can also define the specificity of substrate selection (e.g. a unique surface at the BMI1/RING1B RING-RING dimer interface is required for recognition of short duplex DNA substrates (Bentley, Corn et al. 2011). E3-RING/E3-RING interactions can also represent ligase-substrate interactions as observed for the TM-E3-RING protein AMFR, which is *trans*-ubiquitinated by a second TM-E3-RING protein to provide a signal for AMFR degradation (Shmueli, Tsai et al. 2009). Finally, the dimerization of E3-RING proteins has been shown to enable recruitment of multiple identical or alternative E2-conjugating enzymes for participation in ubiquitination events (Parker and Ulrich 2009).

A recent Y2H based study of soluble E3-RING dimerization events has revealed a high occurrence of both homo- and hetero-dimers (329 interactions were observed in the E3-RING/E3-RING network of which 59 were homo-dimers and 270 hetero-dimers (personal communication Jonathan Woodsmith). However, TM-E3-RING dimers were not investigated in this previous Y2H study and remain poorly defined in the literature with only four known interactions: RNF128/RNF128 (Soares, Seroogy et al. 2004), MARCH9/MARCH9 (Hoer, Smith et al. 2007), PEX10/PEX10 and PEX10/PXMP3 (Okumoto, Abe et al. 2000). Given that the majority of structurally defined E3-RING dimerization events are governed by regions within, or immediately flanking, the RING domain (Linke, Mace et al. 2008; Mace, Linke et al. 2008; Liew, Sun et al. 2010), it was proposed that the use of CRD TM-E3-RING clones in directed Y2H screens would allow the determination of previously unknown TM-E3-RING dimers.

6.3. High-throughput yeast-2-hybrid screen results

To systematically investigate TM-E3-RING/TM-E3-RING interactions CRD TM-E3-RING ORFs were required in both bait and prey Y2H vectors. Utilizing the same *in vivo* gap repair methodology that was used to create the prey TM-E3-RING ORF collection (see Chapter 3.2), 51 sequence-verified TM-E3-RING CRD ORFs were cloned into either pBGD-B (N-terminal) or pGAD-B (C-terminal) bait vectors and systematically tested against the array of 50 prey CRD TM-E3-RING yeast constructs. A total of 2550 protein-protein interactions were tested with 71 reproducible interactions between 28 TM-E3-RING proteins observed on –HIS or multiple reporter arrays (Figure 6.1). As such, approximately 1/35 tested interactions were positive, comparable to the 1/25 positive interaction rate observed for soluble E3-RING/E3-RING interactions and suggesting a high incidence of dimerization events amongst both soluble and transmembrane TM-E3-RINGs.

A higher proportion of interactions (79%) were reported on at least two reporter arrays (-HIS/-ADE) for this class of interaction compared to the TM-E3-RING/E2 screen with the remaining 21% reported on –HIS arrays alone (Figure 6.1B). Interaction data was combined with the four previously known TM-E3-RING dimers to generate an up-to-date TM-E3-RING dimerization network, consisting of 75 interactions between 29 proteins. Despite the prevalence of homo-dimerization events between soluble E3-RING proteins (personal communication Jonathan Woodsmith, unpublished data) and throughout the proteome (Levy, Boeri Erba et al. 2008), only four homo-dimers are present in the combined TM-E3-RING network (TRIM59/TRIM59, PEX10/PEX10, MARCH9/MARCH9, RNF128/RNF128), with the remaining 71 interactions representing hetero-dimer complexes.

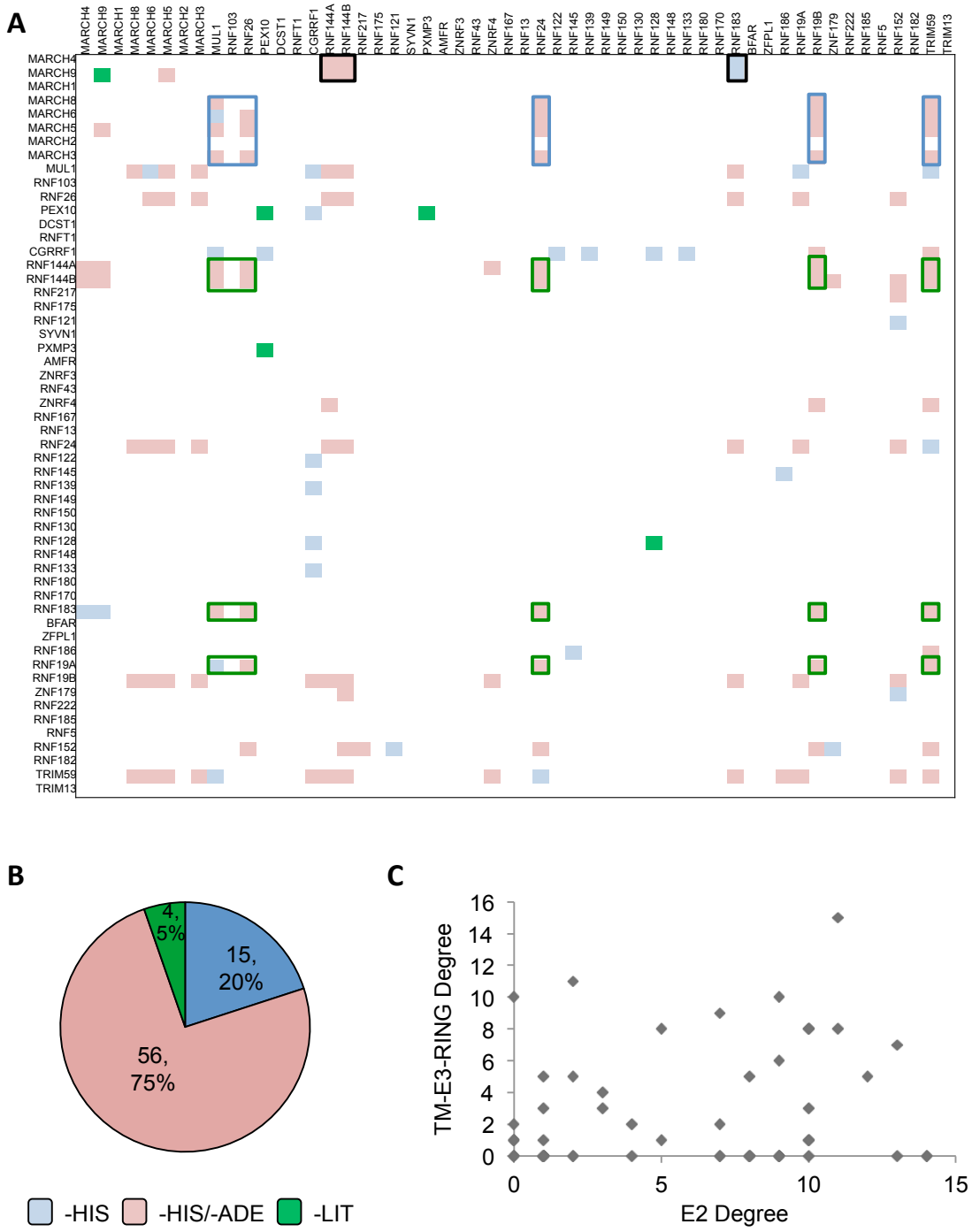

Figure 6.1 TM-E3-RING/TM-E3-RING interaction network. (A) Heatmap representation of TM-E3-RING/TM-E3-RING interactions derived from CRD-Y2H screens or literature curation. TM-E3-RINGs are ordered by primary sequence similarity. **(B)** Breakdown of interactions according to Y2H reporter activation in the CRD-GAL4 screen and number of literature only derived interactions. **(C)** Scatter plot showing TM-E3-RING and E2 degree for each TM-E3-RING protein.

To predict phylogenetic trends TM-E3-RING/TM-E3-RING interaction profiles were displayed in heat-map format and proteins ordered based upon primary sequence similarity (Figure 6.1A). Dimerization events are dispersed amongst TM-E3-RING subfamilies with clusters of closely related TM-E3-RING proteins exhibiting shared interaction partners. For example, MARCH9 and MARCH4 selectively interact RNF144A, RNF144B and RNF183 (black outline) whilst an alternative dimerization profile is common to four other MARCH proteins (blue outline). However, this dimerization profile is also observed for a number of distantly related TM-E3-RING proteins (green boxes) highlighting a current difficulty in the prediction of TM-E3-RING interaction profiles based upon primary sequence similarity alone.

6.4. E2/TM-E3-RING/TM-E3-RING sub-network analysis

To investigate the ability of TM-E3-RINGs to interact with different components of the ubiquitin machinery, the number of E2 and TM-E3-RING interaction partners was calculated for each TM-E3-RING protein. The scatter plot representation of this data revealed no correlation between TM-E3-RING or E2 degree for TM-E3-RING proteins (Figure 6.1C). However, focussing on TM-E3-RING and E2 degree for individual TM-E3-RING proteins allowed identification of four potentially distinct classes of TM-E3-RING proteins (Figure 6.2A) according to whether they bind; TM-E3-RING proteins that interact with: (i) both TM-E3-RINGs and E2s (black bar), (ii) TM-E3-RINGs alone (red bar), (iii) E2s alone (blue bar), (iv) neither TM-E3-RINGs nor E2s (white bar).

5 TM-E3-RING proteins selectively interact with TM-E3-RING but not E2 proteins in the combined TM-E3-RING/TM-E3-RING/E2 network (Figure 6.3B; RNF24, ZNF179,

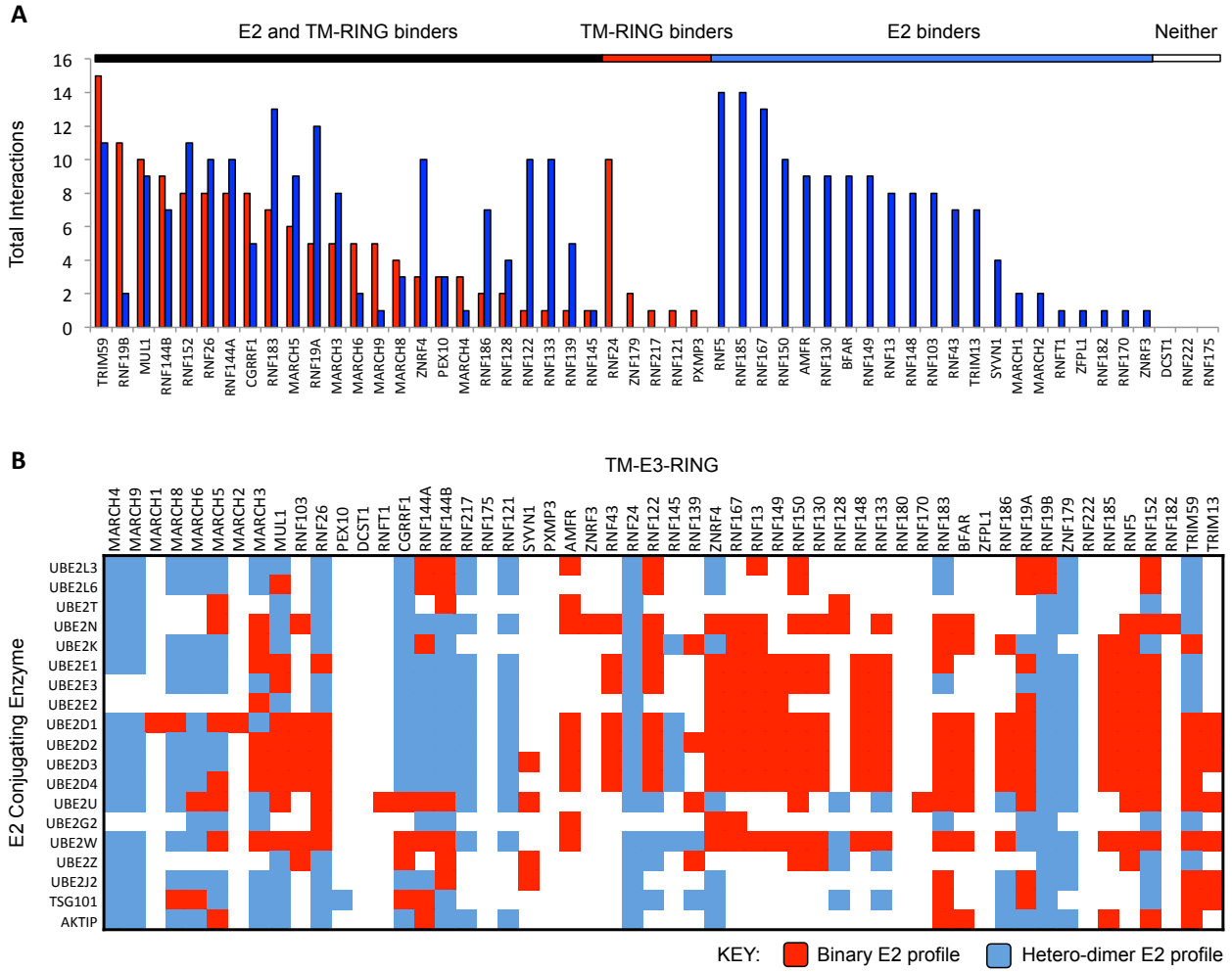

Figure 6.2 TM-E3-RING/TM-E3-RING/E2 interaction network. (A) Bar chart comparing TM-E3-RING and E2 degree for each TM-E3-RING protein. **(B)** Heatmap representation of binary E2 interactions with a given TM-E3-RING protein (red) or with a TM-E3-RING proteins dimeric partner if that E2 does not occur within its own binding profile (blue).

RNF217, RNF121, PXMP3). Each of these proteins interact with at least one E2-binding TM-E3-RING (E.g. Figure 6.3A-C), which may implicate them in structural or activating functions for their dimeric partners such as those described for BARD1/BRCA1, BMI1/RNF2, and MDM4/MDM2 complexes.

A high proportion of TM-E3-RING proteins exhibit both E2 and TM-E3-RING binding (14/24 TM-E3-RINGs have ≥ 3 TM-E3-RING and E2 protein partners). As discussed previously, binary interactions between two E2-binding TM-E3-RING proteins may represent ligase-substrate interactions and serve to negatively regulate TM-E3-RING protein levels (Shmueli, Tsai et al. 2009; de Bie and Ciechanover 2011). Alternatively, E3-RING hetero-dimerization can increase the combinatorial complexity of ubiquitination cascades by facilitated recruitment of the same or different E2 proteins to substrates by each member of the TM-E3-RING pair (Parker and Ulrich 2009). The occurrence of E2 proteins in the binding profile of a TM-E3-RING proteins binding partner that do not occur within its own binding profile was calculated to investigate the potential for recruitment of additional E2 proteins in ubiquitination cascades via selective TM-E3-RING/TM-E3-RING binding. As can be observed in Figure 6.2B the number of E2 proteins that can be potentially recruited to substrates is considerably extended as a result of hetero-dimerization events. In this analysis, binary TM-E3-RING/E2 interactions are shown (red) alongside additional E2 proteins, which occur in the binding profile of each TM-E3-RING proteins' hetero-dimeric partner(s) (blue). Similarly, TM-E3-RING dimers can also recruit the same E2 protein to substrates (supplementary file TMRING dimerization).

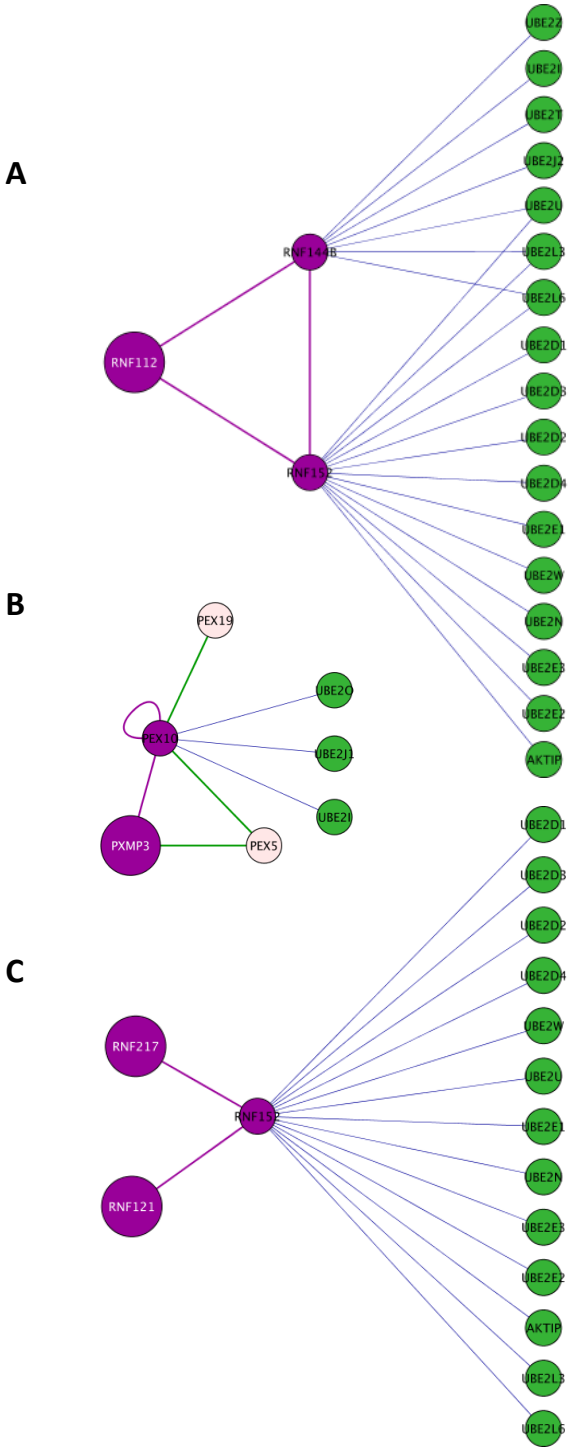

Figure 6.3 TM-E3-RING/TM-E3-RING/E2 sub-networks. (A) RNF112/RNF144B and RNF112/RNF152 heterodimers. **(B)** PEX10/PXMP3 heterodimer. **(C)** RNF217/RNF152 and RNF121/RNF152 heterodimers. TM-E3-RING (purple), E2 conjugating enzyme (green) and non-ubiquitin cascade components (pink) are shown as nodes (circles). Edges (lines) represent binary protein interactions between TM-E3-RING/TM-E3-RING (purple), TM-E3-RING/E2 Enzyme (blue) and TM-E3-RING/non-ubiquitin cascade components (green).

6.5. Systematic E3-RING dimerization characterisation

To characterise potential functional effects of different TM-E3-RING homo- and hetero-dimers the sub-cellular localisation of these components were extracted from HPRD. The subcellular distribution of a significant proportion of TM-E3-RING proteins (21/53) was not reported in this database whilst 11 were reported at a single subcellular compartment and 21 at ≥ 2 locations. The ER and (peri) nuclear compartments are each annotated > 10 TM-E3-RINGs whilst the Golgi, endosome, lysosome and plasma membrane are each reported to contain ≥ 5 TM-E3-RINGs, suggestive of shared or co-operative roles in organelle-specific processes. Finally, a number of additional organelles (mitochondria, peroxisomes, centrosomes, cytoskeleton, and extracellular compartments) have limited numbers of TM-E3-RINGs annotated (≤ 3) (Figure 6.4A).

To represent physiologically relevant complexes, TM-E3-RING proteins of a hetero-dimer complex must be capable of physically interacting in a spatiotemporal manner. Additionally, extension of the 'guilt-by-association' principle dictates that proteins that share common functions are more likely to be physically linked than those involved in disparate processes (Oliver 2000). To investigate this, analyses were performed to determine whether predicted TM-E3-RING interaction partners exhibited a higher incidence of shared subcellular distributions and/or molecular functions compared to tested but non-interacting TM-E3-RING pairs. The subcellular localization of each TM-E3-RING protein was extracted from HPRD and molecular functions from the **P**rotein **An**alysis **Th**rough **E**volutionary **R**elationships (PANTHER) classification database, which classifies genes by their functions using published scientific experimental evidence and evolutionary relationships to predict

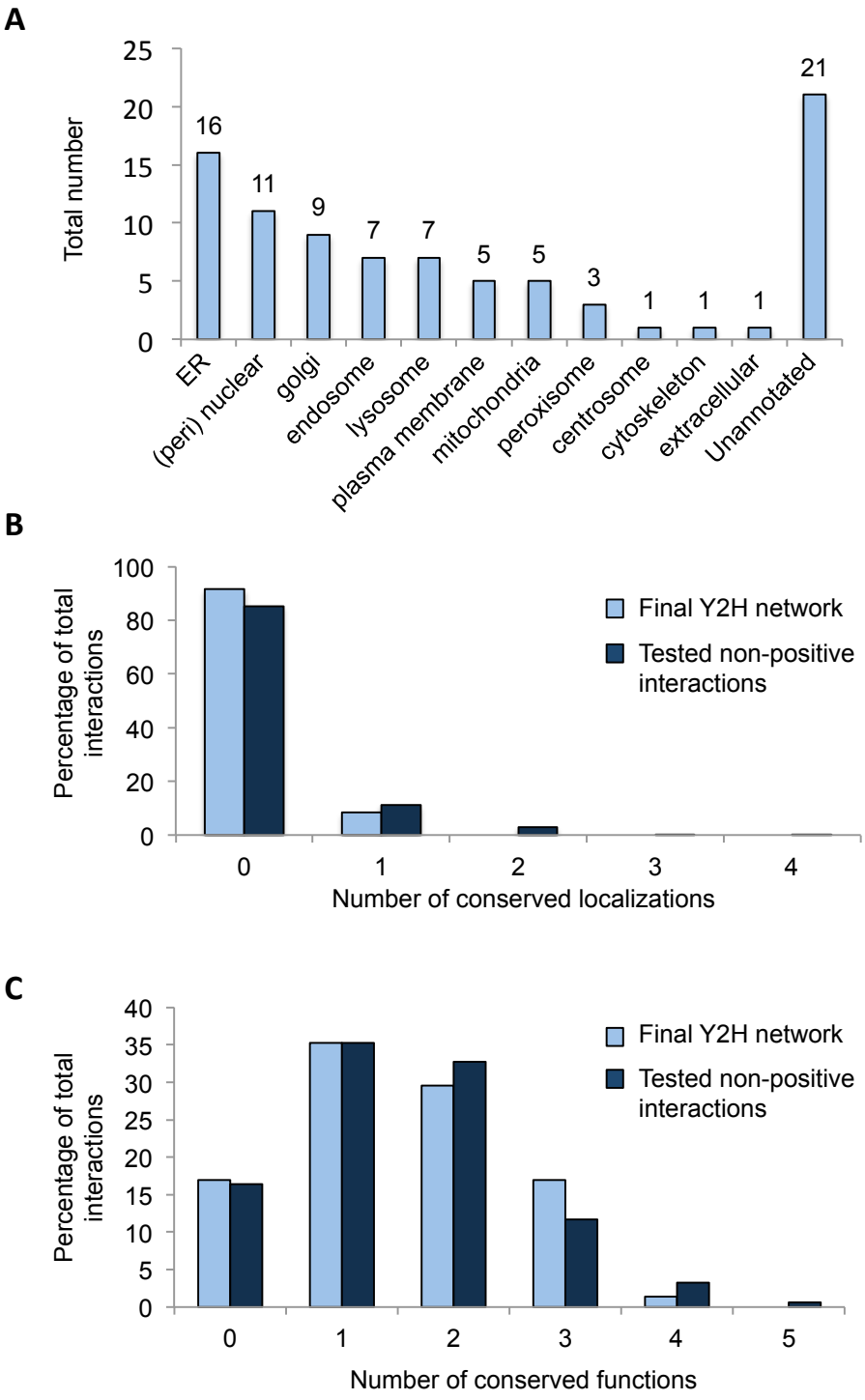

Figure 6.4 Conserved localisations and functions of TM-E3-RING dimers. (A) Number of TM-E3-RING proteins reported at different subcellular organelles within HPRD. Comparison of the number of conserved localisations **(B)** and molecular functions **(C)** across TM-E3-RING/TM-E3-RING pairs observed by CRD-Y2H compared to CRD-Y2H tested but not observed interaction pairs.

function (Thomas, Kejariwal et al. 2003). Following extraction of the molecular functions of the 53 TM-E3-RINGs from the PANTHER database, they were manually condensed into 20 general functional terms prior to comparison (supplementary Figure TMRING dimerization). However, TM-E3-RING hetero-dimers did not reveal any obvious differences in the distribution of common subcellular localisations and molecular functions compared to tested but non-interacting TM-E3-RING protein pairs (Figure 6.4B&C). These analyses rely on the thorough reporting of TM-E3-RINGs subcellular localisation and molecular function and it is therefore likely that incomplete data for TM-E3-RING proteins (exemplified by the fact that 21/53 TM-E3-RINGs are not assigned to a subcellular compartment in HPRD) prevents accurate prediction of potential shared localisations and functions at this time.

To ascertain whether less complex organisms could give insight into functional or phenotypic correlations between TM-E3-RING hetero-dimers, E3-RING orthologs in yeast (*S. cerevisiae*) and worm (*C. elegans*) model organisms were investigated. There has been a significant expansion of the E3-RING family from yeast (~ 50 E3-RINGs) to humans (308 E3-RINGs) with only 10/53 human TM-E3-RING orthologs present in *S. cerevisiae* (Supplementary file E3RING annotation), which hinders meaningful inference of TM-E3-RING dimer functions from *S. cerevisiae*. The *C. elegans* E3-RING system represents a more comprehensive system (~ 150 annotated E3-RINGs) with 31 *C. elegans* genes encoding putative orthologs of human TM-E3-RING proteins. Phenotype information was extracted for *C. elegans* orthologs of human E3-RING proteins from wormbase (http://www.wormbase.org), which provides a catalogue of RNAi knockout phenotype information in the *C. elegans* model (Harris, Antoshechkin et al. 2010). Significantly, > 80% of both

soluble and TM-E3-RINGs exhibit lethality phenotypes following siRNA knockdown. The high percentage of lethality phenotypes associated with (TM)-E3-RINGs is in contrast to E2 proteins, where only 3/25 were lethal upon RNAi knockdown (Jones, Crowe et al. 2002). Whilst this high rate of lethality prevents analysis of conserved functions or phenotypes between TM-E3-RING hetero-dimers, it is however indicative of a non-redundant role for most TM-E3-RING proteins in essential cellular processes (Supplementary file E3RING annotation).

Investigation of conserved interactions between orthologs, termed interologues, of human TM-E3-RING proteins in model organisms revealed only 3 TM-E3-RING/TM-E3-RING interaction pairs (PEX10/PEX10; SYVN1/SYVN1; RNF185/RNF185). Given that *S. cerevisiae* represents the most complete eukaryotic interactome yet contains only 10 predicted TM-E3-RING orthologs (Li, Bengtson et al. 2008; Venancio, Balaji et al. 2009), it is perhaps unsurprising that the interologue interaction network focussed around TM-E3-RING proteins is of low coverage.

6.6. Generation of a TM-E3-RING non-ubiquitome one-step

To identify potential substrates and/or regulators of selective TM-E3-RING/E2 pairs known TM-E3-RING interaction partners that are not core cascade components of the ubiquitin conjugation machinery (E1, E2, E3 or DUB proteins) were extracted from three public databases (HPRD, BioGrid, IntAct). In total, 119 binary interactions were detected between 30 TM-E3-RING proteins and 101 non-ubiquitome proteins (Figure 6.6C). Investigation of the degree of each TM-E3-RING for core cascade components and proteins external to the ubiquitin cascade reveals that whilst many TM-E3-RINGs have known interactions with components of the ubiquitination cascade, few of these TM-E3-RINGs have known interaction partners external to

the core cascade components (Figure 6.5); > 77% (41/53) of TM-E3-RING have ≤ 2 known interactions outside of the ubiquitin system (Figure 6.5; black bar) with 24 of these lacking any known non-ubiquitin cascade component interactions. Furthermore, 33% (39/119) of total TM-E3-RING/non-ubiquitome interactions belong to two extensively studied ERAD related TM-E3-RING proteins, AMFR and SYVN1 (Fang, Ferrone et al. 2001; Shmueli, Tsai et al. 2009), highlighting the need for systematic investigation of TM-E3-RING substrates to further understand TM-E3-RING function.

6.7. Network-driven investigation of the extended TM-E3-RING network

The collation of all data from this study generated an up-to-date TM-E3-RING one-step network encompassing core cascade and non-ubiquitome components (Figure 6.6A-D). Although network coverage is not comprehensive, an analysis of the

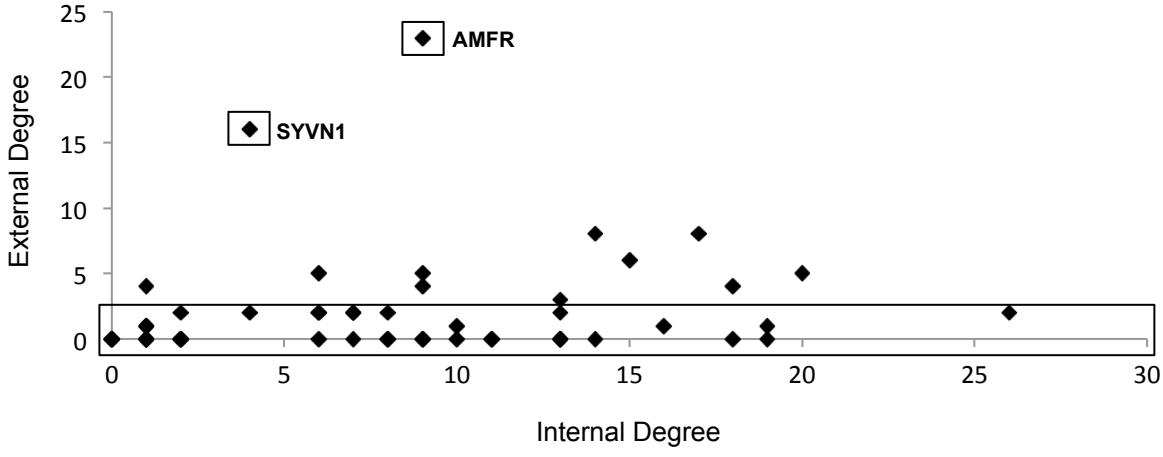

Figure 6.5 Comparison of ubiquitome and non-ubiquitome degree for TM-E3-RINGs. Scatter plot number of TM-E3-RING interactions with ubiquitin core cascade

components (internal degree) and non-ubiquitin cascade components (external degree).

extended TM-E3-RING one-step was undertaken to attempt to identify combinatorial sub-networks based upon common non-ubiquitome binding partners of hetero-meric TM-E3-RING proteins. This analysis revealed one TM-E3-RING hetero-dimer (PEX10/PXMP3) that shared a common non-ubiquitome interaction partner (PEX5) (Figure 6.3B). Whilst both PXMP3 and PEX10 interact with PEX5, only PEX10 has been reported to recruit E2 proteins in CRD-Y2H and literature studies, which may infer a structural or functional role of PXMP3 in this ubiquitination event. Interestingly, PEX10 exhibits a highly restricted E2 partner profile with UBE2O, UBE2J1 and UBE2I. It would therefore, be of interest to determine whether PXMP3 and PEX10 cooperate as a hetero-dimeric complex to selectively ubiquitinate PEX5 through one of these E2 proteins. The undefined role of UBE2O in cellular ubiquitination events and its high specificity for a limited number of E3-RINGs makes this sub-network a potentially interesting module for further investigation.

6.8. Discussion

6.8.1. E3/RING dimerization

Dimerization of E3-RING proteins is emerging as an important mechanism of regulating the specificity or activity of protein ubiquitination complexes (Poyurovsky, Priest et al. 2007; Bentley, Corn et al. 2011; de Bie and Ciechanover 2011; Plechanovova, Jaffray et al. 2011). Investigation of TM-E3-RING homo- and hetero-dimerization on a systematic scale identified a total of 75 TM-E3-RING dimers, increasing the TM-E3-RING dimer network coverage by approximately 20 fold. Also, dimerization events were distributed throughout all phylogenetic sub-groups of TM-E3-RING proteins.

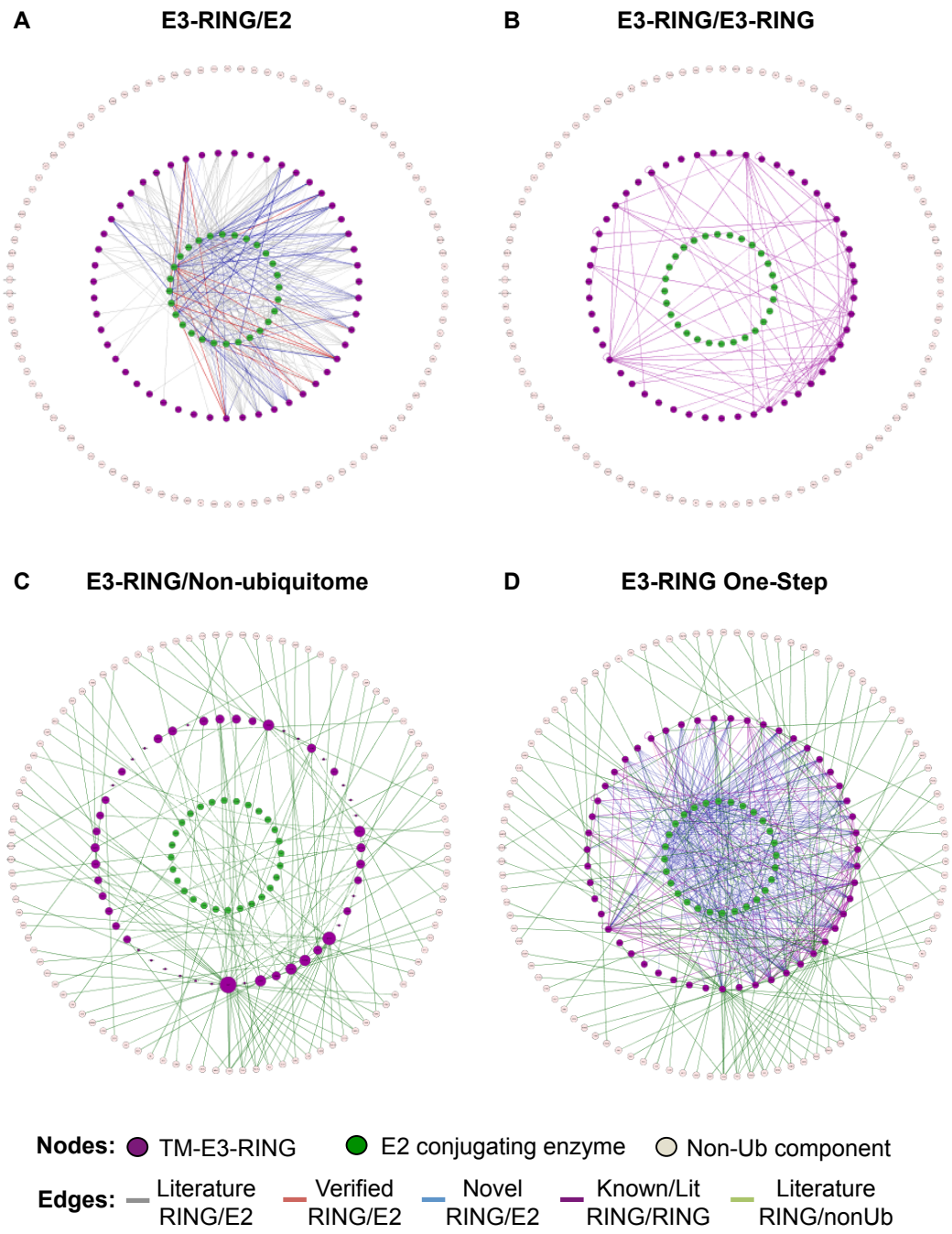

Figure 6.6 TM-E3-RING interaction networks. (A) TM-E3-RING/E2 interaction network. **(B)** TM-E3-RING/TM-E3-RING dimerization network. **(C)** TM-E3-RING/Non-ubiquitome interactions. Relative number of non-ubiquitome interactions is indicated by TM-E3-RING node size. **(D)** Total TM-E3-RING one-step network incorporating ubiquitome and non-ubiquitome components. TM-E3-RING (purple), E2 conjugating enzyme (green) and non-ubiquitin cascade components (pink) are

shown as nodes (circles). Edges (lines) represent binary protein interactions between proteins.

The extent of dimerization events reveals a significant potential for functional linkages between TM-E3-RING proteins and highlights the potential combinatorial complexity in ubiquitin conjugation events. Furthermore, potential mechanisms of complexity can be inferred. For example, differential dimerization profiles for members of the MARCH subfamily may be suggestive of diverse mechanisms of action between MARCH9/MARCH4 and other family members. Indeed, whilst considerable diversity exists between the predicted structures of MARCH proteins, many share extensive homology with another family member (MARCH1/8, MARCH2/3, MARCH4/9) (Nathan and Lehner 2009) that target common substrates: MARCH4/MARCH9, MHCI (Bartee, Mansouri et al. 2004); MARCH1/MARCH8, MHCII (Ohmura-Hoshino, Matsuki et al. 2006; Matsuki, Ohmura-Hoshino et al. 2007); MARCH2/MARCH3, syntaxin 6 (Fukuda, Nakamura et al. 2006).

6.8.2. Generation and analysis of a TM-E3-RING one-step

Despite incomplete network coverage, the ability of network analysis to provide functional insights is demonstrated by the PEX10/PXMP3/PEX5 sub-network. The import of peroxisomal matrix proteins can be divided into four steps: (1) cargo recognition by a cytosolic receptor (PEX5); (2) docking of cargo-loaded receptors at the peroxisome membrane (PEX13, PEX14 and PEX17); (3) translocation into the peroxisome lumen and cargo release; (4) mono-ubiquitin mediated recycling of receptors back to the cytosol for further rounds of protein import (Platta, El Magraoui et al. 2009). The RING peroxins PEX10, PEX2, and PEX12 are thought to function as an “importomer” complex in matrix protein import and PEX5 receptor recycling, yet the precise mechanism remains unclear (Platta, El Magraoui et al. 2007; Brown and Baker 2008). Analysis of the TM-E3-RING one-step network shows that whilst

PEX10 and PXMP3 form heterodimers and both interact with PEX5, only PEX10 recruits E2 proteins. PEX10 selectively interacts with UBE2J1, UBE2I, and the uncharacterised UBE2O protein. Whilst PEX10 ubiquitinates PEX5 in yeast in a Ubc4 (UBE2D)-dependent manner (Williams, van den Berg et al. 2008) and also interacts with a second yeast E2 ubiquitin-conjugating enzyme PEX4 (Eckert and Johnsson 2003), no such role has been observed for PXMP3. As such, PXMP3 may serve a predominantly structural role in the “importomer” complex or ‘activate’ PEX10 in ubiquitination events. Furthermore, as PEX4 does not have a clear human ortholog it will be interesting to investigate the potential role(s) of UBE2J1, UBE2I, or UBE2O in peroxosome specific processes.

Through integration of all E2, TM-E3-RING, and non-ubiquitome interactions for each TM-E3-RING into a more comprehensive network it was hypothesised that the interaction context of each TM-E3-RING dimerization event could be investigated. This analysis revealed considerable potential for recruitment of different E2 proteins to substrates via hetero-dimeric interaction partners. Additionally, the analyses described within this chapter highlight the limited knowledge of putative TM-E3-RING substrates as a major obstacle for prediction of functionally relevant ubiquitination events. The unbiased elucidation of TM-E3-RING substrates would facilitate the prediction of function dependant information flow within the human ubiquitome. Recent advances in mass spectrometric (Meierhofer, Wang et al. 2008; Xu, Paige et al. 2010) and protein microarray (Persaud, Alberts et al. 2009) based methodologies may aid the systematic characterisation of E2/E3-RING/substrate specificity whilst HTP PCA-based systems also hold promise for determination of interaction partners between the integral membrane TM-E3-RING family (Lee, Kim et al. 2011).

7. Chapter 7: Conclusions and Final Discussion

7.1. Introduction

This chapter outlines the key scientific questions that were addressed during this project and summarises the key findings that have resulted from this work. In addition, remaining areas of data paucity and future research are discussed.

Most proteins do not function in isolation but as components of protein complexes or within distinct networks which regulate cellular pathways (Morell, Ventura et al. 2009). Recent advances in mass spectrometric and Y2H interaction detection methods have enabled the unbiased mapping of binary and co-complex interactions on a proteome-wide scale, thereby dramatically increasing network coverage of the human interactome (Rual, Venkatesan et al. 2005; Stelzl, Worm et al. 2005; Ewing, Chu et al. 2007). However, individually these proteome-wide studies are estimated to cover only 10-20% of all possible human protein-protein pairs. The collation of protein-protein interaction information derived from HTP methodologies with data derived from focussed small and medium-scale interaction studies increases network density thus enabling more comprehensive mapping of protein-protein interactions within distinct biological processes or pathways. The recent completion of targeted Y2H studies directed at determining E3-RING/E2 interactions by our group (Markson, Kiel et al. 2009) and others (van Wijk, de Vries et al. 2009) have dramatically increased both network coverage and the density of human E3-RING/E2 partners. Despite the successes of these studies, key areas of data paucity remained within the human ubiquitination network, notably including information relating to interaction profiles for integral membrane E3-RING proteins

(TM-E3-RING proteins), only half (27/53) of which were annotated to have E2 binding partners prior to the initiation of this study.

The primary aim of this study was to systematically identify E2 conjugating enzyme interaction partners for the complement of TM-E3-RING proteins. As such, a comprehensive collection of sequence-verified human cytoplasmic RING domain (CRD) and full-length TM-E3-RING ORF clones was generated in a Gateway™ format, which was amenable for use in CRD-Y2H and complementary interaction detection and functional assay systems.

7.2. Systematic analysis increases the known network of TM-E3-RING/E2 interactions

Literature curation and domain analysis approaches were initially undertaken to establish *bona fide* TM-E3-RING encoding genes. This resulted in the compilation of a final list of 53 unique putative TM-E3-RING proteins. A final panel of 51 unique cytoplasmic RING domain (CRD) and full-length TM-E3-RING ORFs was produced using the Gateway cloning system (Invitrogen), providing a powerful tool for elucidating TM-E3-RING cellular function. This set of TM-E3-RING ORFs was utilized to generate a collection of 51 Y2H bait and prey constructs which were used to define selective interactions between TM-E3-RING preys and an existing collection of 44 E2-conjugating enzyme bait constructs, representing 39 unique genes (Markson, Kiel et al. 2009). Using a targeted CRD-GAL4 Y2H binary interaction assay a total of 196 TM-E3-RING/E2 interactions were identified.

Recent studies have highlighted how utilisation of multiple protein-protein interaction methodologies is necessary to ensure maximal coverage of any interaction space (Braun, Tasan et al. 2009; Chen, Rajagopala et al. 2010). Firstly, comparative

analysis of gold-standard positive reference interaction dataset revealed that each of five distinct interaction methodologies verified 21-36% of known interactions, together reconfirming ~ 60% of the total positive dataset (Braun, Tasan et al. 2009). Subsequently, the identical positive reference dataset was utilized in five alternative Y2H systems and revealed highly similar positive reconfirmation rates were observed compared to entirely different orthogonal assay systems. Therefore, different Y2H and other orthogonal interaction methodologies provide highly similar levels of accuracy and interaction coverage (Chen, Rajagopala et al. 2010). In accordance with these findings, comparative analysis between CRD-Y2H interaction data with that of the two published E3-RING/E2 Y2H interaction networks (Chapter Three), highlighted the complementary nature of different interaction techniques and facilitates the generation of an extended TM-E3-RING/E2 network, consisting of 302 interactions (Markson, Kiel et al. 2009; van Wijk, de Vries et al. 2009).

The CRD-Y2H screening described in this thesis contributes a further 121 novel interactions to the existing combined TM-E3-RING/E2 network, representing a 67% increase in network density. Out of the 121 interactions identified in this study, 49% (71/146) of previously reported Y2H interactions were reconfirmed, in comparison to 43% (10/23) of interactions previously identified by *in vitro* binding or co-immunoprecipitation assays. This reflects a favorable positive reconfirmation rate of TM-E3-RING interactions compared to that expected between orthogonal Y2H or other interaction assay systems (Braun, Tasan et al. 2009; Chen, Rajagopala et al. 2010). As a result of this study coverage of TM-E3-RING proteins in the TM-E3-RING/E2 interaction network now stands at 80% with 45/53 TM-E3-RINGs annotated E2 interaction partners.

7.3. The TM-E3-RING/E2 network provides a frame-work for better global analysis

Comparisons of global trends in the TM-E3-RING/E2 network revealed key trends in E2 binding profiles, providing insight into network architecture and redundancy in the TM-E3-RING/E2 network. Notably, striking differences in E2 binding profiles were observed for different TM-E3-RING proteins. This binding pattern implies that functionally distinct classes of E2 enzymes have evolved, which display broad or highly restricted binding profiles. It will be interesting to determine whether such binding profiles reflect generic and/or specialised roles in different cellular ubiquitination events. For example, the highly specific interaction observed between UBE2O and the peroxisomal PEX10 TM-E3-RING ligase may imply a role of the presently uncharacterised UBE2O protein in ubiquitination events at the peroxisomal membrane where PEX10 resides (Cepinska, Veenhuis et al. 2011)). Equally, the interaction of RNF167 and RNF185 with the NEDD8-specific UBE2M protein may implicate these RINGs in conjugation of this Ubiquitin-like protein.

Several E3-RING proteins have been shown to function with multiple E2s to mediate different forms of ubiquitination (Christensen, Brzovic et al. 2007). In agreement with these findings, integration of data from this study with available literature data reveals 29 TM-E3-RINGs that interact with ≥ 5 E2 partners, highlighting the complex combinatorial nature of the TM-E3-RING/E2 system. By analysing these combinatorial binding profiles, it may be possible to identify novel regulatory features of TM-E3-RING/E2 networks. For example, co-occurrence of E2 proteins in TM-E3-RING profiles shows that UBE2E almost exclusively interacts with a subset of TM-E3-RING proteins that also bind to UBE2D family members, implying a more

restricted role in cellular ubiquitination events consistent with the restricted nuclear expression of UBE2E family members.

7.4. Use of orthogonal protein complementation assays to investigate TM-E3-RING/E2 interactions

Generation of comprehensive protein-protein interaction networks requires close scrutiny of datasets to ensure data quality is of a sufficiently high standard (Braun, Tasan et al. 2009). In particular, it is important to assess the overall quality of data from different methods and studies in order to be perform meaningful analysis of protein interaction information. Furthermore, the use of orthogonal assay systems increases the interaction space that can be analysed (Braun, Tasan et al. 2009). Chapter four describes the Gateway modification and development of an orthogonal protein complementation assay system based upon split firefly luciferase reporter activity to permit the analysis of selective TM-E3-RING/E2 interactions *in vivo*. In total a collection of 16 unique CRD-E3 FLucC constructs and 7 E2 FLucN constructs were generated to analyze the selective interactions between phylogenetically distant TM-E3-RING and E2 proteins in human cells.

CRD-luciferase PCA screening identified 37 potential TM-E3-RING/E2 interactions, representing a 37% overlap with primary CRD-Y2H screens, which is comparable to the observed overlap between other orthogonal assay systems (Braun, Tasan et al. 2009). In addition to the 55% of positive CRD-Y2H interactions verified by luciferase PCA assays, 6 luciferase PCA positive interactions reconfirm previously unverified interactions reported in other HTP Y2H studies that were not detected in CRD-Y2H studies. A further 10 interactions were observed within luciferase PCA screening that had not been reported in any previous interaction studies. Taken together,

these findings further highlight the value of utilising multiple interaction methods to provide maximal coverage of a given interaction space.

Furthermore, it is informative to compare the rate at which CRD-Y2H interactions were reconfirmed within the CRD-luciferase PCA assay. Interestingly, equivalent proportions of CRD-Y2H interactions detected in -HIS (56%), -HIS/-ADE (47%), or -HIS/-ADE/-β-gal (42%) arrays were reconfirmed in orthogonal CRD-luciferase PCAs. These findings implicate interactions reproducibly detected on -HIS only selection as likely to represent true physical positive partners compared to interactions detected on two or three independent Y2H reporters.

7.5. Use of orthogonal PCAs for investigation of full-length TM-E3-RING/E2 interactions

A key advantage of protein complementation assays is the potential to investigate interactions involving full-length clones in live human cells as proteins can be expressed in the context of their normal cellular environment, with appropriate post-translational modifications, and at the correct subcellular localisation (Morell, Ventura et al. 2009). Therefore, the use of this type of orthogonal *in vitro* assay enables both spatial and conditional aspects of TM-E3-RING/E2 protein interactions to be taken into consideration. Preliminary co-expression versus lysate mixing experiments (Chapter Four) indicated that interactions detected within the luciferase PCA assay are predominantly the result of interactions occurring within HEK 293T cells, and not post-lysis association. Furthermore, data from this study demonstrates the applicability of using the luciferase PCA system to analyse interactions between full-length TM-E3-RING and E2 clones; in total 7 full-length TM-E3-RING clones were found to have selective interactions with 5 different E2 proteins. This remains

one of the few binary interaction methods in which the highly labile E3-RING/E2 proteins interactions can be detected.

7.6. Functional analysis of predicted TM-E3-RING/E2 partners

The majority of E3-RING proteins are thought to mediate protein ubiquitination events. However, of the 312 TM-E3-RING/E2 complexes identified in the literature, CRD-Y2H and luciferase PCA data from this study, very few of the predicted complexes have been investigated to test their ability to function as active ligase complexes (Markson, Kiel et al. 2009; van Wijk, de Vries et al. 2009). Chapter Five describes the development and utilisation of an *in vitro* auto-ubiquitination assay system to prescribe *in vitro* functional activity profiles for predicted TM-E3-RING/E2 pairs. The observation that 10 TM-E3-RING proteins, derived from 3 phylogenetically distinct branches of the TM-E3-RING family all exhibit ubiquitin ligase activity *in vitro* highlights the probability that many more predicted E2-binding TM-E3-RING complexes will be functionally active.

Despite these findings, there has been emerging evidence that some E3-RING proteins do not possess intrinsic E3-ligase activity. For example, BARD1, BMI1, and MDMX do not function in isolation with E2 enzymes to ubiquitinate selective substrates. However, these proteins do function to enhance the ubiquitination activity of a second E3-RING protein (BRCA1, RING1B, and MDM2, respectively) through the formation of specific heterodimeric complexes (Hashizume, Fukuda et al. 2001; Linares, Hengstermann et al. 2003; Wang, Wang et al. 2004). It therefore remains to be determined whether TM-E3-RING proteins that have few or no E2 partners function in a mechanistically similar manner or alternatively if these

restricted E2 binding profiles represent a more selective role in substrate ubiquitination events.

In vitro functional data (Chapter Five) also highlights the fact that individual E3-RING proteins, in combination with different E2 partners can yield different forms of ubiquitin modifications, consistent with the prevailing notion that whilst E3-RING proteins serve to select substrates for ubiquitination events, E2 proteins dictate the type of ubiquitin modification conjugated to the selected substrates (David, Ziv et al. 2010). A number of E2 proteins (UBE2D1, UBE2D2, UBE2E1, UBE2E3, UBE2K, UBE2N/V1) were shown to predominantly generate HMW ubiquitin modifications *in vitro* whilst the predominant product formed for active TM-E3-RING/UBE2L3 complexes was mono-ubiquitination. Whilst UBE2L3 has been shown to exhibit a broad specificity for HECT-type E3s (Anan, Nagata et al. 1998) they have recently been reported to have ubiquitin ligase activity in combination with only those E3-RING proteins belonging to RING-in-between-RING subfamilies (Wenzel, Lissounov et al. 2011). Although E3-RING proteins belonging to both RBR and non-RBR families were found to interact with UBE2L3 within CRD-Y2H screens, only those belonging to the RBR (RNF144A and RNF144B) family exhibited ubiquitin ligase activity in our studies. These findings suggest that whilst E3-RING/E2 proteins may form interacting complexes this alone is not sufficient for transfer of ubiquitin moieties. Indeed recent studies have shown that in complex with UBE2L3, RBR proteins serve as RING/HECT hybrids by binding E2s via one RING domain yet Ub transfer occurring via an obligate thioester-linkage with the donor Ub-moiety at a conserved cysteine residue in RING2.

In contrast to the *in vitro* activity profiles of most tested E2 proteins, UBE2W generated different forms of ubiquitin modifications (mono- to poly-ubiquitination) dependent upon TM-E3-RING partner. The implication of these findings is that some E3-RING proteins may contribute to the specificity of ubiquitination architecture on selective substrates. Whilst the precise architecture of HMW TM-E3-RING/E2 ubiquitination remains to be determined the use of a K0-mutant highlighted poly-ubiquitin chains as the major product of these reactions. TM-E3-RING proteins, which form HMW ubiquitin modifications with UBE2W all belong to the closely related PA-TM-RING subfamily, which may reflect a conserved mechanism of poly-ubiquitin chain formation by PA-TM-RING/UBE2W ligase pairs. It would be interesting to elucidate both the molecular determinants and potential physiological relevance of these findings events.

Finally, Y2H screens and previously known interaction data was utilised to generate an extended TM-E3-RING-centric interaction network to identify potential regulators and/or ubiquitin cascade targets. The obtained data increased the TM-E3-RING dimerization identified 71 interactions and may serve as a useful tool in the investigation or prediction of dimerization functions in humans whilst highlights the elucidation of potential substrates as a priority for determination of the control and regulation of specific ubiquitin cascades by TM-E3-RING/E2 pairs.

7.7. Investigating the specificity of ubiquitination events *in vivo*

7.7.1. Tissue specificity of ubiquitome components

The specific interactions that occur between ubiquitin cascade components, substrates and auxiliary proteins dictate the formation of specific ubiquitin signals upon substrates. Whilst the yeast two-hybrid system and other HTP interaction

detection techniques enable generation of high-density interaction maps of potential protein interaction partners, it is unlikely that all reported interactions will occur in the context of the human cell. To represent physiologically relevant interactions it is a prerequisite that protein interaction partners are expressed together in a given tissue/cell at the same time. The integration of secondary datasets, such as tissue mRNA expression profiles, with high-density interaction networks therefore allows for refinement of interactions into more functionally relevant modules for investigation of tissue or cell-type specific interactions (Taylor, Linding et al. 2009).

To assess the tissue specificity of predicted TM E3-RING/E2 protein pairs, the mRNA expression profiles of TM E3-RING and E2 proteins were extracted from a published genome-scale mRNA expression screen incorporating 79 distinct human tissues (Su, Cooke et al. 2002). In accordance with a recent study, a normalised expression level of ≥ 250 was used as a high-confidence measure of gene expression (Bossi and Lehner 2009). 30 TM E3-RING and 40 E2 conjugating enzymes were represented within the mRNA expression dataset. In agreement with previous reports, the majority of E2 conjugating enzymes examined were expressed in the majority of human tissues tested (van Wijk and Timmers 2010) (83% expressed in ≥ 51 tissues; Figure 7.1A). A smaller yet significant subset of TM E3-RING proteins were also reported in a large number of tested tissues 50% expressed in ≥ 51 tissues; Figure 7.1A). Interestingly, 100% of binary interactions reported in the total TM E3-RING/E2 network that were included in the mRNA expression study co-express in 1 or more human tissues. Interestingly, 37% of these TM E3-RING/E2 interactions were reported for TM E3-RING and E2 proteins that co-express in ≥ 51 tissues (Figure 7.1B). Whilst this finding potentially implicates a large proportion of total TM E3-RING/E2 interactions in ubiquitination

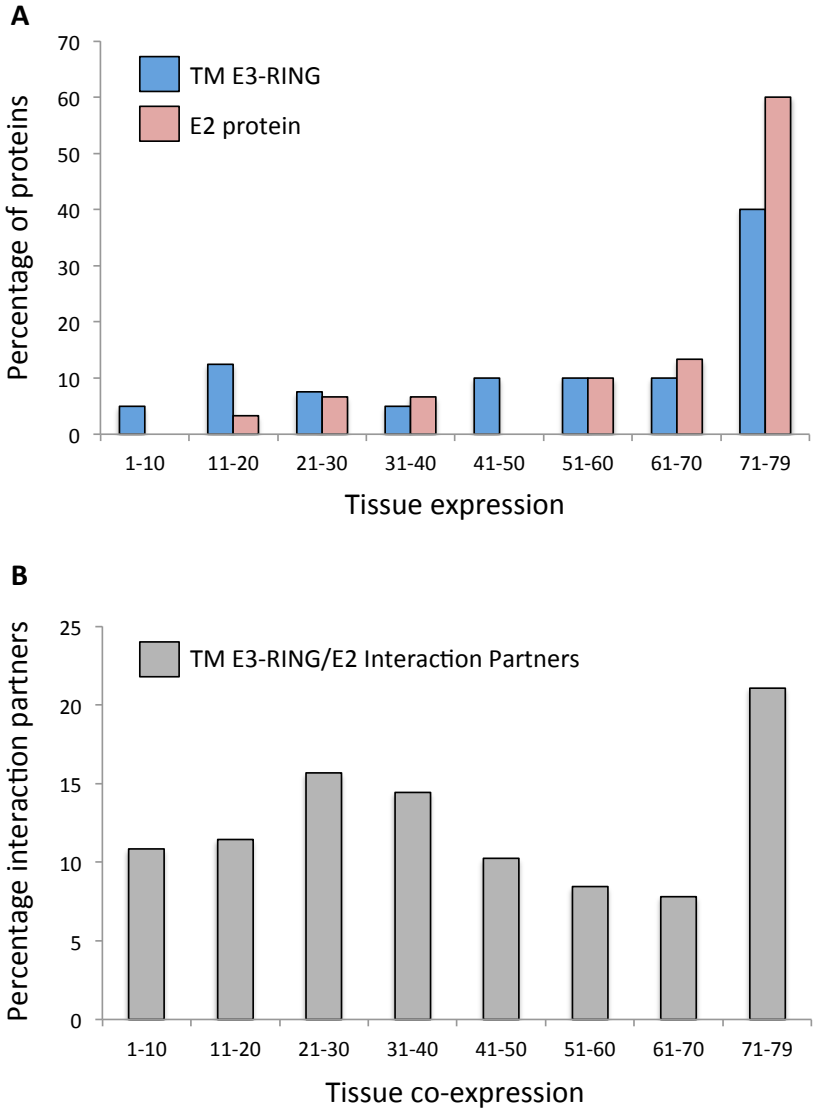

Figure 7.1 TM-E3-RING and E2 tissue expression analysis. (A) TM E3-RING and E2 proteins with positive mRNA expression data in a given number of 79 tested human tissues (Su, Cooke et al. 2002). **(B)** Percentage of binary TM E3-RING/E2 interactions occurring between TM E3-RING and E2 proteins that were co-expressed in a given number of 79 tested human tissues (Su, Cooke et al. 2002).

events that are common to the majority of human tissues, a number of TM E3-RING/E2 interaction pairs co-express in a more limited number of tissues (22% of total protein partners co-occur in ≤ 20 tissues), suggestive of a similarly high degree of tissue-specific ubiquitination events.

As most E2 proteins are expressed in the majority of tested human tissues it is possible that the more selective expression of TM E3-RING proteins may account for a large proportion of the predicted tissue-specific E3-RING/E2 complexes. In agreement with this hypothesis, 91% of the E3-RING/E2 interactions that were restricted to ≤ 20 tissues were attributed to TM E3-RING proteins that were expressed in less than half of tested tissues, compared to only 30% that were attributed to E2 proteins reported in the same number of tissues. Therefore a model could be envisaged whereby a 'core' E2 machinery exists in the majority of human cell types and specificity of ubiquitination may be controlled by the selective expression of interacting TM E3-RING protein partners, with the caveat that the restricted tissue expression of a small number of E2 conjugating enzymes (notably UBE2U (urogenital tract (van Wijk, de Vries et al. 2009)), UBE2O (skeletal and heart muscle (Yokota, Nagai et al. 2001)) and UBE2K (brain (Kikuchi, Furukawa et al. 2000) will also contribute to tissue-specific ubiquitination events. The integration of such secondary datasets can therefore be used to refine large-scale protein-protein interaction networks for guided investigation. For example, Figure 7.2 shows the refinement of the total TM E3-RING/E2 network (A) into brain (B) and ovary (C) tissue specific sub-networks. The number of human tissues with positive mRNA expression (Su, Cooke et al. 2002) and literature curated tissue expression profile for each TM E3-RING and E2 protein is shown in Table 7.1 & 7.2.

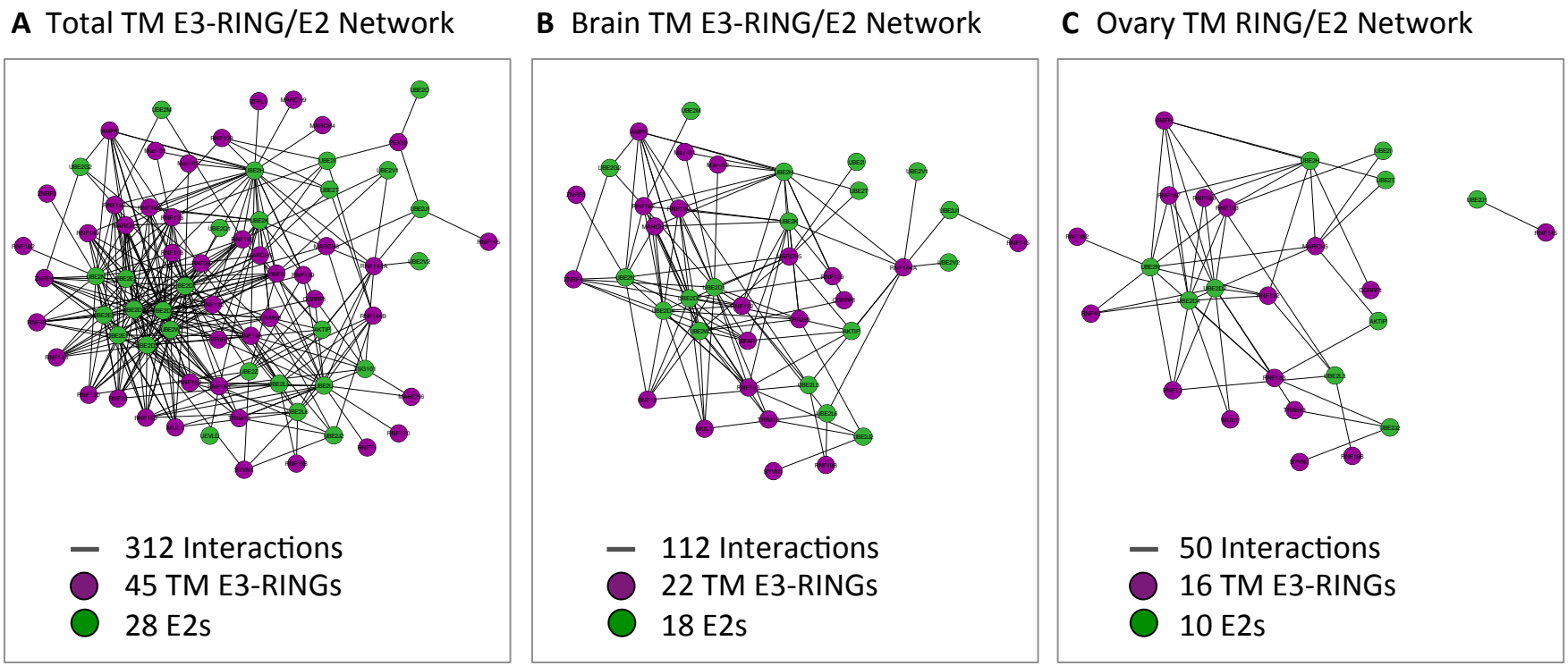

Figure 7.2. Binary TM E3-RING/E2 interaction networks. (A) Total, **(B)** brain-specific and **(C)** ovary-specific TM E3-RING/E2 interaction networks. Nodes (circles) represent proteins and edges (lines) represent binary interactions between proteins.

7.7.2. Subcellular localization of ubiquitome components

To identify the subcellular localisation of TM E3-RING and E2 proteins literature searches were performed (shown in Tables 7.1 & 7.2). Whilst TM E3-RING proteins reside at distinct subcellular organelle membranes, almost half show at least partial localization to the ER membrane suggestive of a key importance of ubiquitination events at this subcellular organelle. Indeed, numerous TM E3-RING proteins have been reported to function in ERAD ubiquitination events (see section 1.4.5.1. Known roles of TM E3-RING proteins). Similarly, the localization of TM E3-RING proteins to other subcellular organelles including endosomes, lysosomes, nucleus, golgi, mitochondria, plasma membrane, peroxisome and centrosomes is likely to reflect their specialized roles in ubiquitination events at these organelles; for example, peroxisomal protein import (PXMP3, PEX10; (Prestele, Hierl et al. 2010)), control of mitochondrial fusion/fission dynamics (MARCH5, (Nakamura, Kimura et al. 2006)) and nuclear signaling (RNF13; (Bocock, Carmicle et al. 2010)).

In stark contrast to the restricted localizations of TM E3-RING proteins, the majority of E2 proteins exhibit diffuse distributions, present in both the cytosol and nucleus. Therefore, most E2 proteins may be capable of interacting spatially with all TM E3-RING proteins resident at any cellular organelle to participate in ubiquitination events at numerous locations dependent upon TM E3-RING partner. The broad subcellular distribution of E2 proteins highlights a difficulty of predicting high-confidence TM E3-RING/E2 partners based upon subcellular localization. Of the 13 E2 conjugating enzymes that display more restricted subcellular localization patterns, 2 are present in the cytosol but excluded from the nucleus, 7 are solely present in the nuclear compartment (UBE2E1-3, UBE2H, UBE2I, and UBE2U) and

4 are anchored to the ER membrane either by transmembrane domains (UBE2J1/2) or via ER-resident protein interaction partners (UBE2G1/2) (Biederer, Volkwein et al. 1997). The more restricted localization for these E2 proteins may underlie organelle-specific roles in cellular ubiquitination events; for example the four ER-associated E2 proteins have been shown to function in ERAD events (Biederer, Volkwein et al. 1997) whilst UBE2I, UBE2W and UBE2E family members have known roles in nuclear substrate ubiquitination events (Spektor, Congdon et al. 2011; Zhang, Zhou et al. 2011).

7.8. Regulation of protein-protein interactions within the ubiquitin system

7.8.1. Spatial and temporal availability of ubiquitin and substrate components

In order to ensure the appropriate timing and duration of selective ubiquitination events additional levels of system regulation exist *in vivo*. The current knowledge of such regulation will be discussed here.

The temporal availability of ubiquitin cascade components, substrate proteins and auxiliary factors represents an initial mechanism of controlling specificity of protein-protein interactions in ubiquitin cascades. Indeed, the activity of SCF E3-RING/E2 ligases are regulated by the availability of their substrates (Vodermaier 2004). From an auxiliary factor perspective, elevated levels of sterols within the ER membrane recruit a TM E3-RING protein (RNF138) to HMG CoA reductase, a critical enzyme in sterol biosynthesis, to signal the substrate for proteasomal degradation, allowing RNF138 to serve as an effective sensor and regulator of appropriate sterol levels in the cell (Jo, Lee et al. 2011).

Table 7.1 TM E3-RING Protein Expression Information

	Subcellular Localization	Tissue Expression: ♯ tissues*|Literature data	Temporal Expression Patterns
RNF19B	Cytolytic granules in NK cells	79	Upregulated in NK cells following IFN/cytokines stimulation
RNF167	Endolysosomal system	79	
MARCH1	Endolysosomal system	17|Widely expressed	Downregulated in dendritic cells upon cell maturation
TRIM59	ER	46	
RNF5	ER	28	
ZNRF4	ER	57	
AMFR	ER	76|Widely expressed	Upregulated following induction of ER stress
RNF133	ER	29|Widely expressed but at low levels; high expression in brain (all cell types)	
RNF148	ER	NT	
TRIM13	ER	79	Upregulated (protein stabilized) following induction of ER stress
BFAR	ER	73	
RNF26	ER	NT	
CGRRF1	ER	74	
MARCH6	ER	74|Widely expressed	
RNFT1	ER	68	
RNF150	ER	NT	
RNF170	ER	11	Important for embryonic development in *D. melanogaster*
MARCH4	ER	NT|Restricted tissue expression: brain, placenta, lung, pancreas	
SYVN1	ER	79|Widely expressed (most cell types)	Upregulated following induction of ER stress
MARCH2	ER|endolysosomal system|plasma membrane	56|Widely expressed	
MARCH8	ER|endosome	NT|Widely expressed	
MARCH3	ER|endosome	50|Widely expressed	
RNF128	ER|endosome|golgi|perinuclear region	20|Expressed in T-cells, brain, kidney, heart, liver, ovary, testes, thymus	In CD4 T-cells expression levels are elevated upon induction of anergy
RNF13	ER|endosome|nucleus	79|Widely expressed	Expression levels are developmentally regulated during myogenesis
RNF122	ER|golgi	78	
RNF185	ER|mitochondria	3	
RNF139	ER|plasma membrane	73|Widely expressed	
RNF24	golgi|nucleus	79	
RNF43	ER|nucleus|extracellular	39|Restricted tissue expression: lung and kidney	

Table 7.1 TM E3-RING Protein Expression Information (continued)

	Subcellular Localization	Tissue Expression: ♯ tissues*|Literature data	Temporal Expression Patterns
RNF152	Lysosome	NT|Expressed in all cancer cell lines tested from multiple origins	
MARCH9	Lysosome	27|Widely expressed	
MARCH5	Mitochondria	78|Widely expressed	
MUL1	Mitochondria|peroxisome	72|Widely expressed	Essential for embryonic development in mice
RNF144A	Nucleus|golgi	42	
ZFPL1	Nucleus|golgi	38|Widely expressed	
RNF19A	Perinuclear region|centrosome	8|Widely expressed	
PEX10	Peroxisome	NT|Widely expressed	
PXMP3	Peroxisome	74|Widely expressed	
RNF149	Plasma membrane	15	
RNF183		69	
RNF186		52	
RNF144B		NT|Widely expressed	Expression is Induced by p53
RNF130		58|Widely expressed	Developmentally expressed during embryonic development *D. melanogaster* |upregulated following induction of apoptosis
RNF145		79	
DCST1	Plasma membrane	NT|human dendritic cells	Selectively expressed in activated but not resting blood dendritic cells
RNF175		NT	
RNF103		NT	
RNF182		16|Restricted tissue expression: enriched in brain	
ZNF179		67|Expressed in a number of tissues: enriched in brain	
RNF121		67	
RNF217		NT	
ZNRF3		42	
RNF222		NT	

Table 7.1. TM E3-RING protein expression information. The known subcellular localization, tissue distribution, and temporal expression patterns for each TM E3-RING protein are shown. For tissue expression, the total number of human tissues with positive mRNA transcripts are shown for each TM E3-RING protein (*79 tested tissues (Su, Cooke et al. 2002)) alongside literature reported data. Further information and references can be found in Supplementary Excel File_TMRING&E2_Expression.

Table 7.2 E2 Protein Expression Information

	Subcellular Localization	Tissue Expression: ♯ tissues*|Literature data	Temporal Expression Patterns
UBE2D1	Nucleus|cytosol	36|Widely expressed	
UBE2D2	Nucleus|cytosol	79|Widely expressed	
UBE2D3	Nucleus|cytosol	NT|Widely expressed	
UBE2D4	Nucleus|cytosol	79|Widely expressed	
TSG101	Nucleus|cytosol	NT|Widely expressed	Expressed at similar levels during all stages of development
AKTIP	Nucleus|cytosol	74|Widely expressed	
UBE2L3	Nucleus|cytosol	79	Expression is cell-cycle regulated (downregulated during S-phase but restored by G2 phase)
UBE2N	Nucleus|cytosol	79|Widely expressed	
UBE2O	Nucleus|cytosol	26|Widely expressed: predominantly skeletal and heart muscle	
UBE2T	Nucleus|cytosol	55|Restriction tissue expression and expressed at low levels - highest in skeletal muscle and testes	
UBE2Z	Nucleus|cytosol	NT|Widely expressed	
CDC34	Nucleus|cytosol	68|Widely expressed	Upregulated in meiotic and postmeiotic haploid germ cells co-inciding with when chromatin modifications occur.
UBE2A	Nucleus|cytosol	79|Widely expressed	Constitutively expressed. Upregulated in testis during spermatogenesis.
UBE2B	Nucleus|cytosol	76|Widely expressed	Constitutively expressed. Upregulated in testis during spermatogenesis.
UBE2V1	Nucleus|cytosol	79|Widely expressed	
UBE2V2	Nucleus|cytosol	57|Widely expressed	
UBE2C	Nucleus|cytosol	79|Widely expressed at low levels	Expression is cell-cycle regulated (transcriptionally activated by the spindle assembly checkpoint protein Cdc20 following chromosome segregation)
BIRC6	Nucleus|cytosol	79|Widely expressed	
UBE2M	Nucleus|cytosol	60|Widely expressed	
UBE2Q1	Nucleus|cytosol	79	

Table 7.2 E2 Protein Expression Information (continued)

	Subcellular Localization	Tissue Expression: ♯ tissues*|Literature data	Temporal Expression Patterns
UBE2K	Cytosol	66|Widely expressed: predominantly brain	
CDC34	Cytosol	79	
UBE2W	Nucleus	40|High expression levels in heart, brain, liver, and pancreas. Marginally expressed in 16 other tissues	
UBE2H	Nucleus	74	
UBE2E1	Nucleus	NT	
UBE2E2	Nucleus	NT|Expressed in majority of tested tissues	
UBE2E3	Nucleus	NT|Widely expressed: predominantly skeletal muscle	
UBE2U	Nucleus	NT|Urogenital tract	
UBCE9	Nucleus	79|Widely expressed	Constitutively expressed throughout all stages of development
UBE2J2	ER	79	
UBE2J1	ER	67	
UBE2G1	ER	79|Widely expressed	
UBE2G2	ER	75|Widely expressed	
UBE2L6	-	28|Preferentially expressed in immune cells	Expression induced following IFNα stimulation
UEVLD	-	16	
UBE2F	-	NT|Widely expressed	
UBE2DNL	-	NT	
UBE2S	-	NT	Expression is cell-cycle regulated
UBE2Q2	-	69	

Table 7.2. E2 protein expression information. The known subcellular localization, tissue distribution, and temporal expression patterns for each E2 conjugating enzyme are shown. For tissue expression, the total number of human tissues with positive mRNA transcripts are shown for each E2 conjugating enzyme (*79 tested tissues (Su, Cooke et al. 2002)) alongside literature reported information. Further information and references can be found in Supplementary Excel File TMRING_E2_Expression.

The spatial redistribution of ubiquitome and/or substrate components in response to certain cellular signals also serves as a mechanism of regulating protein-protein interactions in ubiquitin cascades. For example, in response to activation of PKC signalling the TM E3-RING protein RNF13 undergoes retrograde transport from recycling endosomes to the inner nuclear membrane, exposing the RING domain to the nucleoplasm (Bocock, Carmicle et al. 2010) and altering the available cohort of ubiquitin cascade and substrate proteins for ubiquitination events. Similarly, the redistribution of substrates can also regulate substrate ubiquitination events. For example, nuclear export of the cell-cycle regulatory protein $p27^{Kip1}$ upon quiescent cell re-entry into the cell cycle is necessary for its recognition by cytosolic E3-RING/E2 ligase complexes for ubiquitin-proteasomal degradation (Hara, Kamura et al. 2001).

Regulation of ubiquitin cascade components also provides an effective mechanism of regulating specific ubiquitin cascades. A striking example exists for the cascade components dedicated to the process of ISGylation whereby the expression of ISG15 (Ubl), UBE1L (E1-activating), and UBE2L6 (E2-conjugating) is induced by stimulation with interferons, leading to the specific temporal control of ISG15-conjugation to a variety of targets (Durfee, Kelley et al. 2008). Another example exists for the ERAD-associated TM E3-RING, AMFR, which is stabilized following induction of ER-stress to provide an acute mechanism of increasing degradation of unfolded ER proteins through increased association of AMFR with both E2 and substrate proteins (Shen, Ballar et al. 2007). Finally, the UBE2S and UBE2L3 E2-conjugating enzymes are tightly regulated during the cell cycle allowing for activation and termination of substrate ubiquitination events by the APC/C E3 ligase

complex and control progression through the cell cycle (Williamson, Wickliffe et al. 2009).

7.8.2. Regulation by post-translational modifications

7.8.2.1. Phosphorylation, glycosylation and hydroxylation

Post-translational modifications of ubiquitin cascade and substrate proteins can influence cellular ubiquitination events by altering or increasing the affinity of protein-protein interactions (Pines and Lindon 2005). Phosphorylation has been widely reported to control substrate 'ubiquitination' state (Deshaies and Joazeiro 2009). For example, the phosphorylated but not unmodified Sic1 substrate is recognized and ubiquitinated by the SCF_{Cdc34} ligase (Verma, Annan et al. 1997). In addition, a considerable number of E3-RING substrates are targeted to their ligase by various covalent modifications including glycosylation (Yoshida, Chiba et al. 2002) and proline hydroxylation (Ivan, Kondo et al. 2001). For example the ER-resident E2 protein UBE2J2 specifically targets hydroxylated amino acids upon ER-associated substrates (Wang, Herr et al. 2009). Finally, CDK-mediated phosphorylation of the APC/C E3-RING upon mitotic entry enables interaction between APC/C and specific substrates (Vodermaier 2004), whilst SGK1-mediated phosphorylation of NEDD4-2 prevents its binding to the Epithelial Sodium Channel (ENaC) substrate (Wiemuth, Lott et al. 2010).

Post-translational modifications can also directly regulate the formation of active E3-RING/E2 complexes. For example, the Cdk-mediated phosphorylation of UBE2A affects E2 activity by increasing its association with E3-RING protein partners (Sarcevic, Mawson et al. 2002). Additionally, the casein kinase 2-mediated phosphorylation of CDC34/UBE2R1 exerts a variety of effects on E2 activity

including altered localization, which may influence available E3-RING or substrate interaction partners (Coccetti, Tripodi et al. 2008; Deshaies and Joazeiro 2009).

7.8.2.2. Modification with Ubiquitin or Ubiquitin-like molecules

Specificity of binding events in the ubiquitin conjugational machinery can also be regulated by the covalent conjugation of ubiquitin or ubiquitin-like moieties at multiple stages in the cascade. As discussed in section 1.5.3 many E3-RING proteins are known to be ubiquitinated often by an autocatalytic process in the presence of an appropriate E2 partner (de Bie and Ciechanover 2011), which can lead to downregulation of E3 activity owing to degradation by the proteasome. For example, the autocatalytic turnover of MDM2 has been thought to play a critical role in titrating its activity towards its substrate p53 (Li, Brooks et al. 2004). Additionally, the TM-E3-RING protein, AMFR, is *trans*-ubiquitinated by a second TM-E3-RING protein, SYVN1, to provide a signal for AMFR degradation (Shmueli, Tsai et al. 2009). The conjugation of NEDD8 to the CRLs results in conformation changes that allow binding of CRLs to substrate or facilitates ubiquitin transfer from E2 to substrate potentially through a mechanism involving the tighter binding of E3-RING to E2 proteins (Saha and Deshaies 2008). In contrast, the covalent modification of the E2 enzyme UBE2K by SUMO within helix 1 inhibits interaction with the ubiquitin E1 thus preventing charging of UBE2K with ubiquitin (Pichler, Knipscheer et al. 2005). It is therefore evident multiple levels of regulation exist in the ubiquitin system to control the timing, duration and specificity of ubiquitin/Ubl conjugation events *in vivo*.

The high-density TM-E3-RING interaction maps generated during the course of this study using a variety of binary interaction and functional assays have provided new

insights into specificity and potential regulation within ubiquitination cascades. The identification of potential interaction partners for this subset of proteins can be used to inform hypothesis-driven study into investigation of novel regulatory features within the ubiquitin system and mechanisms of selective ubiquitination events.

Bibliography

Aichem, A., C. Pelzer, et al. (2010). "USE1 is a bispecific conjugating enzyme for ubiquitin and FAT10, which FAT10ylates itself in cis." Nature communications **1**: 13.

Anan, T., Y. Nagata, et al. (1998). "Human ubiquitin-protein ligase Nedd4: expression, subcellular localization and selective interaction with ubiquitin-conjugating enzymes." Genes to cells : devoted to molecular & cellular mechanisms **3**(11): 751-763.

Andersen, P. L., H. Zhou, et al. (2005). "Distinct regulation of Ubc13 functions by the two ubiquitin-conjugating enzyme variants Mms2 and Uev1A." J. Cell Biol. **170**(5): 745-755.

Aranda, B., P. Achuthan, et al. (2010). "The IntAct molecular interaction database in 2010." Nucleic acids research **38**(Database issue): D525-531.

Argenzio, E., T. Bange, et al. (2011). "Proteomic snapshot of the EGF-induced ubiquitin network." Molecular systems biology **7**: 462.

Arrigo, A. P., K. Tanaka, et al. (1988). "Identity of the 19S 'prosome' particle with the large multifunctional protease complex of mammalian cells (the proteasome)." Nature **331**(6152): 192-194.

Bailly, V., S. Lauder, et al. (1997). "Yeast DNA repair proteins Rad6 and Rad18 form a heterodimer that has ubiquitin conjugating, DNA binding, and ATP hydrolytic activities." The Journal of biological chemistry **272**(37): 23360-23365.

Baker, R. T. and P. G. Board (1991). "The human ubiquitin-52 amino acid fusion protein gene shares several structural features with mammalian ribosomal protein genes." Nucleic Acids Res **19**(5): 1035-1040.

Barabasi, A. L. and Z. N. Oltvai (2004). "Network biology: understanding the cell's functional organization." Nat Rev Genet **5**(2): 101-113.

Bartee, E., M. Mansouri, et al. (2004). "Downregulation of major histocompatibility complex class I by human ubiquitin ligases related to viral immune evasion proteins." J Virol **78**(3): 1109-1120.

Bartke, T., C. Pohl, et al. (2004). "Dual Role of BRUCE as an Antiapoptotic IAP and a Chimeric E2/E3 Ubiquitin Ligase." Molecular Cell **14**(6): 801-811.

Bates, E. E., O. Ravel, et al. (1997). "Identification and analysis of a novel member of the ubiquitin family expressed in dendritic cells and mature B cells." Eur J Immunol **27**(10): 2471-2477.

Bentley, M. L., J. E. Corn, et al. (2011). "Recognition of UbcH5c and the nucleosome by the Bmi1/Ring1b ubiquitin ligase complex." The EMBO journal **30**(16): 3285-3297.

Biederer, T., C. Volkwein, et al. (1997). "Role of Cue1p in ubiquitination and degradation at the ER surface." Science **278**(5344): 1806-1809.
Bocock, J. P., S. Carmicle, et al. (2009). "The PA-TM-RING protein RING finger protein 13 is an endosomal integral membrane E3 ubiquitin ligase whose RING finger domain is released to the cytoplasm by proteolysis." The FEBS journal **276**(7): 1860-1877.
Bocock, J. P., S. Carmicle, et al. (2010). "Nuclear targeting of an endosomal E3 ubiquitin ligase." Traffic **11**(6): 756-766.
Bocock, J. P., S. Carmicle, et al. (2011). "Trafficking and proteolytic processing of RNF13, a model PA-TM-RING family endosomal membrane ubiquitin ligase." The FEBS journal **278**(1): 69-77.
Borden, K. L., M. N. Boddy, et al. (1995). "The solution structure of the RING finger domain from the acute promyelocytic leukaemia proto-oncoprotein PML." The EMBO journal **14**(7): 1532-1541.
Bossi, A. and B. Lehner (2009). "Tissue specificity and the human protein interaction network." Molecular systems biology **5**: 260.
Braun, P., M. Tasan, et al. (2010). "Reply to "Exhaustive benchmarking of the yeast two-hybrid system"." Nat Meth **7**(9): 668-668.
Braun, P., M. Tasan, et al. (2009). "An experimentally derived confidence score for binary protein-protein interactions." Nat Methods **6**(1): 91-97.
Breitkreutz, B. J., C. Stark, et al. (2008). "The BioGRID Interaction Database: 2008 update." Nucleic acids research **36**(Database issue): D637-640.
Bremm, A., S. M. V. Freund, et al. (2010). "Lys11-linked ubiquitin chains adopt compact conformations and are preferentially hydrolyzed by the deubiquitinase Cezanne." Nat Struct Mol Biol **17**(8): 939-947.
Brown, L. A. and A. Baker (2008). "Shuttles and cycles: transport of proteins into the peroxisome matrix (review)." Molecular membrane biology **25**(5): 363-375.
Brzovic, P. S., J. R. Keeffe, et al. (2003). "Binding and recognition in the assembly of an active BRCA1/BARD1 ubiquitin-ligase complex." Proceedings of the National Academy of Sciences of the United States of America **100**(10): 5646-5651.
Brzovic, P. S. and R. E. Klevit (2006). "Ubiquitin transfer from the E2 perspective: why is UbcH5 so promiscuous?" Cell Cycle **5**(24): 2867-2873.
Brzovic, P. S., A. Lissounov, et al. (2006). "A UbcH5/ubiquitin noncovalent complex is required for processive BRCA1-directed ubiquitination." Mol Cell **21**(6): 873-880.
Buchwald, G., P. v. d. Stoop, et al. (2006). "Structure and E3-ligase activity of the Ring–Ring complex of Polycomb proteins Bmi1 and Ring1b." The EMBO Journal.
Burr, M. L., F. Cano, et al. (2011). "HRD1 and UBE2J1 target misfolded MHC class I heavy chains for endoplasmic reticulum-associated degradation." Proceedings of the National Academy of Sciences of the United States of America **108**(5): 2034-2039.
Burroughs, A. M., M. Jaffee, et al. (2008). "Anatomy of the E2 ligase fold: Implications for enzymology and evolution of ubiquitin/Ub-like protein conjugation." Journal of Structural Biology **In Press, Corrected Proof**.
Cadwell, K. and L. Coscoy (2005). "Ubiquitination on nonlysine residues by a viral E3 ubiquitin ligase." Science **309**(5731): 127-130.
Ceol, A., A. Chatr Aryamontri, et al. (2010). "MINT, the molecular interaction database: 2009 update." Nucleic acids research **38**(Database issue): D532-539.

Cepinska, M. N., M. Veenhuis, et al. (2011). "Peroxisome fission is associated with reorganization of specific membrane proteins." Traffic **12**(7): 925-937.
Chen, B., J. Mariano, et al. (2006). "The activity of a human endoplasmic reticulum-associated degradation E3, gp78, requires its Cue domain, RING finger, and an E2-binding site." Proceedings of the National Academy of Sciences of the United States of America **103**(2): 341-346.
Chen, Y. C., S. V. Rajagopala, et al. (2010). "Exhaustive benchmarking of the yeast two-hybrid system." Nat Methods **7**(9): 667-668; author reply 668.
Chen, Z. and C. M. Pickart (1990). "A 25-kilodalton ubiquitin carrier protein (E2) catalyzes multi-ubiquitin chain synthesis via lysine 48 of ubiquitin." The Journal of biological chemistry **265**(35): 21835-21842.
Choi, Y. S., Y. H. Jeon, et al. (2009). "60th residues of ubiquitin and Nedd8 are located out of E2-binding surfaces, but are important for K48 ubiquitin-linkage." FEBS letters **583**(20): 3323-3328.
Choudhary, C. and M. Mann (2010). "Decoding signalling networks by mass spectrometry-based proteomics." Nature reviews. Molecular cell biology **11**(6): 427-439.
Christensen, D. E., P. S. Brzovic, et al. (2007). "E2-BRCA1 RING interactions dictate synthesis of mono- or specific polyubiquitin chain linkages." Nat Struct Mol Biol **14**(10): 941-948.
Ciechanover, A. (2005). "Intracellular protein degradation: from a vague idea, through the lysosome and the ubiquitin-proteasome system, and onto human diseases and drug targeting (Nobel lecture)." Angew Chem Int Ed Engl **44**(37): 5944-5967.
Ciechanover, A., S. Elias, et al. (1980). "Characterization of the heat-stable polypeptide of the ATP-dependent proteolytic system from reticulocytes." Journal of Biological Chemistry **255**(16): 7525-7528.
Coccetti, P., F. Tripodi, et al. (2008). "The CK2 phosphorylation of catalytic domain of Cdc34 modulates its activity at the G1 to S transition in Saccharomyces cerevisiae." Cell Cycle **7**(10): 1391-1401.
Cusick, M. E., N. Klitgord, et al. (2005). "Interactome: gateway into systems biology." Human molecular genetics **14 Spec No. 2**: R171-181.
Das, R., J. Mariano, et al. (2009). "Allosteric activation of E2-RING finger-mediated ubiquitylation by a structurally defined specific E2-binding region of gp78." Mol Cell **34**(6): 674-685.
David, Y., T. Ziv, et al. (2010). "The E2 Ubiquitin-conjugating Enzymes Direct Polyubiquitination to Preferred Lysines." Journal of Biological Chemistry **285**(12): 8595-8604.
de Bie, P. and A. Ciechanover (2011). "Ubiquitination of E3 ligases: self-regulation of the ubiquitin system via proteolytic and non-proteolytic mechanisms." Cell Death Differ.
De Duve, C., R. Gianetto, et al. (1953). "Enzymic content of the mitochondria fraction." Nature **172**(4390): 1143-1144.
Denuc, A. and G. Marfany (2010). "SUMO and ubiquitin paths converge." Biochemical Society transactions **38**(Pt 1): 34-39.
Deshaies, R. J. and C. A. Joazeiro (2009). "RING domain E3 ubiquitin ligases." Annu Rev Biochem **78**: 399-434.
Dikic, I., S. Wakatsuki, et al. (2009). "Ubiquitin-binding domains - from structures to functions." Nature reviews. Molecular cell biology **10**(10): 659-671.
Ding, Z., J. Liang, et al. (2006). "A retrovirus-based protein complementation assay screen reveals functional AKT1-binding partners." Proceedings of the

National Academy of Sciences of the United States of America **103**(41): 15014-15019.
Dodd, R. B., M. D. Allen, et al. (2004). "Solution structure of the Kaposi's sarcoma-associated herpesvirus K3 N-terminal domain reveals a Novel E2-binding C4HC3-type RING domain." The Journal of biological chemistry **279**(51): 53840-53847.
Dominguez, C., A. M. Bonvin, et al. (2004). "Structural model of the UbcH5B/CNOT4 complex revealed by combining NMR, mutagenesis, and docking approaches." Structure **12**(4): 633-644.
Durfee, L. A., M. L. Kelley, et al. (2008). "The basis for selective E1-E2 interactions in the ISG15 conjugation system." The Journal of biological chemistry **283**(35): 23895-23902.
Dye, B. T. and B. A. Schulman (2007). "Structural Mechanisms Underlying Posttranslational Modification by Ubiquitin-Like Proteins." Annual Review of Biophysics and Biomolecular Structure **36**(1): 131-150.
Eckert, J. H. and N. Johnsson (2003). "Pex10p links the ubiquitin conjugating enzyme Pex4p to the protein import machinery of the peroxisome." Journal of cell science **116**(Pt 17): 3623-3634.
Eddins, M. J., C. M. Carlile, et al. (2006). "Mms2-Ubc13 covalently bound to ubiquitin reveals the structural basis of linkage-specific polyubiquitin chain formation." Nat Struct Mol Biol **13**(10): 915-920.
Eddins, M. J., R. Varadan, et al. (2007). "Crystal Structure and Solution NMR Studies of Lys48-linked Tetraubiquitin at Neutral pH." Journal of Molecular Biology **367**(1): 204-211.
Eichacker, L. A., B. Granvogl, et al. (2004). "Hiding behind hydrophobicity. Transmembrane segments in mass spectrometry." The Journal of biological chemistry **279**(49): 50915-50922.
Eletr, Z. M., D. T. Huang, et al. (2005). "E2 conjugating enzymes must disengage from their E1 enzymes before E3-dependent ubiquitin and ubiquitin-like transfer." Nature structural & molecular biology **12**(10): 933-934.
Etlinger, J. D. and A. L. Goldberg (1977). "A soluble ATP-dependent proteolytic system responsible for the degradation of abnormal proteins in reticulocytes." Proceedings of the National Academy of Sciences of the United States of America **74**(1): 54-58.
Ewing, R. M., P. Chu, et al. (2007). "Large-scale mapping of human protein-protein interactions by mass spectrometry." Molecular systems biology **3**: 89.
Eyster, C. A., N. B. Cole, et al. (2011). "MARCH ubiquitin ligases alter the itinerary of clathrin-independent cargo from recycling to degradation." Molecular biology of the cell **22**(17): 3218-3230.
Fan, F. and K. V. Wood (2007). "Bioluminescent assays for high-throughput screening." Assay and drug development technologies **5**(1): 127-136.
Fang, S., M. Ferrone, et al. (2001). "The tumor autocrine motility factor receptor, gp78, is a ubiquitin protein ligase implicated in degradation from the endoplasmic reticulum." Proc Natl Acad Sci U S A **98**(25): 14422-14427.
Fang, S., J. P. Jensen, et al. (2000). "Mdm2 is a RING finger-dependent ubiquitin protein ligase for itself and p53." J Biol Chem **275**(12): 8945-8951.
Fields, S. and O. Song (1989). "A novel genetic system to detect protein-protein interactions." Nature **340**(6230): 245-246.
Finley, D., A. Ciechanover, et al. (1984). "Thermolability of ubiquitin-activating enzyme from the mammalian cell cycle mutant ts85." Cell **37**(1): 43-55.

Finn, R. D., J. Mistry, et al. (2009). "The Pfam protein families database." Nucleic Acids Res **38**(Database issue): D211-222.
Freemont, P. S., I. M. Hanson, et al. (1991). "A novel cysteine-rich sequence motif." Cell **64**(3): 483-484.
Fukuda, H., N. Nakamura, et al. (2006). "MARCH-III Is a novel component of endosomes with properties similar to those of MARCH-II." J Biochem **139**(1): 137-145.
Furukawa, K., N. Mizushima, et al. (2000). "A protein conjugation system in yeast with homology to biosynthetic enzyme reaction of prokaryotes." J Biol Chem **275**(11): 7462-7465.
Gareau, J. R. and C. D. Lima (2010). "The SUMO pathway: emerging mechanisms that shape specificity, conjugation and recognition." Nature reviews. Molecular cell biology **11**(12): 861-871.
Garnett, M. J., J. Mansfeld, et al. (2009). "UBE2S elongates ubiquitin chains on APC/C substrates to promote mitotic exit." Nat Cell Biol **11**(11): 1363-1369.
Geng, J. and D. J. Klionsky (2008). "The Atg8 and Atg12 ubiquitin-like conjugation systems in macroautophagy." EMBO Rep **9**(9): 859-864.
Guais, A., S. Siegrist, et al. (2006). "h-Goliath, paralog of GRAIL, is a new E3 ligase protein, expressed in human leukocytes." Gene **374**: 112-120.
Haldeman, M. T., G. Xia, et al. (1997). "Structure and function of ubiquitin conjugating enzyme E2-25K: the tail is a core-dependent activity element." Biochemistry **36**(34): 10526-10537.
Hara, T., T. Kamura, et al. (2001). "Degradation of p27(Kip1) at the G(0)-G(1) transition mediated by a Skp2-independent ubiquitination pathway." The Journal of biological chemistry **276**(52): 48937-48943.
Harris, T. W., I. Antoshechkin, et al. (2010). "WormBase: a comprehensive resource for nematode research." Nucleic acids research **38**(Database issue): D463-467.
Hashizume, R., M. Fukuda, et al. (2001). "The RING heterodimer BRCA1-BARD1 is a ubiquitin ligase inactivated by a breast cancer-derived mutation." The Journal of biological chemistry **276**(18): 14537-14540.
He, H., Y. Dang, et al. (2003). "Post-translational modifications of three members of the human MAP1LC3 family and detection of a novel type of modification for MAP1LC3B." J Biol Chem **278**(31): 29278-29287.
Hicke, L., H. L. Schubert, et al. (2005). "Ubiquitin-binding domains." Nat Rev Mol Cell Biol **6**(8): 610-621.
Hida, N., M. Awais, et al. (2009). "High-sensitivity real-time imaging of dual protein-protein interactions in living subjects using multicolor luciferases." PLoS One **4**(6): e5868.
Hoege, C., B. Pfander, et al. (2002). "RAD6-dependent DNA repair is linked to modification of PCNA by ubiquitin and SUMO." Nature **419**(6903): 135-141.
Hoer, S., L. Smith, et al. (2007). "MARCH-IX mediates ubiquitination and downregulation of ICAM-1." FEBS letters **581**(1): 45-51.
Hofmann, R. M. and C. M. Pickart (1999). "Noncanonical MMS2-encoded ubiquitin-conjugating enzyme functions in assembly of novel polyubiquitin chains for DNA repair." Cell **96**(5): 645-653.
Hough, R., G. Pratt, et al. (1987). "Purification of two high molecular weight proteases from rabbit reticulocyte lysate." J Biol Chem **262**(17): 8303-8313.
Hough, R. and M. Rechsteiner (1986). "Ubiquitin-lysozyme conjugates. Purification and susceptibility to proteolysis." J Biol Chem **261**(5): 2391-2399.

Hu, C. D. and T. K. Kerppola (2003). "Simultaneous visualization of multiple protein interactions in living cells using multicolor fluorescence complementation analysis." Nature biotechnology **21**(5): 539-545.
Huang, A., R. N. de Jong, et al. (2009). "E2-c-Cbl recognition is necessary but not sufficient for ubiquitination activity." Journal of molecular biology **385**(2): 507-519.
Huang, D. T., O. Ayrault, et al. (2009). "E2-RING expansion of the NEDD8 cascade confers specificity to cullin modification." Mol Cell **33**(4): 483-495.
Huang, D. T., H. Walden, et al. (2004). "Ubiquitin-like protein activation." Oncogene **23**(11): 1958-1971.
Huang, L., E. Kinnucan, et al. (1999). "Structure of an E6AP-UbcH7 complex: insights into ubiquitination by the E2-E3 enzyme cascade." Science **286**(5443): 1321-1326.
Huibregtse, J. M., M. Scheffner, et al. (1995). "A family of proteins structurally and functionally related to the E6-AP ubiquitin-protein ligase." Proceedings of the National Academy of Sciences of the United States of America **92**(11): 5249.
Ito, H., Y. Fukuda, et al. (1983). "Transformation of intact yeast cells treated with alkali cations." Journal of bacteriology **153**(1): 163-168.
Ito, T., T. Chiba, et al. (2001). "A comprehensive two-hybrid analysis to explore the yeast protein interactome." Proc Natl Acad Sci U S A **98**(8): 4569-4574.
Ivan, M., K. Kondo, et al. (2001). "HIFalpha targeted for VHL-mediated destruction by proline hydroxylation: implications for O2 sensing." Science **292**(5516): 464-468.
James, P., J. Halladay, et al. (1996). "Genomic libraries and a host strain designed for highly efficient two-hybrid selection in yeast." Genetics **144**(4): 1425-1436.
Jeong, H., S. P. Mason, et al. (2001). "Lethality and centrality in protein networks." Nature **411**(6833): 41-42.
Jo, Y., P. C. Lee, et al. (2011). "Sterol-induced degradation of HMG CoA reductase depends on interplay of two Insigs and two ubiquitin ligases, gp78 and Trc8." Proceedings of the National Academy of Sciences of the United States of America **108**(51): 20503-20508.
Jones, D., E. Crowe, et al. (2002). "Functional and phylogenetic analysis of the ubiquitylation system in Caenorhabditis elegans: ubiquitin-conjugating enzymes, ubiquitin-activating enzymes, and ubiquitin-like proteins." Genome Biol **3**(1): RESEARCH0002.
Kee, Y. and J. M. Huibregtse (2007). "Regulation of catalytic activities of HECT ubiquitin ligases." Biochemical and Biophysical Research Communications **354**(2): 329-333.
Kentsis, A., R. E. Gordon, et al. (2002). "Control of biochemical reactions through supramolecular RING domain self-assembly." Proceedings of the National Academy of Sciences of the United States of America **99**(24): 15404-15409.
Kerscher, O., R. Felberbaum, et al. (2006). "Modification of proteins by ubiquitin and ubiquitin-like proteins." Annual review of cell and developmental biology **22**: 159-180.
Keshava Prasad, T. S., R. Goel, et al. (2009). "Human Protein Reference Database--2009 update." Nucleic acids research **37**(Database issue): D767-772.
Khanin, R. and E. Wit (2006). "How scale-free are biological networks." Journal of computational biology : a journal of computational molecular cell biology **13**(3): 810-818.
Kikuchi, J., Y. Furukawa, et al. (2000). "Induction of ubiquitin-conjugating enzyme by aggregated low density lipoprotein in human macrophages and its

implications for atherosclerosis." Arteriosclerosis, thrombosis, and vascular biology **20**(1): 128-134.
Kim, H. T., K. P. Kim, et al. (2007). "Certain Pairs of Ubiquitin-conjugating Enzymes (E2s) and Ubiquitin-Protein Ligases (E3s) Synthesize Nondegradable Forked Ubiquitin Chains Containing All Possible Isopeptide Linkages." J. Biol. Chem. **282**(24): 17375-17386.
Kim, J., M. Guermah, et al. (2009). "RAD6-Mediated Transcription-Coupled H2B Ubiquitylation Directly Stimulates H3K4 Methylation in Human Cells." Cell **137**(3): 459-471.
Kirisako, T., K. Kamei, et al. (2006). "A ubiquitin ligase complex assembles linear polyubiquitin chains." EMBO Journal **25**(20): 4877-4887.
Kirkpatrick, D. S., C. Denison, et al. (2005). "Weighing in on ubiquitin: the expanding role of mass-spectrometry-based proteomics." Nature cell biology **7**(8): 750-757.
Kleiger, G., A. Saha, et al. (2009). "Rapid E2-E3 assembly and disassembly enable processive ubiquitylation of cullin-RING ubiquitin ligase substrates." Cell **139**(5): 957-968.
Komander, D. (2009). "The emerging complexity of protein ubiquitination." Biochemical Society transactions **37**(Pt 5): 937-953.
Komander, D. (2010). "Mechanism, specificity and structure of the deubiquitinases." Sub-cellular biochemistry **54**: 69-87.
Komander, D., M. J. Clague, et al. (2009). "Breaking the chains: structure and function of the deubiquitinases." Nature reviews. Molecular cell biology **10**(8): 550-563.
Komander, D., F. Reyes-Turcu, et al. (2009). "Molecular discrimination of structurally equivalent Lys 63-linked and linear polyubiquitin chains." EMBO reports **10**(5): 466-473.
Komatsu, M., T. Chiba, et al. (2004). "A novel protein-conjugating system for Ufm1, a ubiquitin-fold modifier." EMBO J **23**(9): 1977-1986.
Krogh, A., B. Larsson, et al. (2001). "Predicting transmembrane protein topology with a hidden Markov model: application to complete genomes." Journal of molecular biology **305**(3): 567-580.
Kumar, S., Y. Yoshida, et al. (1993). "Cloning of a cDNA which encodes a novel ubiquitin-like protein." Biochem Biophys Res Commun **195**(1): 393-399.
Kutner, J., J. Towpik, et al. (2008). "Mitochondrial release factor in yeast: interplay of functional domains." Current genetics **53**(3): 185-192.
Lee, I. and H. Schindelin (2008). "Structural insights into E1-catalyzed ubiquitin activation and transfer to conjugating enzymes." Cell **134**(2): 268-278.
Lee, O. H., H. Kim, et al. (2011). "Genome-wide YFP fluorescence complementation screen identifies new regulators for telomere signaling in human cells." Molecular & cellular proteomics : MCP **10**(2): M110 001628.
Lee, S., S. Hong, et al. (2008). "The ubiquitin-conjugating enzyme UbcH6 regulates the transcriptional repression activity of the SCA1 gene product ataxin-1." Biochemical and Biophysical Research Communications **372**(4): 735-740.
Lee, S. J., J. Y. Choi, et al. (2001). "E3 ligase activity of RING finger proteins that interact with Hip-2, a human ubiquitin-conjugating enzyme." FEBS Lett **503**(1): 61-64.
Lemaire, K., R. F. Moura, et al. (2011). "Ubiquitin fold modifier 1 (UFM1) and its target UFBP1 protect pancreatic beta cells from ER stress-induced apoptosis." PLoS ONE **6**(4): e18517.

Letunic, I. and P. Bork (2007). "Interactive Tree Of Life (iTOL): an online tool for phylogenetic tree display and annotation." Bioinformatics **23**(1): 127-128.
Levy, E. D., E. Boeri Erba, et al. (2008). "Assembly reflects evolution of protein complexes." Nature **453**(7199): 1262-1265.
Li, M., C. L. Brooks, et al. (2004). "A dynamic role of HAUSP in the p53-Mdm2 pathway." Molecular Cell **13**(6): 879-886.
Li, W., M. H. Bengtson, et al. (2008). "Genome-wide and functional annotation of human E3 ubiquitin ligases identifies MULAN, a mitochondrial E3 that regulates the organelle's dynamics and signaling." PLoS ONE **3**(1): e1487.
Li, W., D. Tu, et al. (2007). "A ubiquitin ligase transfers preformed polyubiquitin chains from a conjugating enzyme to a substrate." Nature **446**(7133): 333-337.
Liew, C. W., H. Sun, et al. (2010). "RING domain dimerization is essential for RNF4 function." The Biochemical journal **431**(1): 23-29.
Lima-Mendez, G. and J. van Helden (2009). "The powerful law of the power law and other myths in network biology." Molecular bioSystems **5**(12): 1482-1493.
Linares, L. K., A. Hengstermann, et al. (2003). "HdmX stimulates Hdm2-mediated ubiquitination and degradation of p53." Proceedings of the National Academy of Sciences of the United States of America **100**(21): 12009-12014.
Lineberry, N., L. Su, et al. (2008). "The single subunit transmembrane E3 ligase gene related to anergy in lymphocytes (GRAIL) captures and then ubiquitinates transmembrane proteins across the cell membrane." J Biol Chem **283**(42): 28497-28505.
Lineberry, N. B., L. L. Su, et al. (2008). "Cutting edge: The transmembrane E3 ligase GRAIL ubiquitinates the costimulatory molecule CD40 ligand during the induction of T cell anergy." J Immunol **181**(3): 1622-1626.
Linke, K., P. D. Mace, et al. (2008). "Structure of the MDM2//MDMX RING domain heterodimer reveals dimerization is required for their ubiquitylation in trans." Cell Death Differ.
Loeb, K. R. and A. L. Haas (1992). "The interferon-inducible 15-kDa ubiquitin homolog conjugates to intracellular proteins." J Biol Chem **267**(11): 7806-7813.
Lorick, K. L., J. P. Jensen, et al. (1999). "RING fingers mediate ubiquitin-conjugating enzyme (E2)-dependent ubiquitination." Proc Natl Acad Sci U S A **96**(20): 11364-11369.
Luker, K. E., M. Gupta, et al. (2009). "Imaging ligand-dependent activation of CXCR7." Neoplasia **11**(10): 1022-1035.
Luker, K. E., M. C. Smith, et al. (2004). "Kinetics of regulated protein-protein interactions revealed with firefly luciferase complementation imaging in cells and living animals." Proceedings of the National Academy of Sciences of the United States of America **101**(33): 12288-12293.
Luzio, J. P., P. R. Pryor, et al. (2007). "Lysosomes: fusion and function." Nature reviews. Molecular cell biology **8**(8): 622-632.
Mace, P. D., K. Linke, et al. (2008). "Structures of the cIAP2 RING domain reveal conformational changes associated with ubiquitin-conjugating enzyme (E2) recruitment." The Journal of biological chemistry **283**(46): 31633-31640.
Machida, Y. J., Y. Machida, et al. (2006). "UBE2T Is the E2 in the Fanconi Anemia Pathway and Undergoes Negative Autoregulation." Molecular Cell **23**(4): 589-596.

Magliery, T. J., C. G. Wilson, et al. (2005). "Detecting protein-protein interactions with a green fluorescent protein fragment reassembly trap: scope and mechanism." Journal of the American Chemical Society **127**(1): 146-157.
Mahon, P. and A. Bateman (2000). "The PA domain: a protease-associated domain." Protein science : a publication of the Protein Society **9**(10): 1930-1934.
Markson, G., C. Kiel, et al. (2009). "Analysis of the human E2 ubiquitin conjugating enzyme protein interaction network." Genome Res **19**(10): 1905-1911.
Massoud, T. F. and S. S. Gambhir (2003). "Molecular imaging in living subjects: seeing fundamental biological processes in a new light." Genes Dev **17**(5): 545-580.
Matsuki, Y., M. Ohmura-Hoshino, et al. (2007). "Novel regulation of MHC class II function in B cells." The EMBO journal **26**(3): 846-854.
Matsumoto, M. L., K. E. Wickliffe, et al. (2010). "K11-linked polyubiquitination in cell cycle control revealed by a K11 linkage-specific antibody." Molecular Cell **39**(3): 477-484.
McKenna, S., L. Spyracopoulos, et al. (2001). "Noncovalent interaction between ubiquitin and the human DNA repair protein Mms2 is required for Ubc13-mediated polyubiquitination." The Journal of biological chemistry **276**(43): 40120-40126.
Mehnert, M., T. Sommer, et al. (2010). "ERAD ubiquitin ligases: multifunctional tools for protein quality control and waste disposal in the endoplasmic reticulum." BioEssays : news and reviews in molecular, cellular and developmental biology **32**(10): 905-913.
Meierhofer, D., X. Wang, et al. (2008). "Quantitative Analysis of global Ubiquitination in HeLa Cells by Mass Spectrometry." Journal of Proteome Research **7**(10): 4566-4576.
Misawa, N., A. K. Kafi, et al. (2010). "Rapid and high-sensitivity cell-based assays of protein-protein interactions using split click beetle luciferase complementation: an approach to the study of G-protein-coupled receptors." Analytical chemistry **82**(6): 2552-2560.
Mizushima, N., H. Sugita, et al. (1998). "A new protein conjugation system in human. The counterpart of the yeast Apg12p conjugation system essential for autophagy." J Biol Chem **273**(51): 33889-33892.
Morell, M., A. Espargaro, et al. (2007). "Detection of transient protein-protein interactions by bimolecular fluorescence complementation: the Abl-SH3 case." Proteomics **7**(7): 1023-1036.
Morell, M., S. Ventura, et al. (2009). "Protein complementation assays: approaches for the in vivo analysis of protein interactions." FEBS letters **583**(11): 1684-1691.
Mosesson, Y., K. Shtiegman, et al. (2003). "Endocytosis of receptor tyrosine kinases is driven by monoubiquitylation, not polyubiquitylation." The Journal of biological chemistry **278**(24): 21323-21326.
Nacerddine, K., F. Lehembre, et al. (2005). "The SUMO pathway is essential for nuclear integrity and chromosome segregation in mice." Developmental cell **9**(6): 769-779.
Nakamura, N., Y. Kimura, et al. (2006). "MARCH-V is a novel mitofusin 2- and Drp1-binding protein able to change mitochondrial morphology." EMBO Rep **7**(10): 1019-1022.

Nathan, J. A. and P. J. Lehner (2009). "The trafficking and regulation of membrane receptors by the RING-CH ubiquitin E3 ligases." Experimental cell research **315**(9): 1593-1600.
Neutzner, A., M. Neutzner, et al. (2011). "A systematic search for endoplasmic reticulum (ER) membrane-associated RING finger proteins identifies Nixin/ZNRF4 as a regulator of calnexin stability and ER homeostasis." The Journal of biological chemistry **286**(10): 8633-8643.
Niu, J., Y. Shi, et al. (2011). "LUBAC regulates NF-kappaB activation upon genotoxic stress by promoting linear ubiquitination of NEMO." The EMBO journal **30**(18): 3741-3753.
Nyfeler, B., S. W. Michnick, et al. (2005). "Capturing protein interactions in the secretory pathway of living cells." Proceedings of the National Academy of Sciences of the United States of America **102**(18): 6350-6355.
Ohmura-Hoshino, M., Y. Matsuki, et al. (2006). "Inhibition of MHC class II expression and immune responses by c-MIR." Journal of immunology **177**(1): 341-354.
Ohsumi, Y. (2001). "Molecular dissection of autophagy: two ubiquitin-like systems." Nature reviews. Molecular cell biology **2**(3): 211-216.
Okumoto, K., I. Abe, et al. (2000). "Molecular anatomy of the peroxin Pex12p: ring finger domain is essential for Pex12p function and interacts with the peroxisome-targeting signal type 1-receptor Pex5p and a ring peroxin, Pex10p." The Journal of biological chemistry **275**(33): 25700-25710.
Oliver, S. (2000). "Guilt-by-association goes global." Nature **403**(6770): 601-603.
Ozawa, T., A. Kaihara, et al. (2001). "Split luciferase as an optical probe for detecting protein-protein interactions in mammalian cells based on protein splicing." Analytical chemistry **73**(11): 2516-2521.
Parker, J. L. and H. D. Ulrich (2009). "Mechanistic analysis of PCNA poly-ubiquitylation by the ubiquitin protein ligases Rad18 and Rad5." The EMBO journal **28**(23): 3657-3666.
Paulmurugan, R. and S. S. Gambhir (2003). "Monitoring protein-protein interactions using split synthetic renilla luciferase protein-fragment-assisted complementation." Analytical chemistry **75**(7): 1584-1589.
Paulmurugan, R., Y. Umezawa, et al. (2002). "Noninvasive imaging of protein-protein interactions in living subjects by using reporter protein complementation and reconstitution strategies." Proceedings of the National Academy of Sciences of the United States of America **99**(24): 15608-15613.
Peng, J., D. Schwartz, et al. (2003). "A proteomics approach to understanding protein ubiquitination." Nat Biotech **21**(8): 921-926.
Persaud, A., P. Alberts, et al. (2009). "Comparison of substrate specificity of the ubiquitin ligases Nedd4 and Nedd4-2 using proteome arrays." Mol Syst Biol **5**.
Pichler, A., P. Knipscheer, et al. (2005). "SUMO modification of the ubiquitin-conjugating enzyme E2-25K." Nature structural & molecular biology **12**(3): 264-269.
Pickart, C. M. and R. E. Cohen (2004). "Proteasomes and their kin: proteases in the machine age." Nature reviews. Molecular cell biology **5**(3): 177-187.
Pines, J. and C. Lindon (2005). "Proteolysis: anytime, any place, anywhere?" Nature cell biology **7**(8): 731-735.
Plafker, K. S., J. D. Singer, et al. (2009). "The ubiquitin conjugating enzyme, UbcM2, engages in novel interactions with components of cullin-3 based E3 ligases." Biochemistry **48**(15): 3527-3537.

Plafker, S. M. and I. G. Macara (2000). "Importin-11, a nuclear import receptor for the ubiquitin-conjugating enzyme, UbcM2." EMBO J **19**(20): 5502-5513.
Plafker, S. M., K. S. Plafker, et al. (2004). Ubiquitin charging of human class III ubiquitin-conjugating enzymes triggers their nuclear import. **167:** 649-659.
Platta, H. W., F. El Magraoui, et al. (2009). "Pex2 and pex12 function as protein-ubiquitin ligases in peroxisomal protein import." Molecular and cellular biology **29**(20): 5505-5516.
Platta, H. W., F. El Magraoui, et al. (2007). "Ubiquitination of the peroxisomal import receptor Pex5p is required for its recycling." The Journal of cell biology **177**(2): 197-204.
Plechanovova, A., E. G. Jaffray, et al. (2011). "Mechanism of ubiquitylation by dimeric RING ligase RNF4." Nature structural & molecular biology **18**(9): 1052-1059.
Poetz, O., S. Hoeppe, et al. (2009). "Proteome wide screening using peptide affinity capture." Proteomics **9**(6): 1518-1523.
Poole, B., S. Ohkuma, et al. (1977). "The accumulation of weakly basic substances in lysosomes and the inhibition of intracellular protein degradation." Acta biologica et medica Germanica **36**(11-12): 1777-1788.
Poyurovsky, M. V., C. Priest, et al. (2007). "The Mdm2 RING domain C-terminus is required for supramolecular assembly and ubiquitin ligase activity." The EMBO journal **26**(1): 90-101.
Prasad, T. S., K. Kandasamy, et al. (2009). "Human Protein Reference Database and Human Proteinpedia as discovery tools for systems biology." Methods in molecular biology **577**: 67-79.
Prestele, J., G. Hierl, et al. (2010). "Different functions of the C3HC4 zinc RING finger peroxins PEX10, PEX2, and PEX12 in peroxisome formation and matrix protein import." Proceedings of the National Academy of Sciences of the United States of America **107**(33): 14915-14920.
Raasi, S., R. Varadan, et al. (2005). "Diverse polyubiquitin interaction properties of ubiquitin-associated domains." Nature structural & molecular biology **12**(8): 708-714.
Radoshevich, L., L. Murrow, et al. (2010). "ATG12 conjugation to ATG3 regulates mitochondrial homeostasis and cell death." Cell **142**(4): 590-600.
Rahighi, S., F. Ikeda, et al. (2009). "Specific recognition of linear ubiquitin chains by NEMO is important for NF-kappaB activation." Cell **136**(6): 1098-1109.
Rajagopala, S. V., K. T. Hughes, et al. (2009). "Benchmarking yeast two-hybrid systems using the interactions of bacterial motility proteins." Proteomics **9**(23): 5296-5302.
Reid, B. G. and G. C. Flynn (1997). "Chromophore formation in green fluorescent protein." Biochemistry **36**(22): 6786-6791.
Remy, I. and S. W. Michnick (2001). "Visualization of biochemical networks in living cells." Proceedings of the National Academy of Sciences of the United States of America **98**(14): 7678-7683.
Remy, I. and S. W. Michnick (2006). "A highly sensitive protein-protein interaction assay based on Gaussia luciferase." Nature methods **3**(12): 977-979.
Reverter, D. and C. D. Lima (2006). "Structural basis for SENP2 protease interactions with SUMO precursors and conjugated substrates." Nature structural & molecular biology **13**(12): 1060-1068.
Reymond, A., G. Meroni, et al. (2001). "The tripartite motif family identifies cell compartments." EMBO J **20**(9): 2140-2151.

Rheinbach, H. (2005). "Comparative Analysis of the Ubiquitin-proteasome system in *Homo sapiens* and *Saccharomyces cerevisiae*." Thesis - Mathematisch-Naturwissenschaftlichen Fakultät der Universität zu Köln: 48-50.
Roth, W., P. Kermer, et al. (2003). "Bifunctional apoptosis inhibitor (BAR) protects neurons from diverse cell death pathways." Cell Death Differ **10**(10): 1178-1187.
Rual, J.-F., K. Venkatesan, et al. (2005). "Towards a proteome-scale map of the human protein-protein interaction network." Nature **437**(7062): 1173-1178.
Ryan, P. E., G. C. Davies, et al. (2006). "Regulating the regulator: negative regulation of Cbl ubiquitin ligases." Trends Biochem Sci **31**(2): 79-88.
Saha, A. and R. J. Deshaies (2008). "Multimodal activation of the ubiquitin ligase SCF by Nedd8 conjugation." Molecular Cell **32**(1): 21-31.
Sanderson, C. M. (2009). "The Cartographers toolbox: building bigger and better human protein interaction networks." Briefings in functional genomics & proteomics **8**(1): 1-11.
Sarcevic, B., A. Mawson, et al. (2002). "Regulation of the ubiquitin-conjugating enzyme hHR6A by CDK-mediated phosphorylation." The EMBO journal **21**(8): 2009-2018.
Sato, Y., A. Yoshikawa, et al. (2009). "Structural basis for specific recognition of Lys 63-linked polyubiquitin chains by tandem UIMs of RAP80." EMBO J **28**(16): 2461-2468.
Scheffner, M. and N. J. Whitaker (2003). "Human papillomavirus-induced carcinogenesis and the ubiquitin-proteasome system." Semin Cancer Biol **13**(1): 59-67.
Schoenheimer, R., S. Ratner, et al. (1939). "The Process of Continuous Deamination and Reamination of Amino Acids in the Proteins of Normal Animals." Science **89**(2308): 272-273.
Schulman, B. A. and J. W. Harper (2009). "Ubiquitin-like protein activation by E1 enzymes: the apex for downstream signalling pathways." Nat Rev Mol Cell Biol **10**(5): 319-331.
Semple, J. I., G. Prime, et al. (2005). "Two-hybrid reporter vectors for gap repair cloning." BioTechniques **38**(6): 927-934.
Serebriiskii, I. G. and E. A. Golemis (2001). "Two-hybrid system and false positives. Approaches to detection and elimination." Methods Mol Biol **177**: 123-134.
Shen, Y., P. Ballar, et al. (2007). "ER stress differentially regulates the stabilities of ERAD ubiquitin ligases and their substrates." Biochem Biophys Res Commun **352**(4): 919-924.
Shen, Z., P. E. Pardington-Purtymun, et al. (1996). "UBL1, a human ubiquitin-like protein associating with human RAD51/RAD52 proteins." Genomics **36**(2): 271-279.
Shimizu, Y., Y. Okuda-Shimizu, et al. (2010). "Ubiquitylation of an ERAD substrate occurs on multiple types of amino acids." Molecular Cell **40**(6): 917-926.
Shmueli, A., Y. C. Tsai, et al. (2009). "Targeting of gp78 for ubiquitin-mediated proteasomal degradation by Hrd1: cross-talk between E3s in the endoplasmic reticulum." Biochemical and Biophysical Research Communications **390**(3): 758-762.
Siepmann, T. J., R. N. Bohnsack, et al. (2003). "Protein interactions within the N-end rule ubiquitin ligation pathway." The Journal of biological chemistry **278**(11): 9448-9457.
Soares, L., C. Seroogy, et al. (2004). "Two isoforms of otubain 1 regulate T cell anergy via GRAIL." Nature immunology **5**(1): 45-54.

Souphron, J., M. B. Waddell, et al. (2008). "Structural dissection of a gating mechanism preventing misactivation of ubiquitin by NEDD8's E1." Biochemistry **47**(34): 8961-8969.
Sowa, M. E., E. J. Bennett, et al. (2009). "Defining the human deubiquitinating enzyme interaction landscape." Cell **138**(2): 389-403.
Spektor, T. M., L. M. Congdon, et al. (2011). "The UBC9 E2 SUMO conjugating enzyme binds the PR-Set7 histone methyltransferase to facilitate target gene repression." PLoS ONE **6**(7): e22785.
Stefan, E., S. Aquin, et al. (2007). "Quantification of dynamic protein complexes using Renilla luciferase fragment complementation applied to protein kinase A activities in vivo." Proceedings of the National Academy of Sciences of the United States of America **104**(43): 16916-16921.
Stelzl, U., U. Worm, et al. (2005). "A Human Protein-Protein Interaction Network: A Resource for Annotating the Proteome." Cell **122**(6): 957-968.
Su, A. I., M. P. Cooke, et al. (2002). "Large-scale analysis of the human and mouse transcriptomes." Proceedings of the National Academy of Sciences of the United States of America **99**(7): 4465-4470.
Takeuchi, T., S. Iwahara, et al. (2005). "Link between the ubiquitin conjugation system and the ISG15 conjugation system: ISG15 conjugation to the UbcH6 ubiquitin E2 enzyme." Journal of biochemistry **138**(6): 711-719.
Tarassov, K., V. Messier, et al. (2008). "An in vivo map of the yeast protein interactome." Science **320**(5882): 1465-1470.
Tatsumi, K., Y. S. Sou, et al. (2010). "A novel type of E3 ligase for the Ufm1 conjugation system." The Journal of biological chemistry **285**(8): 5417-5427.
Taylor, I. W., R. Linding, et al. (2009). "Dynamic modularity in protein interaction networks predicts breast cancer outcome." Nature biotechnology **27**(2): 199-204.
Teo, H., D. J. Gill, et al. (2006). "ESCRT-I Core and ESCRT-II GLUE Domain Structures Reveal Role for GLUE in Linking to ESCRT-I and Membranes." Cell **125**(1): 99-111.
Thomas, P. D., A. Kejariwal, et al. (2003). "PANTHER: a browsable database of gene products organized by biological function, using curated protein family and subfamily classification." Nucleic acids research **31**(1): 334-341.
Tiwari, S. and A. M. Weissman (2001). "Endoplasmic reticulum (ER)-associated degradation of T cell receptor subunits. Involvement of ER-associated ubiquitin-conjugating enzymes (E2s)." The Journal of biological chemistry **276**(19): 16193-16200.
Tsai, C. J., B. Ma, et al. (2009). "Protein-protein interaction networks: how can a hub protein bind so many different partners?" Trends in Biochemical Sciences **34**(12): 594-600.
Tsang, H. T., J. W. Connell, et al. (2006). "A systematic analysis of human CHMP protein interactions: additional MIT domain-containing proteins bind to multiple components of the human ESCRT III complex." Genomics **88**(3): 333-346.
Uetz, P., L. Giot, et al. (2000). "A comprehensive analysis of protein-protein interactions in Saccharomyces cerevisiae." Nature **403**(6770): 623-627.
Ulrich, H. D., S. Vogel, et al. (2005). "SUMO keeps a check on recombination during DNA replication." Cell Cycle **4**(12): 1699-1702.
van Wijk, S. J., S. J. de Vries, et al. (2009). "A comprehensive framework of E2-RING E3 interactions of the human ubiquitin-proteasome system." Mol Syst Biol **5**: 295.

van Wijk, S. J. and H. T. Timmers (2010). "The family of ubiquitin-conjugating enzymes (E2s): deciding between life and death of proteins." FASEB J **24**(4): 981-993.
Vander Kooi, C. W., M. D. Ohi, et al. (2006). "The Prp19 U-box crystal structure suggests a common dimeric architecture for a class of oligomeric E3 ubiquitin ligases." Biochemistry **45**(1): 121-130.
Varadan, R., M. Assfalg, et al. (2005). "Structural determinants for selective recognition of a Lys48-linked polyubiquitin chain by a UBA domain." Mol Cell **18**(6): 687-698.
Venancio, T. M., S. Balaji, et al. (2009). "Reconstructing the ubiquitin network: cross-talk with other systems and identification of novel functions." Genome biology **10**(3): R33.
Verma, R., R. S. Annan, et al. (1997). "Phosphorylation of Sic1p by G1 Cdk required for its degradation and entry into S phase." Science **278**(5337): 455-460.
Virdee, S., Y. Ye, et al. (2010). "Engineered diubiquitin synthesis reveals Lys29-isopeptide specificity of an OTU deubiquitinase." Nature chemical biology **6**(10): 750-757.
Vodermaier, H. C. (2004). "APC/C and SCF: controlling each other and the cell cycle." Current biology : CB **14**(18): R787-796.
Walden, H., M. S. Podgorski, et al. (2003). "The structure of the APPBP1-UBA3-NEDD8-ATP complex reveals the basis for selective ubiquitin-like protein activation by an E1." Molecular Cell **12**(6): 1427-1437.
Wang, H., L. Wang, et al. (2004). "Role of histone H2A ubiquitination in Polycomb silencing." Nature **431**(7010): 873-878.
Wang, M., D. Cheng, et al. (2006). "Molecular determinants of polyubiquitin linkage selection by an HECT ubiquitin ligase." EMBO Journal **25**(8): 1710-1719.
Wang, X., R. A. Herr, et al. (2009). "Ube2j2 ubiquitinates hydroxylated amino acids on ER-associated degradation substrates." The Journal of cell biology **187**(5): 655-668.
Weissman, A. M. (2001). "Themes and variations on ubiquitylation." Nat Rev Mol Cell Biol **2**(3): 169-178.
Welchman, R. L., C. Gordon, et al. (2005). "Ubiquitin and ubiquitin-like proteins as multifunctional signals." Nat Rev Mol Cell Biol **6**(8): 599-609.
Wenzel, D. M., A. Lissounov, et al. (2011). "UBCH7 reactivity profile reveals parkin and HHARI to be RING/HECT hybrids." Nature **474**(7349): 105-108.
Wenzel, D. M., K. E. Stoll, et al. (2010). "E2s: structurally economical and functionally replete." The Biochemical journal **433**(1): 31-42.
Whiting, C. C., L. L. Su, et al. (2011). "GRAIL: a unique mediator of CD4 T-lymphocyte unresponsiveness." The FEBS journal **278**(1): 47-58.
Wiborg, O., M. S. Pedersen, et al. (1985). "The human ubiquitin multigene family: some genes contain multiple directly repeated ubiquitin coding sequences." EMBO J **4**(3): 755-759.
Wickliffe, K. E., S. Lorenz, et al. (2011). "The mechanism of linkage-specific ubiquitin chain elongation by a single-subunit E2." Cell **144**(5): 769-781.
Wiemuth, D., J. S. Lott, et al. (2010). "Interaction of serum- and glucocorticoid regulated kinase 1 (SGK1) with the WW-domains of Nedd4-2 is required for epithelial sodium channel regulation." PLoS ONE **5**(8): e12163.
Wilkinson, K. D., M. K. Urban, et al. (1980). "Ubiquitin is the ATP-dependent proteolysis factor I of rabbit reticulocytes." J Biol Chem **255**(16): 7529-7532.

Williams, C., M. van den Berg, et al. (2008). "Pex10p functions as an E3 ligase for the Ubc4p-dependent ubiquitination of Pex5p." Biochemical and Biophysical Research Communications **374**(4): 620-624.
Williamson, A., K. E. Wickliffe, et al. (2009). "Identification of a physiological E2 module for the human anaphase-promoting complex." Proceedings of the National Academy of Sciences of the United States of America **106**(43): 18213-18218.
Wilson, R. C., S. P. Edmondson, et al. (2011). "The E2-25K ubiquitin-associated (UBA) domain aids in polyubiquitin chain synthesis and linkage specificity." Biochemical and Biophysical Research Communications **405**(4): 662-666.
Windheim, M., M. Peggie, et al. (2008). "Two different classes of E2 ubiquitin-conjugating enzymes are required for the mono-ubiquitination of proteins and elongation by polyubiquitin chains with a specific topology." Biochem J **409**(3): 723-729.
Wolfe, M. S. (2009). "Intramembrane proteolysis." Chemical reviews **109**(4): 1599-1612.
Wu, K., J. Kovacev, et al. (2010). "Priming and extending: a UbcH5/Cdc34 E2 handoff mechanism for polyubiquitination on a SCF substrate." Molecular Cell **37**(6): 784-796.
Wu, T., Y. Merbl, et al. (2010). "UBE2S drives elongation of K11-linked ubiquitin chains by the Anaphase-Promoting Complex." Proceedings of the National Academy of Sciences **107**(4): 1355-1360.
Xu, G., J. S. Paige, et al. (2010). "Global analysis of lysine ubiquitination by ubiquitin remnant immunoaffinity profiling." Nat Biotech **28**(8): 868-873.
Xu, P., D. M. Duong, et al. (2009). "Quantitative Proteomics Reveals the Function of Unconventional Ubiquitin Chains in Proteasomal Degradation." Cell **137**(1): 133-145.
Yang, M., Z. Wu, et al. (1995). "Protein-peptide interactions analyzed with the yeast two-hybrid system." Nucleic acids research **23**(7): 1152-1156.
Ye, Y. and M. Rape (2009). "Building ubiquitin chains: E2 enzymes at work." Nat Rev Mol Cell Biol **10**(11): 755-764.
Yin, G., C. Ji, et al. (2006). "Cloning, characterization and subcellular localization of a gene encoding a human Ubiquitin-conjugating enzyme (E2) homologous to the Arabidopsis thaliana UBC-16 gene product." Front Biosci **11**: 1500-1507.
Yin, Q., S. C. Lin, et al. (2009). "E2 interaction and dimerization in the crystal structure of TRAF6." Nature structural & molecular biology **16**(6): 658-666.
Yokota, T., H. Nagai, et al. (2001). "Identification, tissue expression, and chromosomal position of a novel gene encoding human ubiquitin-conjugating enzyme E2-230k." Gene **267**(1): 95-100.
Yoshida, Y., T. Chiba, et al. (2002). "E3 ubiquitin ligase that recognizes sugar chains." Nature **418**(6896): 438-442.
Young, P., Q. Deveraux, et al. (1998). "Characterization of two polyubiquitin binding sites in the 26 S protease subunit 5a." The Journal of biological chemistry **273**(10): 5461-5467.
Yu, H., P. Braun, et al. (2008). "High-quality binary protein interaction map of the yeast interactome network." Science **322**(5898): 104-110.
Yu, H., P. M. Kim, et al. (2007). "The importance of bottlenecks in protein networks: correlation with gene essentiality and expression dynamics." PLoS computational biology **3**(4): e59.

Yunus, A. A. and C. D. Lima (2006). "Lysine activation and functional analysis of E2-mediated conjugation in the SUMO pathway." Nature structural & molecular biology **13**(6): 491-499.

Zhang, Q., K. Wang, et al. (2010). "The myostatin-induced E3 ubiquitin ligase RNF13 negatively regulates the proliferation of chicken myoblasts." The FEBS journal **277**(2): 466-476.

Zhang, Y., X. Zhou, et al. (2011). "UBE2W interacts with FANCL and regulates the monoubiquitination of Fanconi anemia protein FANCD2." Molecules and cells **31**(2): 113-122.

Zhao, C., S. L. Beaudenon, et al. (2004). "The UbcH8 ubiquitin E2 enzyme is also the E2 enzyme for ISG15, an IFN-{alpha}/{beta}-induced ubiquitin-like protein." Proceedings of the National Academy of Sciences **101**(20): 7578-7582.

Zheng, N., B. A. Schulman, et al. (2002). "Structure of the Cul1-Rbx1-Skp1-F boxSkp2 SCF ubiquitin ligase complex." Nature **416**(6882): 703-709.

Zheng, N., P. Wang, et al. (2000). "Structure of a c-Cbl-UbcH7 complex: RING domain function in ubiquitin-protein ligases." Cell **102**(4): 533-539.

Ziv, I., Y. Matiuhin, et al. (2011). "A perturbed ubiquitin landscape distinguishes between ubiquitin in trafficking and in proteolysis." Mol Cell Proteomics **10**(5): M111 009753.